Russian Academy of Sciences
Institute of Applied Physics

## VI International Symposium

# TOPICAL PROBLEMS OF BIOPHOTONICS




*28 July – 03 August , 2017*

*St.-Petersburg – Nizhny Novgorod, Russia*

# Proceedings

Nizhny Novgorod, 2017

## Topical Conferences

**Optical Bioimaging**

**Biophotonics in Cancer Research**

**Novel Laser Applications in Biomedicine**

## Workshops

**Clinical Biophotonics**

**Biophotonics in Stem Cell Research**

# Scientific Advisory Board


| | |
|---|---|
| **Victor Bagratashvili`** | Institute of Laser and Information Technologies RAS, Troitsk, Russia |
| **Sergey Deyev** | Institute of Bioorganic Chemistry RAS, Moscow, Russia |
| **Felix Feldchtein** | Nizhny Novgorod State Medical Academy, Russia |
| **Tayyaba Hasan** | Wellman Center, Harvard Medical School, Massachusetts General Hospital, Boston, USA |
| **Karsten König** | University of Saarland, Germany |
| **Sergey Lukyanov** | Institute of Bioorganic Chemistry RAS, Moscow, Russia |
| **Gerard Mourou** | Laboratoire d'Optique Appliquee, Paris, France |
| **Rudolf Steiner** | Institute of Laser Technologies in Medicine and Metrology at the University of Ulm, Germany |
| **Bruce Tromberg** | Beckman Laser Institute and Medical Clinic, UC Irvine, USA |
| **Valery Tuchin** | Research-Educational Institute of Optics and Biophotonics, Saratov State University, Russia |
| **Yury Vladimirov** | Moscow State University, Russia |
| **Ken-ichi Ueda** | Institute for Laser Science, the University of Electro-Communications, Tokyo, Japan; Institute of Applied Physics RAS, Nizhny Novgorod, Russia |


**Symposium Web site:**
**http://www.biophotonics.sci-nnov.ru**

## Organized by

**Institute of Applied Physics**
**of the Russian Academy of Sciences**
www.iapras.ru

**Nizhny Novgorod State Medical Academy**
www.gma.nnov.ru

**GYCOM Ltd**
www.gycom.ru

**International Center for Advanced Studies in**
**Nizhny Novgorod (INCAS)**
www.incas.iapras.ru

## Supported by

The Government of the Russian Federation

The Russian Foundation for Basic Resear

www.artphotonics.com

www.becker-hickl.de

www.stanfordcomputeroptics.com

LLC "Optical Systems Alliance"
www.opticalalliance.ru

http://bioline.ru

https://www.newport.com

http://www.spectra-physics.com

The electron version of VI International Symposium TPB-2017 materials
was prepared
at the Institute of Applied Physics of the Russian Academy of Sciences,
46 Ulyanov Str., 603950 Nizhny Novgorod, Russia

# CONTENTS

## PLENARY TALKS

*W. Becker*
The multi-dimensional world of TCSPC FLIM ..... 15

*D. Boas*
Optical imaging of oxygen delivery and consumption: novel physiological insights and guiding interpretation of BOLD fMRI ..... 16

*B.N. Chichkov*
Laser printing of Stem and IPS cells ..... 17

*A. Heisterkamp, S. Johannsmeier, P. Heeger, L.M. Torres, D. Heinemann, and T. Ripken*
Optogenetic stimulation using nonlinear optics – Pacing hearts with light and other applications ..... 18

*K. Kondo, M. Kando, H. Sakaki, M. Nishiuchi, H. Kiriyama, K. Mizushima, E. Noda, Y. Iwata, and T. Shirai*
Laser driven injector for a new generation heavy ion cancer therapy machine in Japan ..... 19

*Z. Malik*
The frontiers in ALA-PDT ..... 20

*M. O'Donnell*
Light and sound: integrating photonics with ultrasonics for biomedical applications ..... 21

*F.S. Pavone*
Large scale multidimensional and multilevel imaging of tissue disease: towards the 3D digital histology ..... 22

*M.C. Skala, J.T. Sharick, A.J. Walsh, A.T. Shah, T.M. Heaster, P. Favreau, A. Gillette, T.M. Cannon, C. Pasche, D. Deming, R.M. Cook, and C.L. Arteaga*
Optical imaging of cell-level metabolism ..... 23

# OPTICAL BIOIMAGING (OB)

*P. Stähli, J. Ricka, M. Frenz, and H.G. Akarçay*
Optical extinction measurements on strongly scattering samples by way of imaging (Invited) ..... 26

*J. Gunther and S. Andersson-Engels*
Ultrasound optical tomography (Invited) ..... 27

*T. Anna, S. Chakraborty, A. Chiou, and W.C. Kuo*
Full-field optical coherence microscopy for microstructural assessment of maple leaves ..... 28

*O. Bibikova, U.J. Zabarylo, A. Melenteva, V. Belikova, I. Usenov, T. Sakharova, G. Danielyan, A. Bogomolov, O. Minet, H.J. Eichler, and V. Artyushenko*
Fiber spectroscopy methods for cancer diagnostics *ex-vivo* (Poster) ..... 29

*S. Chakraborty, T. Anna, A. Karmenyan, W. C. Kuo, and A. Chiou*
Fluorescence life-time imaging of senescing leaves ..... 30

*Chia-Yuan Chang, Yong-Da Sie, and Shean-Jen Chen*
Deep-biotissue imaging by temporal focusing widefield multiphoton microscopy ..... 31

*Zhongping Chen*
Advances in Optical Coherence Elastography (Invited) ..... 32

*X.L. Deán-Ben, S. Gottschalk, S. Shoham, and D. Razansky*
The promise of large-scale brain imaging with optoacoustics (Invited) ..... 33

*V.V. Dudenkova, A.S. Bystrova, A.V. Meleshina, O.S. Rogovaya, E.V. Gubarkova, and E.V. Zagaynova*
Quantitative analysis of SHG signal of collagen structure in models and tissue samples ..... 34
*M. Eibl, S. Karpf, H. Hakert, D. Weng, and R. Huber*
Single pulse two-photon fluorescence lifetime imaging (SP-FLIM) with MHz pixel rate and an all fiber based setup ..... 35
*J. Enderlein, N. Karedla, A. Chizhik, and Al. Chizhik*
Metal induced energy transfer and axial superresolution microscopy (Invited) ..... 36
*F.I. Feldchtein, A.A. Moiseev, N.D. Gladkova, M.Yu. Kirillin, G.V. Gelikonov, V.V. Dudenkova, E.B. Kiseleva, E.G. Sharabrin, and E.V. Gubarkova*
Cross-polarization optical coherence tomography in vulnerable atherosclerotic plaque detection ..... 37
*M.A. Franceschini*
Measuring cerebral oxygen delivery & consumption with diffuse correlation spectroscopy in African children (Invited) ..... 38
*M. Frenz, L. Ulrich, L. Ahnen, K.G. Held, M. Jaeger, S. Sanchez Majos, M. Wolf, and H.G. Akarcay*
Quantitative optoacoustic imaging (Invited) ..... 39
*V.M. Gelikonov, V.N. Romashov, D.V. Shabanov, S.Yu. Ksenofontov, D.A. Terpelov, P.A. Shilyagin, G.V. Gelikonov, and A. Vitkin*
Cross-polarization coherent backscattering coefficient and its dependence on probe wave polarization (Poster) ..... 40
*V.A. Hovhannisyan and S.J. Chen*
Drug delivery by natural zeolite particles ..... 41
*A.V. Khilov, M.Yu. Kirillin, D.A. Loginova, and I.V. Turchin*
Estimation of tumor invasion depth for PDT procedure with chlorine photosensitizers from two-wavelength probing ..... 42
*M. Kirillin, M. Shakhova, A. Meller, D. Sapunov, P. Agrba, E. Kiseleva, O. Kondratieva, K. Chikalova, T. Motovilova, E. Sergeeva, I. Turchin, and N. Shakhova*
Optical coherence tomography in pathology recognition and monitoring of photodynamic therapy: benefits from numerical processing in clinical applications (Invited) ..... 43
*E.B. Kiseleva, A.A. Moiseev, E.S. Finagina, M.A. Sirotkina, A.V. Maslennikova, D.V. Shabanov, E.V. Zagaynova, F.I. Feldchtein, L.A. Matveev, A.A. Vitkin, and N.D. Gladkova*
*In vivo* multimodal OCT study of human oral mucosa ..... 44
*Yu.V. Kistenev, A.V. Borisov, V.V. Nikolaev, D.A. Vrazhnov, L.V. Spirina, and O.S. Kurochkina*
Approaches of molecular imaging of bio-tissues and machine learning methods for medical applications ..... 45
*M.V. Kochueva, S.S. Kuznetsov, V.V. Dudenkova, A.V. Varlamova, and A.V. Maslennikova*
Quantitative evaluation of collagen radiation-induced changes by laser scanning microscopy (Poster) ..... 46
*K.V. Larin*
Optical coherence elastography of soft tissue (Invited) ..... 47
*E.N. Lazareva and V.V. Tuchin*
Refraction properties of hemoglobin in a wide temperature and wavelength range (Poster) ..... 48
*M. Leutenegger*
Parallelized RESOLFT nanoscopy (Invited) ..... 49
*D.A. Loginova, E.A. Sergeeva, P.D. Agrba, S.V. Zabotnov, F.V. Kashaev, D.E. Presnov, M.B. Gongalsky, L.A. Golovan, and M.Yu. Kirillin*
Perspectives of silicon nanoparticles in optical biomedical imaging (Poster) ..... 50
*D.A. Loginova, I.I. Fiks, E.A. Sergeeva, and M.Yu. Kirillin*
The impact of measurement configuration on probing depth in optical diffuse reflectometry: A Monte Carlo study (Poster) ..... 51

*I. Meglinski, A. Bykov, N.O. Vera Paz, J.P. Staforelli, A. Doronin, T. Novikova*
Towards application of angular momentum of light for tissue diagnosis (Invited) ..... 52

*I. Mikhailova, M. Jaeger, I. Fiks, I. Turchin, and P. Subochev*
Tikhonov deconvolution filtration in acoustic resolution photoacoustic microscopy ..... 53

*S. Nadkarni*
Intracoronary birefringence microscopy of atherosclerotic plaque (Invited) ..... 54

*G. Paltauf, P. Torke, and R. Nuster*
Overcoming the trade-off between depth of field and lateral resolution in scanning photoacoustic imaging with focused detectors (Invited) ..... 55

*V.V. Perekatova, P.V. Subochev, M.Yu. Kirillin, A.G. Orlova, and I.V. Turchin*
*In vivo* two-wavelength mapping of blood oxygen saturation by acoustic resolution photoacoustic microscopy ..... 56

*V.V. Perekatova, M.Yu. Kirillin, I.V. Turchin, and P.V. Subochev*
A combination of three-dimensional virtual point detector concept and fluence compensation in acoustic resolution photoacoustic microscopy (Poster) ..... 57

*A.V. Priezzhev, K. Lee, F. Yaya, C. Wagner, A.N. Semenov, A.E. Lugovtsov, S.Yu. Nikitin, and E.A. Shirshin*
Multimodal dynamic and structural imaging of erythrocytes and blood capillaries (Invited) ..... 58

*P.A. Shilyagin, V.A. Matkivskiy, A.A. Moiseev, S.Yu. Ksenofontov, I.V. Kasatkina, G.V. Gelikonov, D.V. Shabanov, and V.M. Gelikonov*
Self-acting detection and compensation of the influence of media dispersion in SD OCT images ..... 59

*E.V. Gubarkova, A.A. Sovetsky, V.Yu. Zaitsev, A.A. Moiseev, L.A. Matveev, A.L. Matveyev, S.S. Kuznetsov, D.A. Vorontsov, A.Yu. Vorontsov, N.D. Gladkova, and M.A. Sirotkina*
Combined microstructural, polarization-sensitive and elastographic characterization of breast cancer by optical coherence tomography (Poster) ..... 60

*E. Sobol, O. Baum, and S. Wachsmann-Hogiu*
Structural illuminating microscopy and fluorescent markers in the imaging of laser-induced modification of cartilage and sclera structure ..... 61

*P.T.C. So, Y. Xue, K. Barry, C.J. Rowlands, Y. Takiguchi, and E. Nedivi*
Towards synaptomics (Invited) ..... 62

*P. Subochev, I. Mihailova, M. Kirillin, V. Perekatova, M. Jaeger, A. Orlova, and I. Turchin*
Image enhancement in acoustic resolution photoacoustic microscopy ..... 63

*V.V. Tuchin*
Enhanced imaging of tissues by immersion clearing/contrasting: from X-ray to terahertz (Invited) ..... 64

*A. Vitkin*
Functional Optical Coherence Tomography: preclinical and clinical updates from the Nizhny Novgorod – Toronto collaboration (Invited) ..... 65

*A.B. Voloveckiy, V.S. Sukhov, N.Y. Shilyagina, V.V. Dudenkova, A.V. Feofanov, I.V. Balalayeva, and A.V. Maslennikova*
Fluorescent analysis of pharmacokinetics of chlorine $E_6$ conjugate with BIS(dicarbollide) cobalt for boron neutron capture therapy ..... 66

*H. Wabnitz*
Performance characterization of instrumentation for diffuse optical imaging and spectroscopy (Invited) ..... 67

*V.Y. Zaitsev, A.L. Matveyev, L.A. Matveev, G.V. Gelikonov, A.I. Omelchenko, D.V. Shabanov, A.A. Sovetsky, A. Vitkin, O.I. Baum, and E.N. Sobol*
Applicatons of optical coherence elastography in problems of laser reshaping of cartilages and cornea ..... 68

*V.Y. Zaitsev, A.L. Matveyev, L.A. Matveev, E.V. Gubarkova, A.A. Sovetsky, M.A. Sirotkina, G.V. Gelikonov, E.V. Zagaynova, N.D. Gladkova, and A. Vitkin*
Mitigation of practical obstacles in realization of compressional optical coherence elastography (Poster) ..... 69

*V.P. Zharov*
*In vivo* photoacoustic flow cytometry for early diagnosis and prevention of cancer, infections and cardiovascular disorders (Invited) ..... 70

## BIOPHOTONICS IN CANCER RESEARCH (CR)

*N.A. Aksenova, V.V. Kardumjan, N.N. Glagolev, P.S. Timashev, A.L. Spokoynyy, and A.B. Solovieva*
Photodynamic properties of watersoluble porphyrin-amphiphilic polymer-chitosan systems (Poster) ..... 72

*M. Barroso, A. Rudkouskaya, K. Tubbesing, N. Sinsuebphon, K. Chen, and X. Intes*
Novel insights into transferrin-mediated delivery into tumor cells using *in vitro* and *in vivo* FRET imaging (Invited) ..... 73

*A.S. Belova, A.G. Orlova, K.M. Shchukina, I.V. Balalaeva, N.O. Antonova, and E.V. Zagaynova*
Cisplatin-induced hydrogen peroxide level changes as compared to total ROS level (Poster) ..... 74

*P.J. Campagnola*
Analysis of stromal alterations in ovarian cancers via second harmonic generation microscopy (Invited) ..... 75

*S. Kumar, A. Chaudhary, N. Yadav, R. Kumar, and D. Chandra*
Novel regulation of cancer cell death by OXPHOS complexes, cytokines, and unfolded protein response (Invited) ..... 76

*V.P. Chekhonin, P.V. Mel'nikov, and V.P. Baklaushev*
Internalization of vectorized liposomes into target-cells (Invited) ..... 77

*Z.-R. Lin, Y.-C. Lin, K.-T. Wu, E. Perevedentseva, and C.-L. Cheng*
Drug loading and efficiency of nanodiamond-anticancer drug complex in 2D and 3D cellular model (Invited) ..... 78

*E.S. Plekhanova, I.A. Chernigina, V.V. Chernov, and T.G. Shcherbatyuk*
The effect of low-level blue LED light in oncogenesis ..... 79

*A. Patil, V.K. Unnikrishnan, K.M. Pai, R. Ongole, K. Pai, V.B. Kartha, and S. Chidangil*
Optical biopsy: Journey from laboratory system to public health-care (Invited) ..... 80

*C.R. Day, J. Rodriguez, D.R. Larson, and A. Martin*
Live-cell single-molecule imaging reveals compounds that alter initiation dynamics and transcription kinetics ..... 81

*R.N. Day*
Intravital FRET and FLIM: monitoring biosensor activities and intrinsic metabolic states (Invited) ..... 82

*V. Demidov, A. Maeda, M. Sugita, V. Madge, C. Flueraru, and I.A. Vitkin*
Longitudinal assessment of single-dose radiation-induced tumor vascular changes with optical coherence tomography ..... 83

*M.V. Novoselova, D.N. Bratashov, S.V. German, M. Sarimollaoglu, D.A. Nedosekin, B.N. Khlebtsov, D.A. Gorin, V.P. Zharov, and E.I. Galanzha*
*In vivo* targeted theranostics of circulating tumor cells ..... 84

*M.B. Gongalsky, D.A. Muftieva, J. Saarinen, A. Isomaki, L. Peltonen, C.J. Strachan, H.A. Santos, and L.A. Osminkina*
Coherent anti-Stokes Raman spectroscopy as an imaging tool for the interaction between silicon nanostructures and living systems ..... 85

*N.G. Khlebtsov*
Optimal design of layered plasmonic nanostructures with embedded Raman reporters (Invited) ..... 86

*E.B. Kiseleva, K.S. Yashin, A.A. Moiseev, M.A. Sirotkina, L.B. Timofeeva, V.M. Gelikonov, V.V. Fedoseeva, A.I. Alekseeva, and N.D. Gladkova*
Multimodal OCT-guided detection of infiltrative tumor border in glioblastoma rat model ..... 87

*L.G. Klapshina, S.A. Lermontova, I.S. Grigoryev, N.Yu. Shilyagina, M.S. Muravyeva, D.V. Yuzhakova, I.V. Balalaeva, M.V. Shirmanova, E.V. Zagaynova, and M.K. Kuimova*
Novel-potential anticancer theranostic agents based on the porphyrazine framework for specifically personalized medicine ..... 88

*N.V. Klementieva, K.A. Lukyanov, E.V. Zagaynova, and A.S. Mishin*
A new way to efficient primed conversion of photoactivatable fluorescent protein DENDRA2 ..... 89

*S.A. Lermontova, I.S. Grigoryev, N.N. Peskova, I.V. Balalaeva, and L.G. Klapshina*
Fine-tuning of the photophysical and cytotoxic properties of novel fluorescent molecular rotors and PDT sensitizers based on the porphyrazine pigment platform (Poster)..... 90

*J. Cassidy, V. Betz, and L. Lilge*
Photodynamic treatment planning and dosimetry: development of an universal applicable treatment optimization process (Invited)..... 91

*M.M. Lukina, M.V. Shirmanova, V.V. Dudenkova, N.P. Pavlova, L.B. Snopova, and E.V. Zagaynova*
Metabolic imaging of cancer cells using fluorescence life-time microscopy ..... 92

*Y. Mohammed, W. Sanchez, D. Liu, V.R. Leite-Silva, A. Holmes, H. Studier, I. Haridass, E. Ryan, J. Grice, and M. Roberts*
Zinc oxide nanoparticle penetration into *in vivo* and *in vitro* human skin. Simulating life like experimental conditions and using non-invasive MPT-FLIM imaging can provide accurate toxicological assessment (Invited) ..... 93

*M. Ogawa*
New cancer therapy using near infrared light (Invited)..... 94

*A.G. Orlova, M.Yu. Kirillin, A.B. Volovetsky, N.Yu. Shilyagina, E.A. Sergeeva, G.Yu. Golubiatnikov, and I.V. Turchin*
Diffuse optical spectroscopy monitoring of oxygen state of growing experimental tumor ..... 95

*E. Perevedentseva, A. Karmenyan, Y.-C. Lin, C.-Y. Song, Z.-R. Lin, L.-C. Liu, Ashek-I-Ahmed, and C.-L. Cheng*
Multifunctional nanoparticles for bio-medical researches and theranostics (Invited)..... 96

*A. Periasamy, H. Wallrabe, Z. Svindrych, and S.R. Alam*
Tryptophan as an alternative biomarker for cancer metabolism: FLIM-FRET microscopy (Invited)..... 97

*A. Rudkouskaya, N. Sinsuebphon, X. Intes, and M. Barroso*
Quantification of target engagement using non-invasive MFLI-FRET *in-vivo* imaging of breast cancer xenografts ..... 98

*A. Rück, J. Breymayer, D. Bisinger, P. Schäfer, B. von Einem, C.A.F. von Arnim, and S. Kalinina*
Time resolved luminescence imaging as a new theranostic approach (Invited) ..... 99

*I.D. Solviev, T.V. Ivashina, L.M. Vinokurov, and A.P. Savitsky*
Rational mutagenesis of new photoconvertable fluorescent protein for the live cell microscopy (Invited)..... 100

*M. Lukina, A. Orlova, A. Pavlikov, D. Shirokov, A. Neubauer, H. Studier, E. Zagaynova, W. Becker, V. Yakovlev, M. Shirmanova, and V. Shcheslavskiy*
Probing tumors with time-resolved spectroscopy (Invited) ..... 101

*N.Y. Shilyagina, N.N. Peskova, A.V. Utkina, A.A. Gorokhova, S.A. Lermontova, L.G. Klapshina, and I.V. Balalaeva*
Study of the mechanisms of oxidative stress in response to photodynamic treatment ..... 102

*M.V. Shirmanova, M.M. Lukina, I.N. Druzhkova, T.F. Sergeeva, L.E. Shimolina, L.B. Snopova, V.V. Dudenkova, A.I. Gavrina, M.K. Kuimova, V.I. Shcheslavskiy, and E.V. Zagaynova*
Tumor response to chemotherapy as a complex phenomenon: insight into morphofunctional characteristics using fluorescence imaging (Invited) ..... 103

*M.A. Sirotkina, A.A. Moiseev, S.S. Kuznetsov, M.V. Shirmanova, V.Yu. Zaitsev, V.V. Elagin, G.V. Gelikonov, E.V. Zagaynova, A. Vitkin, and N.D. Gladkova*
Monitoring of tumor treatment by multimodal optical coherence tomography ..... 104

*S. Han, R. Bouchard, S. Emelianov, and K. Sokolov*
Mechanisms of molecular cancer imaging and therapy with ultra-small nanoparticles (Invited)..... 105

*H. Studier, M. Pastore, W. Becker, and M.S. Roberts*
Non-invasive metabolic imaging of melanoma progression (Invited)..... 106

*D.V. Yuzhakova, M.V. Shirmanova, E.O. Serebrovskaya, I.N. Druzhkova, S.A. Lukyanov, and E.V. Zagaynova*
The effect of OX40 ligand on CT26 tumors in mice ..... 107

## NOVEL LASER APPLICATIONS IN BIOMEDICINE (NLAB)

*V. Artyushenko*
Novel laser and fiber optics solutions in optical theranostics (Invited)..... 110

*W. Assmann*
The sound of protons – ionoacoustic range monitoring in proton therapy (Invited)..... 111

*N.M. Bulgakova and V.P. Zhukov*
Spatio-temporal modeling of femtosecond laser effects in transparent dielectrics based on solving Maxwell's equations (Invited)..... 112

*S. Fuchs, M. Wünsche, J. Nathanael, J.J. Abel, Ch. Rödel, J. Reinhard, and G.G. Paulus*
XUV coherence tomography with nanoscale resolution (Invited) ..... 113

*K. Inoue*
Novel classes of eubacterial light-driven ion pumping proteins for optical control tools of cells (Invited)..... 114

*A.V. Korzhimanov, M. Nakatsutsumi, L. Grimellet, and J. Fuchs*
Negative impact of self-generated magnetic fields on energies of ions accelerated by ultra-high intensity laser pulses ..... 115

*Yu.N. Kulchin and S.S. Voznesenskiy*
Optical and sensory characteristics of oceanic biota and organic-inorganic natural and biomimetic materials (Invited)..... 116

*H. Lubatschowski*
Frontiers of femtosecond laser applications in ophthalmology (Invited)..... 117

*U. Masood, T.E. Cowan, W. Enghardt, M. Gotz, T. Herrmannsdörfer, K.M. Hofmann, L. Karsch, F. Kroll, U. Schramm, M. Schürer, J.J. Wilkens, K. Zeil, and J. Pawelke*
Ion beam therapy with laser-accelerated proton beams – Challenges and solutions (Invited)..... 118

*M. Meunier*
Nanoplasmonics enhanced ultrafast laser nanosurgery: modeling and rational design (Invited)..... 119

*V.P. Minaev*
The possibilities realized in surgery and forced therapy by means of devices based on the fiber and diode lasers (Invited)..... 120

*A.A. Seryi*
Recent developments in JAI and UK on X-Ray bio-imaging based on laser-plasma acceleration (Invited)..... 121

*K. Ueda*
Bio-photonics research works in SAKIGAKE program in Japan (Invited)..... 122

*A. Vogel, X.-X. Liang, S. Freidank, and N. Linz*
Cavitation bubble dynamics in plasma-mediated nanosurgery of cells and tissues (Invited) ..... 123

*S. Wada, T. Ogawa, M. Yumoto, and N. Saito*
Development of tunable MID-IR lasers for agriculture and health science applications (Invited) ..... 124

*X. Wang, H. Zhang, J. Li, Z. Hu, Y. Paulus, and X. Yang*
Antivascular effects induced by photo-mediated ultrasound (Invited) ..... 125

*M. Yabashi*
Status and perspective of an X-ray free electron laser SACLA (Invited) ..... 126

*A.A. Lanin, M.S. Pochechuev, I.V. Fedotov, Y.G. Ermakova, A.B. Fedotov, D.A. Sidorov-Biryukov, O.I. Ivashkina, K.V. Anokhin, V.V. Belousov, and A.M. Zheltikov*
Fiber-optic neurointerfaces and multimodal optical neuroimaging in opto- and thermogenetic studies (Invited) ..... 127

## CLINICAL BIOPHOTONICS (CB)

*A. Akopov, G. Papayan*
Contribution of photodiagnosis and photodynamic therapy to the treatment of lung cancer: Saint-Petersburg experience ..... 130

*J. Ng, N. Henriquez, N. Kitchen, and S. Bown*
Bioluminescence-mediated photodynamic therapy: a novel treatment for grade 4 astrocytoma ..... 131

*R. Brinkmann*
Automatic feedback guided retinal laser therapies ..... 132

*E.S. Finagina, E.B. Kiseleva, A.A. Moiseev, M.V. Sirotkina, A.V. Maslennikova, D.V. Shabanov, S. Ksenofontov, G. Gelikonov, L. Matveev, V. Zaitsev, E.V. Zagaynova, N.D. Gladkova, and A. Vitkin*
Effects of Low-Level Laser Therapy (LLLT) in the prevention and treatment of radiation induced mucositis estimated by multimodal optical coherence tomography ..... 133

*S.V. Gamajunov, E.A. Tararova, and O.S. Streltsova*
Intravesical PDT for non-muscle-invasive bladder cancer ..... 134

*E.V. Gubarkova, S.V. Gamayunov, E.V. Zagaynova, E.S. Finagina, M.A. Sirotkina, L.B. Timofeeva, A.A. Moiseev, S.Yu. Ksenofontov, A. Vitkin, and N.D. Gladkova*
Multimodal optical coherence tomography monitoring of basal cell carcinoma treatment with photodynamic therapy ..... 135

*M. Hammer, L. Sauer, J. Schmidt, S. Peters, L. Kreilkamp, and M. Klemm*
Retinal autofluorescence lifetime for ophthalmic diagnostic – what can we learn from *in-vivo* and *in-vitro* FLIM? (Invited) ..... 136

*K.S. Korchagina, S.V. Gamayunov , S.S. Kuznetsov, V.V. Dudenkova, E.A. Sergeeva, and N.M. Shakhova*
Morphology in control of PDT with chlorine photosensitizers ..... 137

*M.A. Lazareva, A. Moiseev, and N.M. Shakhova*
OCT-based microangiography for evaluation of functional vessels ..... 138

*A. Maslennikova, E. Finagina, M. Sirotkina, M. Lazareva, A. Moiseev, S. Ksenofontov, G. Gelikonov, L. Matveev, E. Kiseleva, V. Zaitsev, N. Shakhova, E. Zagaynova, N. Gladkova, and A. Vitkin*
Multimodal optical coherence tomography for evaluation of the normal tissue state during anticancer treatment ..... 139

*A. Meller, M. Shakhova, D. Sapunov, P. Agrba, A. Shakhov, and M. Kirillin*
Differential diagnostics of various forms of chronic rhinitis with Optical Coherence Tomography ..... 140

*N. Mitrakova, M. Gremyakina, V. Nefedov, A. Rozhentsov, and A. Mitrakov*
Morpho-video endoscopic images in diagnostics of an early carcinoma of the stomach ..... 141

*A.A. Mitrakov, R.S. Alieva, V.A. Kryazhov, N.N. Mitrakova, and S.V. Gamayunov*
The palliative role of endoscopic PDT in inoperable cancer ..... 142

*T.M. Motovilova, N.M. Shakhova, K.I. Chikalova, O.A. Kondratieva, S.S. Kuznetsov, O.V. Kachalina, P.A. Shilyagin, and M.Yu. Kirillin*
Novel approach to endometrium evaluation in patients with chronic endometritis using Optical Coherence Tomography ..... 143

*T. Novikova, M. Kupinski, J. Rehbinder, S. Deby, A. Pierangelo, F. Moreau, B. Teig, and A. Nazac*
Tissue imaging with Mueller polarimetry for cancer detection ..... 144

*M.V. Pavlov, P.V. Subochev, T.I. Kalganova, G.Yu. Golubyatnikov, V.I. Plekhanov, O.E. Ilyinskaya, A.G. Orlova, N.M. Shakhova and A.V. Maslennikova*
Noninvasive evaluation of metabolism and blood supply in breast cancer polychemotherapy ..... 145

*D. Sapunov, A. Meller, M. Shakhova, A. Shakhov, and M. Kirillin*
The first clinical experience of photodynamic therapy of pharynx inflammatory diseases ..... 146

*M. Shakhova, A. Meller, D. Sapunov, A. Novozhilov, A. Shakhov, and M. Kirillin*
Optical monitoring for personalization of ENT diseases treatment ..... 147

*R. Sroka*
Developments of 2 µm-laser applications for clinical use ..... 148

*H. Stepp, N. Markwardt, A. Rühm, M. Goetz, P. Zelenkov, V. Loschenov, P. Grachev, and R. Sroka*
Optical spectroscopy for the detection of brain tumor and blood vessels to enhance accuracy and safety of stereotactic brain tumor biopsy ..... 149

*O.S. Streltsova, D.P. Pochtin, I.D. Eranov, R.I. Kositsyin, V.I. Bredichin, O.L. Antipov, and V.A. Kamensky*
Prevention of inflammatory complications of laser lithotripsy ..... 150

*O.S. Streltsova, V.V. Dudenkova, M.V. Kochueva, E.A. Tararova, D.K. Malikov, A.S. Vorobieva, E.B. Kiseleva, K.E. Yunusova, V.N. Krupin, and A.V. Maslennikova*
Laser scanning microscopy study of the bladder extracellular matrix after radiation therapy ..... 151

*V.Y. Toronov, S. Lin, R. Botero, H. Andrade-Caicedo, and T.N. Nguyen*
Hyperspectral NIRS: Development and applications ..... 152

*E. Gerelli, V. Huntosova, D. Horvath, and G. Wagnieres*
*In vivo* measurement of the tissue oxygenation by time-resolved luminescence spectroscopy: Strategies to minimize artefacts associated with the photosensitization and photoproducts ..... 153

*I.A. Medyanik, M.G. Volovik, A.V. Dydykin, K.S. Yashin, S.N. Bugrov, and N.N. Karyakin*
Photodynamic therapy of malignant brain tumors ..... 154

*K.S. Yashin, E.B. Kiseleva, E.V. Gubarkova, A.A. Moiseev, S.S. Kuznetsov, M.M. Karabut, I.A. Medyanik, L.Ya. Kravets, and N.D. Gladkova*
Ex vivo study of human gliomas with cross-polarization optical coherence tomography ..... 155

## Biophotonics in Stem Cell Research (SC)

*M. Kaucka, R. Soldatov, T. Chontorotzea, J. Petersen, M.E. Kastriti, N. Akkuratova, V. Dyachuk, K. Fried, P. Kharchenko, and I. Adameyko*
Single cell transcriptomics reveals fate selection points and early heterogeneity of the neural crest (Invited) ..... 158

*N. Bobrov, D. Kuznetsova, V. Dudenkova, F. Kulagin, N. Kiselev, M. Lukina, V. Zagaynov, and E. Zagaynova*
Label free microstructural analysis of the healthy and diseased liver (Poster) ..... 159

*A.S. Chagin*
3D visualisation of synovial joints revealed novel progenitor cells which form entire adult articular cartilage in mice (Invited) ..... 160

*A.A. Gorkun, I.M. Zurina, A.I. Shpichka, A.V. Koroleva, N.V. Kosheleva, D.V. Butnaru, P.S. Timashev, I.N. Saburina, and V.S. Repin*
Obtainment of capillary-like network from MSC spheroids from umbilical cord MMSC in fibrin gel (Poster) ..... 161

*A.A. Gulin, A.V. Aybush, A.A. Astafiev, A.E. Solodina, A.G. Pogorelov, V.N. Pogorelova, A.I. Panait, and V.A. Nadtochenko*
A new approach for single cell imaging: Mammalian oocyte case ..... 162

*A.A. Gulin, I.V. Shelaev, F.E. Gostev, N.N. Deniso, A.V. Aybush, and V.A. Nadtochenko*
Electron transfer between $Cd_{1-x}SeMn_x$ quantum dots and $MV^{2+}$: Coherent effects revealed by femtosecond laser spectroscopy (Poster) ..... 163

*E.Y. Ivanova, A.V. Selenina, S.A. Sinenko, E.I. Bakhmet, A.N. Tomilin, and A.S. Tsimokha*
The role of immunoproteasomes in mammal cell differentiation ..... 164

*E. Ivashkin, M. Khabarova, A. Obukhova, M. Nikitin, I. Adameyko, and E. Voronezhskaya*
Early monoamines: discovering a new ancient pathways in development (Invited) ..... 165

*A.V. Karmenyan, A.S. Krivokharchenko, E.V. Perevedentseva, H.-H. Chang, Ashek-i-Ahmed, L.-C. Liu, and C.-L. Cheng*
Noninvasive monitoring of living early mammalian embryo development (Invited) ..... 166

*A. Koroleva, A. Deiwick, P. Timashev, D. Kuznetsova, and B. Chichkov*
Two-photon polymerization for fabrication of tissue engineering scaffolds (Invited) ..... 167

*I.M. Zurina, A.A. Gorkun, A.F. Fidarov, N.V. Kosheleva, and I.N. Saburina*
Development of bioengineered construction based on osteoplastic material and VEGF-induced 3D culture of mesenchymal stromal cells (MSC spheroids) (Poster) ..... 168

*J. Krivanek, T. Chontorotzea, K. Fried, and I. Adameyko*
Understanding of developmental and regeneration pathways of tooth using single cell transcriptomics (Invited) ..... 169

*D.S. Kuznetsova, N.N. Prodanets, P.S. Timashev, V.N. Bagratashvili, and E.V. Zagaynova*
The involvement of allogeneic mesenchymal stem cells in bone formation ..... 170

*I.V. Larina*
Reproduction and development *in vivo* with OCT (Invited) ..... 171

*A.V. Meleshina, V.V. Dudenkova, A.S. Bystrova, M.V. Shirmanova, and E.V. Zagaynova*
Metabolic plasticity of mesenchymal stem cells during differentiations by two-photon FLIM ..... 172

*S. Ogasawara*
Precise control of protein expression by light (Invited) ..... 173

*Yu. Rochev*
Temperature-responsive biomaterials design for tissue engineering and drug delivery (Invited) ..... 174

*O.S. Rogovaya, V.V. Dudenkova, A.S. Bystrova, M.M. Lukina, E.A. Vorotelyak, E.V. Zagaynova, and A.V. Meleshina*
The study of the dermal cells cultured in collagen gel by optical and multiphoton tomography ..... 175

*V.Yu. Sysoeva, N.I. Kalinina, P.A. Tyurin-Kuzmin, L.V. Ageeva, and V.A. Tkachuk*
Hormonal regulation of functional heterogeneity of mesenchymal stem cells ..... 176

*P.S. Timashev, S.L. Kotova, T.M. Zharikova, D.V. Butnaru, and A.B. Solovieva*
Collagen morphology in the extracellular matrix as a marker of tissue damage (Invited) ..... 177

*A. Tomilin*
Basic and applied sides of pluripotent stem cells ..... 178

*A.S. Tsimokha, A.V. Selenina, S.A. Sinenko, A.A. Kuzmin, and A.N. Tomilin*
Pluripotent stem cells ..... 179

Author index ..... 180

*Sponsors* ..... 183

*P. Hoess*
Extreme range extension of visual sight hampered by turbid media ..... 184

VI International Symposium

# TOPICAL PROBLEMS OF BIOPHOTONICS




## *Plenary Talks*

# THE MULTI-DIMENSIONAL WORLD OF TCSPC FLIM

**W. Becker**

Becker & Hickl GmbH, Berlin, Germany
E-mail: becker@becker-hickl.com

**Abstract.** TCSPC FLIM delivers a photon distribution over the image coordinates and the time after the excitation pulses. The technique not only reaches an extraordinary time resolution and photon efficiency, it also records the decay data in the individual pixels into a large number of time channels. Such data can be characterised in a multi-parameter data space, yielding complex information on the systems investigated. A new level of multi-dimensionality is reached by extending the photon distribution of TCSPC FLIM with additional parameters of the photons. The technique then opens the way to entirely new experiments, such as recording of fast physiological processes or dynamic protein interaction experiments.

TCSPC FLIM is based on scanning the sample by a high-repetition rate pulsed laser beam and the detection of single photons of the fluorescence signal returning from the sample. Each photon is characterised by its time in the laser pulse period and the coordinates of the laser spot in the scanning area in the moment its detection. The recording process builds up a photon distribution over these parameters [1]. TCSPC FLIM in combination with laser scanning delivers excellent time resolution and near-ideal photon efficiency, and suppresses out-of focus fluorescence and crosstalk by lateral and longitudinal scattering. The result can be interpreted as an array of pixels, each containing a full fluorescence decay curve in a large number of time channels.

Often the decay functions in the pixels are simply characterised by a single 'decay time'. However, this misses the most important point of TCSPC FLIM. TCSPC data are inherently multi-dimensional in a multi-dimensional parameter space. The decay functions in the individual pixels usually contain several exponential components, and are characterised by several independent decay times and amplitude factors. Biological information is often directly related to these parameters. Examples are FRET experiments, where the decay functions represent an interacting and a non-interacting donor fraction, and metabolic imaging, where the components represent bound and unbound NADH.

An entirely new level of complexity is achieved by extending the photon distribution of TCSPC FLIM itself by additional parameters. Examples of such parameters are the wavelength of the photons, the depth of the focus in the sample, the time after a stimulation of the sample, or the time within the period of an additional modulation of the laser. The corresponding photon distributions can be four- or five-dimensional, the data representing multi-spectral FLIM, FLIM Z stacks and lateral FLIM mosaics, time-series FLIM, and simultaneous FLIM-PLIM, or even combinations of these. Possible applications are the investigation of fast physiological effects in live system, such as $Ca^{++}$ transients or chlorophyll transients [2], dynamics of protein interaction, and metabolic imaging in combination with $pO_2$ measurement [3]. There may be more which have not even been considered yet. This paper is an attempt to spread knowledge about advanced TCSPC techniques to potential users and start a discussion about future applications.

## References

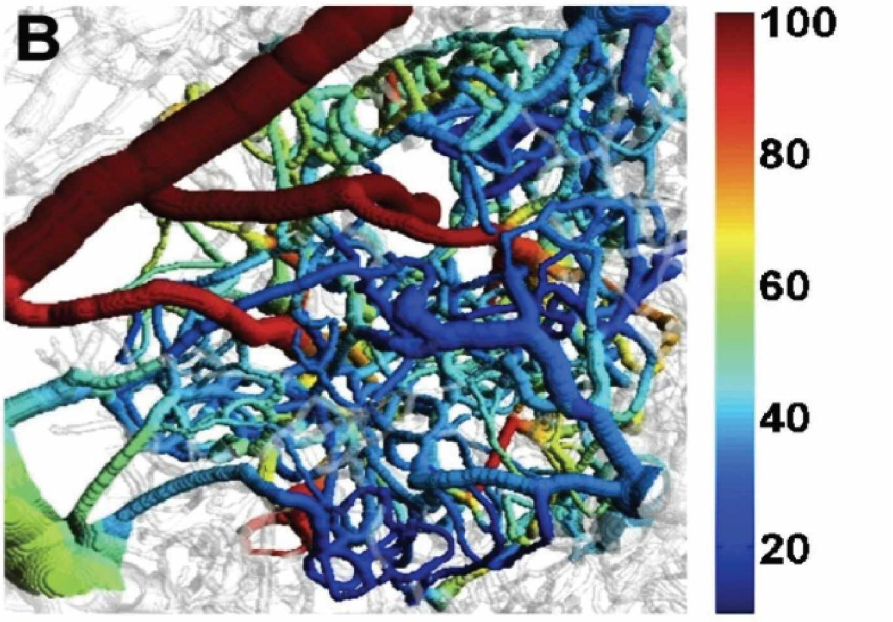
1. W. Becker, ed., "Advanced time-correlated single photon counting applications", *Springer*, 2015.
2. W. Becker, V. Shcheslavkiy, S. Frere, and I. Slutsky, "Spatially Resolved Recording of Transient Fluorescence-Lifetime Effects by Line-Scanning TCSPC", *Microsc. Res. Techn.*, 2014, **77**, 216–224.
3. S. Kalinina, V. Shcheslavskiy, W. Becker, J. Breymayer, P. Schäfer, and A. Rück, "Correlative NAD(P)H-FLIM and oxygen sensing-PLIM for metabolic mapping", *J. Biophotonics*, 2016, **9**(8), 800–811.

# OPTICAL IMAGING OF OXYGEN DELIVERY AND CONSUMPTION: NOVEL PHYSIOLOGICAL INSIGHTS AND GUIDING INTERPRETATION OF BOLD FMRI

**D. Boas**

Neurophotonics Center, Boston University, Martinos Center
Massachusetts General Hospital, Harvard Medical School, USA

BOLD fMRI is used extensively to map out brain activity patterns elicited by varied stimuli. BOLD fMRI measures the vascular response to neuronal activity and is thus not a direct measure of the underlying neuronal response to stimulus. A detailed understanding of neurovascular coupling is required to understand this relationship. Further, BOLD fMRI is an uncalibrated measure of the changes in deoxygenated hemoglobin during brain activation. BOLD is usually calibrated with a hypercapnic procedure and a model of the BOLD signal that itself is not well validated. I will review our efforts to understand the vascular response to neuronal activity at a macroscopic level and our procedures to cross-validate the BOLD calibration procedure. To gain a more microscopic validation of the BOLD signal model, we have performed numerous microscopic studies of the microvascular blood flow and oxygenation response to neuronal activity. I will review these microscopic methods and our validated bottom up model of the BOLD signal and the predictions it made that we have subsequently verified. Along the way, these microscopic studies have provided insight into novel mechanisms of increasing the efficiency of oxygen delivery to the brain in times of increased oxygen demand.



# LASER PRINTING OF STEM AND IPS CELLS

**B.N. Chichkov**

Laser Zentrum Hannover e.V., Hollerithallee 8, 30419 Hannover, Germany

For arranging living cells in 3D patterns, we use laser-assisted bioprinting based on the laser-induced forward transfer. Printing of different cell types, including primary cells, stem cells, and iPS cells embedded in hydrogels as extra-cellular matrix, have been investigated. Laser printing technique is capable of advancing 3D cell culture towards CAD defined and precisely arranged 3D cell models and "organ-on-chip" systems. Printed tissue, for example skin, can be used for analyzing the effect of agents like pharmaceuticals or cosmetics *ex vivo* and, by applying human primary cells it might be applied instead of animal tests. We have proven skin tissue formation by visualizing intercellular junctions and verifying their functionality. We also have observed basal lamina formation. Implanted in mice, the printed skin constructs show an ingrowth of blood vessels and differentiation of the epidermal keratinocytes. Compared to nozzle-based printing techniques such as extrusion or ink-jet printing, laser printing of cells provides the higher resolution and cell densities required for tissue formation.

# OPTOGENETIC STIMULATION USING NONLINEAR OPTICS – PACING HEARTS WITH LIGHT AND OTHER APPLICATIONS

**A. Heisterkamp[1,2,3*], S. Johannsmeier[2,3], P. Heeger[1,3], L.M. Torres[1], D. Heinemann[2], and T. Ripken[2]**

[1] Institute of Quantum Optics, Leibniz Universitaet Hannover, Germany, Heisterkamp@iqo.uni-hannover.de
[2] Laser Zentrum Hannover, Hannover, Germany
[3] Cluster of Excellence REBIRTH, Hannover, Germany

**Abstract.** Optogenetics is a powerful technique using light sensitive molecules within living cells to control cell behavior by light. Dominating field in optogenetics is currently neurobiology in which molecules like Channelrhodopsin-2 (ChR2) are expressed in neuronal cells to induce action potentials upon blue light irradiation. Here we demonstrate the use of laser light to pace cardiomyocytes (heartm muscle cells) expressing ChR2. In order to increase the penetration depth of light, nonlinear excitation like two-photon absorption and other nonlinear techniques using nanoparticles were studied. As an outlook optogenetics allows even more general optical control of cells like gene expression, growth or other cellular functions.

**Introduction.** Optogenetics is a technique based on the genetic modification of cells to allow a light switching or control of cellular processes using light. This switching is achieved by a conformational change of photoactuators like Channelrhodopsin (ChR2) [1], Phytochrome B [2], LOV [3] or other molecules. Widely used is the molecule ChR2 to achieve contraction of muscles [4] or the stimulation of neurons, even in living mice [5]. Further neuronal applications are for the example the stimulation of the auditory pathway at the cochlea [6]. To achieve an optimal control or effect within the target tissue, high penetration depth of the light would be desirable. Therefore, the use of near-infrared wavelength in combination with nonlinear effects for frequency conversion might be a useful to reach higher penetration depth.

**Methods and results.** In our study, we used an optical setup to excite heart muscle cells derived from induced pluripotent stem cells transfected with ChR2 to allow blue light stimulation and light controlled contraction of these tissue constructs. The contraction was studied using a camera with an microscopic imaging setup, the stimulation light was guided over a spatial light modulator to allow spatial and temporal holographic shaping of the excitation pattern.

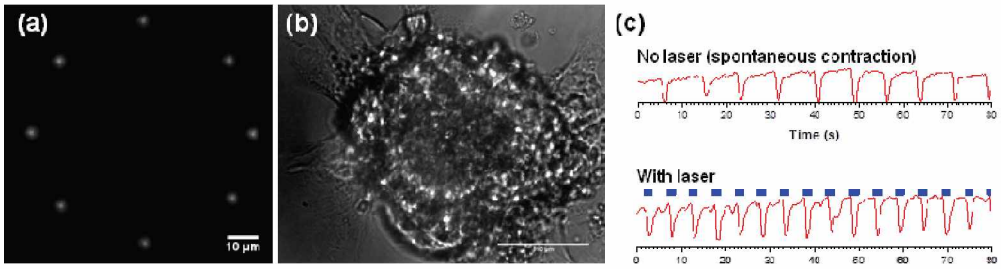



**Fig. 1.** a) 8-spot stimulation pattern for optical excitation of the heart muscle construct. b) Heart muscle construct from iPS derived stem cells. c) Spontaneous and light induced beating of the construct (blue spots – timing of the light application

As shown in Fig. 1 we were able to successfully stimulate heart muscle constructs and observe contraction correlated to both temporal and spatial power distribution of the light incident on the cell clusters using linear excitation at 488 nm as well as using light at 960 nm for two photon excitation. This work can be extended to other fields of optogenetics like spatially or temporally controlled gene expression using constructs like LOV or Phytochrome B.

**Acknowledgements.** This research was funded by the German Research Foundation DFG within the cluster REBIRTH and the Federal Ministry of Education and Research BMBF (FKZ 13N14085) in the BioPACE consortium.

## References

1. Deisseroth, *et al.*, *J. Neurosci.*, 2006, **26**, 10380–10386.
2. Levskaya, *et al.*, *Nature*, 2009, **461**, 997–1001.
3. Y.I. Wu, *et al.*, *Nature*, 2009, **461**, 104–8.
4. Towne, *et al.*, *PLoS One*, 2013, **8**.
5. Krook-Magnuson, *et al.*, *Nat. Commun.*, 2013, **4**, 1376.
6. Hernandez, *et al.*, *J. Clin. Invest.*, 2014, **124**, 1114–1129.

# LASER DRIVEN INJECTOR FOR A NEW GENERATION HEAVY ION CANCER THERAPY MACHINE IN JAPAN

**K. Kondo[1], M. Kando[1], H. Sakaki[1], M. Nishiuchi[1], H. Kiriyama[1], K. Mizushima[2], E. Noda[2], Y. Iwata[2], and T. Shirai[2]**

[1] Kansai Photon Science Institute, Quantum Beam Science Directorate,
National Institutes for Quantum and Radiological Science and Technology, Kyoto, Japan
kondo.kiminori@qst.go.jp
[2] National Institute of Radiological Sciences, National Institutes
for Quantum and Radiological Science and Technology, Chiba, Japan

**Abstract.** In National Institutes for Quantum and Radiological Science and Technology (QST), the project for developing a new generation heavy ion cancer therapy machine, which is called "Quantum Scalpel", has been started. Quantum Scalpel is a very compact and cheap heavy ion cancer therapy machine based on not only the superconducting magnet technology, but also the laser driven ion acceleration technology. The recent Peta-Watt-class power laser technology will make it possible to produce enough number of carbon ions for the compact ion injector to the main synchrotron accelerator in Quantum Scalpel.

Ten years later now, although for metastasis, the molecular target treatment and/or the target isotope therapy will replace the chemical treatment, the surgical operation will still be a very important scheme to treat a primary tumor. Dr. Hirano, who is an immunologist and the first president of National Institutes for Quantum and Radiological Science and Technology (QST), explains the future status of cancer therapy. Not only for giving high QoL (Quality of Life) treatment to patients, but for preserving immune function, the particle cancer therapy, especially the heavy ion cancer therapy has a much higher potential than the surgical operation, although it is hard to put many places because of a very high cost and a gigantic size. If a compact and cheap heavy ion cancer therapy machine is developed, this situation will be drastically improved. Moreover, a high QoL cancer treatment will be received at anytime, at anywhere, and by anyone. Then the project for developing a new generation heavy ion cancer therapy machine, which is called "Quantum Scalpel", has been started in Japan. Quantum Scalpel is the 5th generation heavy ion cancer therapy machine, which could be very compact and cheap. The schematic of Quantum Scalpel is shown in Fig. 1. Actually this new machine is based on not only the superconducting magnet technology for the main synchrotron accelerator ring and the gantry, but also the laser driven ion acceleration technology for the injector. By using a laser driven ion acceleration phenomena, the injector to the main synchrotron accelerator will be placed in the synchrotron ring, while it should be placed outside with a conventional accelerator technology. From our estimation, the required number of carbon ions as the injector is ~ $10^9$ at 4 MeV in ±1% b.w. within 2 seconds. This number is not so serious to develop it during ten years. In this talk, the possibility of the laser driven injector will be discussed with showing not only our recent study in QST, but also some progresses in high power laser science.

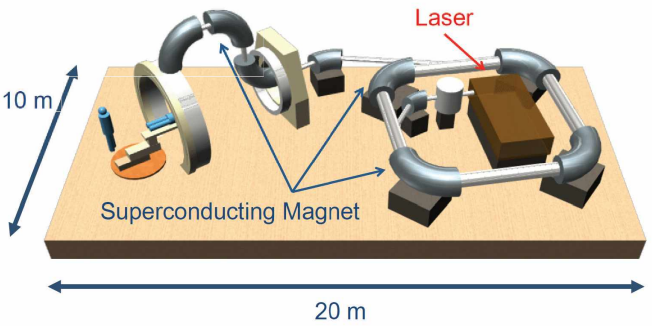



**Fig. 1.** Schematic of a new generation heavy ion cancer therapy machine called Quantum Scalpel

**Acknowledgements**

In this study, K. K is supported by JSPS KAKENHI Grant Number JP15K05236.

# THE FRONTIERS IN ALA-PDT

**Z. Malik**

The Mina and Everard Goodman Faculty of Life Sciences
Bar-Ilan University, Ramat-Gan 5290002, Israel
Zvi.Malik@biu.ac.il

Topical ALA-PDT has gained remarkable success after decades of research, but its medical impact is limited and not the treatment of choice in oncology. It is well documented that topical ALA-PDT enables the treatment of multiple lesions simultaneously with excellent cosmetic results; no acquired multidrug resistance was reported, and the treatment can be repeated with the same efficacy each time in the event of tumor recurrence. Most important, fluorescence-guided resection during surgery is a practical and simple tool that provides straightforward visualization of intraoperative procedures with mm accuracy. The future objectives are to amplify critical, evidence-based results of PDT safety and efficacy, and to validate its unique advantages over other technologies. Strong statistical PDT documentation and the positive predictive values of PpIX-guided surgery can persuade the medical community to implement ALA-based therapeutics into routine oncological treatment and surgery. Research indicates that no multidrug resistance develops as a consequence of PDT; this is of major significance in oncology. A feasible goal should be improving ALA-administration protocols based on recent knowledge that the pre-activation of the PpIx synthesis pathway to promote efficient and selective destruction of tumor tissues. Moreover, the recent introduction of combinatory concepts of multifunctional ALA prodrugs that maximize sensitizer biosynthesis and affect multiple subcellular targets might open new modalities in PDT. In conclusion, well-documented clinical results, new ALA-delivery protocols, and novel multifunctional ALA prodrugs, may render ALA-PDT into a frontline cancer therapy.

# LIGHT AND SOUND: INTEGRATING PHOTONICS WITH ULTRASONICS FOR BIOMEDICAL APPLICATIONS

**M. O'Donnell**

Department of Bioengineering, University of Washington, Seattle, USA
odonnel@uw.edu

**Abstract.** In this talk, the history of integrated photonic-ultrasonic systems will be presented, focusing on examples where light generates sound, light detects sound, and sound "tickles" light. Specific applications of integrated photonic-ultrasonic techniques will be presented, including photoacoustics for molecular imaging, non-contact laser ultrasound systems, and optical coherence elastography (OCE) in which air-coupled ultrasound stimulates propagating shear waves in the eye and skin tracked with real-time, 3-D optical coherence tomography. The talk will conclude by discussing current barriers to clinical translation of these systems and possible ways to overcome the obstacles.

Coherent light and sound have become essential tools in modern medicine. Lasers are routinely used for both therapeutic and diagnostic applications, and real-time ultrasound scanning has become the dominant biomedical imaging modality in the world. Starting over thirty years ago, scientists and engineers have combined these modalities for applications ranging from non-contact sensing to novel molecular imaging techniques. Most applications of integrated photonic-ultrasonic systems use light to generate and/or detect sound, and use ultrasound to modulate or "tickle" light in some way.

A classic example of a system using light to create sound is photoacoustic imaging, in which a temporally modulated light source, usually a pulsed laser, propagates into a biological medium of interest and local light absorption creates acoustic sources within the medium that can be imaged using real-time ultrasound technologies [1]. One of the primary motivations for PA imaging is to bring the molecular sensitivity of optical interactions into ultrasonic measurements within the body. A wide range of nanoscale contrast agents, including both tuned optical absorbers and phase-change nanoemulsions, have been developed to provide both high sensitivity and specificity molecular images using real-time ultrasonic systems integrated with wavelength tunable pulsed lasers. Examples of such agents and imaging systems will be presented [2–3].

Light can be used to detect ultrasound at a surface using interferometric techniques. For nearly thirty years, laser ultrasonic systems have been developed for non-destructive testing using a wide range of different types of interferometers. The recent availability of high repetition-rate pulsed lasers and high intensity broadband light sources such as superluminescent diodes, as well as a wide range of integrated optics devices, has resulted in markedly improved sensitivity and stability of these systems [4]. Examples of how modern laser ultrasound systems can be used for non-contact ultrasound measurements in biomedicine will be presented.

Finally, ultrasound can be used to modulate light in a number of different systems. Recently, air-coupled ultrasound has been used to launch broadband shear waves in soft tissue such as the cornea and skin. These waves can be tracked using real-time, phase-sensitive optical coherence tomography to probe the elastic properties of the medium at high spatial resolution and sensitivity [5]. Recent results on porcine cornea will be presented to demonstrate the capabilities of the system.

### Acknowledgements

This work was supported in part by NIH grants RO1EB016034, R01CA170734, R01EB009682, R01HL093140, R01DC010201, and R01EY026532, and by the Life Sciences Discovery Fund grant # 3292512.

### References

1. S.Y. Emelianov, Pai-Chi Li, and M. O'Donnell, *Physics Today*, 2009, **62**(5), 34–39.
2. C-W Wei, T-M Nguyen, J. Xia, B. Arnal, E. Y. Wong, I. Pelivanov, and M. O'Donnell, *IEEE Transactions on Ultrasonics, Ferroelectrics and Frequency Control*, 2015, **62**(2), 319–328.
3. B. Arnal, C-W Wei, C. Perez, T-M Nguyen, M. Lombardo, I. Pelivanov, L.D. Pozzo, and M. O'Donnell, *Photoacoustics*, 2015, **3**(1), 11–19.
4. I. Pelivanov, T. Buma, J. Xia, C.-W. Wei, and M. O'Donnell, *Photoacoustics*, 2014, **2**(2), 63–74.
5. Ł. Ambroziński, S. Song, S.J. Yoon, I. Pelivanov, D. Li, L. Gao, T.T. Shen, R.K. Wang, and M. O'Donnell, *Sci. Rep.*, 2016, **6**, 38967.

# LARGE SCALE MULTIDIMENSIONAL AND MULTILEVEL IMAGING OF TISSUE DISEASE: TOWARDS THE 3D DIGITAL HISTOLOGY

**F.S. Pavone**

European Laboratory for Non Linear Spectroscopy (LENS)
University of Florence, Sesto Fiorentino (FI), Italy
francesco.pavone@unifi.it

**Abstract.** Modern optics and spectroscopy are offering promising non-invasive solutions to potentially improve diagnostic capability on tissues, as demonstrated by the extensive use of non-linear laser scanning microscopy for tissue imaging in the past decade.

The recent development and integration of multiple non-linear microscopy techniques in a single instrument has provided new opportunities for integrating morphological and functional information and for correlating the observed molecular and cellular changes with disease behaviour. In particular, multimodal non-linear/linear imaging is able to perform a morpho-chemical quantitative analysis in tumour cells and tissue specimens, providing a high-resolution label-free alternative to both histological and immune-histochemical examination of tissues. Although up to now limited to optical research labs, multimodal non-linear imaging is becoming increasingly popular among medical doctors and has the potential to find a stable place in a clinical setting in the near future.

In this talk, a brief overview on the non linear and linear laser brain imaging techniques will be displayed both for label free and specific labeling detection.

Morpho-functional characterization of tissue will be displayed as an interesting tool for early diagnosis of pathologies: different kind of approaches will be shown for in vivo imaging assisted surgery operation or as tools to support anatomo-pathologists decision.

For example, several techniques, useful to create a new 3D histological analysis also on cleared tissue will be shown, and a fiber sensors based on multidimensional spectral will be described with particular applications to tumor detection.

# OPTICAL IMAGING OF CELL-LEVEL METABOLISM

**M.C. Skala[1,2], J.T. Sharick[1,3], A.J. Walsh[3], A.T. Shah[3], T.M. Heaster[1,2], P. Favreau[1], A. Gillette[1,2], T.M. Cannon[3], C. Pasche[2], D. Deming[2], R.M. Cook[3], and C.L. Arteaga[3]**

[1] Morgridge Institute for Research, Madison, WI, USA, mcskala@wisc.edu
[2] University of Wisconsin, Madison, WI, USA
[3] Vanderbilt University, Nashville, TN, USA

**Abstract.** Many cancer patients do not respond to first line therapies, and therefore suffer toxicities from ineffective treatments. We have developed single-cell optical metabolic imaging technologies, and applied them to novel 3D tumor macro-suspensions ("organoids") derived from the patient's tumor. This platform allows for high-sensitivity tests of multiple candidate therapies for each patient, and could provide a personalized predictive screen of optimal therapies for each patient. We have validated this approach in animal models and begun pilot tests in patients with breast, pancreas, and colon cancers. Ongoing work will validate this approach for accuracy in the clinical setting.

Abnormal cellular metabolism is a hallmark of many diseases, yet there is an absence of quantitative methods to dynamically image metabolism with cellular-level resolution. Optical metabolic imaging (OMI) quantifies the fluorescence intensities and lifetimes of the metabolic co-enzymes NAD(P)H and FAD using two-photon microscopy [1–8]. OMI is a label-free, high-resolution, quantitative tool for monitoring cellular metabolism within intact samples. *In vivo* OMI is sensitive to heterogeneous changes in cellular metabolism induced by clinically relevant anti-cancer therapies in mouse models of cancer. The ability to monitor these treatment-resistant sub-populations of cells *in vivo* is important for identifying and eliminating the particularly lethal cells that cause tumor recurrence and metastases.

We have further developed a "tumor-in-a-dish" organoid platform to rapidly test multi-drug response using OMI. This platform has been validated in mouse models of breast and pancreas cancer, and feasibility has been tested in human tumors with chemotherapies, targeted therapies, and experimental drugs. Importantly, the cellular-level assessment of OMI allows for sub-populations of cells with varying response to drug treatment to be tracked over time, to achieve therapeutic effect in all cell populations. This attractive suite of metabolic imaging tools has significant implications for rapid cellular-level assessment of metabolic response to drug treatment (1) *in vivo*, (2) in high-throughput drug efficacy studies, and (3) as a clinical tool to plan individualized treatment regimens. Therefore, these technologies could greatly accelerate cures for cancer patients.

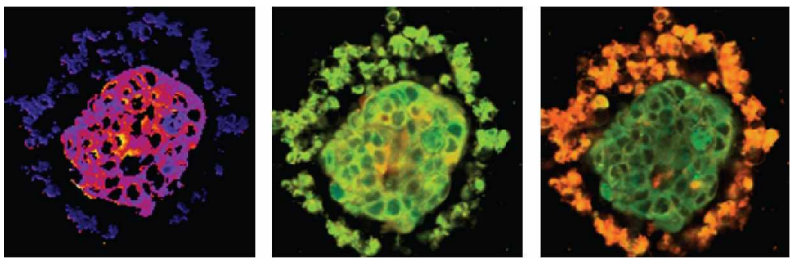


**Fig. 1.** Optical metabolic imaging of breast cancer organoid. *Left* – redox image, *middle* – NAD(P)H fluorescence lifetime image, *right* – FAD fluorescence lifetime image

## References

1. A.T. Shah, T.M. Cannon, J.N. Higginbotham, R.J. Coffey, and M.C. Skala, *J. Biophotonics*, 2016.
2. A.T. Shah, K.E. Diggins, A.J. Walsh, J.M. Irish, and M.C. Skala, *Neoplasia,* 2015, **17**(12), 862–70.
3. A.J. Walsh, J.A. Castellanos, N.S. Nagathihalli, N.B. Merchant, and M.C. Skala, *Pancreas*, 2015.
4. A.J. Walsh, R.S. Cook, H.C. Manning, D.J. Hicks, A. Lafontant, C.L. Arteaga, and M.C. Skala, *Cancer Res*, 2013, **73**(20), 6164–74.
5. A.J. Walsh, R.S. Cook, M.E. Sanders, C.L. Arteaga, and M.C. Skala, *Sci Rep*, 2016, **6**, 18889.
6. A.J. Walsh, R.S. Cook, M.E. Sanders, L. Aurisicchio, G. Ciliberto, C.L. Arteaga, and M.C. Skala, *Cancer Res*, 2014, **74**(18), 5184–94.
7. A.J. Walsh and M.C. Skala, *Biomed Opt Express*, 2015, **6**(2), 559–573.
8. A.T. Shah, T.M. Heaster, and M.C. Skala, *PLoS One*, 2017, **12**(1), e0170415.

VI International Symposium

# TOPICAL PROBLEMS OF BIOPHOTONICS




## *Optical Bioimaging*

# Chairs

**Martin Frenz**
Institute of Applied Physics, University of Bern, Switzerland

**Karsten König**
Saarland University, Germany

**Ilya Turchin**
Institute of Applied Physics RAS, Russia

**Alex Vitkin**
University of Toronto, Canada

*Invited*

# OPTICAL EXTINCTION MEASUREMENTS ON STRONGLY SCATTERING SAMPLES BY WAY OF IMAGING

**P. Stähli, J. Ricka, M. Frenz,** and **H.G. Akarçay***

Institute of Applied Physics, University of Bern, Switzerland
*hidayet.akarcay@iap.unibe.ch

Optical extinction measurements can be challenging to perform on strongly scattering media: this is attributable to the difficulty in distinguishing the scattered light from the illumination beam, which is attenuated upon transmission through said media. We present here a novel approach, where a compact and inexpensive imaging system is used to unambiguously filter out forward-scattered light, without having to recourse to sophisticated calculations. The applicability thereof has been ascertained with experiments on non-interacting, colloidal suspensions, whose optical extinction coefficient can be calculated by means of Mie theory. The scattering cross-section of the suspensions can be determined with $< 0.3\%$ error for line number densities of particles up to 0.25 spheres/micron.

*Invited*

# ULTRASOUND OPTICAL TOMOGRAPHY

**J. Gunther**[1] and **S. Andersson-Engels**[1,2]

[1] IPIC, Tyndall National Institute, Cork, Ireland, stefan.andersson-engels@tyndall.ie
[2] Department of Physics, University College Cork, Cork, Ireland

**Abstract.** Ultrasound optical tomography has a potential to provide molecular contrast information at many centimeters in tissue with tenths of micrometers resolution. The presentation will include a review of the UOT field. It will also include simulation results. The signal contrast-to-noise ratio (CNR) was modeled using Monte Carlo simulations both in reflection and transmission geometries. The target volume contrast in absorption was 50%. In the reflection geometry (using a source-detector distance of 4 cm) the CNR was >1 for depths down to 4.75 cm, while all depths showed a CNR >1 for a 10 cm thick tissue slab.

Optical imaging of biological tissue has good molecular contrast but poor penetration depth and beyond the very superficial tissue also poor spatial resolution. This is the case even using near infrared light under optimal conditions. Ultrasound optical tomography (UOT) has the feature to combine the spatial resolution of ultrasound imaging with the contrast of optical imaging. How deeply it can measure is not fully understood, and will be investigated in this work. In UOT one sends light through an ultrasound focus in a medium, where photons become frequency shifted or "tagged" through a process described by the acousto-optic effect.

In this study, a single Monte Carlo (MC) simulation was run using a CUDAMCML code assuming a semi-infinite medium. Beam convolution was performed in a custom made program in MatLab using the procedures developed by Wang et. al. for the conventionally used MCML code The parameters used in the MC simulation were $10^9$ photon packets launched into a medium. The optical properties of the medium was $\mu_a = 0.2$ cm$^{-1}$, $\mu_s = 50$ cm$^{-1}$, $g = 0.9$, and $n = 1.37$; for the absorption, scattering, anisotropy and refractive index, respectively. The MC simulation yielded a map of the light fluence rate in the semi-infinite medium modeled. This map was used for all convolutions and calculations needed to calculate the final CNR. For these calculations an energy of 0.5 J was considered during a 250 ms light pulse, meeting the laser safety limits. The CNR was found to be in excess of 1 for any depth smaller than 4.75 cm using the reflectance geometry. The performance of the technique was also in the transmission geometry for medium lengths of 4 cm, 6 cm, 8 cm, and 10 cm. For each of these lengths, the CNR decreases close to the front and rear surfaces of the medium, while it remains more or less constant at all depths further from the surface. As the length of the medium increases the CNR decreased. Furthermore, the 8 cm slab had a CNR >10 at all imaging depth for objects with $\mu_a = 0.3$ cm$^{-1}$. Also, a CNR of above 1 was found for all depths of the 10 cm slab medium.

In summary, the results suggest UOT will be able to study tissue deeply located inhomogeneities in tissue. They indicate it is possible to image an inclusion down to about 5 cm in a reflection geometry and within a 10 cm slab in the transmission geometry.

**Acknowledgements**

This research was supported by Science Foundation Ireland. We kindly acknowledge the interesting discussions with Stefan Kröll, Andreas Walther, Lars Rippe and Lihong Wang.

# FULL-FIELD OPTICAL COHERENCE MICROSCOPY FOR MICROSTRUCTURAL ASSESSMENT OF MAPLE LEAVES

**T. Anna[1], S. Chakraborty[1], A. Chiou[1,2], and W.C. Kuo[1,2]**

[1] Biophotonics and Molecular Imaging Research Center (BMIRC), National Yang-Ming University, Taipei-11221, Taiwan, ROC, e-mail: tulsianna@gmail.com
[2] Institute of Biophotonics, National Yang-Ming University, Taipei-11221, Taiwan, ROC

**Abstract.** We present a full-field optical coherence microscopy (FF-OCM) using a single broadband LED to investigate the microstructural changes in senescing maple leaves. Due to senescence/aging, the leaf color changes from green to red. The 2D-interferograms at different depths of the green and red leaves were obtained using CMOS camera and subsequently reconstructed *via* a fast and efficient 4-step derivative algorithm. The axial and lateral resolutions of the present system were 0.9 and 1.4 μm respectively. Our results showed the microstructure of epicuticular wax and upper epidermis layer in red leaves has a significant deterioration as compared to green leaves.

During autumn, the leaf color changes from green to red (senescence, or aging) in maple plants. Senescence is a developmental process accompanied by several metabolic and morphological/microstructural changes at the subcellular level [1]. These microstructural changes are related to the epidermal wax layer (that protects leaves from any entering pathogens and other environmental factors) and stoma of the leaf [2]. Optical coherence microscopy (OCM) has the potential to provide three-dimensional visualization of the microstructural features of the leaves at organ level by collecting the back-scattered light using coherence gating principle [3].

In this study, we used a full-field OCM (FF-OCM) to study the microstructural changes of the green and red *Acer palmatum 'Hogyoku'* leaves without any staining and pretreatment. In the present system, a single broadband LED (470–850 nm, $\lambda_0$ = 630 nm) as illumination source and 2D CMOS detector were used. To reconstruct the *en-face* sectional images, a 4-step derivative-based algorithm was used, which is relatively faster and easier in computation compared to existing approaches in FF-OCM [4].

Figure 1(a)–(b) shows the *en-face* images of the epicuticular wax layer at 8 and 20 μm depths of the green leaves respectively. Similar images for the red leaves are shown in Fig. 1(c)–(d). These results show the intact and well-formed boundaries of the epicuticular wax layer of the green leaf as compared to the red leaf as indicated by arrows in Fig. 1. A diffuse microstructural pattern in red leaves indicates the disintegration of this layer, resulting in the degradation of its function in the leaf protection mechanism. Hence, studying the microstructural changes of the leaves can provide new insights in leaf developmental stage/ autumn phenology using a fast and cost effective FF-OCM.

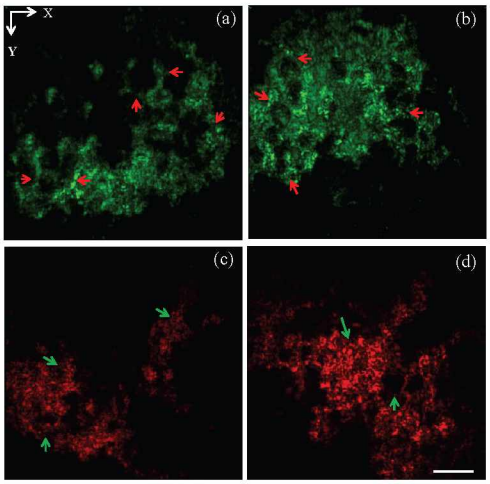



**Fig. 1.** FF-OCM *en-face* sectional images at (a) 8μm, (b) 20 μm, for green and (c) 8μm, and (d) 20μm, for red *Hogyoku* leaf. Scale bar: 125μm. Pseudo color is used for green and red leaves

## Acknowledgements

This work has been supported by the Ministry of Science and Technology, Taiwan, ROC (Project No. NSC 102-2112-M-010-002-MY3).

## References

1. H.R. Woo, H.J. Kim, H.G. Nam, and P.O. Lim, *J. Cell Sci.*, 2013, **126**(pt21), 4823–4833.
2. J. Cao, Y. Song, Hua-Wu, L. Qin, L. Hu, and R. Hao, *Scanning*, 2013, **35**, 336–343.
3. J.W. Hettinger *et al., Plant Physiology*, 2000, **123**(1), 3–16.
4. S. Chang, X. Cai, and C. Fluerau, *Opt. & Las. Eng.*, 2007, **45** (12), 1170–1176.

*Poster*

# FIBER SPECTROSCOPY METHODS FOR CANCER DIAGNOSTICS EX-VIVO

**O. Bibikova[1,2,3,4], U.J. Zabarylo[5], A. Melenteva[6], V. Belikova[6], I. Usenov[1,7], T. Sakharova[1], G. Danielyan[1], A. Bogomolov[6,8], O. Minet[5], H.J. Eichler[7], and V. Artyushenko[1]**

[1] Art photonics GmbH, Berlin, Germany, ob@artphotonics.de
[2] Optoelectronics and Measurement Techniques Research Unit, University of Oulu, Oulu, Finland
[3] Institute of Analytical and Bioanalytical Chemistry, Ulm University, Ulm, Germany
[4] Research-Educational Institute of Optics and Biophotonics, Saratov National Research State University, Saratov, Russia
[5] Center for Radiology C6, Medical Physics and Optical Diagnostics, CBF, Charité-Universitätsmedizin, Berlin Germany
[6] Samara State Technical University, Samara, Russia
[7] Technical University of Berlin, Institute for Optics & Atomic Physics (IOAP), Berlin, Germany
[8] global modelling, Aalen, Germany

**Abstract.** In this study we developed and applied various single and combined fiber probes for four key spectroscopy methods used in the 0.2–16 μm range: Raman scattering, Mid IR-absorption, Diffuse NIR-reflection, and fluorescence – to compare them and select the best one (or their combination) for an *ex-vivo* detection of malignant tissue for cancer surgeries. The most promising fiber spectroscopy methods were defined for selected organs after their tests in laboratory and clinical environment.

According to the World Health Organization (WOH), cancer is one of the leading causes of morbidity and mortality worldwide. However, the current procedure for cancer diagnostics consisting of clinical examination of the suspicious lesion, followed by biopsy and histopathology is invasive, costly, and time-consuming. Non-invasive spectroscopic investigation or "spectral histopathology" is a novel alternative for rapid cancer diagnostics and label-free cancer specification.

Our development of unique Multi-Spectral Fiber (MSF-) systems enables testing various single and combined fiber probes for four key spectroscopy methods: Raman scattering, Mid IR-absorption, Diffuse NIR-reflection, and fluorescence – to select the best method (or their best combination) for a detection of malignant tissue as it´s needed for cancer surgeries. Our recent research in ex-vivo analysis of resected tissues with cancers is presented to demonstrate selection of the best method specific for each organ and cancer type.

Moreover, spectral methods have been applied to analyse not only biopsies of healthy and malignant tissues, but bioliquids, such as blood and urine, of patients before and after surgery. Further multivariate data analysis of spectroscopic data, both individual techniques and their combinations, provided reliable cancer recognition with the strict demand to reach "No false negatives" in oncology diagnostics. Analysis of experimental results by the developed chemometric models of cancer recognition provides a good platform to develop portable Spectral Fiber Tumor Sensors. These new IoT-type Sensors will be customized for specific organs with data exchange via iCloud for a fast and accurate real-time tissue analysis – to guide minimal invasive, but complete tumour removal in oncology, including surgery operations which can be realized in telemedicine mode, in remote robotic mode, etc.

**Acknowledgements**

Funding of the project by the European Union and European Regional Development Fund (Grant 10155837) and ProFIT (ProgrammzurFörderung von Forschung, Innovationen und Technologien) by Investitions bank Berlin is gratefully acknowledged. The Russian Ministry of Education and Science supported this work within the framework of the basic part of state task on the theme: "Adaptive technologies of analytical control based on optical sensors" (Project No. 4.7001.2017/BP).

# FLUORESCENCE LIFE-TIME IMAGING OF SENESCING LEAVES

**S. Chakraborty**[1], **T. Anna**[1], **A. Karmenyan**[2], **W.C. Kuo**[1,3], and **A. Chiou**[1,3]

[1] Biophotonics and Molecular Imaging Research Center (BMIRC), National Yang-Ming University Taipei-11221, Taiwan, ROC, e-mail: sandeep_nanotsk@yahoo.co.in
[2] Department of Physics, National Dong-Hwa University, Hualien-97401, Taiwan, ROC
[3] Institute of Biophotonics, National Yang-Ming University, Taipei-11221, Taiwan, ROC

**Abstract.** Two-photon fluorescence lifetime imaging microscopy (2P-FLIM) was used to monitor the fluorescence life-time of *Acer palmatum 'Hogyoku'* leaves. The Hogyoku plant leaves change color from green to red (leaf senescence or aging) due to autumn phenology. With 760 nm excitation of the blue fluorescence, the average fluorescence lifetime of the red leaves was ~1.442 ns, which is 22% longer ($P < 0.05$) than the corresponding value (1.12 ns) of the green leaves. The source of blue fluorescence may be attributed to hydroxycinnamic acids, NADPH etc. Hence, blue fluorescence lifetime may be used as a signature of ageing in senescing leaves.

Leave is the principal nutrient source of plants. The lifespan and the structure of leaves are influenced by several biotic and abiotic factors. In autumn phenology, the leaves of deciduous plants turn from green to yellow, orange, and to red. Following these, a full programmed cell death occurs and this whole process is termed as leaf senescence [1]. Leaf senescence is a programmed development and can serve as an ideal model to understand aging.

In this work, we have applied two-photon fluorescence lifetime imaging microscopy (2P-FLIM) [2] to determine the blue fluorescence lifetime from the top surface of the green and the red *Acer palmatum 'Hogyoku'* leaves. Hogyoku is a Japanese maple tree variety and shows remarkable autumn phenology. Here, the 2P-FLIM images were obtained using a time-domain technique *viz.* time-correlated single photon counting (TCSPC). 760 nm was used to excite the blue fluorescence and a single band pass filter, 447/60 nm was used to detect the same from the green and the red leaves.

Figure 1 shows the intensity and average fluorescence lifetime images of the top surface of the green and the red *Acer palmatum 'Hogyoku'* leaves. Our preliminary results show that for the red leaves the average blue fluorescence lifetime (1.442 ns) is 22% longer (with $P < 0.05$) than the corresponding value (1.12 ns) for the green leaves. The origin of blue fluorescence is generally attributed to hydroxycinnamic acids attached to the cell walls and NADPH as well. The change in fluorescence property of hydroxycinnamic acids and NADPH is highly correlated with aging/senescing [3]. Hence, blue fluorescence lifetime may serve as a signature to study aging in leaves.

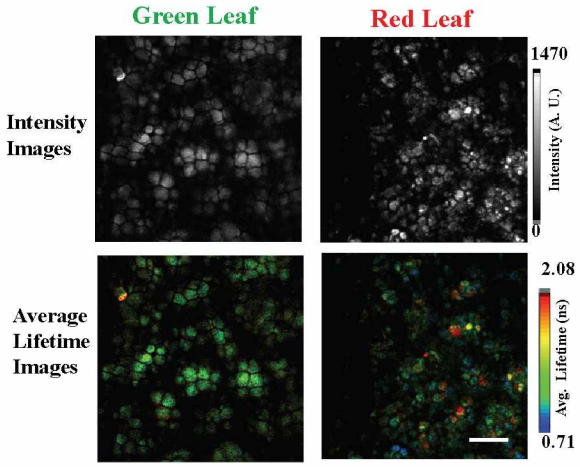



**Fig. 1.** The blue fluorescence intensity and lifetime images of senescing *Acer palmatum 'Hogyoku'* leaves. The Upper panel shows the intensity images while lower panel shows the average fluorescence lifetime images. Scale bar = 20 μm

## Acknowledgements

This work has been supported by the Ministry of Science and Technology, Taiwan, ROC (Project No. NSC102-2218-E-010-003) and the Top University Project from Taiwan Ministry of Education, ROC.

## References

1. P.O. Lim, H.J. Kim, and H.G. Nam, *Annu. Rev. Plant Biol.*, 2007, **58**, 115–136.
2. S. Chakraborty, F. Nian, J-W. Tsai, A. Karmenyan, and A. Chiou, *Sci. Rep.*, 2016, **6**, 19145.
3. S. Meyer, A. Cartelat, I. Moya, and Z.G. Cerovic, *J. Expt. Bot.*, 2003, **54**, 757–769.

# DEEP-BIOTISSUE IMAGING BY TEMPORAL FOCUSING WIDEFIELD MULTIPHOTON MICROSCOPY

**Chia-Yuan Chang[1], Yong-Da Sie[2], and Shean-Jen Chen[3]**

[1] Advanced Optoelectronic Technology Center, National Cheng Kung University, 701 Tainan, Taiwan
[2] Department of Engineering Science, National Cheng Kung University, 701 Tainan, Taiwan
[3] College of Photonics, National Chiao Tung University, 711 Tainan, Taiwan, sheanjen@nctu.edu.tw

**Abstract.** A developed temporal focusing-based multiphoton excitation microscope (TFMPEM) has a digital micromirror device (DMD) which is adopted not only as a blazed grating for light spatial dispersion but also for patterned illumination simultaneously. The TFMPEM has been extended to implement spatially modulated and digital holographic illumination to increase the beam coverage at the back-focal aperture of the objective lens. The axial excitation confinement (AEC) of TFMPEM can be condensed from 3.0 μm to 1.5 μm. By using the TFMPEM with HiLo technique, reconstructed deep-biotissue images according to the condensed AEC structured illumination are shown to be obviously superior in contrast and better scattering suppression.

Temporal focusing-based multiphoton excitation microscopy (TFMPEM) provides direct widefield two-photon excited fluorescence (TPEF) imaging [1], in which the diffraction element (e.g., a blazed grating) separates different spectral components of ultrashort laser pulses into different angles according to the diffraction equation and induces spatial dispersion that broadens the laser pulse width. The constructive interference condition of temporal focusing provides an axial excitation confinement (AEC) of few microns according to the following system parameters, namely the laser pulse width, initial beam size, system magnification, and the NA of the objective [2]. Herein, the TFMPEM has been extended to implement spatially modulated and digital holographic illumination to increase the beam coverage at the back-focal aperture of the objective lens. Furthermore, the TFMPEM with HiLo technique for biotissue has shown that the reconstructed images with the condensed AEC structured illumination are obviously superior in contrast and better scattering distortion suppression.

Figure 1(a) shows the original TPEF image of the eosin-stained mouse cerebellar cortex via the TFMPEM. The images via HiLo technique are presented in Figs. 1(b) and 1(c), with the low-frequency components retrieved from the 1.09 $\mu m^{-1}$ spatial frequency pattern images at 90° and 0° orientations, respectively. Although both images have the same high-frequency components from Fig. 1(a), differences can still be seen in Figs. 1(b) and 1(c) since the 0°-orientation pattern has a superior AEC such that the scattering is reasonably reduced and the modulated information is less distorted. Therefore, the low-frequency component could be retrieved with less noise from the patterned image with the higher pattern contrast and less scattering distortion from the out-of-focus excitation region.

The COS-7 cell line was stained with secondary antibody Alexa Fluor 488 fluorescein, after which the cytoskeleton's α-tubulin was imaged by temporal focusing (TF) alone and TF with the two complementary computer-generated Fourier hologram (CGFH) excitation and mergence approach. The filtered images, after the iterative deconvolution process, are respectively shown in Figs. 2(a) and 2(b). This TF method with DMD-based CGFH diffraction targets AEC improvement; consequently, a portion of the background noise in TFMPEM is rejected. Therefore, the image contrast of Fig. 2(b) respectively compared to that of Fig. 2(a) is superior. From the TPEF image of Fig. 2(b), and with the support of rapid pulse width modulation switching, a near-uniform TPEF image can be achieved even with the binary CGFH pattern excitation.

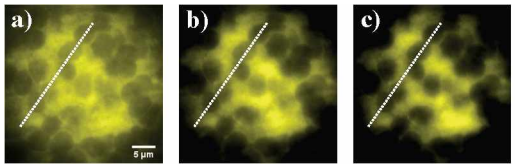



**Fig. 1.** (a) The original TPEF image of the eosin-stained mouse cerebellar cortex. The TFMPEM images with HiLo technique as the low-frequency component analyzed with the 1.09 $\mu m^{-1}$ spatial frequency pattern images at (b) 90° and (c) 0° orientations

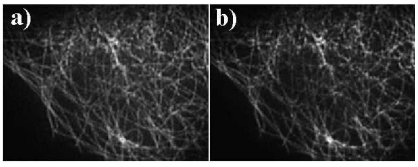



**Fig. 2.** TPEF images of α-tubulin of the COS-7 cell line stained with Alexa Fluor 488 by TF only (a), and TF with the two complementary CGFH excitation (b)

## References

1. D. Oron, E. Tal, and Y. Silberberg, *Opt. Express*, 2005, **13**(5), 1468–1476.
2. H. Dana and S. Shoham, *Opt. Express*, 2011, **19**(6), 4937–4948.

*Invited*

# ADVANCES IN OPTICAL COHERENCE ELASTOGRAPHY

**Zhongping Chen**

Beckman Laser Institute, Dept. of Biomedical Engineering,
Univ. of California Irvine, Irvine, CA 92617, USA

We report on the development of an acoustic radiation force optical coherence elastography (ARF-OCE) technology to image and characterize tissues biomechanical properties. We have applied the ARF-OCE to image post-mortem human coronary artery with atherosclerosis. The result demonstrates the potential of the ARF-OCE as a non-invasive method for imaging and characterizing vulnerable plaques. The ARF-OCE technology have a broad range of clinical applications, including imaging and characterizing cardiovascular atherosclerotic lesions, imaging and diagnosing of early stage cancer, imaging and evaluating ophthalmic diseases such as keratoconus and age-related macular degeneration, and imaging and assessing blood coagulation.

*Invited*

# THE PROMISE OF LARGE-SCALE BRAIN IMAGING WITH OPTOACOUSTICS

**X.L. Deán-Ben**[1], **S. Gottschalk**[1], **S. Shoham**[2], and **D. Razansky**[1,3,*]

[1] Institute for Biological and Medical Imaging, Helmholtz Center Munich, Neuherberg, Germany
[2] Department of Biomedical Engineering, Technion – Israel Institute of Technology, Haifa, Israel
[3] School of Medicine and School of Bioengineering, Technical University of Munich, Germany
[*]E-mail: dr@tum.de

Non-invasive observation of fast spatiotemporal activity patterns of large neural populations is a longstanding goal of neuroscience. We demonstrate a novel optoacoustic imaging platform for direct imaging of fast neural activity across entire light-scattering brains using genetically-encoded calcium indicators. By virtue of combining the contrast abilities of both microscopic and macroscopic functional neuroimaging methods with its unprecedented spatio-temporal resolution performance, our functional optoacoustic neuro-tomography (FONT) method fills an important performance gap in the current neuroimaging technology and opens new prospects for large-scale observations of neural networks.

**Acknowledgements**

This research is supported by the European Research Council grant ERC-2015-CoG-682379 and the US National Institutes of Health grant R21-EY026382.

**References**

1. A. Devor *et al.*, *Neuron,* 2013, **80**, 270–274.
2. N. Ji, J. Freeman, and S.L. Smith, *Nat. Neurosc.*, 2017, **19**(9), 1154–1164.
3. X.L. Deán-Ben, and D. Razansky, *Light Sci. Appl.,* 2014, **3**, e137.
4. X.L. Deán-Ben, S. Gottschalk, B. McLarney, S. Shoham, and D. Razansky, *Chem. Soc. Rev.*, 2017, **46**, 2158–2198.
5. S. Gottschalk, T. Fehm, X.L. Deán-Ben, and D. Razansky, *J. Cer. Blood Flow Metab.,* 2015, **35**, 531–535.
6. X.L. Deán-Ben, G. Sela, A. Lauri, M. Kneipp, V. Ntziachristos, G. Westmeyer, S. Shoham, and D. Razansky, *Light Sci. Appl.,* 2016, **5**, e16201.
7. X.L. Deán-Ben, S. Gottschalk, G. Sela, S. Shoham, and D. Razansky, *Opt. Lett.,* 42017, **42**(5), 959–962.

# QUANTITATIVE ANALYSIS OF SHG SIGNAL OF COLLAGEN STRUCTURE IN MODELS AND TISSUE SAMPLES

**V.V. Dudenkova**[1,2], **A.S. Bystrova**[1,2], **A.V. Meleshina**[2], **O.S. Rogovaya**[3], **E.V. Gubarkova**[2], and **E.V. Zagaynova**[2]

[1] Lobachevsky State University, Nizhny Novgorod, Russia, orange@mail.ru
[2] Nizhny Novgorod State Medical Academy, Nizhny Novgorod, Russia
[3] Koltzov Institute of Developmental Biology of Russian Academy of Sciences, Moscow, Russia

**Abstract.** We propose a combined use of coherence and energy parameters for complex quantitative analysis of SHG signal of a collagen structure both in models and tissue samples. It minimizes potential disadvantages of using a single method, and provides ideal information profile for clinical and research applications. For studying collagen formation on a model structure we used collagen gels constructed by combining dermal fibroblasts or dermal papilla cells and identified the increase in the values of coherence and energy in 3,10,12, and 14 days in collagen gels with fibroblast in comparison with dermal papilla. These parameters were also used for human intraoperative bladder diagnostics and allowed differentiating normal bladder with mild inflammation, severe inflammation, low-grade cancer and cancer on the scar.

Collagen is a main component of the extracellular protein and its characteristics reveal important information related to tissue condition. Second harmonic generation (SHG or 2HG) microscopy in combination with image analysis is a powerful tool for understanding and quantifying collagen organization and has a potential to distinguish different collagen states. Quantitative analysis provides objective metrics for SHG images when accounting for experimental conditions, such as excitation power, detection gain, magnification and resolution.

There is a most relevant approach for each collagen state in density stacking, anisotropy degree, swelling or thinning of fibers, appearance of a preferred direction or organization and disorganization of collagen fiber bundles, The principal methods for quantitative assessment of the state of collagen are the first order statistics (FOS), the second order statistics or GLCM (correlation lengths of gray-level co-occurrence matrix), fast Fourier transform (FFT), curvelet transform (CT), different special coefficients like SHG-to-autofluorescence aging index of dermis (SAAID) and their combination [1].

We propose a combined use of coherence and energy parameters for complex quantitative analysis of SHG signal of collagen structure both in models and tissue samples. Coherence and energy coefficients are based on evaluation of the structure tensor (second-moment matrix) in a local neighborhood [2].

For studying structural collagen formation on a model structure we used special collagen gels constructed by combining dermal fibroblasts (FB) or dermal papilla (DP) cells with type I rat tail collagen. Statistically significant increase of coherence was detected only after 10, 12, 14 days and 12, 14 days for energy. Higher coherence and energy values correspond to less isotropic and more oriented structures. It should be noted that the decrease of energy values after 14 days was probably due to the behavioral changes of DP cells on achieving contraction maximum.

By quantitative evaluation of collagen condition in a tissue model we also used scoring of coherence and energy parameters of SHG signal to human intraoperative bladder diagnostics. We analyzed normal bladder with mild inflammation, severe inflammation, low-grade cancer and cancer on the scar. A high value of coherence in the case of normal bladder submucosa with mild inflammation indicates preservation of collagen orientation and a statistically significant difference from severe inflammation, low-grade cancer and cancer on the scar. The lowest values of coherence and energy are in the case of inflammation and low-grade urothelial cancer that correlate with disorganized structure of collagen fibers. The main result is the possibility to differentiate between inflammation and low-grade cancer. All the diagnostics were confirmed by routine H&E and Van Gieson histology.

### Acknowledgements

This work has been financially supported by Russian Science Foundation (grants No. 14-25-00129П).

### References

1. R. Cicchi, E. Baria, C. Matthäus, M. Lange, and A. Lattermann, *Journal of Biophotonics.*, 2015, **8**, 347–356.
2. R. Rezakhaniha, A. Agianniotis, and J. Schrauwen, *Biomech Model Mechanobiol.*, 2012, **11**, 461–473.

# SINGLE PULSE TWO-PHOTON FLUORESCENCE LIFETIME IMAGING (SP-FLIM) WITH MHZ PIXEL RATE AND AN ALL FIBER BASED SETUP

**M. Eibl[1], S. Karpf[2], H. Hakert[1], D. Weng[1],** and **R. Huber[1]**

[1] Institut für Biomedizinische Optik, Universität zu Lübeck, 23562 Lübeck, Germany
[2] Department of Electrical Engineering, University of California, Los Angeles, California 90095, USA

**Abstract.** We present a two photon microscopy setup using a sub-nanosecond pulsed fiber laser synchronized to a high analog bandwidth signal detection for two-photon-excited fluorescence (TPEF) and single shot fluorescence lifetime imaging (SP-FLIM). Compared to typically used femtosecond excitation, both configurations should yield the same number of fluorescence photons on average when used for TPEF imaging if the same duty cycle and cw-power is applied. However, due to our longer pulse length, more fluorescence photons are generated per shot. In this presentation, we show that this higher number of fluorescence photons together with a high analog bandwidth detection makes it possible to not only use a single pulse per pixel for TPEF imaging but also to acquire FLIM images with pixel rates of 1 MHz.

Two-photon-excited fluorescence lifetime (FLIM) imaging is a powerful 3-D and chemically specific imaging modality in bio-medical research [1–3]. However, the need for a sophisticated ultra-short pulse laser sources and speed limitations of FLIM detection systems hinder a more widespread application. To overcome this limitations, we combined a robust sub-nanosecond fiber laser with a high analog bandwidth detection. The detection concept is similar to the one presented in [4] however we use nanosecond class pulses instead of standard femtosecond pulses. Due to the longer pulse length, more fluorescence photons are generated per pulse in our configuration. This allows us to derive the lifetime with only a single pulse excitation [5] and detect many photons at once, which makes it much faster than the current gold standard time-correlated single photon counting (TCSPC).

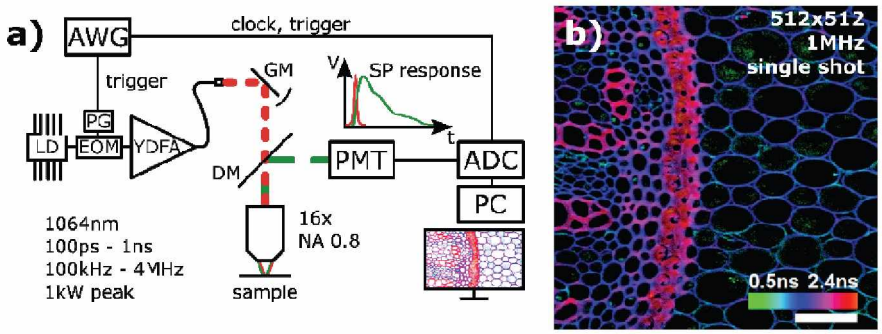



**Fig. 1.** a) Basic setup. b) FLIM image of a plant stem with a pixel rate of 1 MHz (scale bar 100 µm)

Figure 1a shows the basic concept of our single pulse FLIM setup. An actively modulated self-built fiber laser with typically 100 ps long pulses at a repetition rate of 1 MHz is used as excitation laser. The high-speed detection consists of a fast photomultiplier tube (PMT, Hamamatsu, H12056-20) and a high speed analog-to-digital converter (ADC, Alazartech, ATS9373). This combination makes fluorescence lifetime measurements with sub-nanosecond resolution possible. A SP-FLIM image with a pixel rate of 1 MHz is shown in figure 1b). The total acquisition time of the 512×512 pixels sized image was 670 ms (including fly back of galvanometric mirrors, pure measurement time 260 ms).

With the presented results, we show that longer pulses in the many-10ps to nanosecond regime are not only suitable for TPEF imaging but also allow for fast FLIM imaging. SP-FLIM with the all fiber based excitation source and accurate decay time determination is a promising technology to bring FLIM imaging to the workbench of biomedical researchers or into clinics for medical diagnosis.

## References

1. E.E. Hoover and J.A. Squier, *Nat. Photon.*, 2013, **7**(2), 93–101.
2. E.B. van Munster and T.W.J. Gadella, "Fluorescence Lifetime Imaging Microscopy (FLIM)", in *Microscopy Techniques*, 2005, 143–175.
3. K. Svoboda and R. Yasuda, *Neuron,* 2006, **50**(6), 823–839.
4. M.G. Giacomelli, *et al.*, *Biomed. Opt. Express*, 2015, **6**(11), 4317–4325.
5. S. Karpf, *et al.*, *Biomed. Opt. Express*, 2016, **7**(7), 2432–2440.

*Invited*

# METAL INDUCED ENERGY TRANSFER AND AXIAL SUPERRESOLUTION MICROSCOPY

**J. Enderlein**[1,2], **N. Karedla**[1,2], **A. Chizhik**[1], and **Al. Chizhik**[1]

[1] III Institute of Physics – Biophysics, Georg August University,
Friedrich-Hund-Platz 1, 37077 Göttingen, Germany, E-mail: jenderl@gwdg.de
[2] Center for Nanoscale Microscopy and Molecular Physiology of the Brain (CNMPB),
37077 Göttingen, Germany

Classical fluorescence microscopy is limited in resolution by the wavelength of light (diffraction limit) restricting lateral resolution to ca. 200 nm, and axial resolution to ca. 500 nm (at typical excitation and emission wavelengths around 500 nm). However, recent years have seen a tremendous development in high- and super-resolution techniques of fluorescence microscopy, pushing spatial resolution to its diffraction-dictated limits and much beyond. However, for nearly all of the superresolution methods (STED, PALM, STORM etc.), achieving axial superresolution is typically much more difficult than lateral superresolution. A simple approach aiming at nanometer resolution along the optical axis is Metal Induced Energy Transfer or MIET [1]. When placing a fluorescent molecule close to a metal, its fluorescence properties change dramatically. In particular, one observes a strongly modified lifetime of its excited state (Purcell effect). This is due to the efficient electromagnetic coupling of the excited state to surface plasmons in the metal, which is similar to Förster Resonance Energy Transfer (FRET), where the energy of an excited donor molecule transfers into the excited state of an acceptor molecule. We call this effect metal-induced energy transfer or MIET. The MIET-coupling between an excited emitter and a metal film is strongly dependent on the emitter's distance from the metal. We have used this effect for mapping the basal membrane of live cells with an axial accuracy of ~3 nm [1]. We present data of MIET imaging for various biological systems: (i) MIET imaging of the spatio-temporal reorganization of the actin skeleton during stem-to-epithelial cell proliferation, and during the transformation of epithelial to mesenchymal cells; (ii) dual-color MIET imaging of the architecture of focal adhesion complexes; and (iii) dual-color MIET imaging of the protein distribution in the inner and outer membrane of the nuclear envelope.

The method is easy to implement and does not require any change to a conventional fluorescence lifetime microscope. It can be applied to any biological system of interest, and is compatible with most other super-resolution microscopy techniques that enhance the lateral resolution of imaging. Moreover, it is even applicable to localizing individual molecules [2], thus offering the prospect of using single-molecule localization microscopy for structural studies of biomolecules and biomolecular complexes. For that purpose, we have built a dedicated measurement system which does not only allow for single-molecule fluorescence lifetime measurements, but also for recording of defocused images of single molecules for determining the lateral position and three-dimensional orientation [3].

**Acknowledgements**

Part of this work (JE, IG) was supported by the Cluster of Excellence and DFG Research Center Nanoscale Microscopy and Molecular Physiology of the Brain". We are grateful to Andreas Janshoff (Dept. of Chemistry, Georg August University), Jörg Großhans (Dept. of Biology, Georg August University), and Florian Rehfeldt (Dept. of Physics, Georg August University) and their groups for support and collaboration.

**References**

1. A.I. Chizhik, J. Rother, I. Gregor, A. Janshoff, and J. Enderlein, *Nature Photonics*, 2014, **8**, 124–127.
2. N. Karedla, A.I. Chizhik, I. Gregor, and J. Enderlein, *Chem Phys Chem*, 2014, **15**(4), 705–711.
3. N. Karedla, S. Stein, D. Hähnel, I. Gregor, and J. Enderlein, *Phys. Rev. Lett.*, 2015, **115**(17), 173002.

# CROSS-POLARIZATION OPTICAL COHERENCE TOMOGRAPHY IN VULNERABLE ATHEROSCLEROTIC PLAQUE DETECTION

**F.I. Feldchtein[1], A.A. Moiseev[1,2], N.D. Gladkova[1], M.Yu. Kirillin[2], G.V. Gelikonov[1,2], V.V. Dudenkova[1], E.B. Kiseleva[1], E.G. Sharabrin[1], and E.V. Gubarkova[1]**

[1] Nizhny Novgorod State Medical Academy, Nizhny Novgorod, Russia, felixfel00@gmail.com
[2] Institute of Applied Physics RAS, Nizhny Novgorod, Russia

**Abstract.** Different types of atherosclerotic plaques were visualized *ex vivo* using cross-polarization OCT (CP OCT). The developed approach to numerical processing of images allows for automatic detection and classification of vulnerable plaques. A weighted linear combination of average brightness and depolarization factor derived from OCT images is found to be an accurate predictor of plaque vulnerability, better than each of these parameters alone. This finding could be a step towards in vivo detection of vulnerable plaques using OCT.

**Introduction.** Acute coronary syndrome is most often caused by a "vulnerable" plaque rupture. Such plaques are characterized histologically by presence of a necrotic, lipid-rich core at the bottom, and a thin (< 65 μm) fibrous cap [1]. The automatic approach for the OCT detection of "vulnerable" plaque in real time is the most important direction at present. The majority of automated methods are aimed at developing reliable OCT signs, reflecting such microstructural features of "vulnerability" plaques as the degradation of collagen fibers [2], detecting necrotic core lesions [3], accumulation of foam cells and inflammatory cells in the thin fibrous capsule [4].

In particular, the study purpose is to develop an approach for quantitative evaluation of the backscattering and polarization properties changes in the intima/fibrous cap, to characterize and differentiate the atherosclerotic plaques development stages, and to assess their instability.

**Materials and Methods.** This study was performed on 30 *post mortem* samples of coronary artery walls evaluated in parallel by CP OCT and histology. All arterial vessels were excised no later than 24 hours after death.

This study used a CP OCT system with a central wavelength of 1310 nm, radiation power of 20 mW, and a spectral width of 100 nm, resulting in the axial resolution of 15 μm, scanning depth of 1.7 mm, and the OCT images were constructed in two virtual channels, one of which was co-polarized with the incident polarization and the other one was orthogonal (cross-polarized) to the incident polarization, respectively [5]. CP OCT imaging was performed from the intimal side of the samples.

Two quantitative parameters extracted from CP OCT included OCT brightness (Pythagorean sum of both polarizations) and depolarization factor (DF). For the measure of average brightness we chose the maximum probability value from pixel brightness histogram, rather than traditional averaging. Then a linear weighted combination of the brightness and DF with variable weight was optimized to serve as a best predictor of plaque vulnerability.

**Results.** The optimized weighted linear combination of brightness and DF factor can improve reliability of the vulnerable plaques identification, in comparison with using any of these parameters alone. Such combination therefore is called "vulnerability parameter". Based on the ROC curve analysis, it is possible to obtain combination of sensitivity (94-96%) and specificity (91–93%) for plaque vulnerability. Diagnostic accuracy is 95%.

**Acknowledgements**

The development of the CP-OCT equipment were supported by the Ministry of Education and Science of the Russian Federation, grant No. 14.B25.31.0015; OCT image post-processing and data analysis methods development were funded by RFBR project No. 16-32-60178 mol_a_dk.

**References**

1. R. Virmani *et al.*, *J. Am. Coll. Cardiol.*, 2006, **47**, C13–C18.
2. W.C. Kuo *et al.*, *Opt. Express*, 2008, 16, 8117–8125.
3. G. van Soest *et al.*, *J. Biomed Opt.*, 2010, **15**(1), 011105.
4. H. Wang *et al.*, *Biomed Opt Express*, 2015, **6**(4), 1363–75.
5. V.M. Gelikonov and G.V. Gelikonov, *Laser Phys. Lett.*, 2006, **3**, 445–451.

*Invited*

# MEASURING CEREBRAL OXYGEN DELIVERY & CONSUMPTION WITH DIFFUSE CORRELATION SPECTROSCOPY IN AFRICAN CHILDREN

**M.A. Franceschini**

Athinoula A. Martinos Center for Biomedical Imaging, Massachusetts General Hospital, Harvard Medical School, 13th Street, Building 149, Charlestown, MA 02129, USA
mari@nmr.mgh.harvard.edu

**Abstract.** With the foundation of our seminal near-infrared spectroscopy (NIRS) and diffuse correlation spectroscopy (DCS) work on infants, we have developed a novel integrated system, which simultaneously acquires cerebral oximetry and blood flow measurements. We have deployed the device in Africa to assess the feasibility of NIRS studies in low resource settings. Results will be presented.

Frequency domain near infrared spectroscopy (FDNIRS) and diffuse correlation spectroscopy (DCS) have emerged as synergistic techniques for the non-invasive assessment of brain health. Combining FDNIRS cerebral oximetry (hemoglobin concentration (HbT) and oxygenation (SO2)) with DCS measures of cerebral blood flow (CBFi), an index of cerebral metabolic rate of oxygen (CMRO2i) can be quantified. CMRO2 is a parameter more closely linked to underlying physiology and pathology than either NIRS or DCS hemodynamic estimates alone. Here we describe the first commercially available integrated instrument, called the "MetaOx", designed to enable simultaneous FDNIRS and DCS measurements at rates of 10+ Hz, and offering real-time data evaluation. In tissue-like phantoms, we have demonstrated that simultaneous operation of the FDNIRS and DCS components is possible, with performance improvement vs. standalone systems. In the last two years, we have used the Metaox in two studies in African children

For the first study, we have partnered with the CURE Childrens Hospital of Uganda to test initial clinical utility of the FDNIRS-DCS measures to assess the extent of hydrocephalus (HI) and to predict treatment outcomes. We measured 35 HI patients one day pre- and post-treatment and correlated our measures with pre-surgical and 6 months follow up computed tomography (CT) scans. CT pre-surgical scans revealed primary injuries from neonatal infection and severe hydrocephalus resulted in high compression and thinning of the cortical mantle. FDNIRS-DCS pre-surgical measurements on 4 brain locations demonstrated high accuracy in detecting these brain structural damages by quantifying the distortions of the light propagation through the tissue (ROC AUC = 0.93). Differences in tissue scattering one day post-surgery showed a high predictive value (ROC AUC = 0.93) in treatment failure within 6 months. We also found that brain regions with higher CMRO2i tend to recover better than regions with low CMRO2i in agreement with the 6 month follow up CT scans.

For the second study, we are partnering with the Tufts University USDA Human Nutrition Research Center, and participating in an ongoing study aiming to develop a new nutritional supplement formulation focused on enhancing cognitive performance in undernourished children in rural Guinea-Bissau. A 20-week randomized trial (3 groups) is being conducted in 1000 children of age 1.5 – to 7 years old. Preliminary results show correlation of the optical measures with anthropometric or cognitive measure.

These studies show feasibility of FDNIRS-DCS in developing countries and very low resource settings. The results also suggest FDNIRS-DCS can have a direct and immediate impact in predicting therapy success and brain outcomes.

**Acknowledgements**

MetaOx: Stefan Carp and Parisa Farzam, Massachusetts General Hospital; Norin Redes and Dennis Hueber, ISS Inc., IL.

Hydrocephalus study: Pei-Yi Lin, Jason Sutin, Massachusetts General Hospital; Benjamin Warf, Boston Children's Hospital; Peter Ssenyonga, Edith Mbabazi and John Kimbugwe, CURE Children's Hospital of Uganda.

Nutritional study: Pei-Yi Lin and Katherine Hagan, Massachusetts General Hospital; Susan. B. Roberts and Salima Taylor, Tufts University; Augusto Braima de Sa and Raimundo Có, International Partnership for Human Development, Guinea-Bissau.

*Invited*

# QUANTITATIVE OPTOACOUSTIC IMAGING

**M. Frenz[1], L. Ulrich[1], L. Ahnen[2], K.G. Held[1], M. Jaeger[1], S. Sanchez Majos[2], M. Wolf[2], and H.G. Akarcay[1]**

[1] Institute of Applied Physics, University of Bern, Sidlerstrasse 5, CH-3012 Bern, Switzerland
frenz@iap.unibe.ch
[2] Department of Neonatology, University Hospital Zurich, Frauenklinikstrasse 10, CH-8091 Zurich, Switzerland

**Abstract.** Quantitative optoacoustic (OA) imaging exploits the wavelength-dependent absorption of for example hemoglobin, to determine spatially resolved the local blood oxygen saturation, due to the distinct optical absorption spectra of oxy- and deoxygenated hemoglobin. Wavelength-dependent optical attenuation in the bulk tissue, however, distorts the spectral OA signal of the blood and thus renders absolute oxygenation measurements challenging. We show that correction of the spectral distortion is possible without requiring a-priori knowledge of the tissue optical properties. Two different techniques will be presented and compared: (i) Multiple-irradiation sensing and (ii) Near-infrared optical tomography. The experimental results demonstrate that both techniques are promising for quantitative OA imaging combined with handheld clinical ultrasound.

Periventricular diffuse white matter injury (WMI) has become the dominant brain pathology and is the major reason for persisting spastic motor deficits and cognitive abnormalities in preterm infants [1]. Cerebral ischemia is a key initiating factor for WMI. Such brain lesions are localized events and are characterized by drops in oxygen saturation levels (StO2). A safe bedside imaging method that can detect low local StO2 levels and monitor the effects of preventive and neuroprotective interventions and brain development is urgently needed. One promising approach is quantitative OA imaging, which exploits the wavelength-dependent optical absorption properties of oxy- and deoxyhemoglobin in the near-infrared range, to provide quantitative estimates of their spatially varying concentration allowing to image local StO2 levels. This modality, however, faces important challenges, as well-described by [2], among them is the spectral distortion due to wavelength-dependent fluence attenuation. The retrieval of accurate local StO2 values will only be possible if this wavelength-dependency of the optical attenuation in the tissue is taken into account [3]. In this contribution, we propose calculating the fluence distribution by means of multiple-irradiation sensing which employs multiple irradiation positions to estimate optical properties of highly scattering media, a concept similar to optical tomography. However, as opposed to superficial optical detection, it employs optically absorbing structures inside the tissue as intrinsic fluence detectors. The results demonstrate that the multiple optical irradiation approach allows a successful correction of the measured OA spectrum of the inclusions, which was initially distorted by the spectral attenuation of the surrounding medium. A second technique for calculating the local fluence distribution presented is near-infrared optical tomography (NIROT), which provides 3D reconstructions of the probed tissue volume's optical properties [4]. To solve the NIROT inverse problem we used NIRFAST, a software package developed at Dartmouth University [5], that we have modified and optimized for our needs. This Matlab-based code solves the light diffusion equation on a tetrahedral mesh by the finite element (FEM) approach, and relies on Tikhonov regularization to constrain the space of solutions. NIRFAST was also used to calculate the fluence distribution, based on the reconstructed optical properties. Our results indicate that the presented methods of combining OA imaging with multiple irradiation sensing or NIROT is of benefit for achieving spectral correction in highly scattering non-homogeneous media.

**Acknowledgements**

This research was funded in part by the European Community's Framework Programme (FP7/2007-2013) under grant agreement No. 31806 and the SwissTransMed platform "ONIRIUS". The author G. Held acknowledges support the Hans-Sigrist foundation.

**References**

1. J.J. Volpe, *Lancet Neurol*, 2009, **8**(1), 110–24.
2. B.T. Cox, J.G. Laufer, and P.C. Beard, *Proc. SPIE*, 2009, **7177**, 717713-717719.
3. K.G. Held, M. Jaeger, J. Ricka, M. Frenz, and H.G. Akarcay, *Photoacoustics*, 2016, **4**(2), 70–80.
4. J.C. Hebden and T. Austin, *Eur Radiol*, 2007, **17**(11), 2926–33.
5. H. Dehghani, M.E. Eames, P.K. Yalavarthy, S.C. Davis, S. Srinivasan, C.M. Carpenter, B.W. Pogue, and K.D. Paulsen, *International Journal for Numerical Methods in Biomedical Engineering*, 2009, **25**(6), 711–732.

*Poster*

# CROSS-POLARIZATION COHERENT BACKSCATTERING COEFFICIENT AND ITS DEPENDENCE ON PROBE WAVE POLARIZATION

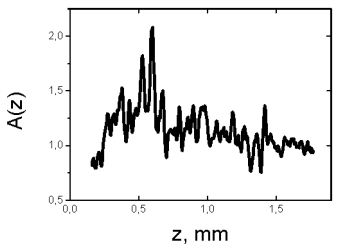
**V.M. Gelikonov[1], V.N. Romashov[1], D.V. Shabanov[1], S.Yu. Ksenofontov[1], D.A. Terpelov[1], P.A. Shilyagin[1], G.V. Gelikonov[1], and A. Vitkin[2,3]**

[1] Institute of Applied Physics RAS, 60390 Nizhny Novgorod, Russia
[2] Nizhny Novgorod State Medical Academy, 603005 Nizhny Novgorod, Russia
[3] University of Toronto and University Health Network, M5G 2M9, Toronto, Ontario, Canada

**Abstract.** A common path OCT setup capable of controlling probe wave polarization state was developed to obtain co- and cross-polarized OCT images. The dependence of the coefficient of cross-polarization coherent backscattering on probe wave polarization state was investigated in experiment. For circularly polarized probe light, this coefficient was shown to be independent of the reciprocal orientation of the probe and object and was 50% higher than for linearly polarized probe light.

The polarization state of the probe wave is the key parameter for the cross-polarization modality of polarization sensitive OCT (CP OCT). Diagnostically significant information in the CP OCT method is contained in two images. The first one (co-polarized image) is a conventional OCT image formed as a result of the interference between the reference wave and the probe wave preserving the initial polarization state during backscattering. The second image (cross-polarized image) is obtained from the probe wave backscattered component in orthogonal polarization state relative to the incident probe wave. Earlier investigations showed that the value of the cross-polarized image strongly depends on both probe wave polarization state and sample orientation relative to the probe. This dependence is unwanted in a clinical diagnostic device [1], because it disturbs uniformity of the obtained results and decreases their repeatability.

The change of the polarization state during backscattering may be described by the ratio of the correlation functions obtained for cross- and co-polarized images: $\tilde{\delta}_{C,L} = I^{\perp}_{C,L} / I^{\parallel}_{C,L} = \left| \left\langle \vec{E}_S \vec{E}^{CROSS*}_{REF} \right\rangle \right| / \left| \left\langle \vec{E}_S \vec{E}^{CO\ *}_{REF} \right\rangle \right|$, where the $C$, $L$ indexes denote circular and linear states, respectively. The optimal condition for the CP OCT images uniformity is to use circular polarization state of the probe light. The experimental investigation shows that for biological tissues, the $\tilde{\delta}_{CIR}(z) / \tilde{\delta}_{LIN}(z) = A(z)$ ratio exceeds 1 for every depth more than 0.1 mm. This coefficient achieves its maximum at the depth of about several mean free paths (0.6 mm in our setup). Minimal values of $A(z)$ correspond to the sample surface (where there is a small number of backscattered photons) and to highest depths, where the number of ballistic photons tends to zero and the signal uncertainty increases due to noise limitations. This behavior of $A(z)$ can be explained by the appearance of backscattering anisotropy inherent in linearly polarized light described in [2, 3].



$A(z)$ for chicken skin fragment

So, the uniformity of measurements in cross-polarized light may be achieved by using circularly polarized probe light for measuring the local coefficient of cross-polarized backscattering. This coefficient is independent of the reciprocal orientation of probe and object and is 50% higher than for linearly polarized probe light.

**Acknowledgements**

The research concerning the development of the method was supported by the State task for the IAP RAS project No. 0035-2014-0018. The experimental validation of the method was supported by the Ministry of Education and Science of the Russian Federation, grant No. 14.B25.31.0015.

**References**

1. E. Kiseleva, M. Kirillin, F. Feldchtein, A. Vitkin, E. Sergeeva, E. Zagaynova, O. Streltzova, B. Shakhov, E. Gubarkova, and N. Gladkova, *Biomedical optics express*, 2015, **6**(4), 1464–1476.
2. P.E. Wolf and M.G. Weak, *Physical Review Letters*, 1985, **55**(24), 2696–2699.
3. V.P. Tishkovets and M.I. Mishchenko, *Journal of Quantitative Spectroscopy and Radiative Transfer*, 2009, **110**(1–2), 139–145.

# DRUG DELIVERY BY NATURAL ZEOLITE PARTICLES

**V.A. Hovhannisyan** and **S.J. Chen**

National Chiao Tung University, Tainan, Taiwan

**Abstract.** Using multiphoton microscopy (MPM), we demonstrated that clinoptilolite type of zeolite (CZ) produced two-photon excited fluorescence (TPEF) and second harmonic generation (SHG) signals by femtosecond laser excitation. In addition, adsorption of PDT active dyes (hypericin, methylene blue, etc) and they release from CZ pores in the presence of biomolecules have been shown. Furthermore, magnetic CZ particles were tested as an effective material for drug delivery and controlled release in biological systems. The results may open new perspectives in application of CZ in biomedical imaging, and introducing optical approaches into the clinical environment.

Natural zeolites are porous alumino-silicates that widely used in agriculture, industry, environmental protection, and biomedicine for several decades [1]. Clinoptilolite type of zeolite (CZ) contains micropores of 0.3 to 1.2 nm sizes and meso- and macro-pores of 2 nm to 100 mm sizes, and it is a promising material for biomedicine and pharmaceutics due to its non-toxicity, thermal stability, expanded surface area, and exceptional ability to adsorb various atoms and organic molecules into the pores. CZ is safe for human and widely used in health industry as a food supplement against many diseases, including cancer, and as adsorbent of free radicals, toxic metals and radioactive elements. In addition, CZ is utilized as effective light harvesting system in solar cells and as dietary supplements in animal diets.

Hypericin (Hyp), a natural pigment found in plants of the Hypericum genus, has recently received increasing attention due to its high photo-toxicity against viruses and anti-tumor photoreactivity. Moreover, it was demonstrated that Hyp was an effective mediator for light-controlled selective modification of collagen in connective tissues, and might be used in biomedical engineering and therapy of collagen-related disorders [2]. However, Hyp in water and PBS tends to aggregate and form non-soluble and non-fluorescent aggregates thereby losing its photoreactive properties.

We showed that CZ particles adsorbed Hyp, methylene blue, chlorin $e_6$ and other PDT molecules, but did not adsorb fluorescein molecules (see Fig. 1). In addition, Hyp molecules were released from the CZ pores in the presence of collagen, hemoglobin and albumin. Hyp release rate was higher in the presence of EtOH, or similar solvents, so it could be controlled by changing of concentration of the solvent [3]. The behavior of Hyp was attributed to its hydrophobic character that served as driving force of release and redistribution of the dye.

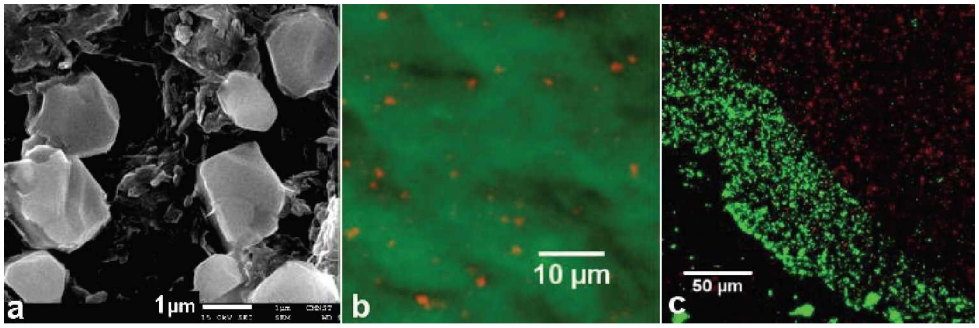



**Fig. 1.** (a) SEM image of microsize CZ particles; (b) CZ in solution of fluorescein, which is not adsorbed by CZ; (c) Droplet of methylene blue (which is adsorbed by CZ), after filling by CZ particles; Green is TPEF from dyes, red is SHG from CZ particles

Furthermore, it was demonstrated that zeolite particles revealed magnetic properties that allowed to manipulate them, separate from other materials and apply for delivery and controlled release of different drugs. Thus, CZ can be considered as a promising multimodal probe for multiphoton optical imaging, as a container for controlled drug delivery and a sensor for photo- and thermo-therapy.

## References

1. F.A. Mumpton, *Proc. Natl. Acad. Sci. USA,* 1999, **96**, 3463–3470.
2. V. Hovhannisyan, *et al.*, *Appl. Phys. Lett.,* 2014, **105,** 263701.
3. V. Hovhannisyan, C.Y. Dong, and S.J. Chen, *Sci. Rep.*, 2017 (in press).

# ESTIMATION OF TUMOR INVASION DEPTH FOR PDT PROCEDURE WITH CHLORINE PHOTOSENSITIZERS FROM TWO-WAVELENGTH PROBING

**A.V. Khilov[1], M.Yu. Kirillin[1], D.A. Loginova[1,2], and I.V. Turchin[1]**

[1] Institute of Applied Physics of the Russian Academy of Sciences, Nizhny Novgorod, Russia
alhil@inbox.ru
[2] Lobachevsky State University of Nizhny Novgorod, Nizhny Novgorod, Russia

**Abstract.** Photodynamic therapy (PDT) is a modern treatment technique efficient for many medical applications, in particular, for tumor treatment. Chlorine series photosensitizers (PSs), such as Fotoditazin, have two absorption peaks, corresponding to 405 nm and 660 nm providing an opportunity to employ multispectral excitation of PS during PDT. For correct choice of the treatment protocol knowledge of depth of tumor invasion into the tissue is required. We present analytical and numerical investigations of the possibility to determine tumor depth by multispectral excitation of PS.

PDT is a modern photochemistry-based approach to the treatment of different pathologies, including cancer [1]. The PDT uses light radiation of specific wavelength and PS. Light radiation imparts cytotoxicity and photochemical reactions inducing singlet oxygen release followed by necrosis and apoptosis of cancer cells.

For a proper choice of PDT treatment protocol it is important to know the depth of a superficial tumor invasion into healthy tissue. We study the possibility to estimate tumor depth based on multispectral excitation of chlorine series PSs, namely, Fotoditazin. Chlorine series PSs have two excitation peaks corresponding to blue and red light allowing for excitation at different probing radiation wavelengths. The difference in biotissue optical properties values at these wavelengths provides additional diagnostic advantages for optical diagnostics.

We developed an analytical model for calculating fluorescence response to multispectral excitation of PS based on diffuse approximation of the Radiative Transfer Equation (RTE). For a cylindrical medium of depth $d$ illuminated with a planar wave we obtained an analytical expression for measured fluorescence which was found to be proportional to $S_{em} \sim (1-\exp(-(\mu^*+\mu)d)$, where $\mu(\lambda)$ is apparent attenuation coefficient, and $\mu^*$ is the effective attenuation coefficient corresponding to emission wavelength [2]. We chose rat brain as a model tissue with known spectral characteristics [3] and varied PS concentration from 0.005 mg/ml to 0.5 mg/ml and tumor invasion depth from 0.25 to 5 mm. Numerical simulations were performed for PS distributed uniformly within the tissue with the excitation at 405 nm and 660 nm applying the developed model and the Monte-Carlo method [4]. The analytical model is consistent with the Monte-Carlo method. It allows differentiating tumor invasion depths up to 1.5–2 mm even for unknown accumulated PS concentration. For larger depths such differentiation becomes impossible due to the limited light penetration in tissue.

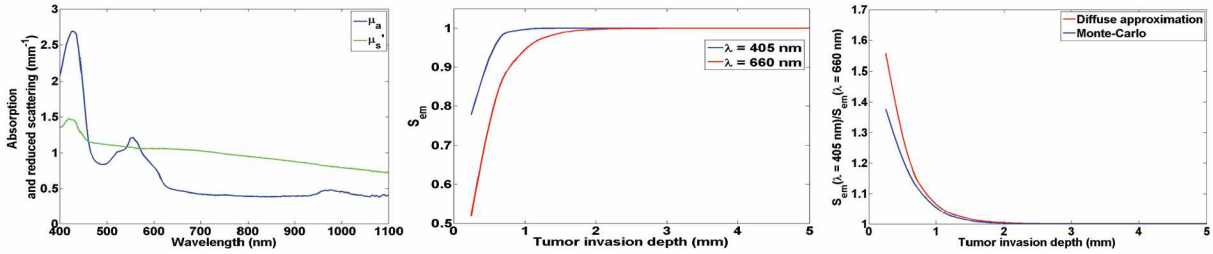



**Fig. 1.** (a) Rat brain spectra. The dependence of fluorescence signals calculated in analytical model (b) and their ratio (c) on tumor invasion depth for 0.05 mg/ml PS concentration

**Acknowledgements.** The investigation was supported by the Russian Science Foundation (project #17-15-01264).

## References

1. J.P. Celli, B.Q. Spring, I. Rizvi, C.L. Evans, K.S. Samkoe, S. Verma, B.W. Pogue, and T. Hasan, *Chem. Rev.*, 2010, **110**, 2795–838.
2. S.L. Jacques, *Journal of Biomedical Optics,* 2010, **15**(5), 051608.
3. D.A. Loginova, E.A. Sergeeva, A.D. Krainov, P.D. Agrba, and M.Yu. Kirillin, *Quantum Electronics,* 2016, **46**(6), 528–533.
4. Q. Fang and D. A. Boas, *Optics express,* 2009, **17**, 20178–90.

*Invited*

# OPTICAL COHERENCE TOMOGRAPHY IN PATHOLOGY RECOGNITION AND MONITORING OF PHOTODYNAMIC THERAPY: BENEFITS FROM NUMERICAL PROCESSING IN CLINICAL APPLICATIONS

**M. Kirillin[1], M. Shakhova[1,2], A. Meller[1,2], D. Sapunov[2], P. Agrba[1,3], E. Kiseleva[2], D. Loginova[1,3], A. Khilov[1], O. Kondratieva[3], K. Chikalova[2], T. Motovilova[2], E. Sergeeva[1], I. Turchin[1], and N. Shakhova[1]**

[1] Institute of Applied Physics RAS, 603950, Ulyanov St., 46, Nizhny Novgorod, Russia, mkirillin@yandex.ru
[2] Nizhny Novgorod State Medical Academy, 603000, Minin Sq., 10/1, Nizhny Novgorod, Russia
[3] N.I. Lobachevsky State University of Nizhny Novgorod, 603950, Gagarin avenue, 23, Nizhny Novgorod, Russia

**Abstract.** Optical coherence tomography (OCT) is a modern imaging modality providing structure visualization with spatial resolution down to units of microns. However, efficient clinical applications of OCT often require additional diagnostic image processing or quantification. In this paper we overview different approaches to OCT image numerical processing that allow enhancing applications of OCT in gynecology, otolaryngology, and aesthetic medicine.

Optical coherence tomography (OCT) is a modern imaging modality based on principles of low-coherence interferometry providing structure visualization with spatial resolution down to units of microns. Currently it is actively introduced into clinical practice, however, visual evaluation of a diagnostic OCT image in some cases is not sufficient for correct interpretation and pathology grading. In this situation numerical techniques are employed for image processing including segmentation and scoring. Additionally, OCT combined with numerical processing can be efficiently employed for treatment monitoring and tracing tissue response to treatment both intra course to correct and personalize the treatment procedure and in the follow-up to evaluate long-term effect and timely reveal pathology recurrence.

In this paper clinical applications of OCT in gynecology, otolaryngology, and aesthetic medicine enhanced by numerical processing are overviewed. Diagnostics was performed both with traditional and cross-polarization OCT modalities employing devices at 1300 nm developed at the IAR RAS (Russia) equipped with an endoscopic fiber optics probe [1]. The study was approved by the Ethical Committee (#45 30/06/2008) for scientific studies with human subjects.

In gynecology OCT was employed for diagnostics of endometritis which is one of the frequent causes of miscarriage and unsuccessful in vitro fertilization in females. OCT demonstrated high potential in detecting signs of edema and sclerosis in the course of standard hysteroscopy procedure. Numerical processing of OCT images based on histogram analysis allowed quantifying the level of sclerosis of endometrium. The results are in good agreement with blind recognition test. In diagnostics of otorhinolaryngology pathologies the potential of OCT in differentiation of different types of rhinitis and pharyngitis was demonstrated.

In otolaryngology OCT was employed for differential diagnostics of rhinitis. Typical features of diagnostic OCT images of relative norm, vasomotor and allergic rhinitis were determined. Application of histogram analysis revealed high potential of image quantification for differentiation of allergic and vasomotor rhinitis which is an important clinical problem.

A promising application of PDT in cosmetology is anti-ageing therapy due to collagen reconstruction induced by PDT. CP OCT modality highly sensitive to collagen presence and ordering allows monitoring this procedure and correcting the treatment protocol based on the registered tissue response. CP OCT was employed in combination with calculation of integral depolarization factor [2] that allowed quantifying the achieved effect of skin rejuvenation.

### Acknowledgements

The study is supported bythe Russian Science Foundation (project # 17-15-01264) except gynecology studies supported by the RFBR (grant 15-42-02572).

### References

1. V. Gelikonov, G. Gelikonov, M. Kirillin *et al.*, *Chapter 16 in Handbook of Photonics for Biomedical Science*, V.V. Tuchin (Ed.), (CRC Press, 2010), 423–444.
2. E. Kiseleva, M. Kirillin, F. Feldchtein, *et al.*, *Biomedical Optics Express*, 2015, **6**(4), 1464–1476.

# *IN VIVO* MULTIMODAL OCT STUDY OF HUMAN ORAL MUCOSA

**E.B. Kiseleva[1], A.A. Moiseev[1,2], E.S. Finagina[1], M.A. Sirotkina[1], A.V. Maslennikova [1], D.V. Shabanov[1,2], E.V. Zagaynova[1], F.I. Feldchtein[1], L.A. Matveev[1,2], A.A. Vitkin[1,3], and N.D. Gladkova[1]**

[1] Nizhny Novgorod State Medical Academy, Nizhny Novgorod, Russia, kiseleva84@gmail.com
[2] Institute of Applied Physics, Russian Academy of Sciences, Nizhny Novgorod, Russia
[3] University of Toronto and University Health Network, Toronto, Ontario, Canada

**Abstract.** Development of the OCT microangiography (OCT MA) allows new potential clinical applications, in particular, studying the human oral mucosa response to different therapies. Such new applications are more sensitive to tissue motion and compression artifacts. Therefore, correction of the previously developed methodology and study of protocols may be required to improve mechanical stabilization of the probe relative to the patient. Also, better tissue compression compensation is needed in case of contact OCT scanning. The objective of this work was to characterize human cheek mucosa using real-time multimodal (MM: cross-polarization and MA) OCT. Some original devices were constructed and several conditions were revealed to be controlled to achieve the goal and optimize *in vivo* MM OCT study of human cheek mucosa.

**Introduction.** Human oral mucosa is a common and fairly well studied object for OCT applications, from malignancy detection to chemo- (radiation) induced oral mucositis [1]. However, development of the OCT system multimodality, in particular OCT microangiography (MA) [2] requires re-evaluation of the same tissues and conditions to understand and characterize new features. The objective of this work was to characterize human cheek mucosa using real-time cross-polarization (CP)OCT/ OCT MA.

**Materials and Methods.** Twelve volunteers aged from 30 to 65 years were studied with MM OCT [3, 4]. The central wavelength of the device was 1310 nm, radiation power 2 mW. The axial resolution was 10 μm, and lateral resolution 15 μm. At least six MM OCT 3D volumetric data sets were acquired from left and right cheeks (3 from each) in one session to verify consistency. The probe was placed on the oral mucosa surface and stayed in contact during 26 sec – the time needed for $3\times3\times1$ mm$^3$ image acquisition. An advantage of the used MM OCT device is real-time image construction. Structural (images in co- and cross-polarizations) and MA images are displayed on the personal computer monitor in the process of scanning, facilitating image quality assessment.

**Results.** Two issues were taken into account for obtaining good quality, informative MM OCT images. For OCT MA images, relative stability of OCT scanning head and of the patient is critical, thus systems of mechanical stabilization of both patients head and the probe were utilized. For acquisition of CP OCT images suitable for comparison, the effect of probe pressure on the mucous membrane must be considered. It was found that a change in the tissue compression impacts greatly layers contrast and epithelial thickness. Also, for monitoring the mucous membrane of the volunteer's cheeks, repeatability of structural and angiographic images was confirmed. Therefore, strict adherence to the developed protocol of MM OCT study is recommended.

**Conclusions.** To optimize *in vivo* MM OCT study of human cheek mucosa, tissue motion and compression should be accurately controlled. MM OCT technology can become important in clinical studies, for example, to predict severity of mucositi in various types of antitumor therapies (chemo-, radiotherapy) by assessing cheek mucosa reaction, as well as identification of various pathological conditions of oral mucosa.

**Acknowledgements**

The study was supported by the Government of the Russian Federation, the Ministry of Education and Science of the Russian Federation, contract No.14.B25.31.0015. The development of OCT image post-processing and data analysis methods was funded by the RFBR project No. 16-32-60178 mol_a_dk.

**References**

1. A. Calantog, L. Hallajian, T. Nabelsi, *et al.*, *Lasers Surg Med,* 2013, **45**, 22–27.
2. W.J. Choi and R.K. Wang, *Biomed Opt Express,* 2014, **5**(8), 2620–2634.
3. V.M. Gelikonov and G.V. Gelikonov, *Laser PhysLett.*, 2006, **3**, 445–451.
4. L. Matveev, V. Zaitsev, G. Gelikonov, *et al.*, *Optics letters*, 2015, **40**(7), 1472–1475.

# APPROACHES OF MOLECULAR IMAGING OF BIO-TISSUES AND MACHINE LEARNING METHODS FOR MEDICAL APPLICATIONS

**Yu.V. Kistenev**[1], **A.V. Borisov**[2], **V.V. Nikolaev**[2], **D.A. Vrazhnov**[2], **L.V. Spirina**[3], and **O.S. Kurochkina**[4]

[1] Tomsk State University, Tomsk, Russia, yuk@iao.ru
[2] Tomsk State University, Tomsk, Russia
[3] Scientific research Institute of Oncology of TomskNational ResearchMedicalCenterofthe RussianAcademyofSciences, Tomsk, Russia
[4] TheInstituteofmicrosurgery, Tomsk, Russia

**Abstract.** The presentation is focused on content analysis of 2D spectroscopic images of bio-tissues using Machine Learning methods. The analysis includes evaluation of the hierarchy of informative features of initial image and classification. The examples of this approach to malignant tumor tissues classification and other applications will be presented.

In this study, we consider the problem of content analysis of 2D spectroscopic images of human tissues.

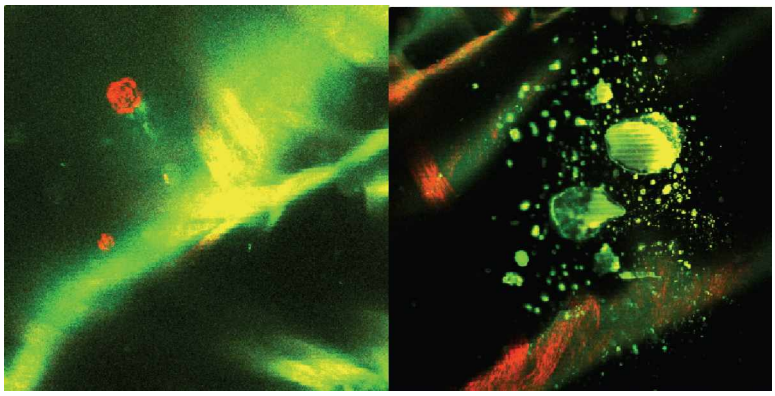
The experimental base includes time-domain THz spectrometer "T-Spec" (EXPLA) with tuning range 0.3–3 THz and ability of regular position in the XY space and MPTflex Multiphoton Laser Tomograph (JenLab) with FLIM module.

The used Data Mining methods include Canonical Correlation Analysis, Principal Component Analysis for selection of most informative features and reduction of the dimension of initial feature space, a number of methods of classification of the results, such as Support Vector Machine, SIMCA, Neural Networks.

The examples of diagnostics using Data Mining analysis of 2D spectroscopic images of human tissues will be presented.

We will consider the problem of diagnostics of malignant tumors biotissues in the THz range.

The second example is connected with visualization of lymphatic vessels in patients with lymphedema, components of lymphatic fluid, including leukocytes (Fig. 1a) and lymphocytes (Fig. 1b).



a) b)

**Fig. 1**

*Poster*

# QUANTITATIVE EVALUATION OF COLLAGEN RADIATION-INDUCED CHANGES BY LASER SCANNING MICROSCOPY

**M.V. Kochueva**[1], **S.S. Kuznetsov**[1], **V.V. Dudenkova**[1,2], **A.V. Varlamova**[2], and **A.V. Maslennikova**[1,2]

[1] Nizhny Novgorod State Medical Academy, Russia
[2] Lobachevsky State University, Nizhny Novgorod, Russian Federation
[3] Institute of Applied Physics RAS, Nizhny Novgorod, Russia

**Abstract.** The objective of our study was quantitative evaluation of the dose-time dependences of changes occurring in the extracellular matrix of bladder and rectum after gamma-irradiation by laser scanning microscopy. LSM microscopy with the detection of second-harmonic generation (SHG) signal allows evaluating radiation-induced changes of normal tissues in addition to standard and special histological staining. Numerical calculation of SHG signal intensity provides additional information about the processes of collagen degradation and subsequent remodeling.

## Introduction

Radiotherapy, like all other cancer treatment modalities, not only results in beneficial effects with regard to tumor control, but is also associated with side effects in disease-free normal tissues [1]. One of the crucial mechanisms of the development of radiation complications is the reaction of the extracellular matrix (ECM) [2]. However, the detailed study of the dynamics of collagen damage and remodeling has not been performed until now.

## Materials and methods

Rat's bladder and rectum were exposed in vivo using a $^{60}$Co external beam unit (Terabalt, UJP, Czech Republic) in single doses equivalent to 2 Gy, 10 Gy and 40 Gy by a local field. Internal organs samples were studied a day, a week and a month after irradiation by LSM Axiovert 510 Meta (Carl Zeiss, Germany) with the following settings: excitation by femtosecond Ti:Sapphire laser at the wavelength of 800 nm and frequency repetition rate of 80 MHz, registration at 362–415 nm (SHG signal of collagen). The same material was prepared using van Gieson staining.

For numerical evaluation of the collagen state regions of interest on the images of 2D distribution of SHG signal intensity of collagen were chosen in the submucosa. The mean signal intensity of SHG signal and its standard deviation were calculated in ImageJ 1.39p (NIH, USA).

## Results

A day after bladder irradiation in the doses of 10 Gy and 40 Gy, a decrease of mean signal intensity was observed. After 40 Gy irradiation, the signal intensity decreased from 1±0.31 a.u. (intact sample) to 0.42±0.04 a.u., after 10 Gy irradiation – to 0.52±0.12 a.u. A week after bladder irradiation, a decrease of signal intensity after 10 Gy and 40 Gy exposure remained. A month after 10 Gy irradiation, the intensity of SHG signal returned to the initial level, but not after 40 Gy irradiation. The dose of 2 Gy did not influence the SHG signal intensity.

A day after rectum irradiation in all doses, a decrease of mean signal intensity was observed. The maximum signal intensity decrease was from 1±0.12 a.u. (intact sample) to 0.48±0.02 a.u. after 40 Gy irradiation. A week after 2 Gy, 10 Gy and 40 Gy exposure, the signal intensity decreased still more. A month after rectum irradiation in the dosesof 2 Gy and 10 Gy, the tendency to return of the signal intensity to the initial level was observed, but after 40 Gy irradiation the intensity decreased again to 0.29±0.011 a.u.

## Conclusions

Numerical calculation of SHG signal intensity provides additional information about the processes of collagen degradation and subsequent remodeling.

## Acknowledgements

This work was supported by the Russian Foundation for Basic Research (16-02-00670).

## References

1. W. Dorr, *Nuklearmedizin*, 2010, **49**(1), 53–58.
2. C. Fiorino, R. Valdagni, T. Rancati, and G. Sanguineti, *RadiotherOncol.*, 2009, **93**, 153–167.

*Invited*

# OPTICAL COHERENCE ELASTOGRAPHY OF SOFT TISSUE

**K.V. Larin**

University of Houston, Houston, USA
klarin@uh.edu

**Abstract.** Optical coherence elastography (OCE) is a relatively new emerging method allowing to assess biomechanical properties of tissues in situ and in vivo in 3D. In this talk I will overview recent progress made in the quantitative assessment of viscoelasticity of ocular and cardiac tissues.

This overview will focus on techniques and methods of *dynamic* optical coherence elastography (OCE). For example, low-amplitude elastic deformations in mice and rabbit ocular tissues and mice hearts (both ex vivo and in vivo) were measured by the OCE system consisting of a phase-sensitive optical coherence tomography (OCT) combined with focused ultrasound (lens excitation) or air-puff (cornea and heart muscle excitation) systems used to produce a transient force on the tissue surface. The amplitude, temporal profile, and the speed of the deformations were used to reconstruct tissue biomechanical properties using novel analytical models. The results of these studies demonstrate that the OCE system can be used for noninvasive analysis and quantification of tissue biomechanical properties in 2D and 3D in normal and pathological tissues and as a function of tissue aging or therapy (e.g. CLX procedures). At the end, I'll introduce our recent advances in ultra-high speed imaging and assessment of the elastic waves using several configurations such as MHz laser swept source and optimizing scanning/imaging methods (such line-field low-coherence holography).

*Poster*

# REFRACTION PROPERTIES OF HEMOGLOBIN IN A WIDE TEMPERATURE AND WAVELENGTH RANGE

**E.N. Lazareva**[1,2,3] and **V.V. Tuchin**[1,3,4]

[1] Research Educational Institute of Optics & Biophotonics, Saratov National Research State University, 83 Astrakhanskaya str., 410012 Saratov, Russia
[2] Center for Functionalized Magnetic Materials (FunMagMa), Immanuel Kant Baltic Federal University, 236041, Kaliningrad, Russia
[3] Interdisciplinary Laboratory of Biophotonics, National Research Tomsk State University, Tomsk, Russia
[4] Laboratory of Laser Diagnostics of Technical and Living Systems, Institute of Precision Mechanics and Control RAS, Saratov, Russia

**Abstract.** Precise measurement of refractive index (RI) of biological materials is of great interest in many areas of biomedical science and engineering, including design and development of optical measurement instruments for biology and medicine, i.e., optical tomography and biopsy. This study is focused on measuring the RI of hemoglobin at different temperatures for visible and near infrared regions. Measurements were carried out using the multi-wavelength Abbe refractometer (Atago, Japan). The RI specific increments for concentration and temperature variations and coefficients for Sellmeier dispersion formula were estimated.

The measurement of optical properties of biological tissues and liquids is one of the topical problems of biophotonics. The refractive index correlates well with density, composition, and temperature of biological materials and wavelength of the probing light [1, 2]. While the RI data of most transparent and semi-transparent materials can be found in handbooks, the RIs of biological materials are not fully available especially for a number of important wavelengths and temperatures. The RI data presented in the literature also varies greatly across publications.

In this study, the RI of hemoglobin was measured at different temperatures for visible and near infrared regions. Measurements were carried out using the multi-wavelength Abbe refractometer (Atago, Japan). Samples of hemoglobin solutions of 80, 120 and 160 g/l were investigated at the wavelengths of 480, 486, 546, 589, 644, 656, 680, 930, 1100, 1300 and 1550 nm. The temperature was varied from room temperature, often used in vitro studies, up to physiological and above that may appear at different electromagnetic wave treatments, i.e., from 25 to 50 °C with the step of 1 °C.

Based on the measurements, the RI specific increments for concentration and temperature variations and coefficients for Sellmeier dispersion formula were evaluated. The specific increments of hemoglobin RI on concentration for temperature T = 25 °C were 0.199±0.005 ml/g for $\lambda$ = 480 nm, 0.195±0.004 ml/g for $\lambda$ = 589 nm, 0.182±0.003 ml/g for $\lambda$ = 930 nm. The temperature dependence of RI was analyzed for the presence of critical temperatures. For example, the temperature 41 °C was determined as critical for hemoglobin solution of 120 g/l. The temperature specific increments of RI for hemoglobin solution of 120 g/l were $-1.85\pm0.07\cdot10^{-4}$ °C$^{-1}$ for $\lambda$ = 480 nm, $-1.85\pm0.04\cdot10^{-4}$ °C$^{-1}$ for $\lambda$ = 589 nm, $-1.79\pm0.05\cdot10^{-4}$ °C$^{-1}$ for $\lambda$ = 930 nm below 41 °C, and $-0.568\pm0.017\cdot10^{-4}$ °C$^{-1}$ for $\lambda$ = 480 nm, $-0.624\pm0.010\cdot10^{-4}$ °C$^{-1}$ for $\lambda$ = 589 nm, $-0.676\pm0.011\cdot10^{-4}$ °C$^{-1}$ for $\lambda$ = 930 nm above 41 °C. The coefficients for Sellmeier dispersion formula A1 = 0.89731, A2 = 1.03737, B1 = 9562.87827 nm$^{-2}$, B2 = $6.61725\cdot10^{7}$ nm$^{-2}$ for 25 °C, A1 = 0.89055, A2 = 1.53725, B1 = 9705.77346 nm$^{-2}$ B2 = $9.88751\cdot10^{7}$ nm$^{-2}$ for 37 °C, and A1 = 0.88678, A2 = 1.22253, B1 = 9828.33162 nm$^{-2}$, B2 = $7.90714\cdot10^{7}$ nm$^{-2}$ for 50 °C were evaluated for hemoglobin solution of 120 g/l.

## Acknowledgements

The work was supported by the Russian Presidential grant 14.Z57.16.7898-NSh.

## References

1. N. Bosschaar, G.J. Edelman, M.C.G. Aalders, T.G. van Leeuwen, and D.J. Faber, *Lasers Med Sci*, 2014, **29**, 453–479.
2. Zh. Deng, J. Wang, Q. Ye, T. Sun, W. Zhou, J. Mei, Ch. Zhang, and J. Tiann, *J. Biomed. Opt.*, 2016, **21**(1), 015003.

*Invited*

# PARALLELIZED RESOLFT NANOSCOPY

**M. Leutenegger**

Max Planck Institute for Biophysical Chemistry, Department of NanoBiophotonics, Göttingen, Germany
marcel.leutenegger@mpibpc.mpg.de.

**Abstract.** Optical nanoscopy based on the RESOLFT concept has recently been parallelized to image larger fields of view more rapidly. This advance relies on using light patterns with arrays of intensity minima for discerning objects by switching their fluorophores between fluorescent and non-emissive states. We demonstrate highly parallelized, multicolor RESOLFT nanoscopy in living cells at 80–100 nm resolution and discuss novel image reconstruction algorithms that incorporate background rejection and image formation models.

Fluorescence microscopy is rapidly turning into optical nanoscopy. Among the various nanoscopy methods, the STED (stimulated emission depletion) and RESOLFT (reversible saturable/switchable optical linear fluorescence transitions) super-resolution family has recently been expanded to image larger fields of view within a few seconds. STED/RESOLFT directly discerns sample features located within subdiffraction length scales by transiently preparing their fluorescent labels in two distinct states (fluorescence 'on' and 'off') using patterns of light featuring one or more intensity minima.

Switching of reversibly photo-switchable fluorescent proteins at low light intensities has rendered the implementation of parallelized RESOLFT with ~100,000 simultaneous intensity minima possible [1]. Parallelized RESOLFT demands for coaligned switching and read-out patterns of equal periodicity at different wavelengths. We have split the light with a grating and recombine it in the focal plane of the objective lens to render arrays of minima with wavelength-independent periodicity [2]. Applying up to three such periodic patterns on the switchable fluorescent proteins Dreiklang and rsCherryRev1.4, we demonstrate highly parallelized, multicolor RESOLFT nanoscopy in living cells at ~80–100 nm resolution in up to 100×100 μm$^2$ fields of view.

Parallelized RESOLFT implementations to date suffer from the blurry background stemming from out-of-focus features, as is well-known in wide-field microscopy. We addressed this issue by novel image reconstruction methods based on either a spatial bandpass filtering or a maximum likelihood fitting of the acquired images [2]. This analysis features background rejection and greatly improved the contrast of the RESOLFT images without sacrificing spatial resolution (see figure 1).

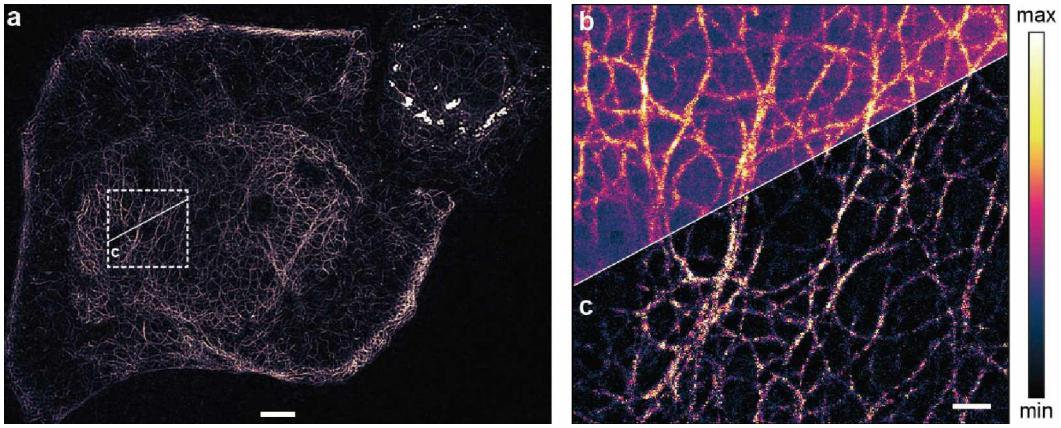



**Fig. 1.** Parallelized RESOLFT nanoscopy of living HeLa cells expressing proteins fused to Dreiklang. RESOLFT image reconstructed with local pinholes [1] (b) and by incorporating an image formation model (a, c). Scale bars: 5 μm (a), 1 μm (b, c). Displayed fields of view: 78×61 μm$^2$ (a), 11×11 μm$^2$ (b, c)

## Acknowledgements

This work was funded by the German Federal Ministry of Education and Research (BMBF) within the project "Ultraschnelle RESOLFT-Mikroskopie (VideoRES)" (FKZ: 13N12993, 13N12995).

## References

1. A. Chmyrov, J. Keller, T. Grotjohann, M. Ratz, E. d'Este, S. Jakobs, C. Eggeling, and S.W. Hell, *Nat. Methods*, 2013, **10**, 737–740.
2. A. Chmyrov, M. Leutenegger, T. Grotjohann, A. Schönle, J. Keller-Findeisen, L. Kastrup, S. Jakobs, G. Donnert, S.J. Sahl, and S.W. Hell, *Sci. Rep.*, 2017, **7**, 44619.

*Poster*

# PERSPECTIVES OF SILICON NANOPARTICLES IN OPTICAL BIOMEDICAL IMAGING

**D.A. Loginova[1,2], E.A. Sergeeva[1], P.D. Agrba[1,2], S.V. Zabotnov[3], F.V. Kashaev[3], D.E. Presnov[3,4], M.B. Gongalsky[3], L.A. Golovan[3],** and **M.Yu. Kirillin[1]**

[1] Institute of Applied Physics RAS, Nizhny Novgorod, Russia
[2] Lobachevsky State University of Nizhny Novgorod, Nizhny Novgorod, Russia
[3] Lomonosov Moscow State University, Faculty of Physics, Moscow, Russia
[4] Lomonosov Moscow State University, Skobeltsyn Institute of Nuclear Physics, Moscow, Russia

**Abstract.** We study the optical properties of silicon nanoparticle suspensions and demonstrate their efficiency as contrasting agents in different optical bioimaging techniques in experiment and in Monte Carlo simulations. Upon administration, the silicon nanoparticles locally change biotissue optical properties thus affecting images acquired by optical techniques.

Nowadays biocompatible nanoparticles are widely used in biomedical applications. In particular, gold nanoparticles were earlier demonstrated as efficient contrasting agents in optical tomography modalities [1], however, their toxicity is still a point of discussion. Recent studies demonstrated silicon nanostructures as anon-toxic, biocompatible and biodegradable nanoparticle class [2]. A high refractive index and optical properties controlled through manufacturing technologies promise silicon nanoparticles a great potential as contrasting agents in bioimaging problems.

In this work, silicon nanoparticle ensembles fabricated through electrochemical etching (porous silicon) followed by picosecond laser ablation (1064 nm, 34 ps, 10 mJ, 10 Hz) in water were studied. Nanoparticles size varied in the range between 30 and 300 nm in accordance with scanning electron microscopy and dynamic light scattering data. The optical properties of nanoparticle suspensions in the range of 400–1100 nm were reconstructed from spectrophotometry measurements employing an analytical model [3]. The scattering coefficient varied in the 0.09–0.14 $mm^{-1}$ range. The absorption coefficient slightly declined from 0.22 $mm^{-1}$ to 0.001 $mm^{-1}$ with wavelength increase.

The potential of silicon nanoparticles for contrasting structural elements in bioimaging applications was studied in *ex vivo* experiment on controlling optical properties of murine biotissues with nanoparticle administration. The experiments were performed with brain and hind limb muscle tissue samples extracted from 4 laboratory mice and subsequently homogenized. Two samples were prepared for each tissue types: i) composition of homogenized tissue and phosphate buffered saline; ii) composition of homogenized tissue and silicon nanoparticle suspensions. The ratio of concentrations was considered to be 1:1 for both samples. Comparison of scattering coefficient spectra demonstrated the increase in their values on the average by 30% for both tissue samples in the presence of silicon nanoparticles. The increase in absorption coefficient amounted to 30% for brain tissue and 5% for muscle tissue.

### Acknowledgements

This work was supported by the RFBR (grant 15-29-01185).

### References

1. M.Yu. Kirillin, M.V. Shirmanova, M.A. Sirotkina, M.L. Bugrova, B.N. Khlebtsov, and E.V. Zagaynova, *J. Biomed. Opt.*, 2009, **14**, 021017.
2. M. Kilpeläinen, J. Riikonen, M.A. Vlasova, A. Huotari, V.P. Lehto, J. Salonen, K.H. Herzig, and K. Järvinen, *J. Control. Release*, 2009, **137**(2), 166–170.
3. D.A. Loginova, E.A. Sergeeva, A.D. Krainov, P.D. Agrba, and M.Yu. Kirillin, *Quantum Electronics*, 2016, **46**(6), 528–533.

# THE IMPACT OF MEASUREMENT CONFIGURATION ON PROBING DEPTH IN OPTICAL DIFFUSE REFLECTOMETRY: A MONTE CARLO STUDY

**D.A. Loginova**[1,2], **I.I. Fiks**[1], **E.A. Sergeeva**[1], and **M.Yu. Kirillin**[1]

[1] Institute of Applied Physics RAS, Nizhny Novgorod, Russia, vekfy@inbox.ru
[2] Lobachevsky State University of Nizhny Novgorod, Nizhny Novgorod, Russia

**Abstract.** We report on Monte Carlo study of the probing volume in diffuse optical spectroscopy and its modification employing structured illumination. Different configurations of probing illumination including collimated point source, one-dimension sinusoidal and rectangular patterns with various spatial characteristics are considered. Simulation has been performed for a turbid medium with optical properties corresponding to cutaneous tissues at 600 nm and their variations in the range of ±60%.

Diffuse optical spectroscopy (DOS) is a widely used technique in biotissue monitoring. However, for its efficient applications it is important to know the exact probing volume that cannot be measured experimentally. The Monte Carlo technique implying modeling of a large number of random photon trajectories in turbid media with following statistical processing of the results, allows simulating fluence distribution generated by probing illumination and at the same time analyzing an individual photon trajectory. Tracing of maximal depth reached in a turbid medium (photon probing depth) provides information about probing volume.

Employment of structured illumination is a recent DOS modification based on projection of the illumination pattern on the studied object surface and registration of backward scattering signal. The advantage of the technique consists in controlling probing volume through variation of spatial characteristics of illumination patterns.

In this work we performed a series of Monte Carlo numerical experiments on illumination of a biotissue sample by sources with different spatial configuration, including a point source and one-dimensional modulated illumination pattern, and studied the dependence of probing depth on source geometry, source-detector separation (SR), and tissue optical properties.

## Materials and methods

Simulation was performed for a uniform slab sized 10x10 mm in transversal directions and 5 mm in-depth with optical properties corresponding to human skin at the wavelength of 600 nm and their variation in the range of ±60%. The refractive index was set to 1.4. Monte Carlo simulations were performed for a collimated point source located at the medium surface. To model structured illumination, the results obtained for point-source illumination were convolved with the distribution functions of probing patterns. In this study we considered two pattern types: one-dimensional sinusoidal patterns with spatial frequency in the range of 0.3–2.5 $mm^{-1}$ and one-dimensional rectangular patterns with 0.1 mm stripe width and duty cycles varying in the 0.03–0.25 range.

A custom developed MATLAB-based implementation of Monte Carlo algorithm was employed simultaneously processing $10^7$ photon trajectories with recording of the maximal depth reached in the medium by each photon. As a result of Monte Carlo simulation, photon distribution maps over maximum were derived for different source configurations and tissue optical properties.

## Results and discussion

For a collimated point source, the photon fraction diffusively reflected from the medium decreases with probing depth for SR = 0 and has maximum at a definite depth for SR different from zero. The position of this maximum shifts to higher probing depths with $\mu_a$ decrease.

For structured illumination, the photon distributions over probing depth have different trends for detector location corresponding to the centers of bright and dark stripes of the probing pattern. The distribution peak remains close to the surface for the bright stripe center and, on the contrary, shifts towards higher depths for the dark stripe center with decreasing spatial frequency and duty cycle of the considered sinusoidal and rectangular patterns, respectively. The distributions demonstrate stronger dependence on spatial configuration in case of rectangular patterns.

## Acknowledgements

The study is supported by the Russian Foundation for Basic Research (grant # 15-02-04270).

*Invited*

# TOWARDS APPLICATION OF ANGULAR MOMENTUM OF LIGHT FOR TISSUE DIAGNOSIS

**I. Meglinski[1], A. Bykov[1], N.O. Vera Paz[2], J.P. Staforelli[2], A. Doronin[3], T. Novikova[4]**

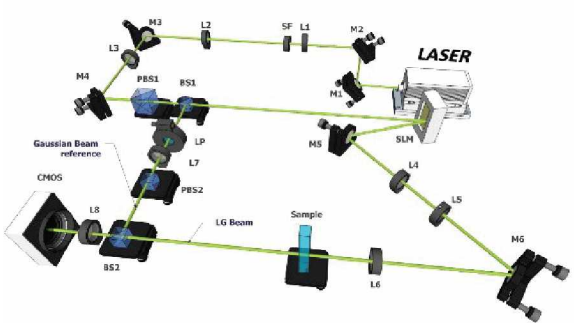
[1] Optoelectronics and Measurement Techniques, University of Oulu, Oulu, 90014 Finland
[2] Facultad de CienciasFísicas y Matemáticas, University of Concepción, Concepción, Chile
[3] Department of Computer Science, Yale University, New Haven, CT 06520-8285, USA
[4] LPICM, CNRS, EcolePolytechnique, Université Paris–Saclay, 91128 Palaiseau, France

**Abstract.** We investigate how the spin-orbit interaction leads to the mutual influence of the polarization and the trajectories of twisted photons (or vector beams) propagating in turbid tissue-like scattering media, and how sensitive are the vector light beams to subtle alterations in biological tissue morphology. An overall aim of the study is to explore the potential applicability of vector light beams for non-invasive tissue diagnosis (optical biopsy) and provide the proof of concept by developing the operating prototype of the instrument for the characterization of complex scattering anisotropic and/or chiral media with vector light beams.

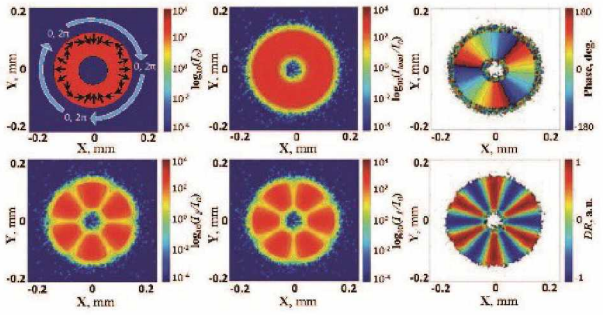
Polarization is the fundamental property of light that has been attracting great attention in various practical applications from space to modern biology and medicine. When the polarized light interacts with the matter its state of polarization is changed. The state of polarization of linearly, elliptically or circularly polarized light ("simple" light) has long been used to characterize material surfaces, thin films and transparent media. In fact, the structure of light can be more "complex", i.e. the light beams can be radially or azimuthally polarized and carry orbital angular momentum. The light with orbital momentum, Laguerre-Gaussian (LG) beams, plays an emerging role in both classical and quantum science, and offers fascinating opportunities for exploring new fundamental ideas, as well as for being used as a tool for practical applications.

We investigate (i) how the spin-orbit interaction leads to the mutual influence of the polarization and the trajectories of twisted photons propagating in turbid tissue-like scattering media, and (ii) how sensitive are the vector light beams to subtle alterations in the scattering medium. Thus, an overall aim is to investigate the potential applicability of LG laser beams for non- invasive tissue diagnosis (optical biopsy).

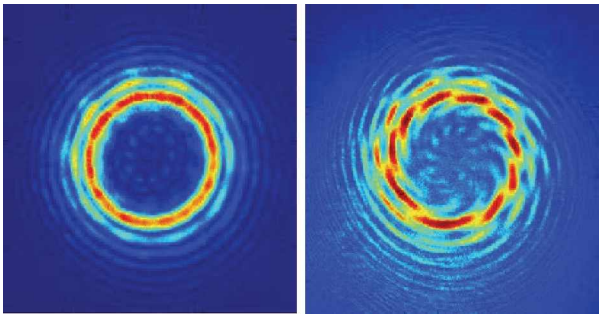
The results of propagation of LG laser beams in the scattering medium obtained by using specially developed Monte Carlo model are presented in comparison with the results of experimental studies (Fig. 1).




(a)




(b)



(c)

**Fig. 1**. (a) Schematic presentation of the experimental system used to the studies of LG beams propagation through the turbid tissue-like scattering medium. (b) The results of Monte Carlo modeling of LG beam ($l = +3$, $\sigma = -1$) transmitted through the scattering medium ($g = 0.9$, $\mu s = 100$ mm$^{-1}$). (c) The experimental results of LG10 propagation through scattering medium.

# TIKHONOV DECONVOLUTION FILTRATION IN ACOUSTIC RESOLUTION PHOTOACOUSTIC MICROSCOPY

**I. Mikhailova**[1], **M. Jaeger**[2], **I. Fiks**[1], **I. Turchin**[1], and **P. Subochev**[1]

[1] Institute of Applied Physics RAS, Nizhny Novgorod, Russia, Pavel.Subochev@gmail.com
[2] Institute of Applied Physics, University of Bern, Switzerland

**Abstract.** Acoustic resolution photoacoustic microscopy (AR-PAM) is a raster-scan imaging technique based on focused ultrasonic detection of wideband optoacoustic (OA) transients thermoelastically induced by nanosecond laser pulses in light-absorbing tissue chromophores. However, a spatial low-pass filter provided by frequency-dependent ultrasonic attenuation of the tissue limits the effective bandwidth of the detected OA pulses reducing spatial resolution. Our poster presentation will be devoted to one-dimensional Tikhonov deconvolution filtration allowing 2-fold improvement in spatial resolution for both phantom and *in vivo* objects.

Acoustical-resolution photoacoustic microscopy (AR-PAM) is a raster-scan imaging technique based on focused ultrasonic detection of wideband optoacoustic (OA) transients thermoelastically induced by nanosecond laser pulses in light-absorbing tissue chromophores. For the given numerical aperture (NA) of a spherically focused ultrasonic detector, theoretical spatial resolution of AR-PAM technique is determined by the detector bandwidth $\Delta f$. However, frequency-dependent ultrasonic attenuation acts like a low-pass filter for a broad spectrum of OA pulses $\Delta f \sim 100$ MHz provided by the smallest blood vessels. As a result, the capillaries can be hardly resolved at raw AR-PAM angiography images [1].

To recover ultra-wideband spectral content of OA transients and therefore improve the spatial resolution, one needs to use post-acquisition software algorithms.This manuscript is devoted to the Tikhonov L-2 norm regularized matrix inversion method, which demonstrated better performance for OA imaging as compared to Fourier division technique and the Wiener deconvolution filtration [2].We applied Tikhonov deconvolution filtration to raw A-scans acquired by AR-PAM system [1] based on spherically focused polyvinylidene fluoride detector ($\Delta f = 30$ MHz, NA = 0.5 corresponding to lateral resolution LR ~ 50 μm and axial resolution AR ~ 38 μm).To optimize two parameters of Tikhonov deconvolution filter (regularization parameter β and the rank of convolution matrix $L$),we introduced contrast enhancement parameter (CEP) for AR-PAM B-scan of the wire phantom:

$$CEP(\beta, L) = \sum OA(x^*, z^*)/\sum[OA(x^* \pm LR/3, z^* \pm AR/2)]/SDN(z^*)], \quad (1)$$

with $x^*$ and $z^*$ – lateral and axial coordinates of local maxima at OA B-scan corresponding to different wires and SDN – standard deviation of noise. After applying the optimized deconvolution filter corresponding to maximum of CEP ($L = 4$, $\beta = 0.3$) the signal-to-noise ratio (SNR) of OA signals at wire positions did not change significantly, while ~2-fold improvement in spatial resolution was achieved. The effect of AR-PAM image enhancement by means of the optimized deconvolution filter was also tested for a raw AR-PAM image of rabbit ear *in vivo*. After Tikhnonov deconvolution filtration, smaller blood vessels corresponding to higher acoustic frequencies could be visualized.

**Acknowledgements**

The study was supported by the Russian Science Foundation (project #14-15-00709). Dr. Pavel Subochev was partly supported by the Scholarship of the President of the Russian Federation (project #SP-3196.2016.4).

**References**

1. P. Subochev, A. Orlova, I. Mikhailova, N. Shilyagina, and I. Turchin, *Biomedical Optics Express*, 2016, 7(10), 3951–3957.
2. D. Van de Sompel, L.S. Sasportas, J.V. Jokerst, and S.S. Gambhir, *PloS one,* 2016, **11**(3), e0152597.

*Invited*

# INTRACORONARY BIREFRINGENCE MICROSCOPY OF ATHEROSCLEROTIC PLAQUE

**S. Nadkarni**

Wellman Center for Photomedicine, Massachusetts General Hospital, Harvard Medical School, USA

*Invited*

# OVERCOMING THE TRADE-OFF BETWEEN DEPTH OF FIELD AND LATERAL RESOLUTION IN SCANNING PHOTOACOUSTIC IMAGING WITH FOCUSED DETECTORS

**G. Paltauf, P. Torke,** and **R. Nuster**

Department of Physics, University of Graz, Austria,
guenther.paltauf@uni-graz.at

**Abstract.** Photoacoustic imaging with a scanning, focused detector yields images with high resolution and signal to noise ratio. However, there is a trade-off between the lateral resolution and the depth of field, similar to optical microscopy techniques. Several methods to overcome this trade-off are presented, including reconstruction of out-of-focus structures from scanning data and hardware solutions, where the focusing element has an extended focal region. The latter include annular arrays of flat or inclined piezoelectric elements.

Photoacoustic (or optoacoustic) imaging reveals structures with optical absorption contrast in strongly scattering biological tissue. Several ways to reconstruct the distribution of absorbed optical energy from the recorded photoacoustic signals are known, such as tomographic algorithms that employ large datasets recorded at multiple detector positions in an ultrasound array. A less complex but very sensitive approach is the scanning of a single, focused sensor across the tissue surface. Particularly in an acoustic resolution mode, where the lateral resolution is given by the acoustic focusing, there exists the known trade-off between resolution and depth of field: If a large numerical aperture lens is used, high resolution in the focus can be achieved but structures located outside the focus will quickly become blurred. On the other hand, large depth of field can be achieved at the expense of lateral resolution. In this work, several approaches to address this trade-off will be discussed, involving both reconstruction (software) and special focusing (hardware) techniques.

Since the axial resolution is given by the temporal resolution of the sensor, it is decoupled from the lateral resolution. Moreover, structures lying before or behind the focus can be discriminated via the time of flight of the corresponding acoustic signals. This allows the application of reconstruction methods for recovering structures lying out of focus with improved lateral resolution [1, 2]. The full lateral resolution given by the numerical aperture of the acoustic lens can be achieved, but only if the sensor is scanned a distance that is larger than the size of the resolved structure.

Hardware solutions, which are the main focus of this study, use special detectors that have the possibility to focus to an extended depth range without suffering a degrading of the lateral resolution and without requiring extended scanning. We have investigated conical sensors that work like optical axicon lenses and have an extended acoustic focus with a range given by the geometry of the sensor [3]. Since such detectors tend to create strong, "X"-shaped artifacts, a more flexible approach uses an annular array detector [4]. Signals recorded at several flat rings can be combined to achieve dynamic focusing into an extended depth of field. However, the outer rings in such an array receive waves at a relatively large angle of incidence, limiting their sensitivity. Therefore, in a modified annular array sensor, the ring elements are inclined towards the symmetry axis to achieve good sensitivity and high resolution at the same time.

### Acknowledgment

This work has been supported by the Austrian Research Promotion Agency (FFG), project No. 846559 and by the Austrian Science Fund (FWF), Project No. P 28032.

### References

1. M. Li, H.F. Zhang, K. Maslov, G. Stoica, and L.V. Wang, "Improved *in vivo* photoacoustic microscopy based on a virtual-detector concept," *Opt. Lett.*, 2006, **31,** 474–476.
2. M.A.A. Caballero, A. Rosenthal, J. Gateau, D. Razansky, and V. Ntziachristos, "Model-based optoacoustic imaging using focused detector scanning," *Opt. Lett.*, 2012, **37,** 4080–4082.
3. G. Paltauf, S. Gratt, K. Passler, R. Nuster, and P. Burgholzer, "Photoacoustic imaging with limited diffraction beam transducers", *Proc. SPIE*, 2009, **7177**, 71770S.
4. K. Passler, R. Nuster, S. Gratt, P. Burgholzer, and G. Paltauf, "Piezoelectric annular array for large depth of field photoacoustic imaging," *Biomed. Opt. Express*, 2011, **2,** 2655–2664.

# IN VIVO TWO-WAVELENGTH MAPPING OF BLOOD OXYGEN SATURATION BY ACOUSTIC RESOLUTION PHOTOACOUSTIC MICROSCOPY

**V.V. Perekatova, P.V. Subochev, M.Yu. Kirillin, A.G. Orlova,** and **I.V. Turchin**

Institute of Applied Physics RAS, Nizhny Novgorod, Russia
ValeriyaPerekatova@gmail.com

**Abstract.** Spectral approach in optoacoustic (OA) imaging allows simultaneous mapping of the structure and oxygenation status of the vasculature, which makes this approach well suited for different biomedical applications. We report on the novel OA system operating at the wavelengths of 658 and 1069 nm, which enabled *in vivo* blood oxygen saturation mapping in rabbit ear at depths up to 1.5 mm.

Multispectral optoacoustic (OA) measurements in addition to structural imaging allow obtaining important functional information about inspected biological tissue, such as blood oxygen saturation. The ability to map the structure and oxygenation status of the vasculature makes OA imaging well suited for different biomedical applications. Oxygen saturation of hemoglobin in biological tissues is critical in assessment of tumor response to treatment, including chemotherapy, monitoring of brain hemodynamics, wound healing and other processes characterized by local alterations in tissue oxygenation.

Since oxygenated and deoxygenated hemoglobin have different absorption spectra, blood oxygen saturation can be extracted from OA measurements at two wavelengths with high accuracy and high spatial resolution. However, quantitative OA measurements of optical absorption face significant challenges [1]. The OA signal from an elementary volume will depends both on local absorption spectrum of this volume and on local spectral distribution of optical probing radiation fluence, which depends on local absorption and scattering. Therefore, for precise multispectral OA measurements of blood oxygen saturation both spatial and spectral dependencies of the optical fluence in the tissue should be taken into account.

The goal of this study was to evaluate the capabilities of *in vivo* OA measurements of oxygen saturation of hemoglobin ($StO_2$) at previously determined optimal wavelengths of 658 nm and 1069 nm [2], taking into account fluence distribution in the tissue.

*In vivo* estimations of blood oxygen saturation distribution were performed in an ear of a rabbit, fixed and anesthetized with an intramuscular injection of Zoletil 100 (15 mg/kg) and with Rometar (5 mg/kg). All *in vivo* experiments were conducted using OA system [3], providing confocal laser illumination and ultrasonic detection. A three-dimensional OA image of vasculature map was obtained at the wavelength of 532 nm by mechanical scanning with 25 μm step in the X and Y axis direction (corresponding to the range of scanning 10 mm by 10 mm). Further, 10 B-scans corresponding to scanning along the X axis for different Y positions with step 1 mm at the wavelengths of 658 nm and 1069 nm were recorded. Afterwards, blood oxygen saturation maps were reconstructed based both on the recorded OA data and the results of Monte Carlo simulations of axial fluence distribution at two wavelengths for ring-shaped geometry of the OA illumination system and optical properties typical for biological tissues. The obtained saturation maps in different cross-sections featured arteries and veins in rabbit ear that were consistent with the physiological structure of ear vasculature.

### Acknowledgements

The work was supported by the Russian Science Foundation, project no. 14-15-00709. The authors thank A.V. Khilov for helpful discussions of the results.

### References

1. B. Cox, J. Laufer, and P. Beard, *SPIE BiOS: Biomedical Optics – International Society for Optics and Photonics*, 2009, 717713-717713-9.
2. V. Perekatova, P. Subochev, M. Kleshnin, and I. Turchin, *Biomedical Optics Express*, 2016, **7**(10), 3979–3995.
3. P. Subochev, *Optics Letters*, 2016, **41**(5), 1006–1009.

*Poster*

# A COMBINATION OF THREE-DIMENSIONAL VIRTUAL POINT DETECTOR CONCEPT AND FLUENCE COMPENSATION IN ACOUSTIC RESOLUTION PHOTOACOUSTIC MICROSCOPY

**V.V. Perekatova, M.Yu. Kirillin, I.V. Turchin,** and **P.V. Subochev**

Institute of Applied Physics RAS, Nizhny Novgorod, Russia, ValeriyaPerekatova@gmail.com

**Abstract.** We report on combined application of the synthetic aperture focusing technique approach and fluence compensation in acoustic resolution photoacoustic microscopy. Both software post-acquisition procedures are performed in full-3D allowing significant enhancement of resultant image quality.

Optoacoustic (OA) imaging is based on wideband detection of ultrasonic waves generated in the studied biological tissue by chromophores absorbing optical nanosecond-pulsed radiation. One of the simplest hardware implementations of 3D OA imaging is acoustic resolution photoacoustic microscopy (AR-PAM) based on raster-scanning of an investigated object by a spherically focused ultrasonic detector with target bandwidth and numerical aperture defining the spatial resolution [1]. The drawback in using focused ultrasonic transducers with high numerical aperture is limited depth of the focus. To improve resolution of 3D AR-PAM imaging, the studied sample is often scanned in additional focal planes [2], although software post-acquisition algorithms of acoustic inversion [3] are also very effective.

The synthetic aperture focusing technique (SAFT) based on the simple virtual-point-detector (VPD) concept [1] was proposed to improve the lateral resolution outside the focus by means of axial resolution of AR-PAM modality. Nevertheless, application of the original 2D SAFT technique [1] to 3D AR-PAM data set comes at a cost of artifacts provided by the signals along the third, unaccounted for dimension. Although quasi-3D implementations of 2D SAFT technique in two perpendicular directions [4] further improve lateral spatial resolution of AR-PAM images, 3D directionality of spherically focused detector can only be accounted for within accurate full-3D implementation of the SAFT technique, which has been done in [5].

Another limitation of AR-PAM 3D imaging is a rapid in-depth attenuation of probing laser radiation due to strong scattering and absorption in biological tissues, which limits the diagnostics depth. In order to cope with this limitation, the compensation of fluence distribution is needed. The optical illumination system of AR-PAM usually employs conical laser-beam geometry aiming at confocal probing. Accurate calculation of fluence distribution with a sample produced by such beams can hardly be achieved by analytical techniques, especially, if the sample is optically inhomogeneous. In this situation, Monte Carlo simulation of light transport accounting for complex geometry of laser illumination seems to be an optimal tool.

In this paper we report on the novel approach combining the three-dimensional synthetic aperture focusing technique with three-dimensional fluence compensation based on Monte Carlo simulation. Monte Carlo code previously customized for accounting for the exact geometry of the probing beam is employed to produce 3D distribution of optical fluence within a ample for optical properties typical for the tissue under study [6]. Three-dimensional raw AR-PAM data is compensated for the produced fluence map at the first stage of processing prior to the SAFT procedure. At the second stage, the SAFT procedure is performed in full-3D [5] unlike the initially proposed approaches [1, 4].

AR-PAM with combined SAFT and fluence compensation techniques was employed for both phantom objects and *in vivo* imaging demonstrating significant enhancement of image quality.

**Acknowledgements**

The work was supported by the Russian Science Foundation, project no. 14-15-00709. Dr. Pavel Subochev was partly supported by the Scholarship of the President of the Russian Federation (project #SP-3196.2016.4).

**References**

1. M.-L. Li, H.F. Zhang, K. Maslov, G. Stoica, L.V. Wang, *Optics Letters*, 2006, **31**(4), 474–476.
2. M. Omar, J. Rebling, K. Wicker, T. Schmitt-Manderbach, M. Schwarz, J. Gateau, H. López-Schier, T. Mappes, and V. Ntziachristos, *Light: Science & Applications*, 2017, **6**(1), e16186.
3. L. Ding, X.L. Deán-Ben, and D. Razansky, *IEEE Transactions On Medical Imaging*, 2017.
4. Z. Deng, X. Yang, H. Gong, and Q. Luo, *Optics Express*, 2012, **20**(7), 7555–63.
5. D. Cai, Z. Li, Y. Li, Z. Guo, and S.-L. Chen, *Optics Express*, 2017, **25**(2), 1421–1434.
6. V. Perekatova, P. Subochev, M. Kirillin, and I. Turchin, *Proc. of SPIE*, 2017, **10064**, 100645K-1.

*Invited*

# MULTIMODAL DYNAMIC AND STRUCTURAL IMAGING OF ERYTHROCYTES AND BLOOD CAPILLARIES

**A.V. Priezzhev[1], K. Lee[1,2], F. Yaya[2], C. Wagner[2], A.N. Semenov[1], A.E. Lugovtsov[1], S.Yu. Nikitin[1], and E.A. Shirshin[1]**

[1] Physics Department and International Laser Center of Lomonosov Moscow State University, Moscow, Russia
avp2@mail.ru
[2] Experimental Physics, Saarland University, Saarbrücken, Germany

**Abstract.** Several optical techniques were used to make a complex study of various parameters related to the fundamental properties of erythrocytes, aggregation and deformation, by means of imaging and measurement. Diffuse light scattering, laser diffractometry, and dual- and multiple channel laser tweezers were applied in the experiments *in vitro*. Computerized capillaroscopy and laser two-photon lifetime imaging microscopy were used for imaging the structure of the terminal capillaries and papillary dermis in the fingernail bed and the inner forearm area *in vivo*.

The ability of the erythrocytes to perform their functions is mostly due to their two intrinsic properties: reversible erythrocyte aggregation (EA) and erythrocyte deformability (ED). The former one optimizes the interaction of the moving cells with the walls in the vessels of various sizes, while the latter one enables the erythrocytes to squeeze through the terminal capillaries, given that the diameters of the capillaries are smaller than those of the cells in some parts of the body. The dynamic processes of EA and ED are tightly connected with the structural changes of the cells and the terminal capillaries. Both EA and ED were given a lot of attention especially during the last several decades. Many techniques were designed and applied to assess the mechanisms of EA and ED and their dependences on blood content and changes at various diseases. The same is true in relation to the terminal vessels and the surrounding tissues where the gas and liquid exchange with blood takes place. However many important issues are still to be studied.

In this work, we combined several optical techniques to perform a complex study of various parameters related to EA and ED by means of imaging and measurement. We used: 1) diffuse light scattering; 2) laser diffractometry; 3) dual- and multiple channel laser tweezers, also combined with microfluidics,. The above mentioned imaging and measurement experiments were performed *in vitro*. Also we used: 4) computerized capillaroscopy and 5) laser fluorescence lifetime imaging microscopy (FLIM) for imaging the terminal capillaries and papillary dermis in the fingernail bed and the inner forearm area *in vivo*.

Imaging of a pair of individual erythrocytes trapped by laser tweezers in the process of their interaction allowed us to measure the range of the interaction forces in dependence of their interaction surface area, velocity of relative movement and the proteins content in the suspending medium. We showed that the aggregating and disaggregating forces are significantly different from each other. The studies of the cells interaction kinetics in model solutions revealed a significant importance of the synergy of the contributions of different proteins or other blood components, especially for initiating the spontaneous aggregation. The diffraction imaging of erythrocyte suspensions at different shear stresses allowed to quantitatively estimate the first several moments of the erythrocyte deformability distributions characteristic of various diseases. Using FLIM of endogenous compounds allowed us to assess the molecular structure of internal and external regions of skin capillaries. It was shown that the capillaries are characterized by a fast fluorescence decay, which is originated from the blood cells and blood plasma. Using the SHG signal, FLIM segmentation was performed, which provided for spatial localization and fluorescence decay parameters distribution of collagen I and elastin in the dermal papillae. It was demonstrated that the lifetime distribution was different for the inner area of dermal papillae around the capillary loop that was suggested to be due to collagen III.

## Acknowledgements

This study was supported by RFBR grants 17-02-01200 and 17-02-00249.

## References

1. A.V. Priezzhev and K. Lee, *Clin. Hemorheol.Microcirc.*, 2016, **4**, 587–592.
2. E.A. Shirshin, Yu.I. Gurfinkel, A.V. Priezzhev, *et al.*, *Sci. Reports*, 2017, **7**, 1171.

# SELF-ACTING DETECTION AND COMPENSATION OF THE INFLUENCE OF MEDIA DISPERSION IN SD OCT IMAGES

**P.A. Shilyagin, V.A. Matkivskiy, A.A. Moiseev, S.Yu. Ksenofontov, I.V. Kasatkina, G.V. Gelikonov, D.V. Shabanov, and V.M. Gelikonov**

Institute of Applied Physics RAS, Nizhny Novgorod, Russia
paulo-s@mail.ru

**Abstract.** A method for determining and correcting distortions in SD OCT images caused by medium dispersion was developed. The method is based on analysing the phase distribution of the interference signal recorded by an OCT device using the iteration approach to find and compensate the influence of medium chromatic dispersion on PSF broadening in OCT. This allows compensating the impact of medium dispersion to an accuracy of tens of fractions of radian (units of percent) avoiding additional measurements and solution of the optimization problem. The robustness of the method was demonstrated experimentally on model and biological objects.

The proposed method operates with a number of separate fragments of an OCT image assuming that the impact of medium dispersion is similar for a large number of scatterers in a highlighted area of the image. The method is realized iterationally, each iteration consisting of two stages.

At the first stage a number of depth-localized complex-valued optical frequency combs are generated. At the first iteration, an inverse Fourier transformation is performed for each complex-valued optical frequency comb $F(k, x)$ from the set corresponding to an OCT B-scan yielding a complex-valued image $Q(z, x)$. The next step is to automatically select a number of A-scans containing strong local maxima in a certain range of depth $z$. Each selected A-scan is multiplied by a window function centered at the A-scan maximum. The truncated A-scans are used to reconstruct localized spectra in a quasi-harmonic representation.

At the second stage the dispersion-induced image distortions are found and eliminated. As the first step, gradients of the argument of the localized spectra are obtained. The dispersion caused deposit should be equal for every localized spectrum, so averaging of all obtained spectral gradients excluding their constant part gives the value of dispersion gradient. After integration of the result, the approximated dispersion part is obtained and further used to reconstruct the improved complex-valued image.

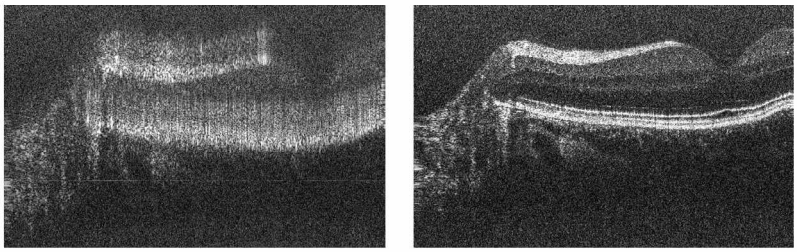


**Fig. 1.** The image improvement provided by the proposed method: the initial image (*left*) and the restored image (*right*) of the volunteer eye obtained in ultrabroadband SD OCT setup

The proposed method has been verified using the common-path spectral-domain OCT setup based on a light source with 980 nm central wavelength and about 200 nm bandwidth (Superlum diodes Ltd). The dispersion-induced distortion results in dramatic broadening of PSF, and some layers (including the inner/outer segment junction layer) are not visible in the left image. The use of the proposed method results in appreciable decrease of the PSF width (the right image) and appearance of layers that were indistinguishable before.

**Acknowledgements**

The research concerning the development of the method was partly supported by the Russian Foundation for Basic Research (grant No. 15-29-03897). The experimental verification part was supported by the State task for IAP RAS project No. 0035-2014-0018.

*Poster*

# COMBINED MICROSTRUCTURAL, POLARIZATION-SENSITIVE AND ELASTOGRAPHIC CHARACTERIZATION OF BREAST CANCER BY OPTICAL COHERENCE TOMOGRAPHY

**E.V. Gubarkova[1], A.A. Sovetsky[2], V.Yu. Zaitsev[1,2], A.A. Moiseev[1,2], L.A. Matveev[1,2], A.L. Matveyev[1,2], S.S. Kuznetsov[1], D.A. Vorontsov[3], A.Yu. Vorontsov[3], N.D. Gladkova[1], and M.A. Sirotkina[1]**

[1] Nizhny Novgorod State Medical Academy, Nizhny Novgorod, Russia, sirotkina_m@mail.ru
[2] Institute of Applied Physics, Russian Academy of Sciences, Nizhny Novgorod, Russia
[3] Nizhny Novgorod Regional Oncologic Hospital, Nizhny Novgorod, Russia

**Abstract.** We have studied feasibility of multimodal OCT (MM OCT) that combines cross-polarization imaging and elastographic stiffness mapping to assess spatial structural organization and heterogeneity of breast cancer (morphological and immuno-histochemical) in the tumor center in comparison with normal mammary gland tissue.

**Introduction.** Breast cancer is the most widespread type of cancer among women all over the world. Complexity of breast cancer is related to the fact that this carcinoma has a broad variability of morphological features. Several morphological types and subtypes of breast cancer such as ductal (infiltrating, non-infiltrating), lobular (infiltrating, non-infiltrating), colloidal, and medullary carcinomas are known [1]. Promising results of using a high-speed polarization-sensitive OCT system for *ex vivo* visualization of human mammary glands was demonstrated in [2]. Mechanical properties of tissues are known to be related to their function and structure that can be changed due to pathology development, as well as in the course of treatment. Application of OCT-based elastography for characterization of tissue mechanical properties was demonstrated *in vivo* [3] and proposed for soft tissues tumor visualization, including breast-cancer margin detection [4, 5].

**Materials and Methods.** The research was carried out using human breast tissue mastectomy surgical samples including different histological types of breast cancer: invasive lobular and ductal carcinoma, fibroadenoma, and normal tissue. All samples were imaged within 2 hours after surgical excision. In this study we used a common path spectral domain MM OCT system with a central wavelength of 1310 nm and spectral width of 100 nm, resulting in axial resolution of 15 μm, scanning depth of 1.7 mm, scanning speed of 20 000 A-scans per second. The system was capable of cross-polarization visualization [6] of connective tissue component, as well as compressional phase-sensitive OCT-elastography [7, 8] was used to visualize inter-frame strains in the tissue. For quantification of the tissue Young's modulus, a reference silicon layer with preliminary calibrated stiffness was used.

**Results.** MM OCT is capable of seeing the difference between microstructure or elastic properties of lobular and ductal breast cancer, fibroadenoma and normal tissue. The obtained results were compared with morphological data and immuno-histochemical status of patients. The lesions showed structural features, as well as increased stiffness typical of tumor tissue. In the case of invasive ductal carcinoma, the CP OCT image shows a more heterogeneous high level of OCT signal and higher stiffness in comparison with lobular breast cancer or fibroadenoma. These results indicate that assessing microstuctures and elasticity changes yields complementary information about the microstructural features of breast cancer, which is important for selection of treatment tactics.

## Acknowledgments

The study was supported by the Russian President grant for young scientists No. MK-905.2017.7. The development of the MM-OCT equipment were supported by the Ministry of Education and Science of the Russian Federation, grant No. 14.B25.31.0015.

## References

1. G.A. Frank, "A practical guide for clinicians", ed. G.A. Frank *et al.*, 2014, 171 p.
2. Boppart *et al.*, *Biomed. Opt. Express*, 2014, **5**(10), 3417–3426.
3. Kennedy *et al.*, *Opt Express,* 2009, **17**(24), 21762–21772.
4. Wang *et al.*, *Opt. Lett.*, 2012, **37** (24), 5184–6.
5. Allen *et al.*, *Biomed. Opt. Express*, **7**(10), 4139–4152 (2016).
6. Zaitsev *et al.*, *Radiophys. and Quantum Electron.*, 2014, **57**(1), 52–66.
7. Zaitsev *et al.*, *J. Biophotonics,* 2016, **9**(5), 499–509.
8. Zaitsev *et al.*, *J. Biomed. Optics*, 2016, **21**(11), 116005.

# STRUCTURAL ILLUMINATING MICROSCOPY AND FLUORESCENT MARKERS IN THE IMAGING OF LASER-INDUCED MODIFICATION OF CARTILAGE AND SCLERA STRUCTURE

**E. Sobol[1], O. Baum[1], and S. Wachsmann-Hogiu[2,3]**

[1] Institute of Photonic Technologies, Federal Scientific Research Centre "Crystallography and Photonics" of the Russian Academy of Sciences, Troitsk, Moscow, Russia
esobol@rambler.ru
[2] University of California, Department of Pathology and Laboratory Medicine and Center for Biophotonics, One Shields Avenue, Davis, Sacramento, USA
[3] Department of Bioengineering, McGill University, Montreal, Canada

**Abstract.** Recent results in laser modification of pore system structure of the tissues toward development of new methods for healing of osteoarthritis and glaucoma are presented. The effect of 1.56 mcm laser radiation on porcine articular cartilage and eye sclera was studied using atomic force microscopy and super resolution structured irradiation microscopy with fluorescent markers. The stabilization of laser-assisted gas and pore systems in the tissues can explain the long lasting healing effect in laser reconstruction of spine discs and in laser creation the uveoscleral pathway for aqueous in glaucomatous eyes.

The paper presents recent results in laser modification of pore system structure of the tissues toward development new methods for healing of osteoarthritis and glaucoma. Laser-induced pores play important role in the process of cartilage regeneration [1]. Pores in eye sclera can be crucial for normalization of intraocular pressure. Effect of 1.56 mcm laser radiation on porcine articular cartilage and eye sclera was studied using atomic force microscopy and super resolution structured irradiation microscopy with fluorescent markers. It is shown that in cartilage the pores and gas bubbles arise predominately near chondrocytes that promotes nutrition and signaling molecules transfer that activates regeneration of cartilage. The images demonstrated that laser-generated gas nanobubbles coated with calcium ions stabilize the pores in sclera. The stabilization of laser-assisted gas and pore systems in the tissues can explain the long lasting healing effect in laser reconstruction of spine discs and in laser creation the uveoscleral pathway for aqueous in glaucomatous eyes.

**Acknowledgements**

The work was supposed by Russian Science Foundation, grant16-15-10274 and Russian Foundation for Basic Research, grant 15-29-04810.

**References**

1. O. Baum, S. Wachsmann-Hogiu, T. Milner, and E. Sobol, *Laser Physics Letters*, 2017, **14**(6), 065601.

*Invited*

# TOWARDS SYNAPTOMICS

**P.T.C. So**[1,2,3,4], **Y. Xue**[1,3], **K. Barry**[5], **C.J. Rowlands**[2,3], **Y. Takiguchi**[6], and **E. Nedivi**[5,7]

[1] Department of Mechanical Engineering, MIT, Cambridge, USA, ptso@mit.edu
[2] Department of Biological Engineering, MIT, Cambridge, USA
[3] Laser Biomedical Research Center, MIT, Cambridge, USA
[4] BioSym, Singapore-MIT Alliance Research and Technology Ctr., Singapore, Singapore
[5] Department of Brain and Cognitive Science, MIT, Cambridge, USA
[6] Hamamatsu Photonics, Hamamatsu, Japan
[7] Picower Institute, MIT, Cambridge, USA

**Abstract.** Synaptomics: we seek to study how a single neuron in the brain integrates, processes, and responses to all tis inputs. Toward this goal, we are developing a novel multiphoton holographic microscope that is capable of monitoring up to hundreds of locations simultaneously in living brain offering functional studies with unprecedented signal to noise ratio.

It is important to understand how neurons receive and integrate synaptic signals. A single neuron has approximately ten thousand excitatory synapses; monitoring signal initiation and propagation require near simultaneous imaging of all these synaptic locations sites and other strategic locations along the dendrite. We demonstrate the selective access multifoci multiphoton microscopy, which improves imaging speed and signal-to-noise ratio. A spatial light modulator is used to generate multifoci excitation in 3D. More importantly, a Gaussian-Laguerre phase plate is used to detect fluorescence from these spots simultaneously throughout the volume. We illustrate the performance of this system by recording calcium dynamics of cultured neurons simultaneous at 10Hz from 149 planer locations distributed across the field of view (Fig. 1). Simultaneously excitation and detection at multiple locations in 3D is also demonstrated. This "3D imaging in a single shot" strategy allows strictly synchronized dynamic recording, which is used for accurate determination of signal propagation speed across different dendrites.

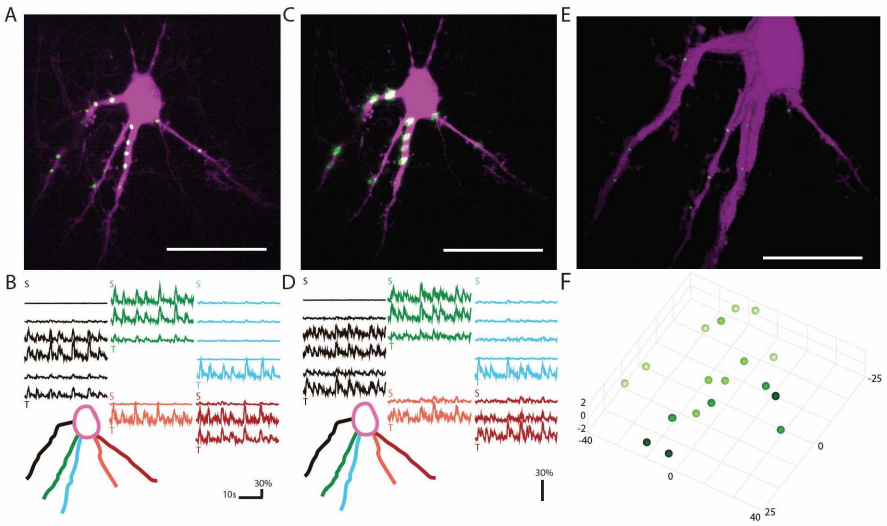



**Fig. 1.** The comparison of Gaussian spots and Gaussian-Laguerre (GL) spots for 3D simultaneously excitation and detection of neuronal calcium signals and the 3D reconstruction of a GL encoded image

## Acknowledgements

This work was supported by grant from NIH/NINDS (1U01NS090438-01). We further acknowledge supports by NIH (9P41EB015871-26A1, 5R01NS051320, 4R44EB012415, and 1R01HL121386-01A1), Hamamatsu Corp., and Singapore-MIT Alliance for Science and Technology Center, BioSym IRG. We thank Coherent Inc for loaning Fidelity-10 laser for the experiment data in all the figures.

# IMAGE ENHANCEMENT IN ACOUSTIC RESOLUTION PHOTOACOUSTIC MICROSCOPY

**P. Subochev[1], I. Mihailova[1], M. Kirillin[1], V. Perekatova[1], M. Jaeger[2], A. Orlova[1], and I. Turchin[1]**

[1] Institute of Applied Physics RAS, Nizhny Novgorod, Russia
Pavel.Subochev@gmail.com
[2] Institute of Applied Physics, University of Bern, Switzerland

**Abstract.** Acoustic resolution photoacoustic microscopy (or raster-scan optoacoustic mesoscopy) is based on mechanical scanning of a sample with a focused ultrasonic detector tuned to optimal frequency and geometry defining the system spatial resolution. However, practical realization of an efficient AR-PAM system faces several challenges related to the limited depth of focus, frequency-dependent ultrasonic attenuation, and inhomogeneous spatial distribution of optical fluence within sample. In this presentation we review the experience of our group in AR-PAM image enhancement by means of Fourier reconstruction, Tikhonov deconvolution filtration, and optical fluence compensation based on Monte Carlo simulations.

Acoustical-resolution photoacoustic microscopy (AR-PAM) is a raster-scan imaging technique based on focused ultrasonic detection of wideband optoacoustic (OA) transients thermoelastically induced by nanosecond laser pulses in light-absorbing tissue chromophores. The most cost-effective modality for *in vivo* AR-PAM imaging is OA angiography with commercially available source at optical wavelength of 532 nm, which lies within the absorption band of hemoglobin. For the given parameters of optical excitation, theoretical lateral and axial resolutions of AR-PAM angiography are determined by the numerical aperture NA and the bandwidth $\Delta f$ of the focused ultrasonic detector. However, along with the development of ultrasonic detector with optimal frequency and geometry, practical realization of an efficient AR-PAM system faces additional challenges.

The first problem is the trade-off between the lateral resolution (LR) and the depth of focus (DOF), which are both dependent on the detector's numerical aperture (NA). For example, a spherically focused ultrasonic detector with NA ~1 corresponds to low DOF/LRratio ~3. As a result, raw AR-PAM angiography images cannot provide high lateral resolution for the out-of-focus region. To improve the spatial resolution above and below the position of focus of high-NA detector one can use the virtual-detector concept [1] along with some synthetic-aperture focusing technique, such as Fourier reconstruction [2].

The second problem is frequency dependent ultrasonic attenuation that acts like a low-pass filter for a broad spectrum of OA pulses $\Delta f$ ~100 MHz provided by the smallest blood vessels, the capillaries. As a result, the capillary bed fine structure can be hardly resolved in raw AR-PAM angiography images. To maintain ultra-wideband spectral content one can use additional post-acquisition algorithms, for example, Tikhonov deconvolution filtration [3].

Another challenge of AR-PAM angiography is an effective optical attenuation coefficient $\mu_{eff}$ ~ 1 $mm^{-1}$ typical for biological tissues at 532 nm wavelength. Without fluence compensation, raw AR-PAM images are usually characterized by low OA contrast of blood vessels located at the millimeter diagnostic depths. To estimate effective in-depth fluence profiles for AR-PAM systems with dark-field optical illumination, we use Monte Carlo simulation of light transport accounting for complex geometry of laser illumination and acoustic detection [4].

In my talk I will review the experience of our group in AR-PAM image enhancement by means of practical implementation of all these highlighted approaches [1–4].

### Acknowledgements

The study was supported by the Russian Science Foundation (project #14-15-00709). Dr. Subochev was partly supported by the Scholarship of the President of the Russian Federation (project #SP-3196.2016.4).

### References

1. M.-L. Li *et al.*, *Optics letters*, 2006, **31**(4), 474.
2. M. Jaeger *et al.*, *Inverse Problems*, 2007, **23**(6), S51.
3. D.Van de Sompel *et al.*, *PloS one*, 2016, **11**(3), e0152597.
4. A. Gorshkov and M. Kirillin, *Journal of biomedical optics*, 2015, **20**(8), 085002.

*Invited*

# ENHANCED IMAGING OF TISSUES BY IMMERSION CLEARING/CONTRASTING: FROM X-RAY TO TERAHERTZ

**V.V. Tuchin**

Research Educational Institute of Optics & Biophotonics, Saratov National Research State University
83 Astrakhanskaya str., 410012 Saratov, Russia
Interdisciplinary Laboratory of Biophotonics, National Research Tomsk State University, Tomsk, Russia
Laboratory of Laser Diagnostics of Technical and Living Systems
Institute of Precision Mechanics and Control RAS, Saratov, Russia

**Abstract.** Optical immersion clearing/contrasting technology is aimed to enhance imaging of living tissues and cells. The method explores controllable and reversible modification of tissue/cell properties by their impregnation with a biocompatible clearing/contrasting agent (CCA). The multimodal diagnostic medical technologies with the targeting by a unified CCA (THz/optical, x-ray/optical, MRT/optical) is discussed. Water transport and modification of tissue mechanical properties under CCA action is analyzed. The enhancement of probing depth and image contrast for human and animal tissues is demonstrated using diffuse spectroscopy, OCT, photoacoustic, linear and nonlinear fluorescence, SHG and Raman microscopies, polarization and speckle imaging.

Optical immersion clearing/contrasting technology aiming at enhancement of living tissue and cell imaging using different diagnostic modalities working in a broad range of the wavelengths from x-ray to terahertz is presented. The method is based on controllable and reversible modification of tissue or cell properties by their impregnation with a biocompatible clearing/contrasting agent (CCA). The multimodal diagnostic medical technologies with the targeting by a unified CCA (THz/optical, x-ray/optical, MRT/optical) are proposed and discussed. Water transport and modification of tissue mechanical properties under CCA action such as reversible dehydration and shrinkage, balance of free and bound water is analyzed. The enhancement of probing depth and image contrast for different human and animal tissues is demonstrated using diffuse spectroscopy, OCT, photoacoustic microscopy, linear and nonlinear fluorescence, SHG and Raman microscopies, polarization and speckle imaging.

Perspectives of application of immersion optical clearing method to improve cell imaging mediated by plasmonic nanoparticles and to detect weak luminescence from upconversion nanoparticles deeply inserted into living tissue and Cherenkov's fluorescence excited by free electrons or protons in tissue depth are discussed.

Experimental data on diffusivity and permeability of glucose, glycerol, PEG, OmnipaqueTM (x-ray contrast) and other CCAs applied to normal and pathological tissues are presented.

**Acknowledgements**

The work was supported by Russian Presidential grant 14.Z57.16.7898-NSh, RFBR grant 17-02-00358, and Russian Ministry of Education and Science grant 17.1223.2017/AP.

**References**

1. D. Zhu, K.V. Larin, Q. Luo, and V.V. Tuchin, *Laser Photonics Rev.*, 2013, 7(5), 732–757.
2. E.A. Genina, A.N. Bashkatov, Yu.P. Sinichkin, I.Yu. Yanina, and V.V. Tuchin, *J. Biomed. Photonics & Eng.*, 2015, **1**(1), 22–58.
3. V.V. Tuchin, *BioPhotonics, IEEE International Conference*, 2015, pp. 1–10.
4. V.V. Tuchin, *J. Biomed. Opt.*, 2016, **21**(7), 071114-1-37.

*Invited*

# FUNCTIONAL OPTICAL COHERENCE TOMOGRAPHY: PRECLINICAL AND CLINICAL UPDATES FROM THE NIZHNY NOVGOROD – TORONTO COLLABORATION

**A. Vitkin**

University of Toronto, Canada

Functional monitoring of treatment response could enable patient-specific treatment adjustments thereby improving therapy effectiveness. In this Nizhny Novgorod + Toronto collaboration, optical coherence tomography (OCT) is being extended to include structural, polarization-sensitive, angiographic, and elastographic regimes. The ability of these complimentary information channels to detect treatment-induced changes is investigated in normal and tumour-bearing small animals (mice, hamsters) undergoing chemo-, radio-, and photodynamic therapies. Representative project results, including initial human studies, will be highlighted in this presentation. The multimodal OCT technologies and treatment response metrics thus developed may help usher in the era of "personalized cancer treatments" of the 21st century.

# FLUORESCENT ANALYSIS OF PHARMACOKINETICS OF CHLORINE $E_6$ CONJUGATE WITH BIS(DICARBOLLIDE) COBALT FOR BORON NEUTRON CAPTURE THERAPY

**A.B. Voloveckiy**[1], **V.S. Sukhov**[1], **N.Y. Shilyagina**[1], **V.V. Dudenkova**[1], **A.V. Feofanov**[2], **I.V. Balalayeva**[1], and **A.V. Maslennikova**[1,3]

[1] N.I. Lobachevsky State University of Nizhny Novgorod, Russia, voloveckiy91@gmail.com
[2] M.M. Shemyakin and Yu.A. Ovchinnikov Institute of bioorganic chemistry of the Russian Academy of Sciences, Moscow, Russia
[3] Nizhny Novgorod State Medical Academy, Russia

**Abstract.** The study objective was the evaluation of tissue distribution of boron-containing chlorin e6 derivative by detecting the fluorescence signal intensity in tumor and normal tissues *ex vivo*, and developing a descriptive mathematical model for the accumulation and excretion of boron based on experimental data. The study was performed on 20 tumor-bearing Balb/c mice. The solution of preparation was injected into a tail vein in a dose of 10 mg/kg of body weight. Animals were euthanized 1, 3, 6 and 24 hours after injection. *Ex vivo* microscopic fluorescent imaging of tumor, liver and muscle was performed. Analysis of the content of boron in blood, tumor, liver and muscle was performed by inductively coupled plasma mass spectrometry. A strong positive correlation between the fluorescence value and the content of boron in tissues was shown.

An obligatory condition of the efficiency of boron-neutron capture therapy (BNCT) is the control of the $^{10}B$ isotope content in tumor and normal tissues. Since $^{10}B$ is not a radioactive isotope and cannot serve as a label for quantitative analysis, an important aspect of BNCT is the development of methods for studying the biodistribution of boron-containing compounds in the patient's body [1]. In case of fluorescent boron-containing compounds, this property can be used to quantify the content of boron in biological tissues. A new promising class of compounds for BNCT are boron-containing porphyrin derivatives [2]. Recent *in vivo* studies have demonstrated their increased accumulation in the tumor compared to normal tissues [3]. The question is to what extent the fluorescence level of the conjugate correctly reflects the boron content in the tissues.

The study objective was the evaluation of boron-containing chlorin e6 derivative distribution by detecting the fluorescence signal intensity of the compound in tumor and normal tissues *ex vivo*, and developing a descriptive mathematical model for boron accumulation and excretion.

The study was performed on 20 tumor-bearing (mice colon carcinoma CT-26) Balb/c mice. The solution of boron containing chlorine $e_6$ conjugate was injected into a tail vein in a dose of 10 mg/kg of body weight. Animals were euthanized 1, 3, 6 and 24 hours after injection. Imaging of tumor, liver and muscle was carried out by AxioObserver Z1 LSM 710 DUO RP NLO system (Carl Zeiss, Germany). For microscopic imaging, excitation was implemented at 633 nm and emission of chlorin $e_6$ derivate was registered at 653–730 nm. The average fluorescence signal intensity was calculated in the regions of interest (ROI) of each image of the examined tumor samples and normal tissues.

Analysis of boron content in blood, tumor, liver and muscle was performed by inductively coupled plasma mass spectrometry (Ltd «Micronutrients», Moscow). The correlation between the fluorescence intensity signal and boron content was studied by Spearmen's method. To analyze the dynamics of the boron compound, a simple multi-compartment model [4] was used, in which blood and the organs (liver, muscles, tumor) were considered as different chambers.

The study demonstrated a strong positive correlation ($r > 0.9$, $p < 0.01$) between the fluorescent signal intensity and boron content in the tissues. The comparison of the experimental data (fluorescence signal intensity) and the results obtained by solving the mathematical model demonstrated a high level of compliance with experimental data, which is confirmed by the high value of the coefficient of determination ($R^2 > 0.91$), and means that the model adequately describes the kinetics of the redistribution of the borated compound between the organs and tissues studied.

## References

1. W.A.G. Sauerwein, A. Wittig, R. Moss, and Y. Nakagawa, *Neutron Capture Therapy – Principles and Applications*, Springer-Verlag, Berlin-Heidelberg, 2012, p. 543.
2. M.A. Grin, R.A. Titeev, D.I. Brittal, A.V. Chestnova, A.V. Feofanov, I.A. Lobanova, I.B. Sivaev, V.I. Bregadze, and A.F. Mironov, *RUCB*, 2010, **59**(1), 219–224.
3. A.B. Volovetskiy, N.Y. Shilyagina, V.V. Dudenkova, S.O. Pasynkova, A.A. Ignatova, A.F. Mironov, M.A. Grin, V.I. Bregadze, A.V. Feofanov, I.V. Balalaeva, and A.V. Maslennikova, *Biophisics*, 2016, **61**(1), 158–164.
4. S.D. Varfolomeev, and K.G. Gurevich, *Biokinetics*, Fairpress, Moscow, 1999, p. 720.

*Invited*

# PERFORMANCE CHARACTERIZATION OF INSTRUMENTATION FOR DIFFUSE OPTICAL IMAGING AND SPECTROSCOPY

**H. Wabnitz**

Physikalisch-Technische Bundesanstalt (PTB), Abbestrasse 2-12, 10587 Berlin, Germany
heidrun.wabnitz@ptb.de

**Abstract.** The quantitative assessment of system performances based on tissue-like phantoms plays an important role in the validation and quality assurance of diffuse optics instrumentation for clinical diagnostics and monitoring. Several dedicated protocols and guidelines have been developed and applied for performance comparison of instrumentation in multilaboratory efforts, in particular the nEUROPt protocol. Two sets of tests will be discussed in detail, (1) the quantification of the responsivity of the detection system in diffuse optics, (2) the assessment of sensitivity, spatial resolution and quantification of localized absorption changes in the context of time-domain functional brain imaging.

In the field of diffuse optical imaging and spectroscopy, the first systematic study of the performance of various instruments was undertaken on the basis of the MEDPHOT protocol [1]. It was focused on the capability of instruments to measure homogeneous optical properties. Two other protocols were developed and applied as part of the European project nEUROPt that was focused on time-domain optical brain imaging. The "Basic Instrumental Performance" (BIP) protocol [2] addresses the key instrumental characteristics while the "nEUROPt" protocol [3] utilizes specific inhomogeneous phantoms and a number of tests to quantify the capability of optical brain imaging systems to detect, localize, and quantify absorption changes in the human brain.

To quantify the responsivity of the detection system as a measure of the overall efficiency to detect light diffusely emerging from tissue, solid homogeneous phantoms were used. They had been characterized in terms of their diffuse transmittance, to provide a source of known radiance. For the different time-domain optical brain imagers investigated the responsivity was found to be of the order of 0.1 $m^2sr$. Differences between the values for the various devices could be attributed to the spectral sensitivity of the particular detectors or to the fiber bundles and optics used to transfer the light from tissue to detector.

The tests of the nEUROPt protocol were implemented with two types of inhomogeneous liquid phantoms that were based on Intralipid and India ink with well-defined optical properties [4]. First, small black cylinders of varying size were used to mimic localized changes of the absorption coefficient [5], to address, e.g., depth-dependent contrast and lateral spatial resolution. Second, two-layered liquid phantoms with variable absorption coefficients were employed to study, in particular, depth selectivity that compares the sensitivity of the measurement to absorption changes in a lower and upper layer of the turbid medium representing, e.g., brain and extracerebral tissues. Depth-dependent contrast and depth selectivity were studied for different instruments as well as methods to analyze the measured time-of flight distributions of photons based on time-window and moments approaches.

Quantification of such characteristics is beneficial, e.g. during development of instrumentation and algorithms for data analysis as well as for quality assurance during routine clinical use. The application of the BIP and nEUROPt protocols is not restricted to time-domain techniques and brain imaging but can be applied to other kinds of diffuse optical spectroscopy and imaging techniques. The protocols could be a useful step toward performance tests for future standards in these fields.

### Acknowledgements

The research leading to these results has received funding from the European Community (FP7/2007-2013) under grant agreement no. FP7-HEALTH-F5-2008-201076 and LASERLAB EUROPE no. 284464. The work presented here was a joint effort of project partners from six institutions in Europe. The valuable contribution of all collaborators is gratefully acknowledged.

### References

1. A. Pifferi, A. Torricelli, A. Bassi *et al.*, *Appl. Opt.*, 2005, **44**(11), 2104–2114.
2. H. Wabnitz, D.R. Taubert, M. Mazurenka *et al.*, *J. Biomed. Opt.*, 2014, **19**(8), 086010.
3. H. Wabnitz, A. Jelzow, M. Mazurenka *et al.*, *J. Biomed. Opt.*, 2014, **19**(8), 086012.
4. L. Spinelli, M. Botwicz, N. Zolek *et al.*, *Biomed. Opt. Express*, 2014, **5**, 2037–2053.
5. F. Martelli, P.D. Ninni, G. Zaccanti *et al.*, *J. Biomed. Opt.*, 2014, **19**(7), 076011.

# APPLICATONS OF OPTICAL COHERENCE ELASTOGRAPHY IN PROBLEMS OF LASER RESHAPING OF CARTILAGES AND CORNEA

**V.Y. Zaitsev[1], A.L. Matveyev[1], L.A. Matveev[1], G.V. Gelikonov[1], A.I. Omelchenko[1,2], D.V. Shabanov[1], A.A. Sovetsky, A. Vitkin, O.I. Baum[2], and E.N. Sobol[1,2]**

[1] Institute of Applied Physics, Russian Academy of Sciences, Nizhny Novgorod, Russia; vyuzai@ipfran.ru
[2] Institute of Photonic Technologies, Centre "Crystallography and Photonics", Russian Academy of Sciences

**Abstract.** In the context of the development of emerging laser-assisted thermo-mechanical technologies of non-destructive reshaping of avascular collagenous tissues (cartilages and cornea), we demonstrate the application of phase-sensitive optical coherence tomography (OCT) for visualizing transient strains involving supra-wavelength inter-frame displacements of scatterers. The proposed approach allows direct estimation of elevated strains $\sim 10^{-2}$ (close to the onset of intense speckle blinking) obviating the necessity of averaging and phase unwrapping for supra-wavelength inter-frame displacements. We demonstrate a possibility of mapping aperiodic thermally-induced transient strains with resultant large deformations >10%. Such strains are typical in laser tissue reshaping, but are far beyond the range of conventionally discussed OCT-based strain mapping.

**Introduction.** Thermo-mechanical laser-induced reshaping of cartilages and eye cornea is an emerging technology that opens unprecedented possibilities for biologically non-destructive modification of collagenous-tissue shape for various applications, such as preparation of cartilaginous implants in otolaryngology (e.g. forming annular-shape implants from planar pieces of rib cartilage) or non-surgical correction of nasal-septum shape by moderate heating of the cartilage by irradiation of a IR laser. A challenging problem is the transfer of the similar approach in ophthalmology, for non-surgical reshaping of cornea in vision-correction problems. By the evident reasons in the latter application one needs to ensure especially precise control of the heating regime, monitoring of current deformations of the tissue during reshaping and certainly evaluation of the resultant shape of cornea. In this report we present some preliminary results on application of OCT-based elastography for real-time monitoring of thermomechanically-induced shape variations of avascular collagenous tissues.

**Materials and Methods.** The research was carried out using samples of porcine rib cartilage and excised rabbit eyes. For tissue heating, we applied a fiber IR erbium laser operating at 1.56 μm with variable power output in the range of 0.5–1 W. The characteristic distance of the irradiation absorption in the tissues was ~1 mm. For visualization, we used a common path spectral domain OCT system with a central wavelength of 1310 nm and spectral width of 100 nm, resulting in axial resolution of 15 μm, scanning depth of 2 mm in air, scanning speed of 80 000 spectral fringes per second. Due to utilisation of $\pi/2$ modulation of the reference arm the system was able to form complex-valued A-scans at a rate of 40 kAscan/s. Typically, B-scans consisting of 1024 A-scans and covering 4 mm in the lateral direction were obtained at a rate of 20 f/s, which made it possible to limit the data volumes to ~4 Gb for 50-second records that was sufficient to reshape cornea (or similar in size cartilage samples) by applying pulse-periodic heating (with characteristic pulse/pause durations of 1–2 s). Elastographic processing of complex-valued OCT scans was used to estimate inter-frame phase gradients and visualize strains [1, 2].

**Results.** The proposed OCT-based elastographic method is capable of visualizing thermo-mechanically induced reversible and irreversible deformations in the tissue, including both transitional inter-frame strains (below 1%) and cumulative ones (that can reach tens per cent). An exponential relationship between the temporal and spatial profiles of measured cumulative strains and simulated temperature variations (based on preliminary calibrations) was found. The ability of OCT to detect threshold temperatures required for producing irreversible deformations has been confirmed. Micropore formation in the treated regions via combined assessment of local deformations and Young modulus reduction has been demonstrated for the first time.

### Acknowledgments

The study was supported by the Russian Science Foundation, project No 16-15-10274.

### References

1. Zaitsev *et al.*, *J. Biophotonics,* 2016, **9**(5), 499–509.
2. Zaitsev *et al.*, *J. Biomed. Optics*, 2016, **21**(11), 116005.

# MITIGATION OF PRACTICAL OBSTACLES IN REALIZATION OF COMPRESSIONAL OPTICAL COHERENCE ELASTOGRAPHY

**V.Y. Zaitsev[1], A.L. Matveyev[1,2], L.A. Matveev[1,2], E.V. Gubarkova[2], A.A. Sovetsky[1], M.A. Sirotkina[2], G.V. Gelikonov[1,2], E.V. Zagaynova[2], N.D. Gladkova[2], and A. Vitkin[2,3]**

[1] Institute of Applied Physics, Russian Academy of Sciences
e-mail: vyuzai@ipfran.ru
[2] Nizhny Novgorod State Medical Academy, 10/1 Minina Square, Nizhny Novgorod 603005, Russia;
[3] University of Toronto and University Health Network, 610 University Ave., Toronto, M5G 2M9, Canada

**Abstract.** In this presentation we point out some practical obstacles arising in realization of compressional optical coherence elastography (OCE) that have not attracted sufficient attention before. Specifically, we discuss (i) complications in quantification of the Young modulus of tissues related to partial adhesion between the OCE probe and soft intervening reference layer-sensor, (ii) distorting influence of tissue surface curvature/corrugation on the subsurface strain distribution mapping, (iii) ways of signal-to-noise ratio (SNR) enhancement in OCE strain mapping when periodic averaging is not realized, and (iv) potentially significant influence of tissue elastic nonlinearity on quantification of its stiffness. Potential practical approaches to mitigate the effects of these complications are also described.

**Introduction.** Elastography (evaluation and visualization of spatial distribution of mechanical shear modulus $G$ of biological tissues) is a diagnostic imaging modality that complements conventional structural bio-imaging. Specifically, we focus on the compressional variant of elastography initially proposed in medical ultrasound [1] and now actively developed in optical coherence elastography. In this method, the rigid OCT-probe creates approximately uniaxial stress in the vicinity of the probe and the resultant axial strain is evaluated by comparing consequent OCT scans. This strain should be inversely proportional to the Young modulus $E$. Since for soft biological tissues $E \approx 3G$ to a high accuracy, the as-found strain map is equivalent to tissue stiffness (or rather inverse stiffness) map. Placing between the probe and tissue an intervenient soft layer (e.g., translucent silicone) with pre-calibrated stiffness opens a possibility to quantify the tissue stiffness. However, non-planar form of the tissue surface, adhesion influence at the interface with the OCT probe, and nonlinearity of the tissue elasticity may significantly distort the actual strain distribution.

**Materials and Methods.** The experimental demonstrations were made using a custom-made common path spectral domain OCT systems with a central wavelength of 1310 nm and spectral width of 100 nm, resulting in axial resolution of 15 μm, scanning depth of 2 mm in air, with scanning speed of either 20 000 or 80 000 spectral fringes per second. Elastographic processing of complex-valued OCT scans was used to estimate inter-frame phase gradients to visualize strains [2, 3].

**Results.** The proposed method visualizes local strains in the reference silicone layer and tissue in a unified manner. This allows one to detect sticktion at the interface via artefactual stiffening of the reference layer near the OCT-probe and to reduce distorting sticktion influence, e.g., by adding lubrication. The use of sufficiently soft intervenient layer also helps to efficiently mitigate the influence of non-planar shape of the tissue surface. Next, obviating the necessity of phase unwrapping in the proposed method allows one to use fairly large interframe strains ~1%, which improves the effective SNR in estimating phase gradients, which is favorable for hand-held operation. Finally, the use of linearly-elastic layer revealed pronounced nonlinearity of some tissues even for strains ~ a few per cent. In such cases, the current Young modulus may vary several times depending on the precompression, but more complete stress-strain curve (up to ~10% strain) may be helpful for discriminating different tissue states/types. The corresponding experimental examples are presented.

**Acknowledgments.** The study was supported by the Russian Federation Government contract No 14.B25.31.0015.

**References**

1. K.J. Parker, M.M. Doyley, D.J. Rubens, *Phys. Med. Biol.* 56(1), R1–R29 (2011).
2. Zaitsev *et al.*, *J. Biophotonics*, **9**(5), 499–509 (2016).
3. Zaitsev *et al.*, *J. Biomed. Optics*, **21**(11), 116005 (2016).

*Invited*

# *IN VIVO* PHOTOACOUSTIC FLOW CYTOMETRY FOR EARLY DIAGNOSIS AND PREVENTION OF CANCER, INFECTIONS AND CARDIOVASCULAR DISORDERS

**V.P. Zharov**

University of Arkansas for Medical Sciences, Little Rock, Arkansas, USA
zharovvladimirp@uams.edu

**Abstract.** This report summarizes our novel concept of early disease diagnosis with ~1000-fold improved sensitivity using *in vivo* noninvasive photoacoustic (PA) flow cytometry (PAFC) platform for detection of circulating biomarkers with intrinsic PA contrasts (e.g., melanin in melanoma and hemozoin in malaria) or molecularly targeted with the functionalized nanoparticles. The integration in real-time diagnosis and therapy (called theranostics) can eradicate circulating abnormal cells, and thus can potentially prevent, or at least inhibit deadly metastasis, sepsis or stroke. Recent advances of this theranostic platform are presented with focus on the pre-clinical and clinical trials associated with cancer, malaria, thrombosis, and stroke.

Cardiovascular diseases, cancer, and infections remain the main causes of death in the worldwide. The diagnosis of these and other diseases begins with a common medical procedure: the examination of blood samples. The sensitivity of current blood tests is limited by the small volume of blood collected, in which no less than one disease-specific biomarker (e.g., tumor cell, clot, or pathogen) can be detected. This can miss many thousands of abnormal cells and biomarkers in the whole blood volume (~5 liter in adults), which can be sufficient for disease progression to difficult-to-treat if not already incurable complications (e.g., metastasis, stroke, or sepsis). This report summarizes our novel concept of early disease diagnosis with ~1000-fold improved sensitivity using *in vivo* noninvasive photoacoustic (PA) flow cytometry (PAFC) platform for identification and enumeration of rare circulating biomarkers with intrinsic PA contrasts (e.g., melanin in melanoma and hemozoin in malaria) or molecularly targeted with the functionalized gold nanoparticles [1–5]. The principle of PAFC is based on the irradiation of the superficial blood vessels with near-infrared laser pulses followed by detection of laser-induced acoustic waves from single biomarkers with small ultrasound transducer attached to skin. In addition, the integration in real-time diagnosis and therapy (called theranostics) can eradicate circulating abnormal cells, and thus can potentially prevent, or at least inhibit deadly metastasis, sepsis or stroke. Recent advances of this label-free theranostic platform are presented with focus on its pre-clinical and clinical trials associated with cancer, malaria, venous thrombosis, lung embolism, and stroke.

Most cancer deaths are related to metastases to distant organs due to disease dissemination by circulating tumor cells (CTCs) shed from the primary tumor. For many years oncologists believed that some medical procedures may provoke metastasis; however no convincing data were reported. Recently we obtained direct evidence using PAFC platform that typical medical procedures such as palpation, biopsy, tumor resection, or laser surgery might enhance the penetration of cancer cells from the primary tumor into the circulatory system, and thus increase the risk of metastases.

We also introduce an advanced *in vivo* PAFC-based test for the earliest presymptomatic diagnosis of malaria through ultrasensitive detection of circulating malaria markers directly in the bloodstream, without the drawing of blood. By quick examination of almost the entire volume of blood, this technology provides up to a $10^5$-fold improvement in diagnostic sensitivity that enables determining an unprecedented low level of parasitemia of 0.00000001%, which is equivalent to ~50 parasites in 1 liter of blood [4, 5]. In addition to high sensitivity and spectral specificity to *Plasmodium* subspecies, the PAFC test is noninvasive (needle-free), label-free (no contrast agents), and safe (e.g., no pain, skin damage, or contamination concerns) and is not influenced by environment noise, hand movement, or skin pigmentation. Gentle contact of the PA probe with the intact skin can identify malaria-positive asymptomatic individuals in just 5–10 seconds.

**Acknowledgements**

This work was supported in part by the NIH grants R01CA131164 and R01EB017217, the NSF grants OIA 1457888 and DBI 1556068, and the Translational Research Institute grant from UAMS.

**References**

1. E. Galanzha and V. Zharov, *Methods*, 2012, **57**, 280–296.
2. W. Kim, E.I. Galanzha, D.A. Zaharoff, R.J. Griffin, and V.P. Zharov, *Mol. Pharm.*, 2013,**10**, 813-830.
3. J. Nolan *et al.*, *Anal Cell Pathol (Amst).*, 2016, 1628057.
4. Y. Menyaev *et al., Biomed Opt Express*, 2016, **7**, 3643–3658.
5. C. Cai, *et al., Cytometry A*, 2016, **89**, 531–542.

VI International Symposium

# TOPICAL PROBLEMS OF BIOPHOTONICS




## *Biophotonics in Cancer Research*

## Chairs

**Lothar Lilge**
Princess Margaret Cancer Centre, University of Toronto, Canada

**Ammasi Periasamy**
University of Virginia, USA

**Elena Zagaynova**
Nizhny Novgorod State Medical Academy, Russia

*Poster*

# PHOTODYNAMIC PROPERTIES OF WATERSOLUBLE PORPHYRIN-AMPHIPHILIC POLYMER-CHITOSAN SYSTEMS

**N.A. Aksenova[1], V.V. Kardumjan[1], N.N. Glagolev[1], P.S. Timashev[2,3], A.L. Spokoynyy[1], and A.B. Solovieva[1]**

[1] N.N.Semenov Institute of chemical physics of RAS, Moscow, Russia, e-mail: naksenova@mail.ru
[2] Institute for Regenerative Medicine, I.M. Sechenov First Moscow State Medical University
[3] Institute of Photonic Technologies, Research center "Crystallography and Photonics", RAS

**Abstract.** The aim of this study was to create effective porphyrin-containing photosensitizing systems based on chitosan and amphiphilic polymer (AP) Pluronic F127. The photosensitizing activity of porphyrin–AP–chitosan systems was estimated in the reaction of tryptophan oxidation in solution. The photosensitizing systems based on chitosan are effective for use in the photodynamic therapy (PDT) of various skin injuries (purulent wounds, tumors).

The creation of chlorine (CPS) or porphyrin photosensitizers (PPS) – polymer systems is of great interest owing to possible applications of such formulations in photodynamic therapy, an effective method of treatment of oncological diseases. In recent years, this method has been used throughout the world for the treatment of wounds, burns, trophic ulcers, and other skin injuries, with the photosensitizers being used in the immobilized state. The mechanism of photodynamic therapy is based on the ability of CPS or PPS localized on the membranes of organelles to generate, when illuminated with light, a highly reactive singlet oxygen $^1O_2$, which oxidizes the cell components and initiates tissue cell death. The effects of Fotoditazin, an e6 chlorine derivative, and its complexes with AP were analyzed at the early stage of wound healing in a rat model by the PDT method [1]. A skin excision wound model with prevented contraction was developed in male albino rats divided into eight groups according to the treatment mode. All animals received injections of one of the studied compositions into their wound beds and underwent low-intensity laser irradiation or stayed un-irradiated. The clinical monitoring and histological examination of the wounds were performed. It has been found that all the Fotoditazin formulations have significant effects on the early stage of wound healing. The superposition of the inflammation and regeneration was the main difference between the groups. The aqueous solution of CPS alone induced a significant capillary hemorrhage, while its combinations with amphiphilic polymers did not. The best clinical and morphological results were obtained for the Fotoditazin–Pluronic F127 composition. Compositions of CPS and AP, especially Pluronic F127, probably, have a great potential for therapy of wounds. Their effects can be attributed to the increased regeneration and suppressed reactions changes at the early stages of repair. It is known that the polymers used in medicine must be nontoxic and biocompatible. In this context, the natural polysaccharide chitosan is of special interest as a carrier for porphyrin immobilization. Chitosan has bactericidal properties that make it versatile for applications in medicine, for example, in burns and wounds healing. However, as was shown previously, owing to the processes of CPS and PPS aggregation, the activity of photosensitizers in the reaction of tryptophan oxidation in water decreases in the presence of water soluble polymers containing amino groups. The aggregation is initiated by formation of ionic complexes between amino groups of chitosan and carboxylate ions of water soluble porphyrins or chlorins. Thus, in chitosan-based chlorine- or porphyrin-containing photosystems, AP should be added, for example, Pluronic or polyvinylpirrolidone. In this work the photosensitizing properties of such triple systems in model reaction of tryptophane oxidation have been considered. The features of wound healing in a rat model by the PDT method have also been addressed.

**Acknowledgments**

This work was supported by the Russian Foundation for Basic Research (project № 16-32-00722-mol_a) and the Russian Science Foundation (project № 16-13-10295).

**References**

1. T.G. Rudenko, A.B. Shekhter, and A.E. Guller, *Photochem.Photobiol.*, 2014, **90**(6), 1413–1422.

*Invited*

# NOVEL INSIGHTS INTO TRANSFERRIN-MEDIATED DELIVERY INTO TUMOR CELLS USING *IN VITRO* AND *IN VIVO* FRET IMAGING

**M. Barroso[1], A. Rudkouskaya[1], K. Tubbesing[1], N. Sinsuebphon[2], K. Chen[2], and X. Intes[2]**

[1] Albany Medical College, Albany, NY, USA, barrosm@mail.amc.edu
[2] Rensselaer Polytechnic Institute, Troy, NY, USA

**Abstract.** Our main goal is to integrate basic cell biology with methodological advances in imaging technology to develop novel approaches to visualize, quantitate and optimize receptor-mediated targeted delivery into tumor cells. By integrating our knowledge on the endocytic trafficking of receptor-ligand complexes with our expertise on Förster Resonance Energy Transfer (FRET) and fluorescence lifetime (FLIM) imaging, we have developed novel *in vivo* and *in vitro* imaging approaches to measure target engagement in tumors, a crucial parameter to accelerate the prioritization of the most efficient targeted anti-cancer therapy.

**Introduction**: To guide the development of targeted therapies with improved efficacy and accelerated clinical acceptance, novel imaging methodologies need to be established. Current *in vivo* non-invasive imaging techniques are limited to monitoring only the pooling of the labeled drug at the pathologic site and cannot distinguish between co-localization and actual ligand-receptor engagement. Our goal is to develop non-invasive *in vivo* optical imaging assays for optimization of anti-cancer drug targeted therapy by achieving the direct visualization of receptor engagement, dimerization and internalization into tumor cells. Whole-body near-infrared (NIR) *in vivo* Macroscopy Fluorescence Lifetime Forster Resonance Energy Transfer (MFLI-FRET) has been performed to quantitate the receptor-mediated uptake of NIR-labeled ligands into tumor xenografts in live animals [1, 2]. Since transferrin receptor (TfR) level is significantly elevated in cancer cells compared to non-cancerous cells, transferrin (Tf) has been successfully used in molecular imaging and targeted anti-cancer drug delivery. The homodimeric nature of TfR allows for the quantification of Tf binding and internalization into cancer cells by measuring FRET between receptor-bound NIR-labeled donor-Tf and acceptor-Tf, based on the reduction of donor fluorophore lifetime in live mice (Figure 1) [1, 2].

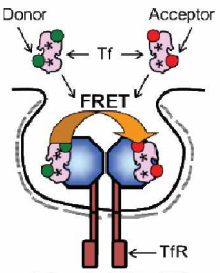



**Fig. 1.** TfR-Tf MFLI-FRET assay. *, iron

**Results:** MFLI-FRET imaging *in vivo* has been used to measure the internalization of tail-vein injected NIR-labeled Tf at different acceptor:donor (A:D) ratios into human breast T47D tumor xenografts in live nude mice. Quantification of FRET donor fraction (FD%) indicates a relative higher FD% for holo-Tf (iron-loaded) compared to that of apo-Tf (iron-depleted). Since apo-Tf shows reduced uptake into cancer cells *in vitro*, these results showing a similar behavior *in vivo*, demonstrate specific TfR-mediated uptake of holo-Tf into T47D tumor xenografts (Figure 2). Thus, MFLI-FRET can discriminate between TfR-Tf engagement and internalization into tumor cells from receptor-independent accumulation of Tf at the tumor region.

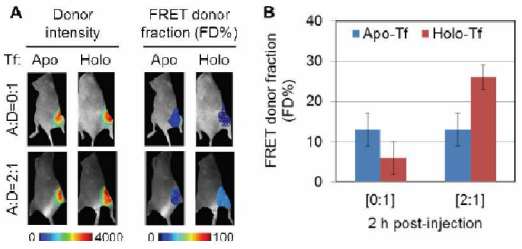



**Fig. 2.** (A) Tumor-carrying mice were injected with apo-Tf or holo-Tf and subjected to MFLI-FRET imaging at 2h post-injection. (B) Increasing FD% values are shown upon injection of Holo-Tf at A:D 2:1. Error bars indicate standard deviation

**Conclusion**: We have successfully demonstrated the quantitative receptor-mediated uptake of Tf into human breast tumors *in vivo* using a novel non-invasive NIR MFLI-FRET imaging assay. This novel approach can be extended to other receptors, currently targeted in oncology. Hence, MFLI-FRET ability to measure target engagement *in vivo* can find numerous applications in pre-clinical drug delivery and targeted therapy assessment and optimization.

## References

1. K. Abe, L. Zhao, A. Periasamy, X. Intes, M. Barroso, A. Periasamy, *PLoS One.*, 2013, **8**, e80269.
2. S. Rajoria, L. Zhao, X. Intes, M. Barroso, *Curr Mol Imaging*, 2014, **3**, 144–61.

*Poster*

# CISPLATIN-INDUCED HYDROGEN PEROXIDE LEVEL CHANGES AS COMPARED TO TOTAL ROS LEVEL

**A.S. Belova[1], A.G. Orlova[1], K.M. Shchukina[2], I.V. Balalaeva[2], N.O. Antonova[2], and E.V. Zagaynova[3]**

[1] Institute of Applied Physics RAS, Nizhny Novgorod, Russia, belova-as@mail.ru
[2] N.I. Lobachevsky State University of Nizhny Novgorod, Nizhny Novgorod, Russia
[3] Nizhny Novgorod State Medical Academy, Nizhny Novgorod, Russia

**Abstract.** Cisplatin is a chemotherapeutic drug which causes not only DNA damage, but also induces production of reactive oxygen species (ROS) that can initiate tumor cell death. Using genetically encoded fluorescent sensor, apoptosis marker and vital dye, dose-dependent increase of hydrogen peroxide level was demonstrated by flow cytometry under cisplatin action in viable and apoptotic tumor cells separately. In parallel, a decrease of total ROS amount was demonstrated using DCFH-DA.

Hydrogen peroxide ($H_2O_2$) is assumed to be the key component of the tumor cell reaction to chemotherapy. There is an assumption that cancer cells produce an increased amount of ROS than normal cells and a direct increase of intracellular $H_2O_2$ may lead to a selective and effective cancer cells death [1].

## Materials and methods

For investigation of total ROS under cisplatin treatment human cervical carcinoma HeLa Kyoto cell line was used. The intracellular ROS level was measured using a fluorescent dye, 2', 7' dichlorofluorescein diacetate (DCFH-DA). Cells were treated with cisplatin at the doses of 0.0 μg/ml (control probe), 5.0 μg/ml, 10.0 μg/ml for 24 hours. For studying the ways of cell death under cisplatin action PE–Annexin V apoptosis detection kit I (BD Biosciences, USA) comprising PE Annexin V and 7-amino-actinomycin D (7-AAD) was used. All fluorescence dyes were registered using the flow cytometer FACSCalibur (Becton Dickinson, USA). For measurement of changes in the level of hydrogen peroxide, human cervical carcinoma HeLa Kyoto cell line stably expressing HyPer2 was employed [2].

## Results and discussion

Analysis of the data have shown that the addition of cisplatin at a concentration of 5.00 μg/ml results in the "migration" of cells from the population of viable cells to the population of cells undergoing early apoptosis.

Histogram of DCFH-DA staining shows separation of cells in the control sample and in the sample after exposure to cisplatin in a concentration of 5.00 μg/ml into 2 fractions: weakly fluorescent and strongly fluorescent cells; the latter fraction demonstrates increased fluorescence intensity after cisplatin exposure with respect to the control group. Administration of high concentrations of the drug led to the formation of a fraction with weak fluorescence of the DCF. HyPer2 fluorescence histogram shows the increase in fluorescence intensity in fractions of viable cells and cells in early stages of apoptosis after drug treatment as compared to control (unlike DCF fluorescence).

## Conclusions

In this study we show that most of the viable cells are characterized by high DCFH-DA fluorescence indicating active oxidative processes and high levels of ROS, while for the cells at early stages of apoptosis levels of ROS in cells treated with cisplatin is lower than in control cells. Experiments with HyPer2 show the increase in the level of hydrogen peroxide in viable cells and in cells in early stages of apoptosis. We can conclude that an increase in the amount of $H_2O_2$ induced by cisplatin in viable and apoptotic cells occurs in parallel with a decrease of total ROS amount.

## Acknowledgements

The reported study was funded by the RFBR under to the research project No. 16-34-01112 мол_а.

## References

1. M. López-Lázaro, *Cancer Lett,* 2007, **252**(1), 1–8.
2. K.N. Markvicheva, D.S. Bilan, N.M. Mishina, A.Y. Gorokhovatsky, L.M. Vinokurov, S. Lukyanov, and V.V. Belousov, *Bioorganic & Medicinal Chemistry*, 2011, **19**(3), 1079–1084.

*Invited*

# ANALYSIS OF STROMAL ALTERATIONS IN OVARIAN CANCERS VIA SECOND HARMONIC GENERATION MICROSCOPY

**P.J. Campagnola**

University of Wisconsin Madison, Madison, WI, USA, pcampagnola@wisc.edu

**Abstract.** Ovarian cancer is the most deadly gynecological cancer with a poor aggregate survival rate. To improve upon this situation, we utilized collagen-specific Second Harmonic Generation (SHG) imaging microscopy to probe structural differences in the extracellular matrix of normal stroma, benign tumors, endometrioid tumors, and low and high-grade serous (LGS and HGS) tumors. We extract quantitative differences at all levels of assembly using texture analysis for fiber pattern classification, SHG creation physics for fibril size and packing, and polarization resolved SHG for changes in macromolecular structure across this spectrum of disease type and grade.

## Introduction

Ovarian cancer remains the most deadly gynecological cancer with a poor aggregate survival rate. To improve upon this situation, we utilized collagen-specific Second Harmonic Generation (SHG) imaging microscopy to probe structural differences in the extracellular matrix of normal stroma, benign tumors, endometrioid tumors, and low and high-grade serous (LGS and HGS) tumors. We perform specific analyses that probe collagen alterations across all size scales, namely fiber, fibril, and macromolecular.

## Methods and Results

For analysis of fiber patterns, we implemented a form of 3D texture analysis method to delineate the fibrillar morphology. Here we developed a tailored set of 3D filters which extract textural features in the 3D image sets to build (or learn) statistical models of each tissue class. By applying k-nearest neighbor classification using these learned models, we achieved 83–91% accuracies for the six classes [1]. The 3D method outperformed the analogous 2D classification on the same tissues, where we suggest this is due the increased information content. For the fibril level, we utilized SHG signatures of the emission directionality and conversion efficiency as well as the optical scattering are related to the organization of collagen on the sub-micron size. The wavelength dependence of these readouts adds additional characterization of the size and distribution of collagen fibrils/fibers relative to the interrogating wavelengths. We found strong wavelength dependent dependencies of these metrics that were different between the different tumors that are related to respective structural attributes in the collagen organization. The SHG metrics and optical scattering measurements were then used to form a linear discriminant model to classify the tissues, and we obtained high accuracy (~90%) between the tissue types [2]. This delineation is superior to current clinical performance and has potential applicability in supplementing histological analysis and provide better understanding the etiology. To examine molecular changes, we employed three SHG polarization metrics to probe ECM remodeling in human ovarian cancer which determine i) the helical pitch angle via the single axis molecular model, ii) dipole alignment via anisotropy, and iii) chirality via SHG circular dichroism. These methods differentiate Col I and Col III in fibrillar gel models and also human ovarian tissues due to differences in the α-helix angle of the isoforms and are consistent with immunofluorescence and gene expression measurements.

## Conclusions

Collectively, these SHG probes interrogate collagen changes over all levels of organization and can serve as label-free biomarkers for ovarian cancer as well as provide insight into disease etiology. Additionally, the methods are quite general applicable to other cancers, as well as other diseases with collagen alterations such as fibroses and connective tissue disorders.

## Acknowledgements

We acknowledge support under NSF CBET 1402757 and 0959525; and NIH R21 HL 126190.

## References

1. B. Wen, K.R. Campbell, K. Tilbury, O. Nadiarnykh, M.A. Brewer, M. Patankar, V. Singh, K.W. Eliceiri, and P.J. Campagnola, *Sci Rep-Uk,* 2016, **6**.
2. K.B. Tilbury, K.R. Campbell, K.W. Eliceiri, S.M. Salih, M. Patankar, and P.J. Campagnola, *BMC Cancer,* 2017, **17**, 102.

*Invited*

# NOVEL REGULATION OF CANCER CELL DEATH BY OXPHOS COMPLEXES, CYTOKINES, AND UNFOLDED PROTEIN RESPONSE

**S. Kumar, A. Chaudhary, N. Yadav, R. Kumar,** and **D. Chandra**

Department of Pharmacology and Therapeutics, Roswell Park Cancer Institute, Buffalo, New York 14263, USA

Apoptotic cell death machinery is defective in cancer leading to the development of resistance to current therapy. Thus cancer cells develop resistance to multiple types of anticancer agents, however, whether they adopt similar or differential mechanisms to evade cell death in response to a broad spectrum of cancer therapeutics is not fully defined. We recently demonstrated that DNA-damaging agents (etoposide and doxorubicin), endoplasmic reticulum stressor (thapsigargin), and histone deacetylase inhibitor (apicidin) target oxidative phosphorylation (OXPHOS) for apoptosis induction, whereas other anticancer agents including staurosporine, taxol, and sorafenib induced apoptosis in an OXPHOS-independent manner. Thapsigargin-induced caspase activation was reduced upon abrogation of complex-I or gross-complexes, whereas a reverse trend was observed with apicidin.

Cytokines and inflammation regulate mitochondrial complexes, cell survival, and cellular apoptosis. Our findings suggest that apicidin and thapsigargin target different OXPHOS complexes, we further investigated the effect of thapsigargin or apicidin on functional significance of cytokines in mitochondrial function and apoptotic cell death. We first screened modulation of various cytokines in response to anticancer agents. Then we further investigated the cytokines in cell survival and apoptotic cell death. Altered release of various cytokines were observed in the medium of colon and prostate cancer cells treated with anticancer drugs including apicidin and thapsigargin. Dose dependent up-regulation of cytokines was observed upon apicidin and thapsigargin treatment, which was corroborated with cytochrome-c release from mitochondrial compartment. Significantly elevated caspase-3 was observed upon combined exposure of apicidin and thapsigargin with altered cytokines expression and release. Interestingly, knock down of *caspase-8* and *caspase-9* down-regulated cytokines expression, suggesting the involvement of caspases on regulation of cytokine-mediated cellular and mitochondrial function. These findings suggest that mitochondrial dysfunction is required for cytokine-mediated cancer cell survival. Further mechanistic analysis demonstrated that unfolded protein response plays a critical role in the regulation of cytokine-induced cellular proliferation and death. Using tumor xenograft mouse model, we further defined the role of unfolded protein response as well as cytokine in tumorigenesis and tumor regression. Together, we dissect the novel role of cytokines, OXPHOS complexes, and unfolded protein response in regulating cancer cell survival and death, which may have significance in understanding tumorigenesis, drug resistance, and tumor recurrence.

*Invited*

# INTERNALIZATION OF VECTORIZED LIPOSOMES INTO TARGET-CELLS

**V.P. Chekhonin, P.V. Mel'nikov,** and **V.P. Baklaushev**

Chair and Department of Medical Nanobiotechnologies of the Russian State Medical University

**Abstract.** The development of nanocontainers capable of selective accumulation in tumor cells enhances bioavailability and selectivity of the delivered drugs and diagnostic preparations, including the ones with apparent antitumor properties. Internalization of vectorized nanocontainers with antitumor metabolites and plasmid DNA into glyoma C6 cells has been studied in a series of works.

For increasing the selectivity of delivery, pegilated liposomes were conjugated with anti-VEGF and/or with anti-VEGFR2 monoclonal antibodies. The phenomenon of more than three-fold increase of penetration and accumulation of vectorized liposomes into the glioma C6 cells was demonstrated by the methods of flow cytometry and laser scanning confocal microscopy. Using quantitative analysis of fluorescent signal it was shown that cationized immunoliposomes are able to deliver plasmid DNApCopGreenN into the cells much more effectively, providing efficient transfection of the glioma C6 cells.

It was shown that vectorization of the cationized liposomes with anti-VEGF and/or anti/VEGF2 monoclonal antibodies can reliably increase the efficiency of transfection. However, it does not affect the final concentration of the fluorescent product in the cells 24 hours after the beginning of the transfection.

*Invited*

# DRUG LOADING AND EFFICIENCY OF NANODIAMOND-ANTICANCER DRUG COMPLEX IN 2D AND 3D CELLULAR MODEL

**Z.-R. Lin, Y.-C. Lin, K.-T. Wu, E. Perevedentseva,** and **C.-L. Cheng**

Department of Physics, National Dong Hwa University, Hualien, Taiwan
clcheng@gms.ndhu.edu.tw

**Abstract.** Nanodiamond (ND) has been considered as a biocompatible and feasible platform for efficient cancer drug delivery. Examples have been successfully demonstrated for various cellular and animal models. However, to date very few or no studies include the assessment on the effects and efficiency in a quantitative fashion; and the transportation of these ND-drugs to the cancer/tumor sites are still in a less understood state. For drug delivery, ND can interact with blood circulatory system and enter the peripheral tissues; where ND interacts with target cells. When cell encounters and engulfs ND, the cell may try to digest it in a process named autophagy, a survival mechanism for cells.

In this work, we study autophagy effect of ND and ND conjugated with clinically used anti-cancer drug doxorubicin (Dox). ND and Dox internalization in Human Oral Squamous Carcinoma cell, SAS and the effect of autophagy in the SAS cell are analyzed. To observe ND internalization by SAS cell, the cell was treated with ND for several hours. To visualize ND engulfing by cells, confocal microscopy to observe ND's NV center fluorescence was used. To observe ND's effect on autophagy in SAS cells, the cells were subject to immunofluorescence analysis by staining with an anti-LC3 antibody. The LC3 protein aggregates during autophagic process and its fluorescence can be monitored via BD Pathway 435 Benchtop System. Analyzing spatial distribution of anti-LC3 antibody allows detecting whether ND induces the autophagy. The conditions and ND properties to induce an autophagy are discussed in terms of optimization of the ND use for drug delivery.

The efficiency of the ND-drug as compared to pure drug in the 2D- and 3D-cellular model was assessed. 3D cell culture system mimicking tumor model was adopted to evaluate the toxicity and toxicity mechanism of ND-drug complex. This will demonstrate the real effects of drug delivery to tumor inside the animal body. The ND-drug transportation in the animal model is investigated. *In vivo* investigation of ND in Rat model and laser-scanning confocal microscopic analysis found ND attachment on RBC membrane. Further, 100 nm carboxylated ND (cND) was conjugated with human serum albumin (HSA) to achieve well dispersed suspension in buffer solution. Then the clinically used anticancer drug Doxorubicin (DOX) was adsorbed on the particles surface. To characterize the conjugation, UV/Visible, Raman and infrared spectroscopies were used. The particle sizes and surface charges of the complex cND-HSA-DOX were measured by Dynamic Light Scattering (DLS). The stability of cND-HSA-DOX in the buffer solution with pH of 7.4 for 1 week was analyzed via UV/Visible spectroscopy. Besides, DOX release from cND-HSA-DOX at different pH was measured. The Cell viability test was performed using SAS cell line to compare the cytotoxic effect of DOX and ND-HSA-DOX complex. The cytotoxic effect of Dox and cND-HSA-Dox complex was assessed in the 2D- and 3D-cultured SAS cell via MTT assay. A possible mechanism of the drug transportation and delivery will be discussed in the work. The results show ND can be well dispersed and to have stable particles size in buffer solution after the HSA conjugation; pH-dependent drug release from cND-HSA-DOX complex is demonstrated. ND-HSA-Dox is more efficient in the 3D-cultured cell compare to 2D-cultured cell.

**Acknowledgement**

The authors appreciate the financial support of this research by the Ministry of Science and Technology (MoST) of Taiwan, Grant No. MOST 103-2112-M-259 -001 -MY3.

# THE EFFECT OF LOW-LEVEL BLUE LED LIGHT IN ONCOGENESIS

**E.S. Plekhanova[1], I.A. Chernigina[1], V.V. Chernov[2], and T.G. Shcherbatyuk[1]**

[1] Nizhny Novgorod State Medical Academy, Nizhny Novgorod, Russia, ozone_stg@mail.ru
[2] Institute of Applied Physics of the Russian Academy of Sciences, Nizhny Novgorod, Russia

**Abstract.** The impact of low-level LED light (LLL) at the wavelengths of 400 nm and 460 nm on outbred rats (healthy animals and with transplanted tumor) was studied in experiments *in vitro* and *in vivo*. The photolytic action of LLL on nitrosyl complexes of hemoglobin of red blood cells, the antitumor effect and the restoration of oxidative homeostasis in animals with transplanted tumor were demonstrated.

## Objectives

The goal of the study was to determine the influence of low-level LED light at the wavelengths of 400 nm and 460 nm on erythrocyte hemoglobin, on the growth of experimental tumor and on the level of free radical activity in red blood.

## Materials and methods

Twenty seven mature outbred male rats were used in this study (7 animals for experiments *in vitro* and 20 *in vivo* tests). Healthy animals and rats with transplanted cholangiocellular RS-1 carcinoma [1] of late development were divided into several groups: *healthy*, *RS-1–control*, *RS-1+LLL 400 nm*, and *RS-1+LLL 460 nm*.

Erythrocytes were exposed to LLL in experiments *in vitro*. The exposure time at the wavelengths of 400 nm and 460 nm was 42 and 60 seconds, respectively. The radiation dose for each wavelength was 0.2 J/cm$^2$.

In the test *in vivo*, LED was applied transcutaneously, and the irradiation was performed on belly and at several tumor locations for 60 seconds. The radiation dose at the wavelengths of 400 nm and 460 nm was 0.3 and 0.2 J/cm$^2$, respectively. The LLL was applied for 10 days.

The experimental LLL generators made at the *Institute of Applied Physics RAS, Nizhny Novgorod, Russia*) were used for irradiation. The antitumor effect of the therapy was evaluated using the coefficient of absolute tumor growth (C) [2]. Hemoglobin concentration was measured spectrophotometrically by the cyanmethaemoglobin method using a commercial kit (Hemoglobin Agate, LLC "Agat-Med", Moscow, Russia). The state of free-radical oxidation in rat organisms was verified using the method of chemiluminescence induced by hydrogen peroxide and ferric sulfate (Kuzmina E.I. et al., 1983) based on the content of malondialdehyde (MDA) (Fletcher D.L. et al., 1973) and superoxide dismutase (SOD) activity (Nishiňimi M. et al., 1972).

## Results

It was found that the hemoglobin concentration in erythrocytes of animals with late stages of tumor growth increased on exposure to LLL *in vitro*.

The results indicate that low-level LED light at the wavelength of 400 nm does not affect growth of experimental tumors, but exposure to LLL at the wavelength of 460 nm leads to inhibition of neoplasia growth by 69% ($p = 0.008$). The enzyme activity of superoxide dismutase reduces to the level of healthy animals on exposure to LED light ($p < 0.05$). However, the chemiluminescence activity and the product of lipid peroxidation in plasma decreases only after irradiation by light at the wavelength of 460 nm (10% ($p = 0.042$) and 19% ($p = 0.018$), respectively).

## Conclusions

Our experiments point to the presence of the antitumor effect and restoration of oxidative homeostasis in cancerous animals as a result of photolysis of nitrosyl complexes of hemoglobin and release of NO on exposure to LLL. The effect is most pronounced for LLL at the wavelength of 460 nm.

## References

1. E.M. Treshalina, "Protivoopukholevaya aktivnost' veshchestv prirodnogo proiskhozhdeniya", *Prakticheskaya Meditsina*, Moscow, 2005, p. 272.
2. E.V. Yaroslavtseva-Isaeva, M.A. Kaplan, Yu.S. Romanko, and N.I. Sokol, *Russian Journal of Biotherapy*, 2003, **2**, 19–22.

*Invited*

# OPTICAL BIOPSY: JOURNEY FROM LABORATORY SYSTEM TO PUBLIC HEALTH-CARE

**Ajeetkumar Patil[1], V.K. Unnikrishnan[1], Keerthilatha M. Pai[2], Ravikiran Ongole[3], Kanthilatha Pai[2], V.B. Kartha[1],** and **Santhosh Chidangil[1]**

[1] Department of Atomic and Molecular Physics, Manipal University, Manipal,
[2] Department of Oral Medicine and Radiology, Manipal University, Manipal,
[3] Department of Oral Medicine and Radiology, Mangalore
Email: santhosh.cls@manipal.edu

**Abstract.** Under-developed countries constitute 85% of the world population and almost 80% of them live in rural areas. More than 60% of this population are in conditions of grossly inadequate health care, without any modern medical facilities for diagnosis from conditions (e.g. cancers) which remain clinically silent for long periods. The solution for this issue is the development of screening methods, which can be used in small hospitals or medical camps. The paper will discuss development of non-invasive *Optical Biopsy* systems for early detection of epithelial cancers (oral and cervical cancers), capable of repeated application and screen large susceptible population groups.

85% of the world population exists in the under-developed countries and almost 80% of them live in rural areas. This number constitutes a large fraction of the world population – more than 60% – who are living in conditions of grossly inadequate health care, without any modern medical facilities for therapy, or relief from conditions like coronary problems, various types of cancers, diabetes etc., diseases which remain clinically silent for long periods. For all these diseases, overt symptoms start appearing only in the final stages, by that time therapy is almost always unsuccessful, and serves only palliative purposes. The solution for this is provided by development of screening and diagnostic methods, which are cost-effective, can be used even in small hospitals and community health-care centers, or medical camps organized in rural areas. The present work deal with the possibility of using Optical methods for early detection of clinically silent diseases with emphasis on cancers. The invited talk will discuss the results of the successful development of an "Optical Biopsy" system, which is non-invasive, capable of repeated application, can be used in hospitals to screen large susceptible population groups (tobacco users) for oral pre-malignancy and malignancy conditions.

**Acknowledgements**

Authors are thankful to the financial support of Board of Research in Nuclear Research Sciences (BRNS) for setting up of the experimental facility and Manipal University for fellowship to one of the authors.

# LIVE-CELL SINGLE-MOLECULE IMAGING REVEALS COMPOUNDS THAT ALTER INITIATION DYNAMICS AND TRANSCRIPTION KINETICS

**C.R. Day[1,2], J. Rodriguez[2], D.R. Larson[2], and A. Martin[1]**

[1] Department of Biological Sciences, The George Washington University, 800 22nd Street, N.W., Washington D.C. 20052
[2] Laboratory of Receptor Biology and Gene Expression, Center for Cancer Research, National Cancer Institute, Bethesda, Maryland 20892

**Abstract.** Transcription is a highly-ordered process involving distinct steps of coordinated enzyme activities. Using a reporter gene with PP7 and MS2 stem loops we have developed a high-throughput single-cell imaging screen to identify compounds that alter the kinetics of each step in the transcription process. To further understand how endogenous genes are regulated we have used CRISPR to integrate MS2 stem loops into the endogenous loci of an estrogen-responsive gene, *TFF1*. By live-cell imaging of the MS2 tagged *TFF1* locus the dynamics of ER-dependent gene expression were studied in single cells over long time courses.

Transcription of DNA into messenger RNA (mRNA) requires the coordination of many enzymatic processes that are catalyzed by large protein complexes [1]. The activity of these enzymatic complexes is modified by transcription factors responsible for initiating transcription, but transcriptional events including elongation and splicing require separate enzymes to function. A reporter for human β-globin gene transcription was constructed by inserting 24 bacteriophage PP7 stem loops in the terminal intron and 24 bacteriophage MS2 repeats in the 3' untranslated region (UTR) [2]. This reporter gene approach enabled direct measurement of elongation rates, splicing kinetics, and cell-to-cell variability. A high-throughput method was designed using this system to screen compounds that inhibit chromatin modifiers [3]. Compounds targeting bromodomain proteins were identified that slow elongation rates while increasing co-transcriptional splicing.

To better understand how endogenous gene expression is regulated, CRISPR/Cas9 was used to insert 24 MS2 stem loops into the 3' UTR of the well-characterized estrogen responsive gene, *TFF1* [4], allowing the visualization of transcription dynamics. *TFF1* is regulated by the estrogen receptor alpha (ERα), which is a ligand-activated transcription factor. ERα bound by agonist ligand acts in combination with other coactivator proteins to recruit chromatin modifying proteins that are responsible for opening chromatin and initiating transcription [5]. In contrast, ERα bound by antagonists, like tamoxifen, adopts an altered conformation that allows the recruitment of corepressor proteins, thus inhibiting the expression of estrogen-dependent genes [6]. Small molecule inhibitors have been developed that target the DNA binding activities of some proteins that associate with ERα and function to coordinate the activation of target gene expression. Little is known about how these compounds affect estrogen-dependent gene expression at the single cell level or how they affect the dynamics of gene expression.

Here, the dynamics of estrogen-dependent gene expression is monitored in single cells by visualizing *TFF1* transcription sites in MCF7 human breast cancer cells. Time-lapse imaging of the diffraction limited transcription sites allows quantification of the on- and off-rates for *TFF1* gene transcription. In addition, fluorescence *in situ* hybridization (FISH) was used to determine the average number of *TFF1* mRNAs per cell under different perturbations of the ERα complex. The EC50 of each compound was used for live cell imaging and the effect of each compound on *TFF1* transcription dynamics was determined and the inhibitors altered the off time of *TFF1*.

**Acknowledgments.** This research was supported by the Intramural Research Program of the NIH, National Cancer Institute, Center for Cancer Research.

## References

1. G. Orphanides and D. Reinberg, *Cell*, 2002, **108**, 439–451.
2. A. Coulon, M.L. Ferguson, V. de Turris, M. Palangat, C.C. Chow, and D.R. Larson, *Elife*, 2014, **3**.
3. C.R. Day, H. Chen, A. Coulon, J.L. Meier, and D.R. Larson, *Methods*, 2016, **96**, 59–68.
4. A.M. Brown, J.M. Jeltsch, M. Roberts, and P. Chambon, *Proc. Natl. Acad. Sci. USA*, 1984, **81**, 6344–6348.
5. Z. Liu, D. Merkurjev, F. Yang, W. Li, S. Oh, M.J. Friedman, X. Song, F. Zhang, Q. Ma, K.A. Ohgi, A. Krones, and M.G. Rosenfeld, *Cell*, 2014, **159**, 358–373.
6. F.E. May and B.R. Westley, *J. Biol. Chem.*, 1987, **262**, 15894–15899.

*Invited*

# INTRAVITAL FRET AND FLIM: MONITORING BIOSENSOR ACTIVITIES AND INTRINSIC METABOLIC STATES

**R.N. Day**

Department of Cellular and Integrative Physiology, Indiana University School of Medicine, 635 Barnhill Dr., Indianapolis, IN 46202, USA

**Abstract.** Intravital microscopy (IVM) is an imaging tool capable of detecting subcellular signaling or metabolic events as they occur in tissues in the living animal. Imaging in highly scattering biological tissues, however, is challenging, and quantitative measurements by IVM require methods that use internal standardization, or alternatively, a completely different way of evaluating the signals. For example, ratiometric imaging of genetically encoded biosensor probes can provide quantitative measurements of changes in cell signaling pathways in intact tissues. Alternatively, lifetime imaging of intrinsic fluorescence can be used for label-free measurements of the metabolic states of cells within the living animal.

IVM has become an essential tool for evaluating cellular physiology in the context of the living animal [1]. This method uses two-photon excitation (2PE) to gain access to the cellular environments within living tissues that are not typically accessible by conventional microscopy. The near infrared illumination used in IVM allows deeper penetration of the excitation light into highly scattering tissues. In addition, because of the quadratic dependence of the 2PE process the fluorescence emissions emanating from cellular sources are limited to the focal plane. Consequently, IVM provides some of the most relevant information available about cellular physiology and pathophysiology in the context of the intact tissue within the living animal. This is critically important, since cellular pathologies develop *in vivo* while integrated within the complex tissue environment [2].

The use of IVM to detect specific cellular events in intact organs presents some unique challenges. The main concern is preserving the physiological welfare of the animal while on the microscope stage. The surgically exposed organ is secured to a glass-bottomed dish on an environmentally controlled microscope stage to reduce motion artifacts, and distortions in the collected images can be corrected in the digital image analysis [3]. Another major challenge is the quantitative analysis of the optical signals. When imaging in highly scattering biological tissues, the signals are attenuated in a wavelength- and depth-dependent fashion. The loss of signal prevents the direct comparison of intensities acquired at different depths in a tissue. Therefore, quantitative measurements of signals acquired by IVM require methods that use internal standardization [4].

I will describe how ratiometric Förster resonance energy transfer (FRET) imaging of genetically encoded biosensor probes can be used in IVM to obtain quantitative measurements of changes in cell signaling pathways. Because these ratiometric probes are internally calibrated, they are less affected by depth-dependent signal attenuation than intensity-based imaging methods. The use of a single 2PE wavelength allows rapid measurements of the spatial and temporal characteristics of cell signaling, but it is particularly important to use standards to validate the IVM measurements of biosensor probes [4, 5]. Alternatively, IVM can exploit a completely different way of evaluating the signals to achieve quantitative measurements of cellular events. I will describe how intravital fluorescence lifetime imaging microscopy (FLIM) of cellular auto-fluorescence signals can identify the unique metabolic states of different cell-types within a tissue. Intravital FLIM enables a bias-free approach to characterize and monitor metabolism *in vivo* and offers the unique opportunity to uncover dynamic metabolic changes in the living animal.

## Acknowledgments

This research is supported by the National Institutes of Health O'Brien Center for Advanced Renal Microscopic Analysis (NIH-NIDDK P30DK079312).

## References

1. M.J. Pittet and R. Weissleder, *Cell*, 2011, **147**, 983–991.
2. G. Follain, L. Mercier, N. Osmani, S. Harlepp, and J.G. Goetz, *J. Cell Sci.*, 2016, DOI: 10.1242/jcs.189001.
3. R.G. Presson, Jr., M.B. Brown, A.J. Fisher, R.M. Sandoval, K.W. Dunn, K.S. Lorenz, E.J. Delp, P. Salama, B.A. Molitoris, and I. Petrache, *Am J Pathol*, 2011, **179**, 75–82.
4. W. Tao, M. Rubart, J. Ryan, X. Xiao, C. Qiao, T. Hato, M.W. Davidson, K.W. Dunn, and R.N. Day, *American journal of physiology. Cell physiology*, 2015, **309**, C724–735.
5. R.N. Day, W. Tao, and K.W. Dunn, *Nat. Protoc.*, 2016, **11**, 2066–2080.

# LONGITUDINAL ASSESSMENT OF SINGLE-DOSE RADIATION-INDUCED TUMOR VASCULAR CHANGES WITH OPTICAL COHERENCE TOMOGRAPHY

**V. Demidov[1], A. Maeda[1], M. Sugita[1], V. Madge[2], C. Flueraru[3], and I.A. Vitkin[1,4]**

[1] University of Toronto, Toronto, Canada, email: val.demidov@mail.utoronto.ca
[2] Carleton University, Ottawa, Canada
[3] Institute for Microstructural Sciencesof National Research Council, Ottawa, Canada
[4] University Health Network, Princess Margaret Cancer Centre, Toronto, Canada

**Abstract.** Here we report the optical coherence tomography (OCT) quantitative assessment of early (up to 6 weeks) microvascular response of engrafted tumors in mouse dorsal skin window chamber model, subjected to a high-dose single-fraction radiation treatment of 10, 20, and 30Gy. Acquisition of structural images of tumor tissues with OCT and their real-time processing with speckle variance (svOCT) algorithm to obtain vascular volumetric images provided highly detailed view of vasculature remodeling in tumors following RT.OCT pre-clinical evaluation of tumor vascular response offers a shedding light opportunity on early RT effects and is likely to be extended into the clinic.

Radiation therapy (RT) is widely used for cancer treatment alone or in combination with other therapies. It is effective and powerful, however, as with every form of treatment, has its side effects. In order to personalize the treatment course for every patient, these effects need to be promptly understood and mid-course corrections offered. Microvasculature is a potentially sensitive functional biomarker of RT early response [1], but is (1) difficult to measure directly and non-invasively, (2) even if successfully measured and quantified, its time course, dose dependencies, and overall importance in RT effect are unclear. This is mostly due to the lack of ability to study the dynamic response of multiple tumor components longitudinally and in-situ at the capillary level. Here we propose a new insight into this problem using a novel preclinical experimental platform to study radiobiological response of tumor microvasculature based on functional OCT.

Early microvascular response was evaluated for engrafted pancreatic cancer tumors (DS-Red labeled BxPC-3 cell line) in mouse dorsal skin window chamber model (NRG strain mice, total number of 60) subjected to a high-dose single-fraction radiation treatment delivered by a commercial X-ray micro-irradiator system XRad225Cx. Volumetric tissue structures were imaged with built-in-house OCT machine [2] in optimized speckle variance mode [3] in order to obtain three-dimensional vascular images. Those images were post-processed for vascular volume density (VVD) calculation and depth encoded representation. Changes in tumor size (measured with caliper) and cancer cell metabolic activity (evaluated from cancer cells fluorescence images) were tracked before and after irradiation. Tissue sections were stained at various time points post RT to assess tumor proliferation and vascularization.

Main results: (i) Four stages of tumor microvascular response were distinct within 6 weeks post RT (moderate vessel damage, decreased vessel function, revascularization, vessel growth); (ii) Tumor capillaries shutdown was detected 30 minutes post-RT with following recovery to the pre-RT state at 90 min time point (more pronounced for higher doses); (iii) Vasculature at tumor rim was found to be less sensitive to radiation than vasculature at tumor core; (iv) Functional vasculature collapsed weeks faster at higher doses; (v) VVD decreased more at higher doses at maximum response period; (vi) It took longer time for vasculature to re-grow to the pre-RT volume density at higher doses; (vii) Vasculature re-growth originated from adjacent healthy tissues.

## Acknowledgements

This study was supported by the Canadian Institutes of Health Research and the Ministry of Science and Education, Russian Federation (I.A.V.). V.D. was also supported by the Alexander Graham Bell Canada Graduate Scholarship from the Natural Sciences and Engineering Research Council of Canada.

## References

1. M. Garcia-Barros, T. Thin, J. Maj, Z. Fuks, R. Kolesnick,*Cancer Res.,* 2010,**70**, 8179–8186.
2. Y. Mao, C. Flueraru, S. Chang, D. Popescu, M. Sowa, IEEE Trans. Instrum. Meas., 2011, **60**, 3376–3383.

# *IN VIVO* TARGETED THERANOSTICS OF CIRCULATING TUMOR CELLS

**M.V. Novoselova[1], D.N. Bratashov[1], S.V. German[1], M. Sarimollaoglu[2], D.A. Nedosekin[2], B.N. Khlebtsov[1,3], D.A. Gorin[1], V.P. Zharov[2],** and **E.I. Galanzha[2]**

[1] Saratov State University, Saratov, Russian Federation
[2] University of Arkansas for Medical Sciences, Little Rock, AR
[3] Institute of Biochemistry and Physiology of Plants and Microorganisms, Saratov, Russian Federation

Approximately 90% of all cancer deaths are caused by metastases produced by circulating tumor cells (CTCs). Detection and therapy (theranostics) of CTCs holds promise to prevent metastasis. However, the existing methods including the FDA-approved CellSearchsystem (Veridex, LLC) are only able to detect CTCs and evaluate whether their amount is associated with a worse prognosis. The existing CTC assays are burdened with 1) low sensitivity at the level of 1–10 CTCs/mL (i.e., missing up to 5,000–50,000, CTCs in whole 5 L blood volume) due to the small volume of blood sampled (i.e., untreatable metastatic disease may already be established at the time of the initial diagnosis); 2) low throughput (e.g., 0.1–8 mL/h) requiring up to a whole day to assess typical blood samples of 10 mL; and 3) multiple sample-processing resulting in the loss of 60–97.5% of CTCs. As a result, CTCs can actually be detected only in 30 to 65% patients with clinically confirmed metastases. Furthermore, it is important that in vitro approaches cannot provide therapy (killing) of CTCs. This challenge has been solved by the development of CTC theranostics *in vivo* using photoacoustic (PA) flowcytometry (PAFC) with nanoparticles as PA contrast agents (Zharov VP, Galanzha EI, Tuchin VV., 2004). Our PAFC already demonstrated ultrasensitive counting CTCs (the sensitivity threshold >100 times higher than in the existing assays) in relatively deep (1–3 cm) blood vessels with a fast flow (up to 5–20 cm per sec) using laser parameters safe for humans. Here we introduce nanocomposite microcapsules (NMs) as new low-toxic advanced high-contrast PA agents. The PA characteristics of different NMs were tested *in vitro* and *in vivo*. In a preclinical mouse models, we demonstrated (1) PA imaging and counting of NMs and nanoparticle-labeled CTCs; (2) *in vivo* MRI imaging and magnetic manipulations with cells and NMs containing magnetite nanoparticles and gold nanorods; and (3) targeted cancer cell therapy with immediate estimation of therapy efficacy. Overall, our findings show that PAFC with nanoparticles and NMs as PA, PT and MRI contrast agents provides a unique multifunctional and clinically-relevant platform for early theranostics of CTCs for prevention of metastases, which is unachievable with other existing techniques.

# COHERENT ANTI-STOKES RAMAN SPECTROSCOPY AS IMAGING TOOL FOR INTERACTION BETWEEN SILICON NANOSTRUCTURES AND LIVING SYSTEMS

**M.B. Gongalsky**[1], **D.A. Muftieva**[1], **J. Saarinen**[2], **A. Isomaki**[3], **L. Peltonen**[2], **C.J. Strachan**[2], **H.A. Santos**[2], and **L.A. Osminkina**[1]

[1] M.V. Lomonosov Moscow State University, Faculty of Physics, Moscow, Russia, mgongalsky@gmail.com
[2] Division of Pharmaceutical Chemistry and Technology, Faculty of Pharmacy, University of Helsinki, Helsinki, Finland
[3] Institute of Biomedicine, Anatomy, Faculty of Medicine, University of Helsinki, Helsinki, Finland

**Abstract.** Silicon nanoparticles (SiNPs) are known to be promising biocompatible and biodegradable agents for both diagnostics and therapy of cancer. Here we apply a powerful non-linear optical imaging technique (coherent anti-Stokes Raman spectroscopy – CARS) for bioimaging SiNPs in vitro. A very efficient contrast was provided by SiNPs because of high third-order non-linear susceptibility of silicon by comparison with biological medium. All the images were obtained for the concentration below cytotoxic concentration of SiNPs. The proposed approach may be used for drug release and SiNPs biodegradation studies *in vitro*, and also for investigation of antibacterial or antiviral activity of SiNPs.

## Results

Today, scientists pay a lot of attention to the study of nanoparticles. Silicon nanoparticles (SiNPs) are promising as agents for diagnosis and therapy of cancer due to their low toxicity and biodegradability [1, 2]. SiNPs were also shown to be efficient sensitizers of anticancer therapy [3–5].

Coherent anti-Stokes Raman Spectroscopy (CARS) was used for visualization of SiNPs inside cells. The advantages of this technique are fast image acquisition, confocal geometry, sensitivity to chemical composition of the sample, non-linear contrasting possibilities. Those advantages perfectly fit with SiNPs, which have strong nonlinear-optical response due to high third-order non-linear susceptibility.

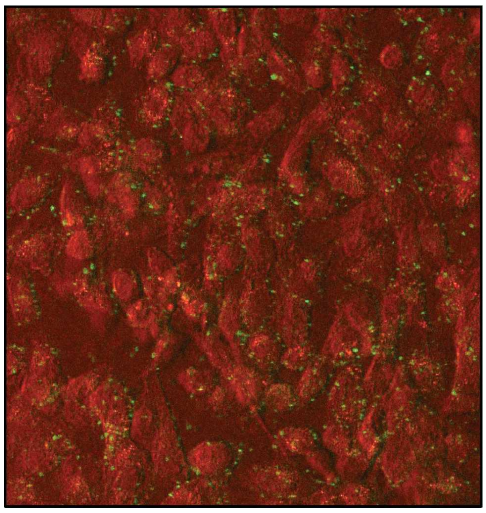


**Fig. 1.** CARS image of silicon nanoparticles (colored green) in MD 231 cell culture (colored red)

This work is aimed to the visualization of SiNPs in MD 231 cancer cells. Three types of samples were used for this: mesoporous (MP) SiNPs obtained by electrochemical etching, and porous and nonporous silicon nanowires obtained by metal-assisted chemical etching.

Spectrally-resolved experiments showed maximum in spectrum, typical for CARS. The toxicity of SiNPs was studied, and the non-toxic concentration (0.1 mg/mL) was chosen for carrying out bioimaging experiments in cells. Typical image of SiNPs (colored green) in cell culture (cells are colored red) visualized by CARS microscopy is shown on Fig. 1.

These results open pathway for further research: one can visualize drug loaded SiNPs by means of CARS with subsequent drug release, investigate how SiNPs degrade in the cells over time.

## Acknowledgements

This work was supported by the Russian Science Foundation (Grant № 17-12-01386).

## References

1. S. Park *et al.*, *Mater. Chem. B*, 2015, **3**, 198206.
2. A.D. Durnev *et al.*, *Int. J. Biomed. Nanosci. Nanotechnol.*, 2010, **1**, 70.
3. L.A. Osminkina *et al.*, *Appl. Phys. B Lasers Opt.*, 2011, **105**, 665668.
4. K.P. Tamarov *et al.*, *Sci. Rep.*, 2014, **4**, 7034.
5. A.P. Sviridov *et al.*, *Appl. Phys. Lett.*, 2013, **103**, 193110.

*Invited*

# OPTIMAL DESIGN OF LAYERED PLASMONIC NANOSTRUCTURES WITH EMBEDDED RAMAN REPORTERS

**N.G. Khlebtsov**[1,2]

[1] Institute of Biochemistry and Physiology of Plants and Microorganisms, Russian Academy of Sciences
[2] Saratov State University, Saratov, Russia
khlebtsov@ibppm.eu

**Abstract.** Recently, several research groups reported on highly efficient multilayer SERS tags (also called nanomatryoshkas, NMs), in which Raman molecules were embedded in a nanometer-sized interior gap between the metallic core and shell. Here, we report a detail analysis of EM enhancement in a (core/gap/shell) Au NMs as a function of NM structure, including the core size, the gap and shell thicknesses, and the gap refractive index.

Recently, several research groups reported on highly efficient multilayer SERS tags (also called nanomatryoshkas, NMs), in which Raman molecules were embedded in a nanometer-sized interior gap between the metallic core and shell [1–5]. Such multilayered structures have great potential for biomedical applications due to several advantages: (1) Raman molecules are protected from desorption, subjected to a strongly enhanced electromagnetic (EM) field in the gap, and their SERS response does not depend on the environmental conditions and NM aggregation; (2) owing to bright and uniform spectral pattern, NMs provide a linear correlation between probe concentration and SERS intensity and allow for a real-time *in vivo* imaging and high throughput sensing with short integration times; (3) NM size and spectral properties can be designed for effective cellular uptake and tissue imaging with negligible background from sample autofluorescence; (4) NM probes can be multiplexed by incorporating different Raman molecules into two-layered or multilayered NMs. However, the synthesis and design of optimal gold NMs remain still challenging. Here, we report a detail analysis of EM enhancement in a (core/gap/shell) Au NMs as a function of NM structure, including the core size, the gap and shell thicknesses, and the gap refractive index. The optimization strategy is based on efficient rigorous solution for internal EM fields in a layered sphere and explicit analytical solutions for the surface and volume averaged EM intensities within a particular layer and around the NM. The SERS enhancement is shown to be strongly dependent, in a resonance manner, on the core and gap size, whereas the shell thickness plays a minor role. The simulation data are exemplified with experimental measurements of SERS spectra for Au NMs with 1,4 benzenedithiol molecules embedded in a subnanometer gap.

**Acknowledgements**

This work was supported by RNF grant No. 14-13-01167 (particle fabrication) and by RFBR grant 16-02-00054 (particle characterization).

**References**

1. D.K. Lim, *et al.*, *Nat. Nanotechnol.*, 2011, **6**, 452–460.
2. L. Lin, *et al.*, *Nano Lett.*, 2015, **15**, 6419; *Chem. Commun.*, 2015, **51**, 17740–17743.
3. B.N. Khlebtsov and N.G. Khlebtsov, *J. Phys. Chem. C*, 2016, **120**, 1538–15394.
4. N. Gandra, *et al.*, *Nanoscale*, 2016, **8**, 8486–8494.
5. J.-H. Lee, *et al.*, *Small*, 2016, **12**, 4726–4734.

# MULTIMODAL OCT-GUIDED DETECTION OF INFILTRATIVE TUMOR BORDER IN GLIOBLASTOMA RAT MODEL

**E.B. Kiseleva[1], K.S. Yashin[1,2], A.A. Moiseev[1,3], M.A. Sirotkina[1], L.B. Timofeeva[1], V.M. Gelikonov[1,3], V.V. Fedoseeva[4], A.I. Alekseeva[4],** and **N.D. Gladkova[1]**

[1] Nizhny Novgorod State Medical Academy, Nizhny Novgorod, Russia, kiseleva84@gmail.com
[2] Privolzhsky Federal Medical Research Center, Nizhny Novgorod, Russia
[3] Institute of Applied Physics, Russian Academy of Sciences, Nizhny Novgorod, Russia
[4] Research Institute of Human Morphology, Moscow, Russia

**Abstract.** Determining the boundaries of infiltrative glial tumors is still a challenging problem in neurooncology. Optical coherence tomography (OCT) with cross-polarization and real-time microangiography visualization is a promising technique for a possible surgical guidance. This study is aimed to develop a robust quantitative approach for multimodal OCT data to differentiate cancer from non-cancer tissues in glioblastoma rat model. Processing of structural and microvasculature images gave an advantage for more accurate determination of tumor borders.

**Introduction.** More extensive brain cancer resection can prolong survival and delay recurrence [1]. Infiltrative growth of brain tumors causes difficulties in achieving total tumor resection. An introduction of innovative minimally invasive methods like multimodal OCT for intrasurgical guidance appears to be a critical challenge for modern neuromedicine. Various approaches to qualitative evaluation of OCT images and scoring algorithms for gliomas/normal differentiation criteria have been actively developed [2, 3], but still remain an actual scientific task.

**Materials and Methods.** The study was carried out on C6rat glioblastoma model injected into the brain of female Wistar rats (n = 10). The MM OCT imaging was performed on days 17–19 after the transplantation of glioblastoma, when the tumor had formed and was visible on the brain surface. The spectral domain MM OCT device that provides two modes of investigation – cross-polarization OCT (CP OCT) and microangiographic OCT (OCTMA) was used in the study [4, 5]. The light source was a superluminescent diode with a central wavelength of 1310 nm, a spectral width of 100 nm, resulting in axial resolution of 10 μm. The lateral resolution was 15 μm. MM OCT images of the tumor, its border with cortex and the visually normal cortex were collected *in vivo*, tumor-white matter border and normal white matter were studied *ex vivo*.

**Results.** The C6 model is morphologically similar to human glioblastoma multiforme showing regions of necrosis and hemorrhage with infiltration into the surrounding brain tissues. Based on histopathology data, 5 groups of CP OCT images – normal cortex (group 1), normal white matter (group 2), tumor cells infiltration of cortex (group 3) and white matter (group 4), and tumor only (group 5) were formed and assessed quantitatively. CP OCT parameters were developed to distinguish between tumor cells infiltrative areas of brain tissue vs healthy one. Microvasculature bed changes in glioblastoma compared to normal brain tissue were also demonstrated.

**Conclusions.** The potential of MM OCT as an effective instrument for *in vivo* OCT-guided infiltrative gliomas growth borders detection was demonstrated. The MM OCT method has further prospects of intraoperative application for one of the most complex clinical problems in neurosurgery.

### Acknowledgements

The study was supported by the Russian Scientific Foundation grant No.16-15-10391 and the RFBR project No. 16-32-60178 mol_a_dk. The MM OCT device development was funded by the Ministry of Education and Science of the Russian Federation, grant No. 14.B25.31.0015.

### References

1. N. Sanai, M.Y. Polley, M.W. McDermott, *et al.*, *J Neurosurg*, 2011, **115**(1), 3–8.
2. C. Kut, K.L. Chaichana, J. Xi, *et al.*, *SciTransl Med*, 2015, **7**(292), 292ra100.
3. O. Assayag, K. Grieve, B. Devaux, *et al.*, *Neuroimage Clin.*, 2013, **2.** 549–557.
4. V.M. Gelikonov and G.V. Gelikonov, *Laser Phys. Lett.*, 2006, **3**, 445–451.
5. L. Matveev, V. Zaitsev, G. Gelikonov, *et al.*, *Optics letters*, 2015, **40**(7), 1472–1475.

# NOVEL-POTENTIAL ANTICANCER THERANOSTIC AGENTS BASED ON THE PORPHYRAZINE FRAMEWORK FOR SPECIFICALLY PERSONALIZED MEDICINE

**L.G. Klapshina[1,2], S.A. Lermontova[1,2], I.S. Grigoryev[1], N.Yu. Shilyagina[1], M.S. Muravyeva[1], D.V. Yuzhakova[3], I.V. Balalaeva[2], M.V. Shirmanova[3], E.V. Zagaynova[3], and M.K. Kuimova[4]**

[1] N.I. Lobachevsky State University, Nizhny Novgorod, Russia, klarisa@iomc.ras.ru
[2] Institute of Organometallic Chemistry, Russian Academy of Sciences, Nizhny Novgorod, Russia[2]
[3] Nizhny Novgorod State Medical Academy
[4] Department of Chemistry, Imperial College London, UK

**Abstract.** We report on a series of novel tetracyanotetra(aryl) porphyrasine dyes which are found to be red-emitting fluorescent 'molecular rotor' *i.e.* the fluorescence lifetime and the quantum yield of these macrocycles strongly increase as a function of environment viscosity. They work also as an efficient PDT agent. Photosensitizers prepared on the cyano-aryl porphyrazine pigment platform bound to gadolinium cation demonstrate the potential to become an extraordinarily effective multimodal agent for theranostics, representing a new approach to PDT based on real-time monitoring of the therapy in combination with precise MRI /fluorescence diagnostics of tumor.

The various techniques available for cancer diagnosis and therapy are traditionally considered as separate approaches in medical care. But nowadays the development of the multifunctional agents which combine modalities for cancer diagnosis, treatment and real-time monitoring of treatment progress is a real imperative for specifically personalized medicine. Here we report on a series of novel tetracyanotetra(aryl)porphyrasine dyes which are found to be a red-emitting fluorescent 'molecular rotor', *i.e.* the fluorescence lifetime and the quantum yield of these macrocycles strongly increase as a function of environment viscosity [1]. On the other hand, they work as an efficient PDT sensitizer that induces apoptosis and necrosis in cells upon irradiation with red light through formation of singlet oxygen. We demonstrated that PDT *in vitro* using the new cyano-aryl porphyrasinemacrocycles is accompanied by a significant viscosity increase by monitoring the fluorescence lifetime of the macrocyclicrotor [2]. We suggest that this increase could be used as a completely new type of diagnostic and dosimetry tool during a PDT treatment providing feedback information about individual therapy status. Recently we obtained the integral curves of porphyrazine fluorescence delay within the area of model tumor of experimental animal (mouse) during PDT treatment. Thus, the significant increase of porphyrazine molecular rotor fluorescence lifetime upon irradiation was demonstrated *in vivo*.

In addition, the results of *in vivo* experiments showed that PDT sensitizers prepared on the cyano-aryl porphyrazine pigment platform bound to gadolinium cation demonstrate the potential to become an extraordinarily effective multimodal agent for specifically personalized medicine, representing a new approach to PDT based on real-time monitoring of the therapy in combination with precise MRI /fluorescence diagnostics of tumors.

**Acknowledgements**

The reported study was funded by the RFBR under the research projects №15-02-05468,15-02-05189,16-34-60117. It was also partially supported by the Ministry of Education and Science of the Russian Federation grant (Contract 14.Z50.31.0022).

**References**

1. M.K. Kuimova, S.W. Botchway, A.W. Parker, M. Balaz, H.A. Collins, H.L. Anderson, K. Suhling, and P.R. Ogilby, *Nat. Chem.*, 2009, **1**, 69–73.
2. M.A. Izquierdo, A. Vyšniauskas, S.A. Lermontova, I.S. Grigoryev, N.Y. Shilyagina, I.V. Balalaeva, L.G. Klapshina, M.K. Kuimova, *J. Mater. Chem. (B)*, 2015, **3**, 1089–1102.

# A NEW WAY TO EFFICIENT PRIMED CONVERSION OF PHOTOACTIVATABLE FLUORESCENT PROTEIN DENDRA2

**N.V. Klementieva**[1], **K.A. Lukyanov**[1,2], **E.V. Zagaynova**[1], and **A.S. Mishin**[1,2]

[1] Nizhny Novgorod State Medical Academy, Nizhny Novgorod, Russia, nvklementieva@gmail.com
[2] Shemyakin-Ovchinnikov Institute of Bioorganic Chemistry, RAS, Moscow, Russia

**Abstract.** Dendra2 is one of the most useful and effective fluorescent tools both for confocal and single-molecule detection live-cell microscopy. However, this protein requires phototoxic violet light to be photoactivated. Recently, a strategy utilizing blue and near-infrared lasers for the so-called primed conversion of Dendra2 was reported. In our study we suggested a new way to induce primed conversion by co-illumination with blue and red light sources that are more available for researchers. The efficiency of the proposed approach has been proved using various imaging modes, including super-resolution microscopy of living cells.

Photoactivatable fluorescent proteins are genetically encoded probes perfectly suitable for live-cell imaging, including super-resolution localization-based microscopy [1]. Among them, Dendra2 is a widely used marker, allowing studies of different targets, from individual proteins to cells, both in vitro and in vivo. Dendra2 is commonly photoconverted from green to red form upon illumination with violet (~405 nm) light. Such a process can also be induced by blue light sources but with much lower efficiency [2]. Recently, the phenomenon of the so-called primed photoconversion has been reported by a combination of blue and near-infrared lasers [3]. We, in turn, have proposed a new way to induce primed photoconversion, avoiding cytotoxic violet light and the need for special optics, by simultaneous irradiation of Dendra2 with blue and red lasers.

Primed photoconversion of Dendra2 by blue and red light was studied in different modes. The experiments included the illumination of purified protein in solution by light emitting diodes, laser scanning confocal microscopy of beads with immobilized protein, and, finally, live-cell single-molecule localization imaging of Dendra2-labelled beta-actin. As a result, we observed a strong increase in photoconversion efficiency of Dendra2 in case of combined illumination with red and blue lasers compared to illumination with single blue or red one. This effect was evaluated in a wide range of laser intensities. We also selected the optimized conditions for Dendra2 primed conversion to perform localization-based super-resolution microscopy. No difference between the traditional 405 nm laser-induced photoconversion and suggested dual-laser illumination scheme was found. Therefore, we could reconstruct high-quality sub-diffraction images and visualize actin ultrastructure in living cells.

In summary, a new approach for primed photoconversion of Dendra2 was demonstrated. We showed that red lasers in combination with blue ones can be used to increase photoconversion efficiency of the photoactivatable fluorescent protein. This allows avoiding the irradiation by 405 nm laser and related phototoxic effects on cells. Additionally, most microscopists seem to be able to easily implement this approach in practice due to the availability of red lasers and suitable optics.

### Acknowledgements

This work was supported by the Russian Science Foundation (grant 14-25-00129).

### References

1. D. Bourgeois, A. Regis-Faro, and V. Adam, *Biochem. Soc. Trans.*, 2012, **40**, 531–538.
2. N.G. Gurskaya, V.V. Verkhusha, A.S. Shcheglov, D.B. Staroverov, T.V. Chepurnykh, A.F. Fradkov, S. Lukyanov, and K.A. Lukyanov, *Nat. Biotechnol.*, 2006, **24**, 461–465.
3. W.P. Dempsey, L. Georgieva, P.M. Helbling, A.Y. Sonay, T.V. Truong, M. Haffner, and P. Pantazis, *Nat. Methods*, 2015, **12**, 645–648.

*Poster*

# FINE-TUNING OF THE PHOTOPHYSICAL AND CYTOTOXIC PROPERTIES OF NOVEL FLUORESCENT MOLECULAR ROTORS AND PDT SENSITIZERS BASED ON THE PORPHYRAZINE PIGMENT PLATFORM

**S.A. Lermontova[1,2], I.S. Grigoryev[2], N.N. Peskova[1], I.V. Balalaeva[1], and L.G. Klapshina[1,2]**

[1] N.I. Lobachevsky University of Nizhny Novgorod, Russia, lermontovasa@rambler.ru
[2] G.A. Razuvaev Institute of Organometallic Chemistry, Nizhny Novgorod, Russia

**Abstract.** Novel fluorescent molecular rotors based on the porphyrazine framework have been obtained in the form of free bases via a template assembly of a variety of aryltricyanoethylenes as structural units of the macrocycle. The unique combination of photodynamic activity with high sensitivity of the fluorescent properties to viscosity has been demonstrated for the prepared series of fluorophores which have a good prospect to be applied in biomedicine as optical sensors of intracellular viscosity and highly efficient PDT sensitizers.The chemical modification of macrocycle peripheral frame is found to be an effective tool for fine-tuning of the required photophysical properties and photodynamic activity enhancement.

This research was aimed at the synthesis of a series of new tetra(aryl)tetracyanoporphyrazine pigments in the form of free bases (Fig. 1) via a template assembly of various aryltricyanoethylenes [1] and to study photophysical properties and photodynamic activity of the products.

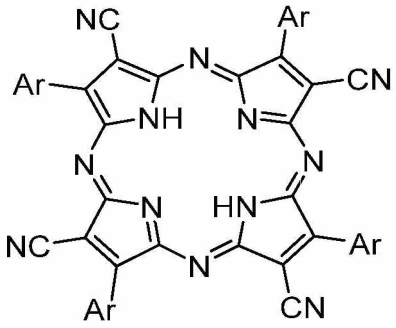



**Fig. 1.** The structure of tetra(aryl)tetracyanoporphyrazine pigments

The high sensitivity of fluorescence parameters of the prepared porphyrazines to the medium viscosity resulted in a unique combination of properties of optical sensor of local viscosity and sensitizers of photodynamic therapy. It is important to notice that viscosity is an important parameter determining the rate of diffusion (and, hence, that of the bimolecular reactions) in the condensed phase. A change in the local viscosity in the biological systems can cause serious diseases and cell dysfunction or even death. Therefore, the preparation of compounds acting as highly sensitive non-invasive optical sensors of intracellular viscosity is a topical issue. High sensitivity of their fluorescence parameters to viscosity is an additional advantage for PDT sensitizers since it allows the new theranostic approach to oncological disease treatment based on the real time monitoring of intracellular viscosity during the photodynamic therapy procedure [2].

We introduced a wide variety of Ar-groups into peripheral frame of the prepared porphyrazines. The spectral properties, fluorescence quantum yield sensitivity to the viscosity and cytotoxicity under dark and light conditions were investigated for the prepared products. It was established that all these characteristics significantly depend on the chemical nature of peripheral groups framing macrocycle. For example, the introduction of nitrogen atoms into substituents in *para*-position of aryl ring causes a substantial decrease of half maximal inhibitory concentration (IC50) under the light condition and strong increase of in the dark. Thus, the chemical design of macrocycle peripheral frame is found to be an effective tool for fine-tuning of the required photophysical properties and photodynamic activity enhancement.

## Acknowledgements

The reported study was funded by the RFBR under the research projects №15-02-05468,16-34-60117. It was also partially supported by the Ministry of Education and Science of the Russian Federation grant (Contract 14.Z50.31.0022).

## References

1. L.G. Klapshina, W.E. Douglas, I.S. Grigoryev, *et al., J. Mater. Chem.* 2009, **19,** 3668–3673.
2. M.A. Izquierdo, A. Vyšniauskas, S.A. Lermontova, I.S. Grigoryev, N.Y. Shilyagina, I.V. Balalaeva, L.G. Klapshina, M.K. Kuimova, *J. Mater. Chem. (B)*, 2015, **3**,1089–1102.

*Invited*

# PHOTODYNAMIC TREATMENT PLANNING AND DOSIMETRY: DEVELOPMENT OF AN UNIVERSAL APPLICABLE TREATMENT OPTIMIZATION PROCESS

**J. Cassidy[1], V. Betz[1], and L. Lilge[2]**

[1] Department of Electrical and Computer Engineering, University of Toronto, Toronto, Canada
[2] Department of Medical Biophysics, University of Toronto and University Health Network, Toronto, Canada

**Abstract.** Personalized Cancer Therapy is the focus of a concerted research effort in North America and other high-income countries. The aim is to improve survival while simultaneously reduce toxicity to normal organs. While local, minimally invasive physical therapies would satisfy these requirements, planning their implementation for an individual patient is but in its infancy. Here we present a workflow for Photodynamic Therapy, leading to personalized therapy delivery.

The majority of novel cancers are being diagnosed in low and middle-income countries (LMICs) [1], with an increase of 68% in incidence predicted by 2030. Cancer is not a major focus currently for LMICs, which also often lack the resources to present a similar range of therapeutic options to the patients as available in high-income countries. LMICs often can not even remotely consider Personalize Cancer Therapy. However, minimally invasive therapies such as Photodynamic Therapy (PDT) or photothermal therapies (PTT) are attractive treatment options, albeit widespread acceptance is hindered by multiple factors ranging from training of surgeons in optical therapeutic techniques, lack of easily usable treatment optimizing tools [2] and prediction of the anticipated treatment outcome.

Based on the publicly available FullMonte software [3], in combination with other open source image processing tools, a work plan is proposed that allows for personalized treatment planning. Starting with, generating in silico 3D tetrahedral models, from clinical images, execution of the Monte Carlo simulation and presentation of the 3D fluence rate distribution a treatment plan is presented which minimizes the number of light sources to be placed while attaining the prescribed energy density for the target and the organs at risk.

Calculation of a forward photon transport map in biological tissues is executed in < 1 minute even for a $10^6$ tetrahedral elements 3D models. Optimization of the source placement requires 1–2 hours.

Largest sources of errors are uncertainties in the contouring and unknown tissue optical properties. Hence, the proposed workflow includes also perturbation of the planning tissue optical properties, uncertainties in the photon source placement and contouring errors, to validate the invariance of the attained solution against these unknowns.

Lastly, the Monte Carlo simulations will also identify the locations for the most opportune photon density sensors to obtain the true tissue optical properties and quantify the uncertainty of the source fiber placement.

The accuracy of the fluence rate contours, as well as the predicted photon density at the sensor positions, were validated using 3D printed models.

The PDT treatment optimization process can accelerate the training or physicians, currently only available for ophthalmological applications, and thus accelerating the implementation of this therapy in various LMICs clinical centers.

### Acknowledgements

The work is funded through the OCE/NSERC CRD (PI Vaughn Betz) and the ORF (PI Lothar Lilge) funding mechanism by the Government of Ontario and Canada. Additional support was provided by Altera, IBM Canada, and Theralase Inc.

### References

1. L.A. Torre, R.L. Siegel, E.M. Ward, and A. Jemal, *Cancer Epidemiology Biomarkers & Prevention*, 2015; DOI: 10.1158/1055-9965.EPI-15-0578.
2. A. Rendon, R. Weersink, and L. Lilge, *Phys. Med. Biol.*, 2006, **51**, 5967–5975.
3. J. Cassidy, V. Betz, and L. Lilge, *Front. Phys.*, 2015, Doi:10.3389/fphy.2015.00006.

# METABOLIC IMAGING OF CANCER CELLS USING FLUORESCENCE LIFE-TIME MICROSCOPY

**M.M. Lukina**[1,2], **M.V. Shirmanova**[1], **V.V. Dudenkova**[1,2], **N.P. Pavlova**[1], **L.B. Snopova**[1], and **E.V. Zagaynova**[1]

[1] Nizhny Novgorod State Medical Academy, Russia, kuznetsova.m.m@yandex.ru
[2] Lobachevsky State University of Nizhny Novgorod, Russia.

**Abstract.** The aim of our work was to investigate metabolic activity of cancer cells by FLIM. Cellular metabolism was examined by monitoring the fluorescence lifetimes NAD(P)H and FAD. Cellular metabolism was analyzed in Hela cancer cells co-cultured with fibroblasts and in Hela tumor xenografts transplanted to nude mice. In the co-culture we observed a metabolic shift from OXPHOS toward glycolysis in cancer cells, and a reverse shift in fibroblasts. Metabolic heterogeneity within a tumor node was detected in the tumor tissue.

**Introduction.**The use of the glycolytic metabolism even in the presence of oxygen is a principal metabolic feature of cancer cells that exhibit aberrant growth rate and demand an elevated level of ATP to support the biogenesis of major macromolecules [1]. An important role in regulation of energy metabolism of cancer cells belongs to stromal components - collagen and cancer-associated fibroblasts (CAFs) [2]. NAD(P)H and FAD are the main metabolic cofactors that transfer electrons to molecular oxygen in a mitochondria electron transport chain. Since these co-factors are fluorescent, their relative content and state (free or protein-bound) can be assessed using Fluorescence Lifetime Imaging (FLIM) [3, 4].

**The aim** of our work was to study energy metabolism in human cervical carcinoma cells in the models of tumor-stroma interactionsin vitro and in vivo using FLIM.

**Materials and Methods.** The study was performed on the cervical cancer cells HeLa Kyoto. For *in vitro* investigation we used LSM 710 (Carl Zeiss, Germany) fluorescence laser-scanning microscope equipped with a FLIM module (Becker &Hickl GmbH, Germany). Cancer cells and fibroblasts were plated in the ratio of 1:5 and analyzed during 5 days. *In vivo* study of Hela tumor metabolism was implemented using multiphoton tomography MPTflex (JenLab GmbH, Germane) equipped with a FLIM module (Becker &Hickl GmbH, Germany). The histopathology examination and second harmonic generation (SHG) were used to analyze the tissue structure.

**Results.** It was found *in vitro* that the relative contribution of free NAD(P)H ($\alpha 1$) in cancer cells co-cultured with fibroblasts increased from 76.9 % on Day 1 to 79.45 % on Day 2, and remained at that increased level during the whole period of co-culturing. The relative contribution of free FAD ($\alpha 2$) in these cells also increased, which presumably indicates a shift of metabolism to glycolysis. By contrast, in the fibroblasts co-cultured with cancer cells, the relative contributions of free NAD(P)H and FAD gradually decreased, indicating a shift toward oxidative metabolism [2]. The relative contributions of free and protein-bound NAD(P)H in cancer cells *in vivo* were different at various tumor sites. In tumor areas with a denser cellular structure and low content of fibrotic stroma, the relative contribution of free NAD(P)H was 75.5±2.4 %. Whereas zones enriched with connective tissue fibers and containing a small amount of cancer cells, the relative contribution of free NAD(P)H increased to 80.8±2.7 %. Therefore, we detected heterogeneity of cellular metabolism within a tumor node with more glycolytic metabolism in stroma-rich zones [5].

**Conclusion**. In summary, the results of the study are of great importance for understanding metabolic behavior of tumors and for development of anticancer drugs targeted to metabolic pathways.

**Acknowledgements**

The work has been financially supported by the Russian Science Foundation (grant #14-15-00646-П).

**References**

1. J.C. Tung, *et al.*, *Free Radical Biology and Medicine,* 2015, **79**, 269–280.
2. I. Druzhkova, *et al.*, *Cell Cycle*, 2016, **1**, 1–10.
3. I. Georgakoudi, W.L. Rice, M. Hronik-Tupaj, D.L. Kaplan, *Tissue Eng*, 2008, **14**(4), 321–340.
4. M.C. Skala, *et al.*, *Journal of Biomedical Optics*, 2007, **12**(2), 1–10.
5. M.M. Lukina, *et al.*, *SPIE pross,* 2017, **42**, 731–734.

*Invited*

# ZINC OXIDE NANOPARTICLE PENETRATION INTO *IN VIVO* AND *IN VITRO* HUMAN SKIN. SIMULATING LIFE LIKE EXPERIMENTAL CONDITIONS AND USING NON-INVASIVE MPT-FLIM IMAGING CAN PROVIDE ACCURATE TOXICOLOGICAL ASSESSMENT

**Y. Mohammed[1], W. Sanchez[1], D. Liu[1], V.R. Leite-Silva[1], A. Holmes[2], H. Studier[2], I. Haridass[1], E. Ryan[1], J. Grice[1], and M. Roberts[1,2]**

[1] Therapeutics Research Centre, School of Medicine, The University of Queensland, Translational Research Institute, QLD, Australia. y.mohammed@uq.edu.au
[2] Therapeutics Research Centre, School of Pharmacy and Medical Sciences, University of South Australia, SA, Australia

**Abstract.** Zinc oxide nanoparticles (ZnO-NP) have been widely used in sunscreens and provide good broad spectrum protection against UV induced photo damage and skin cancer. Recent encouraging findings have attributed better sun protection to a slight reduction in Melanoma cases in Australia. However, controversies surrounding the safety of nanoparticles applied topically to the skin remain. We have over the last several years looked at simulating real life experimental conditions when assessing nanoparticle penetration into the human skin. Non-invasive Multiphoton Microscopy coupled with Florescence Lifetime Imaging Microscopy enables real-time, accurate detection of NP penetration into volunteer skin *in vivo*.

## Methods

We used multiphoton tomography with fluorescence lifetime imaging microscopy to measure zinc oxide nanoparticle penetration and the metabolic changes within the viable epidermis. The effects of life like conditions such as massaging, flexing, occlusion, barrier impairment as well as routine bathing/swimming in different water sources was assessed on volunteer skin penetration of ZnO NPs. We also looked at the effect of short and long time repeated dosing of ZnO NPs.

## Results

Zinc oxide nanoparticles failed to penetrate into the viable epidermis of human volunteer skin with or without occlusion, massage or flexing. In barrier-impaired skin, achieved by tape-stripping, occlusion resulted in greater penetration of zinc oxide into the viable epidermis. Water from different sources simulating daily habits such as tap water (bathing), pool water (swimming) and ocean/beach water (swimming) resulted in different hydration/dehydration states of the skin. This did not result in ZnO NP penetration but rather caused an increased accumulation into the skin appendages (furrows and follicles). Repeated application (both short and long time) did not cause an increase in penetration. However, an increase in labile Zinc species as a result of hydrolysis/ dissolution was observed in ex vivo skin. We observed no measurable changes in the metabolic and redox state of the viable epidermis after treatment with zinc oxide, suggesting the lack of any toxicity.

## Conclusions

MPT-FLIM allows for simultaneous penetration and toxicity assessment in vivo reducing the need for separate experiments to be carried out. By simulating real-life experimental conditions during and prior to nanoparticle application on human volunteers myths and concerns regarding nanoparticle penetration and the subsequent damage caused by them can be effectively dispelled.

## Acknowledgements

Funding for this project was made possible, in part, by continued support provided by the NH&MRC Australia.

*Invited*

# NEW CANCER THERAPY USING NEAR INFRARED LIGHT

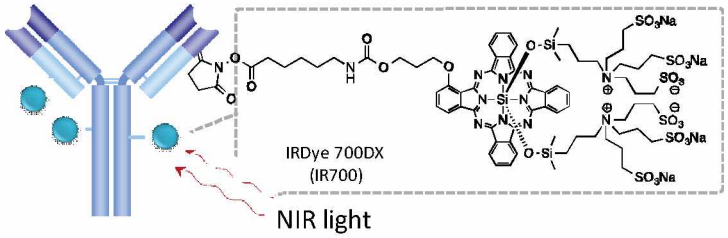
**M. Ogawa**[1,2]

[1] Hokkaido University, Sapporo, Japan, mogawa@pharm.hokudai.ac.jp
[2] JST, PRESTO, Saitama, Japan

**Abstract.** Near infrared photoimmunotherapy (NIR-PIT) is a new cancer therapy using antibody and hydrophilic photosensitizer conjugates. However, the mechanisms for killing the cells are not elucidated yet, and it is necessary to elucidate them for developing better NIR-PIT. In this study, we investigated the mechanism of NIR-PIT by evaluating cell membrane damage, immunologic reactions induced by NIR-PIT.

## Introduction

Near infrared photoimmunotherapy (NIR-PIT) is a new method of treating cancers by exposing them to an antibody-photosensitizer conjugate (APC) consisting of an antibody directed at a cell surface antigen overexpressed on the plasma membrane and a photo-activated silica-phthalocyanine dye (IR700) [1]. The APC binds to cells expressing antigen and after NIR light exposure (690 nm), induces highly selective cancer cell death with immediately adjacent non-target expressing cells suffering no toxic effects. A phase I study of an antibody conjugate consisting of cetuximab (anti-HER1 antibody) linked to IR700, for the treatment of inoperable head and neck cancers is ongoing in USA (NCT02422979). However, the mechanism for killing the cells are not elucidated yet. To make the more potent and effective drug for PIT, it is necessary to know the mechanism.




IR700 conjugated antibody binds to the target cancer cell membrane, and the exposure to near infrared light induces target-specific cell killing

## Methods

We have investigated dynamic morphological changes after NIR-PIT using three-dimensional dynamic low coherence quantitative phase microscopy (3D LC-QPM). Additionally, cell membrane permeability was studied using various sized molecules. Furthermore, we have performed immunologic analyses of the events induced by NIR-PIT.

## Results and discussion

Based on LC-QPM observation, the cells were dramatically and rapidly expanded by PIT, and PIT induced sufficient cumulative damage to the cell membrane within 5 seconds to induce rapid cell death. We found that initial damage of the cell plasma membrane was large enough to penetrate small ions, but not other molecules. Then, the size of the membrane damage increased to a few nanometers without obvious changes in bright field images. Thus, PIT-induced damage to the cell membrane impairs the membrane function as a pressurized barrier, allowing flow-in or flow-out of molecules by compensating the unbalanced osmotic pressure. Also, we observed the process that induces relocation of the immunogenic cell death bio-markers [2]. These observations suggest that necrotic cell death due to cell membrane damage is one of the potential causes for inducing cell death by PIT.

## Acknowledgements

This research was supported by JST, PRESTO. I would like to sincerely thank Dr. Kobayashi, NCI/NIH, USA, for his grateful guidance, advice and support.

## References

1. M. Mitsunaga, M. Ogawa, N. Kosaka, LT. Rosenblum, PL. Choyke, and H. Kobayashi, *Nat. Med.*, 2011, **17**(12), 1685–1691.
2. M. Ogawa, Y. Tomita, Y. Nakamura, M.-J. Lee, S. Lee, S. Tomita, T. Nagaya, K. Sato, T. Yamauchi, H. Iwai, A. Kumar, T. Haystead, H. Shroff, P.L. Choyke, J.B. Trepel, and H. Kobayashi, *Oncotarget.*, 2017, **8**(6), 10425–10436.

# DIFFUSE OPTICAL SPECTROSCOPY MONITORING OF OXYGEN STATE OF GROWING EXPERIMENTAL TUMOR

**A.G. Orlova[1], M.Yu. Kirillin[1], A.B. Volovetsky[2], N.Yu. Shilyagina[2], E.A. Sergeeva[1], G.Yu. Golubiatnikov[1], and I.V. Turchin[1]**

[1] Institute of Applied Physics RAS, Nizhny Novgorod, Russia
[2] N.I. Lobachevsky State University of Nizhny Novgorod, Nizhny Novgorod, Russia

**Abstract.** *In vivo* monitoring of oxygenation level and blood content in the course of experimental tumor growth was performed using the diffuse optical spectroscopy (DOS) technique. Results of oxygen saturation measurements were confirmed by measurements of $pO_2$. Differences in the level of oxygenation and blood content between experimental tumor and normal tissue were revealed. Rapid decrease of oxygenation level preceded the acceleration of tumor growth during which oxygen state has remained low. The increase of tumor volume was accompanied by the gradual increase in blood content.

Tumor hypoxia determines poor prognosis, rapid tumor progression and therapy resistance. The study of the mechanisms of tumor hypoxia formation makes it possible to develop novel methods for its correction. In recent years diffuse optical spectroscopy (DOS) demonstrated its potential in evaluation of the parameters of tissue oxygenation and blood content for preclinical tumor models [1–2]. DOS enables reconstruction of concentration of principal tissue chromophores: oxy-($HbO_2$), deoxy-hemoglobin (HHb), water and lipids from evaluation of tissue absorption coefficient [3]. In this work we employed DOS for monitoring the dynamics of oxygen saturation ($StO_2$) and hemoglobin content in animal model of human breast adenocarcinoma SKBR-3 during its growth.

We used a continuous wave fiber probe based DOS system in reflectance configuration [4]. Probing radiation with a spectral range of 400–900 nm is delivered to the tissue surface through a 200 μm optical fiber. Scattered radiation is collected from the surface by a detecting fiber located 1.5 mm from the probing one. The exact values of concentrations of total hemoglobin (tHb), HHb, $HbO_2$, and oxygen $StO_2$ are extracted by a two-step reconstruction algorithm: at the first step, the absorption coefficient spectra are derived from DOS measurements using the algorithm based on the diffusion theory; at the second step, the concentrations of HHb and $HbO_2$ are reconstructed.

The DOS measurements were started from the 12th day after tumor inoculation and continued for 11 days every 24 hours. Diffuse optical transmittance spectra were measured from the animal body surface in the tumor region and in the normal muscle region. For verification of DOS data, oxygen partial pressure ($pO_2$) was measured in the tumor and muscle tissues using Clark microelectrode OX-N in two mice.

$StO_2$ level in tumor tissue as compared to baseline and to normal muscle tissue decreased and remained reduced by up to three times starting from 14th day of tumor growth. Comparison of data on blood oxygen saturation obtained by DOS for normal and tumor tissues and $pO_2$ measurements showed good compliance, correlation coefficient was 0.80 ($p < 0.05$). For the content of tHb statistically significant differences with the baseline as well as between the tumor and muscle were detected on day 15 of tumor growth. THb concentration continued to increase gradually to the level about three times higher as compared to the initial one. The gradual growth of tHb concentration which indicates an increase of tumor blood content was observed in parallel with an increase of tumor volume. Unlike the changes in blood content, reduction of the tumor oxygenation level occurred quickly and preceded the tumor growth acceleration. We demonstrated that the rise in the level of hemoglobin is associated with the increase in tumor node size. According to $\chi^2$–test, strong dependence of the tHb concentration on tumor volume (with significance level $p < 0.01$) was revealed, while the values of $StO_2$ and tumor volume were shown to be independent ($p = 0.11$).

**Acknowledgements**

The study is supported by the RFBR (project 15-02-04270).

**References**

1. J.W. Spliethoff, D.J. Evers, *et al.*, *TranslOncol.*, 2014, **7**(2), 230–239.
2. N. Rajaram, A.F. Reesor, C.S. Mulvey, A.E. Frees, & N. Ramanujam, *PLoS One*, 2015, **10**(1), e0117132.
3. T. Durduran, R. Choe, W.B. Baker, and A.G. Yodh, *Rep. Prog. Phys.*, 2010, **73**, 076701.
4. N. Shakhova, I. Turchin, *et al.*, *Proc. SPIE*, 2007, **6430**, 64300N.

*Invited*

# MULTIFUNCTIONAL NANOPARTICLES FOR BIO-MEDICAL RESEARCHES AND THERANOSTICS

**E. Perevedentseva[1,2], A. Karmenyan[1], Y.-C. Lin[1,3], C.-Y. Song[1], Z.-R. Lin[1], L.-C. Liu[1], Ashek-I-Ahmed[1], and C.-L. Cheng[1*]**

[1] National Dong Hwa University, Taiwan, elena@gms.ndhu.edu.tw, *clcheng@gms.ndhu.edu.tw
[2] P.N. Lebedev Physics Institute of Russian Academy of Science, Moscow, Russia
[3] Institute of Physics, Academia Sinica, Taipei, Taiwan

**Abstract.** Recently, an important trend is the development of multifunctional nanoparticles (NP) for bio-medical applications. To integrate diverse functionalities, the methods to vary particles surface properties, size, shape and structure, composition, optical-spectroscopic and other physical properties are developed. Number of NP can reveal wide variability of the properties: noble metals nanoparticles, C- and Si-based NP of different structure, polymer NP, etc., as well as their composites. Among these NP nanodiamond (ND), noble metal and ND-metal NP reveal promising variability of the properties. Some examples, including magnetic-, Au-, fluorescent drug-modified ND, are considered in the presented work.

Nanoparticles which have the potential to integrate various functionalities useful for bio-medical applications attract now much attention. Particularly, discussing the NP theranostic applications always considers such multifunctional NP, designed to co-deliver multiple components, control the delivery, realizingdrug and diagnosis simultaneously [1]. To integrate several functionalities, different methods of surface functionalization and modifying the particles optical-spectroscopic and other physical properties are developed. Number of NP can reveal wide variability of utilized properties: noble metals NP, carbon- and silicon-based NP of different structure, polymer NP, etc., as well as their composites.

Among these NP nanodiamond (ND) ispromising for development of multifunctional complex [2] due to their widely variable features in sizes, structure, surface chemistry, physical properties and biocompatibility [3]. In this work we consider like example magnetic-modified ND (Ray Technologies, Israel). The strong magnetic susceptibility of this ND has been demonstrated; however the origin of magnetism is unclear. It is important, that simultaneously the ND reveals strong fluorescence both at one-photon and two-photon excitation, and at fluorescence lifetime analysis. The origins of the fluorescence are also discussed. The combining fluorescence and magnetic properties of ND with its biocompatibility make it promising for various imaging and delivery bioapplications. Simultaneous utilizing ND fluorescence and magnetic properties applications, e.g. to realize and observe magnetic filtration, magnetic-guided delivery, magnetic-assisted 3D cellular growth are discussed.

Very different kinds of surface design and modification can be considered to increase ND's functional modalities. Plasmonic properties of Au nanostructures make them promising for multimodal imaging using surface enhanced Raman scattering and two-photon excitation. Combining Au with ND in core-shell Au@NDNP joins Au plasmon resonance properties and ND fluorescence and makes the nanoparticles an excellent multimodal-imaging probe [4]. As another example, ND complex with surface-adsorbed drug berberine and the study utilizing both ND and berberine fluorescence properties, is presented [5].

Note, that we discuss here only limited examples. However they are already enough to demonstrate the wide perspectives of development of NP with new synergy properties for fundamental studies and for applications.

**Acknowledgements**

The authors appreciate the financial support of this research by the Ministry of Science and Technology (MoST) of Taiwan, Grant No. MOST 103-2112-M-259-001-MY3.

**References**

1. G. Bao, *et al.*, *Annu. Rev. Biomed. Eng.*, 2013, **15**, 253–282.
2. L.C. Cheng, *et al.*, *Nanoscale*, 2013, **5**, 3931–3940.
3. E. Perevedentseva, *et al.*, *Future Medicine. Nanomedicine*, 2013, **8**(12), 2041–2060.
4. L. Minati, *et al.*, *Dia. Relat. Mater.*, 2015, **53**, 23–28.
5. Y.C. Lin, *et al.*, *J. Biomedical Photonics & Engineering*, 2017, in press.

*Invited*

# TRYPTOPHAN AS AN ALTERNATIVE BIOMARKER FOR CANCER METABOLISM: FLIM-FRET MICROSCOPY

**A. Periasamy, H. Wallrabe, Z. Svindrych,** and **S.R. Alam**

The W.M. Keck Center for Cellular Imaging, Departments of Biology and Biomedical Engineering, University of Virginia, Charlottesville, Virginia 22903, USA
Email: ap3t@virginia.edu

**Abstract.** Tryptophan (Trp) is another endogenous fluorophore that can be considered as a biomarker in cancer investigation. In this study we investigated the quenching of Trp in the presence of NAD(P)H in the prostate cancer cells using three-photon excitation FLIM and FRET Microscopy. We developed an image segmentation analysis and correlated the E% (energy transfer efficiency) with FLIM based optical redox ratio. The quenching of Trp clearly shows the drug response between Caucasian-American and African-American prostate cancer cell lines.

The molecular native fluorescence (autofluorescence) can be used as a research tool to understand the underlying mechanisms of molecular interactions and cellular processes under native conditions in cells and tissues. The intrinsically fluorescent NADH and flavins (FAD) are widely utilized as a biomarker for cellular energy metabolism. Tryptophan (Trp) is another endogenous fluorophore which is being reported as a biomarker in cancer investigations [1, 2]. Trp is an essential amino acid, is a precursor of niacin, which in turn is a precursor of NAD(P)H. Increased Trp catabolism and increased Indoleamine 2,3-dioxygenase (IDO) activity in the Kynurenine pathway are linked to cancer development and progression. Probing Trp is therefore, clinically relevant. In general, Trp fluorescence intensity and lifetime mainly provide information on the protein composition, protein structure of which they are a part of and changes in overall cellular microenvironment. Trp is used as a marker for protein abundance. Like NAD(P)H and FAD, Trp could also have two possible lifetime components. The shorter and longer lifetimes of Trp represent the "protein-bound" (as residues in proteins) and "free" (free amino acid) components, respectively. One of the major applications of fluorescence lifetime imaging is the measurement of FRET (Förster resonance energy transfer) [3, 4]. In FLIM-FRET measurements, FRET events are identified if there is reduction in the donor lifetimes, as a result of quenching of fluorescence in the presence of the acceptor. Trp-NADH is known pair [1, 5–7]. The NAD(P)H-interacting enzymes carrying Trp residues from different metabolic pathways, may be responsible for the quenching of Trp resulting in FRET interaction (E%). Trp is the most useful for imaging because of its attractive spectral features—with excitation and emission maxima at 280 and 350 nm, respectively, it has relatively high molar absorptivity (5500 $M^{-1}$ $cm^{-1}$) and modest quantum yield ($\Phi$) of 0.13 in the 300–400 nm range [8]. Excited state fluorescence of Trp decays bi-exponentially with an average lifetime of 3.03 ns. We have demonstrated that Tryptophan-NADH interactions can be used as a reporter of metabolic activity [1, 5].

In prostate cancer, since, there is a direct link amongst defective OXPHOS activity, cancer cell metabolism and apoptosis, we have investigated the doxorubicin drug response of an aggressive (African-American, E006AA) and responsive (Caucasian-American, LNCaP) prostate cancer cells. Through, this study we clearly demonstrate the earlier molecular changes associated with the increased mitochondrial oxidative phosphorylation that precede the effector caspase-3 activation and apoptosis.

## References

1. V. Jyothikumar, Y. Sun, and A. Periasamy, *J. Biomed. Opt.,* 2013, **18**, 060501.
2. P. Diagaradjane, *et al.*, *Lasers Surg. Med.* 2005, **37**(5), 382–395.
3. A. Periasamy and R.M. Clegg, *FLIM Microscopy in Biology and Medicine*, CRC Press, New York, 2010.
4. Y. Sun, R.N. Day, and A. Periasamy, *Nature Protocols*, 2011, **6**, 1324–1340.
5. V. Ghukasyan & A. Heikal, *Natural Biomarkers for Cellular Metabolsm: Biology, Techniques, and Applications*, CRC Press; Taylor & Francis Group, New York, 2015, p. 157.
6. T. Torikata, *et al.*, *J Biol Chem*, 1979, **254**(9), 3516–3520.
7. J.R. Lakowicz, *Principles of fluorescence spectroscopy*, 3rd ed. Springer US; 2006.
8. R.F. Chen, *Analytical Letters* 1967, **1**(1), 35–42.

# QUANTIFICATION OF TARGET ENGAGEMENT USING NON-INVASIVE MFLI-FRET *IN-VIVO* IMAGING OF BREAST CANCER XENOGRAFTS

**A. Rudkouskaya[1], N. Sinsuebphon[2], X. Intes[2], and M. Barroso[1]**

[1] Albany Medical College, Albany, NY USA, rudkoua@mail.amc.edu
[2] Rensselaer Polytechnic Institute, Troy, NY USA

**Abstract.** We employ Macroscopy Fluorescence Lifetime Imaging (MFLI) FRET to quantify the internalization of NIR labeled transferrin in T47D breast cancer xenografts *in vivo*. We report that *in vivo* MFLI-FRET data correlate with transferrin accumulation in dissected tumors based on quantification analysis of immunofluorescent staining. In contrast, no correlation between FRET levels and transferrin receptor density was found. This study demonstrates MFLI-FRET as a robust non-invasive quantitative measure of the target engagement of ligand-dimerized receptor in cancer cells which could accelerate the optimization of targeted drug delivery efficacy.

**Introduction.** The ability to non-invasively monitor and quantify the target engagement in preclinical studies of oncologic drug delivery remains a great challenge. MFLI-FRET offers a unique approach to detect NIR labeled ligand binding to dimeric receptors followed by their uptake into cancer cells in live mice. The dimeric nature of Transferrin receptor (TfR), which is overexpressed in most cancer cells, allows for the quantification of Tfn internalization into the cells by measuring FRET between receptor-bound Tf donor and acceptor NIR fluorophore pairs, based on the reduction of donor fluorophore lifetime in live mice [1].

**Methods.** Athymic nude mice carrying T47D breast cancer xenografts were injected intravenously with Tfn-AF700 and Tfn-AF750 at an A:D ratio of 2:1 and used for live imaging experiments. Widefield MFLI was performed on a time-domain fluorescence lifetime imaging tomographic system using a gated intensified CCD (ICCD) as detailed in [2]. After imaging, tumors were dissected and processed for immunohistochemical (IHC) and immunofluorescent (IF) staining.

**Results.** We compared the data from two independent imaging experiments (six mice total) with thorough IHC and IF analysis of dissected xenografts. Despite significant heterogeneity of tumors regarding size, cell density and TfR expression levels, we found a strong correlation between FRET donor fraction (FD%), which indicates the internalized Tf, and Tf accumulation in cancer cells based on quantification of Tf staining (Fig. 1, A and C). Surprisingly, no correlation was found between FD% and TfR density which suggests receptor overexpression doesn't guarantee an efficient drug delivery.

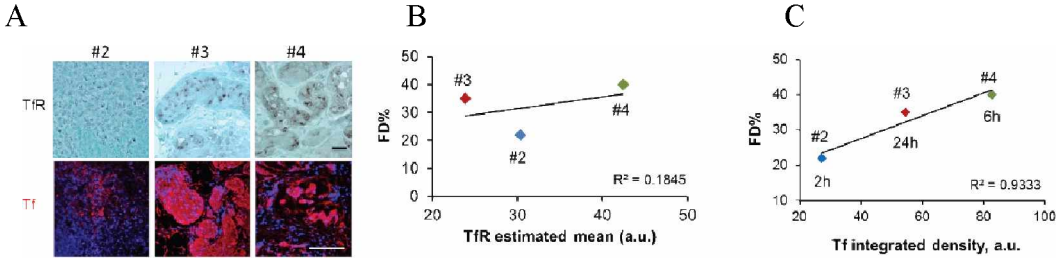



**Fig. 1.** (A) Representative images of TfR IHC staining and confocal Tf IF staining in tumors from mice#2-4. Scale bar 100 µm. (B) FD% does not correlate with TfR estimated mean obtained from quantification of IHC staining histograms. (C) Strong correlation between FD% and Tf integrated density calculated using whole tissue scan images

**Conclusion.** We demonstrated in heterogeneous breast cancer xenografts a strong correlation between FRET levels and transferrin accumulation inside the cancer cells, but not TfR levels. Thus, MFLI-FRET represents a robust measure of the target engagement in tumor cells *in vivo*. This approach may dramatically transform the field of targeted drug delivery.

**Acknowledgements**

This work was funded by the National Institutes of Health grant R01EB019443.

**References**

1. K. Abe, *et al.*, *PLoS One*, 2013, **8**, e80269.
2. V. Venugopal, *et al.*, *Biomed. Optics Express*, 2010, **1**, 143.

*Invited*

# TIME RESOLVED LUMINESCENCE IMAGING AS A NEW THERANOSTIC APPROACH

**A. Rück[1], J. Breymayer[1], D. Bisinger[1], P. Schäfer[2], B. von Einem[2], C.A.F. von Arnim[2], and S. Kalinina[1]**

[1] University Ulm, Core Facility Confocal and Multiphoton Microscopy, N24, Albert-Einstein-Allee 11, 89081 Ulm, Germany, angelika.rueck@uni-ulm.de
[2] Dept. of Neurology, University Hospital Ulm, Oberer Eselsberg 45, 89081 Ulm, Germany

**Abstract.** Cellular responses to oxygen tension have been studied extensively, optical techniques based on time resolved luminescence imaging to detect oxygen concentration and distribution are therefore of prominent interest. They offer the possibility by inspecting fluorescence decay characteristics of intrinsic coenzymes to directly image metabolic pathways, whereas oxygen tension can be determined by considering the phosphorescence lifetime of a phosphorescent probe. The combination of both fluorescence lifetime imaging (FLIM) of coenzymes like NAD(P)H and FAD and phosphorescence lifetime (PLIM) of phosphorescent dyes could provide valuable information about correlation of metabolic pathways and oxygen tension and offers new ways in theranostic procedures.

The photophysical basis of fluorescence lifetime imaging (FLIM) and phosphorescence lifetime imaging (PLIM) is demonstrated in the Jablonski diagram in figure 1. The fluorescence lifetime describes the decay from the first excited singlet state of a molecule and is the reciprocal of the sum of all the rate constants leading to relaxation. FLIM of metabolic coenzymes is the basis for optical metabolic imaging (OMI). Intersystem crossing from the first excited singlet state to the triplet state is the prerequisite for a spin forbidden process called phosphorescence. The phosphorescence lifetime is the reciprocal of the sum of the decaying processes from the triplet state and is the parameter of interest during PLIM. The phosphorescence lifetime can decrease in the presence of quenchers as oxygen. Oxygen is the most abundant quencher in cells. From this oxygen concentration can be determined leading to oxygen imaging (OXI). Main interest is focused on techniques which enable simultaneous analysis of OMI and OXI by correlated FLIM and PLIM. Within this presentation new efforts in time resolved luminescence imaging are presented and promising theranostic applications are discussed. This includes metabolic studies in neurological disorders as well as new approaches in PDT.

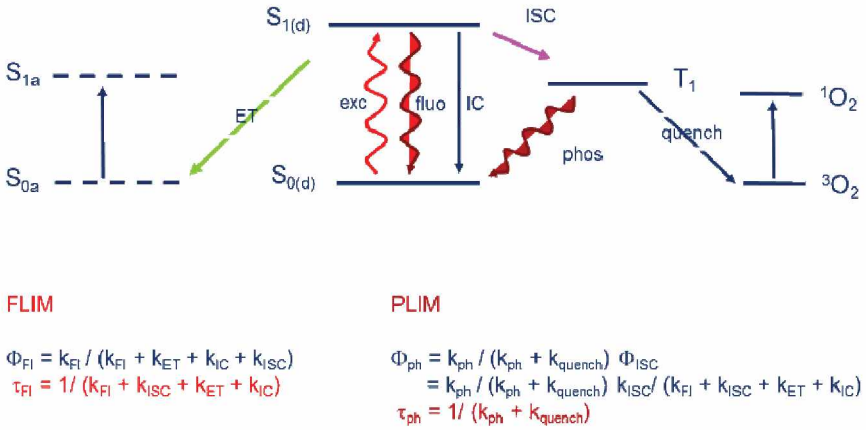



**Fig. 1.** Jablonski diagram of FLIM and PLIM

## Acknowledgements

This work was carried out with financial support by the Ministry of Financial Affairs of Germany, FKZ order: KF2122510AK2 ("PLIMOX"), FKZ order: IGF 18239 N/3 ("MITOSKOPIE").

## References

1. A. Rück, C. Hauser, S. Mosch, and S. Kalinina, "Spectrally resolved fluorescence lifetime imaging to investigate cell metabolism in malignant and nonmalignant oral mucosa cells", *Journal of Biomedical Optics*, 2014, **19**(9), 096005.
2. S. Kalinina, J. Breymayer, P. Schäfer, E. Calzia, V. Shcheslavskiy, W. Becker, and A. Rück, "Correlative NAD(P)H-FLIM and oxygen sensing-PLIM for metabolic mapping", *J. Biophotonics*, 2016, 1–12, DOI 10.1002/jbio.201500297 (2016).

*Invited*

# RATIONAL MUTAGENESIS OF NEW PHOTOCONVERTABLE FLUORESCENT PROTEIN FOR THE LIVE CELL MICROSCOPY

**I.D. Solviev[1,2], T.V. Ivashina[3], L.M. Vinokurov[4], and A.P. Savitsky[1,2]**

[1] Chemistry Department, Lomonosov Moscow State University, 119991,Moscow, Russia
[2] Federal Research Centre "Fundamentals of Biotechnology" of the Russian Academy of Sciences, Moscow
apsavitsky@inbi.ras.ru
[3] The Branch of Shemyakin and Ovchinnikov Institute of Bioorganic Chemistry Pushchino, Moscow region, Russia
[4] Skryabin Institute of Biochemistry and Physiology of Microorganisms, Russian Academy of Sciences, Pushchino, Moscow Region, Russia

GFP-like fluorescent proteins are widely used as markers for the visualization of intracellular processes and for sub-difractional localization microscopy. In this work we describe a new photoconvertible protein, SAASOti, obtained from the Stylocoeniellaarmata coral [1]. Wild type of the protein is tetramer with strong tendency to oligomerization. Wild type SAASOtiwas monomerized using rational mutagenesis. It is well known that tetramers of fluorescent proteins have two interfaces: electrostatic AB and hydrophobic AC. Site-directed mutagenesis was used to introduce mutations in both interfaces. Substitution in electrostatic interface (K145E) gives tetrameric structure and totally excludes oligomerization. Substitution in hydrophobic interface (V127T) gives monomeric protein up to millimolar concentration. Data on oligomerization state was supported by fluorescence correlation spectroscopy. Using FCS method we calculated diffusion coefficients D = 50±10 μm2/s for SAASotiK145E and wild type SAASOti. The data obtained is consistent with tetramer FP diffusion coefficient. Diffusion coefficient for SAASotiV127T variant was estimated as D = 100±20 μm2/s and is similar to the D value for eGFP. Thus, SAASOtiV127T is supposed to be presented in monomeric state that has cytoplasmic localization and no cytotoxicity. Monomeric proteins in both green and red forms have high extinction coefficient and quantum yield. Monomeric protein SAASotiV127Tcapable of rapid green to red photoconversion and rapid photobleaching of the red form, which allows the protein to be used in sub-diffractional microscopy approaches in living cells with low light intensity.

**Acknowledgements**

This work was supported by Russian Science Foundation (project 15-14-30019).

**References**

1. G. Lapshin, A. Salih, P. Kolosov, M. Golovkina, Y. Zavorotnyi, T. Ivashina, L. Vinokurov, V. Bagratashvili, A. Savitsky, "Fluorescence color diversity of great barrier reef corals", *Journal of Innovative Optical Health Sciences*, 2015, 1550028.

*Invited*

# PROBING TUMORS WITH TIME-RESOLVED SPECTROSCOPY

**M. Lukina[1], A. Orlova[1,2], A. Pavlikov[1], D. Shirokov[1], A. Neubauer[3], H. Studier[2], E. Zagaynova[1], W. Becker[3], V. Yakovlev[4], M. Shirmanova[1], and V. Shcheslavskiy[1,3]**

[1] Institute of Biomedical Technologies, Nizhny Novgorod State Medical Academy, Minin and Pozharsky Square, 10/1, Nizhny Novgorod, Russia 603005
[2] Institute of Applied Physics RAS, Ulyanov Street 46, Nizhny Novgorod, Russia 603950
[3] Becker&Hickl GmbH, Nahmitzer Damm 30, Berlin 12277, Germany
[4] Department of Biomedical Engineering, Texas A&M University, TX 77843-3120 USA

**Abstract.** Time-resolved fluorescence and phosphorescence spectroscopy of a tumor based on Time-Correlated Single Photon Counting (TCSPC) may deliver valuable information about its metabolic and oxygen states. We present the results on optical interrogation of tumors *in vivo* based on the novel fiber optical probes. We also discuss the potential of the TCSPC approach for label-free spectroscopy of biological samples.

The study of metabolic and oxygen states of cells in a tumor *in vivo* is crucial for understanding of the mechanisms responsible for the tumor development and provides background for the relevant tumor's treatment. Here, we show that a specially designed implantable fiber-optical probe provides a promising tool for optical interrogation of metabolic and oxygen states of a tumor *in vivo*. In our experiments, the excitation light from a ps diode laser source is delivered to the sample through an exchangeable tip via a multimode fiber, and the emission light is transferred to the detector by another multimode fiber (Fig. 1).

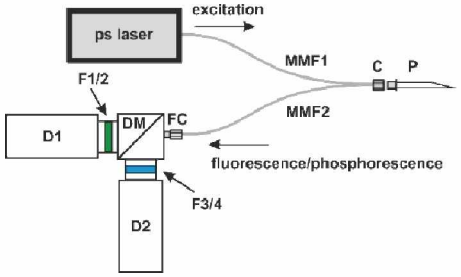



**Fig. 1.** Experimental setup for fluorescence/phosphorescence spectroscopy measurements. MMF1: Multimode fiber (core diameter: 50 μm, cladding diameter: 65 μm); MMF2: Multimode fiber (core diameter: 200 μm, cladding diameter: 220 μm); C: miniature connector; P: exchangeable probe with a multimode fiber (core diameter: 300 μm, cladding diameter: 350 μm) in a needle G26); FC-FC connector; D1 and D2: HPM-100-40 detector. F1/2: emission filters 510LP and 632/90 BP. F3/4: 405LP and 450/60BP. DM: 510 LP dichroic mirror

Fluorescence lifetime of nicotinamid adenine dinucleotide (NAD(P)H) and phosphorescence lifetime of an oxygen sensor based on iridium (III) complex of enzothienylpyridine (BTPDM1) are explored both in model experiment in solutions, and in living mice.

We also present a developed system, based on Time-Correlated Single Photon Counting that can be used for Raman spectroscopy of interrogated samples. This system is compact, cost-effective, and therefore, is suitable for clinical applications.

**Acknowledgements**

This work was partially funded by Russian foundation for basic research (grant # 15-32-20324). We also thank Prof. Tobita from Gunma University, Japan for providing oxygen sensors and Anastasia Shumilova (Nizhnii Novgorod State Medical Academy) for preparation of tissue cryosections.

# STUDY OF THE MECHANISMS OF OXIDATIVE STRESS IN RESPONSE TO PHOTODYNAMIC TREATMENT

**N.Y. Shilyagina**[1], **N.N. Peskova**[1], **A.V. Utkina**[1], **A.A. Gorokhova**[1], **S.A. Lermontova**[2], **L.G. Klapshina**[2], and **I.V. Balalaeva**[1]

[1] N.I. Lobachevsky University, Nizhny Novgorod, Russia, nat-lekanova@yandex.ru
[2] Nizhny Novgorod Institute of Organometallic Chemistry, Nizhny Novgorod, Russia

**Abstract.** Photodynamic therapy (PDT) is a modern minimally invasive treatment technique, which provides selective damage of tumor tissue. Despite extensive use of PDT in clinical practice, there is still no clear understanding of the nature of photodynamic response development. It is true for both initial physicochemical processes and subsequent chain of events developing at the level of the whole organism and leading to a recorded local tissue and systemic response. The present work is devoted to the study of the hydrogen peroxide production dynamics during photodynamic reaction and its correlation with cell functional state using viscosity-sensitive photosensitizes.

In order to study the role of hydrogen peroxide in the development of the photodynamic reaction, we have obtained lines of human epidermoid carcinoma A431cells stably expressing peroxide-sensitive HyPer sensor in the cytoplasm (A431-HyPer-cyto), mitochondria (A431-HyPer-mito) or nucleus (A431-HyPer-nuc). The localization of HyPer protein and the level of its expression in cells were confirmed by confocal microscopy and flow cytometry, respectively. At the first stage of the study the intracellular localization of porphyrazines (Pz) was investigated for all cell lines obtained. Earlier Pzs were shown to demonstrate correlation between their photo-physical characteristics (fluorescence quantum yield and life-time) and viscosity properties of the cell [1]. The confocal microscopy study showed the nuclear envelope and vesicular structures (presumably endosomes and lysosomes) to be the main targets of Pz intracellular uptake. Using the MTT assay a significant difference between dark and photo-induced cytotoxicity of Pz was shown for the obtained cell lines. At the second stage of the study the method of registration of the dynamics of hydrogen-peroxide content in cells was adapted using HyPer sensor. This method is based on the analysis of the HyPer fluorescence under excitation at two wavelengths (I488/I405). With this method, we monitored the hydrogen-peroxide content in cytoplasm and mitochondria of A431-HyPer-mito and A431-HyPer-cyto cells, respectively, after treatment with clinically approved photosensitizes (Photosens and Phtalosens). The increase in the hydrogen-peroxide content in cells in response to photodynamic treatment was shown for both photosensitizes mentioned above (fig. 1).

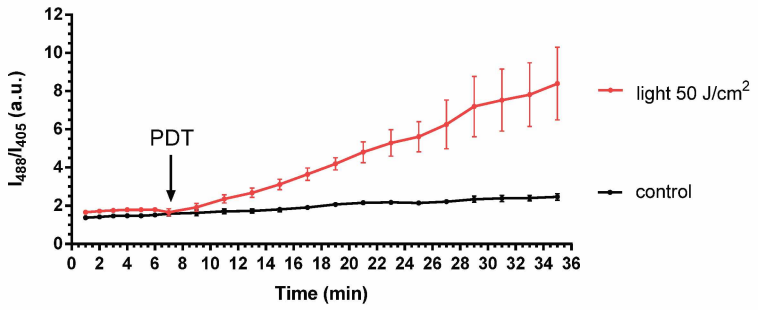



**Fig. 1.** The increase of the hydrogen peroxide presence after irradiation of A431-HyPer-cyto cells, under 5 μM Photosens exposure

The next step in our study will be a comparison of the time parameters of hydrogen peroxide production in various cell compartments and the functional state of the cell estimated by its viscosity using porphyrazines as viscosity sensors.

**Acknowledgements**

The work was partially supported by the Russian Foundation for Basic Research (project no.16-04-01676), and the Ministry of Education and Science of the Russian Federation (contracts no. 14.Z50.31.0022; no. MK-980.2017.4).

## References

1. Izquierdo M. Angeles, Vyšniauskas Aurimas, S.A. Lermontova, I.S. Grigoryev, N.Y. Shilyagina, I.V. Balalaeva, L.G. Klapshina, and M.K. Kuimova, *Journal of Materials Chemistry B,* 2015, **3**, 1089–1096.

*Invited*

# TUMOR RESPONSE TO CHEMOTHERAPY AS A COMPLEX PHENOMENON: INSIGHT INTO MORPHOFUNCTIONAL CHARACTERISTICS USING FLUORESCENCE IMAGING

**M.V. Shirmanova[1], M.M. Lukina[1,2], I.N. Druzhkova[1], T.F. Sergeeva[1], L.E. Shimolina[1,2], L.B. Snopova[1], V.V. Dudenkova[1,2], A.I. Gavrina[1,2], M.K. Kuimova[3], V.I. Shcheslavskiy[4], and E.V. Zagaynova[1]**

[1] Nizhny Novgorod State Medical Academy, Nizhny Novgorod, Russia, shirmanovam@mail.ru
[2] Lobachevsky State University of Nizhny Novgorod, Nizhny Novgorod, Russia
[3] Imperial College London, South Kensington, London
[4] Becker&Hickl GmbH, Germany

**Abstract.** Recent advances in our understanding of cancer behaviors have suggested that multiple drug-induced physiological changes are involved in the development of therapeutic responses. The focus of our studies is multimodal fluorescence imaging of cancer cell reactions to treatment with cytotoxic agents with different mechanisms of action to identify relevant biomarker(s) of early therapeutic effects.

Conventional criteria of assessment of solid tumor response to chemotherapy are based on measuring of the tumor burden size in the course of treatment and pathomorphological analysis of the tumor tissue at the end of treatment. Recent advances in our understanding of cancer behaviors have suggested that multiple drug-induced physiological changes are involved in the development of therapeutic responses. It has become clear that identification of relevant biomarker(s) among these changes is crucial to develop approaches to monitoring early therapeutic effects.

Modern achievements with fluorescence imaging methods and genetically encoded fluorescent probes open up new possibilities for noninvasive examination of cellular functions in living cells and tissues. The focus of our studies is multimodal imaging of cancer cell reactions to treatment with cytotoxic agents with different mechanisms of action. Using advanced fluorescence imaging techniques (two-photon fluorescence laser scanning microscopy, time-resolved fluorescence microscopy and spectroscopy, fluorescence whole-body imaging etc.), fluorescence from endogenous metabolic cofactors, genetically encoded and chemical sensors, we investigate the changes in energy metabolism, intracellular pH (pHi) and microviscosity in cancer cells exposed to chemotherapy. The experiments are performed on monolayer cell cultures, tumor spheroids and animal tumor models.

To examine bioenergetics of cells, we registered fluorescence intensity of metabolic cofactors NAD(P)H and FAD to calculate the optical redox ratio and fluorescence lifetime to assess a state ("free" or "protein-bound") of the cofactors [1]. To measure pHi, ratiometric (dual excitation) genetically encoded sensor SypHer2 on the basis of cpYFP chromophore was used [2]. Fluorescent BODIPY-based molecular rotor was used to imagemicroscopic viscosity [3].

Our results describe functional alterations specific for different scenarios of cell response to chemotherapy (cell death by apoptosis or necrosis or proliferative disorder). Apoptotic process was monitored by FLIM/FRET sensor for caspase-3 activity, mKate2-DEVD-iRFP [4].

For example, in case of cisplatin we found that a greater ability to maintain an alkaline pHi in the presence of drug was a principal difference between surviving cells and those that died. Although at long-term treatment, the surviving cells showed decrease in pHi, both in vitro and in vivo, which possibly promoted metabolic shift to more oxidative status. This, in turn, resulted in inhibition of cultured cells proliferation and of tumor growth in mice. Additionally, cisplatin-induced fluctuations of plasma membrane viscosity were detected in dying cells. The present study indicates that these parameters can serve as markers of responsiveness to chemotherapeutic agents.

### Acknowledgements

This research was supported by the Russian Science Foundation (#14-15-00129-П).

### References

1. I.N. Druzhkova, *et al.*, *Cell Cycle.*, 2016, **15**(9), 1257–66.
2. M.V. Shirmanova, *et al.*, *BBA*, 2015, **1850**(9), 1905–11.
3. L.E. Shimolina, *et al.*, *Sci. Rep.*, 2017, 41097.
4. T.F. Sergeeva, *et al.*, *BBA*, 2017, **1864**, 604–611.

# MONITORING OF TUMOR TREATMENT BY MULTIMODAL OPTICAL COHERENCE TOMOGRAPHY

**M.A. Sirotkina**[1], **A.A. Moiseev**[1,2], **S.S. Kuznetsov**[1], **M.V. Shirmanova**[1], **V.Yu. Zaitsev**[1,2], **V.V. Elagin**[1], **G.V. Gelikonov**[1,2], **E.V. Zagaynova**[1], **A. Vitkin**[1,3], and **N.D. Gladkova**[1]

[1] Nizhny Novgorod State Medical Academy, Nizhny Novgorod, Russia, sirotkina_m@mail.ru
[2] Institute of Applied Physic, Russian Academy of Sciences, Nizhny Novgorod, Russia
[3] University of Toronto and University Health Network, Toronto, Ontario, Canada

**Abstract.** The study objective was to monitor the microcirculation reaction on photodynamic therapyusing multimodal OCT. Using OCT microangiography on an experimental tumor model we investigated the microvascular reaction in the tumor side and in the collateral tissue. The dependence of tumor response on the initial state of tumor microvasculature was studied. Complete disappearance of vessels in OCT images within 24 hours after exposure led to the total tumor necrosis on the 7th day. 40% of poorly vascularized tumors and 87% of highly vascularized tumors were killed by PDT, and OCT microangiography can visualize vascular changes related to the PDT treatment and correlate them with clinical outcome.

**Introduction.** Photodynamic therapy (PDT) is an actively developed method of antitumor therapy for superficial localization. For PDT success, several factors are very important. One of them is tissue oxygenation [1]. The level of tissue blood supply may be an direct sign of tumor oxygenation. Multimodal OCT with angiography function can become a valuable tool for individual reaction to PDT assessment [2]. It is known that one of the main targets for PDT toxicity are endothelial cells. Their damage results in blood vessel damage and in disruption of a blood flow [3].

**Materials and Methods.** The study was carried out on mouse ear tumor model murine colon carcinoma transplanted subcutaneously on female BALB/c mice (n = 20). Animals were randomly divided into two groups: treated by PDT (n = 15) and untreated (control, n = 5). PDT was performed on small-size tumors (poorly vascularized) and medium-size tumor (highly vascularized). PDT with total exposure 100 J/cm$^2$ was done 1hour after Photosensitizer (Chlorine e6) administration. The photosensitizer accumulation in the tumor and photobleaching after PDT were controlled by fluorescent bioimaging. Epi-fluorescence imaging was performed using IVIS-Spectrum system (Caliper Life Sciences, USA) with excitation at 640 nm, emission at 720 nm. The microvasculature reaction was observed in the tumor area and in the surrounding normal tissue using OCT microangiangiography based on speckle variance [4]. On day 7, all tumors were excised for histopathology.

**Results.** The study revealed that complete irreversible blood vessels disappearance on OCT microangiography images within 24 hours after exposure led to the total tumor necrosis on day 7, which was confirmed by histology examination. In the group of poorly vascularized tumor, approximately 40% of tumors were killed by PDT in comparison with 87% in the group of highly vascularized tumors.

**Conclusions.** Optical coherence tomography microangiography can visualize vascular changes related to the PDT treatment and correlate them with clinical outcome.

### Acknowledgments

The study was supported by the Russian Federation Government contract No 14.B25.31.0015 and the Russian President grant for young scientists No MK-905.2017.7.

### References

1. R.R. Allison, K. Moghissi, *ClinEndosc.*, 2013, **46**, 24–29.
2. M.A. Sirotkina, L.A. Matveev, M.V. Shirmanova, *et al.*, *SciRep*, 2017, **7**, 41506. DOI: 10.1038/srep41506.
3. V.H. Fingar, *et al.*, *Br J Cancer*, 1999, **79**, 1702–1708.
4. L.A. Matveev, V.Y. Zaitsev, G.V. Gelikonov, *et al.*, *Optics Letters*, 2015, **40**(7), 1472–1475.

*Invited*

# MECHANISMS OF MOLECULAR CANCER IMAGING AND THERAPY WITH ULTRA-SMALL NANOPARTICLES

**S. Han[1,2], R. Bouchard[2], S. Emelianov[3], and K. Sokolov[1,2,4*]**

[1] Bioengineering, Rice University, Houston, TX
[2] Imaging Physics, The University of Texas MD Anderson Cancer Center, Houston, TX
[3] Electrical & Computer Engineering and Biomedical Engineering,
Georgia Institute of Technology and Emory University School of Medicine, Atlanta, GA
[4] Biomedical Engineering, The University of Texas at Austin, Austin, TX
[*] ksokolov@mdanderson.org

**Abstract.** This work explores the application of 5 nm diameter gold nanoparticles for molecular photoacoustic (PA) imaging of cancer micrometastasis. Isolated 5 nm particles exhibit negligible PA signal in the near-infrared (NIR) spectral region. However, our results show that trafficking and processing of antibody-targeted 5 nm gold particles in cancer cells lead to a strong PA signal in the NIR region, allowing for highly specific and sensitive cancer imaging. Furthermore, nanoparticles can also suppress proliferation of cancer cells, opening exciting opportunities for theranostic applications. Confocal microscopy studies revealed that specific mechanism of 5 nm gold nanoparticle interactions with cancer cells is essential for their applications in cancer imaging and therapy.

Nanoparticles with sizes less than 10 nm are comparable to large biomolecules such as antibodies and, therefore, present a very interesting opportunity for biomedical applications. These ultra-small nanoparticles can improve biodistribution and pharmacokinetics, including more uniform intratumoral distribution. Furthermore, these nanoparticles can undergo efficient body clearance, which is a critical requirement for clinical translation of non-biodegradable nanoparticles such as gold. We apply the combination of ultra-small (5 nm) spherical gold nanoparticles and spectroscopic photoacoustic (PA) imaging to two important clinical problems: (i) detection of cancer micrometastasis in lymphatics; and (ii) detection of microscopic ovarian cancer disease. Both applications can have lifesaving implications in management of cancer patients.

Plasmonic gold nanoparticles (AuNPs) are ideally suited for PA imaging because of their high optical absorption. Conjugation of AuNPs with probe molecules (e.g., antibodies) renders them with molecular specificity [1]. However, the challenge is that isolated spherical gold nanoparticles do not exhibit appreciable NIR absorbance that is required for in vivo applications. Recently, we turned this challenge into opportunity by leveraging the change in NIR absorption between aggregated and non-aggregated gold nanospheres that results from plasmon coupling for specific detection *in vivo* of metastatic foci in lymph nodes as small as 50 μm and with as few as 30 cells [2]. We used 40 nm AuNPs targeted to epidermal growth factor receptor (EGFR), which is a key cancer biomarker. We showed that receptor-mediated uptake of AuNPs in cancer cells resulted in a strong PA signal in the NIR region.

In the study presented herein, we validated the use of clinically translatable 5nm gold nanoparticles. Study results showed a 10-fold increase in PA signal of EGFR(+) cancer cells labeled with EGFR-targeted 5 nm nanoparticles as compared to EGFR(-) cells. Detailed confocal microscopy studies of nanoparticle trafficking inside cancer cells revealed that unique mechanism of nanoparticles' coating degradation inside cells is a major contributor to the observed PA signal. Furthermore, nanoparticle uptake was associated with suppression of cancer cell proliferation. Therefore, understanding mechanisms of nanoparticle processing inside live cells will allow further optimization of molecular targeted ultra-small gold nanoparticles as a theranostic platform.

### Acknowledgements

We acknowledge support from National Health Institute grants R01 EB008101 and R01 CA103830.

### References

1. S. Kumar, J. Aaron, and K.V. Sokolov, *Nat Protoc.*, 2008, **3**(2), 314–20.
2. G.P. Luke, J.N. Myers, S.Y. Emelianov, and K.V. Sokolov, *Cancer Research*, 2014, **74**, 5397–408.

*Invited*

# NON-INVASIVE METABOLIC IMAGING OF MELANOMA PROGRESSION

**H. Studier**[1,2], **M. Pastore**[1], **W. Becker**[2], and **M.S. Roberts**[1,3]

[1] School of Pharmacy and Medical Sciences, University of South Australia, Adelaide, Australia
[2] Becker & Hickl GmbH, Berlin, Germany, studier@becker-hickl.com
[3] Therapeutics Research Centre, School of Medicine, University of Queensland, Princess Alexandra Hospital, Brisbane, Australia

**Abstract.** Skin cancer is associated with abnormal cellular metabolism which if identified early introduces the possibility of intervention to prevent its progress to a deadly metastatic stage. This study combines multiphoton microscopy with FLIM using a melanoma mouse model, to detect changes in redox states of single epidermal cells as a metabolic marker to monitor the progress of tumor growth. We found a significant increase in the free-to-bound NADH ratio with the growth of the tumor, while concurrently the short and long lifetime components remained constant. These results demonstrate the potential of FLIM for rapid, non-invasive assessment of melanoma progression.

Skin cancer is associated with abnormal cellular metabolism which if identified early introduces the possibility of intervention to prevent its progress to a deadly metastatic stage [1]. This study combines multiphoton microscopy with fluorescence lifetime imaging (FLIM) using an orthotopic melanoma mouse model [2, 3], to detect changes in redox states of single epidermal cells as a metabolic marker to monitor the progress of tumor growth. This method utilizes imaging of the ratio of the amounts of the free and protein-bound forms of the intracellular autofluorescent metabolic co-enzyme nicotinamide adenine dinucleotide (NADH) [4–6]. Here we investigate the impact of the primary tumor lesion on the epidermal layers at three different growth stages of melanoma lesion compared to normal skin as a control. We show a significant increase in the free-to-bound NADH ratio with the growth of the solid melanoma tumor, while concurrently the short and the long lifetime components of NADH remained constant. These results demonstrate the potential of FLIM for rapid, non-invasive and sensitive assessment of melanoma progression revealing its potential as a diagnostic tool for melanoma detection and as an aid for melanoma staging.

## References

1. F. Tas, "Metastatic behavior in melanoma: timing, pattern, survival, and influencing factors", *J. Oncol.* 2012, 647684.
2. L. Ha, F.P. Noonan, E.C. De Fabo, *et al.,* "Animal models of melanoma", *J. Invest Dermatol,* 2005, **10**, 86-8.
3. J.W. Wilson, S. Degan, C.S. Gainey, *et al.,* "Comparing in vivo pump-probe and multiphoton fluorescence microscopy of melanoma and pigmented lesions", *J. Biomed. Opt.,* 2015, **20**, 051012.
4. O. Warburg, "On the origin of cancer cells", *Science*, 1956, **123**, 309–14.
5. L. Pires, M.S. Nogueira, S. Pratavieira, *et al.,* "Time-resolved fluorescence lifetime for cutaneous melanoma detection", *Biomed. Opt. Express*, 2014, **5**, 3080–9.
6. S. Seidenari, F. Arginelli, and M. Manfredini, "Multiphoton Laser Microscopy with Fluorescence Lifetime Imaging and Skin Cancer", In: *Skin Cancer* (Baldi A, Pasquali P, Spugnini EP, eds), 2014, Springer New York, 279–90.

# THE EFFECT OF OX40 LIGAND ON CT26TUMORS IN MICE

**D.V. Yuzhakova**[1,2], **M.V. Shirmanova**[1], **E.O. Serebrovskaya**[1,3], **I.N. Druzhkova**[1], **S.A. Lukyanov**[1,3,4], and **E.V. Zagaynova**[1]

[1] Nizhny Novgorod State Medical Academy, Nizhny Novgorod, Russia, yuzhakova-diana@mail.ru
[2] Lobachevsky State University of Nizhny Novgorod, Nizhny Novgorod, Russia
[3] Shemyakin-Ovchinnikov Institute of Bioorganic Chemistry RAS, Moscow, Russia
[4] Pirogov Russian National Research Medical University, Moscow, Russia

**Abstract.** The OX40 ligand (OX40L) is a potential agent for immunotherapy, a promising therapeutic strategy for cancer. The purpose of this study was to investigate the effect of soluble extracellular domain of OX40L (OX40Lexo) on CT26 colon carcinoma in mice. Our results showed that gene transfer of OX40L into tumor cells resulted in lower tumor incidence, resistance to spontaneous metastases and development of immunological memory. Therefore, we report for the first time on the antitumor effect of OX40Lexo in a mouse tumor model.

## Introduction

The OX40 ligand (OX40L) is a potential agent for immunotherapy, a promising therapeutic strategy for cancer. OX40L is a member of the TNF (Tumor Necrosis Factor) family that has shown antitumor potential in several murine tumor models [1, 2]. In the present study we developed the novel soluble extracellular variant of OX40L – OX40Lexo for more effective interaction with the tumor infiltrating immune cells. Therefore, the purpose of this study was to investigate the effect OX40Lexo, on CT26 tumors in mice.

## Materials and Methods

CT26 murine colon carcinoma cell lines stably expressing EGFP (Enhanced Green Fluorescent Protein) or co-expressing EGFP and soluble murine OX40Lexo were obtained by lentiviral transduction. CT26, CT26-EGFP or CT26-EGFP-OX40Lexo tumors were induced by subcutaneous (s.c.) injection of $2 \cdot 10^5$ cancer cells into the leg of immunocompetent Balb/c mice. The evaluations of tumor incidence, growth rate, number of lung metastases and *in vivo* fluorescence imaging were performed. To assess the formation of antitumor immune protection, a passive transfer of spleen cells was conducted from mice inoculated with CT26-EGFP-OX40Lexo, CT26-EGFP or CT26 cells, and from naïve mice, as a control.

## Results

The expression of OX40Lexo in tumor cells inhibited the development of tumor in mice [3]. It was found that the tumor incidence of CT26-EGFP-OX40Lexo tumors was 10% (1 out of 10 mice), while the tumor incidence of CT26-EGFP or non-modified CT26 tumors was 90% (9 out of 10 mice). Mice challenged with CT26-EGFP-OX40Lexo cells demonstrated complete resistance to formation of spontaneous metastases. Besides, all tumor-free mice rejected CT26-EGFP-OX40Lexo showed resistance to rechallenge with $5 \cdot 10^5$ CT26-EGFPcells, indicating the development of immunological memory. The results of the adoptive immune transfer showed that all the mice (20 of 20) treated with spleen cells from donors previously challenged with CT26-EGFP-OX40Lexo cells rejected the CT26-EGFP tumors. Tumor susceptibility was 47% (7 of 15) in the case of spleen cell transfer from naïve mice, and 50% (5 of 10) or 33% (2 of 6) where CT26 or CT26-EGFP bearing mice were the donors.

In summary, the results of this study show that OX40Lexo demonstrated strong antitumor effects manifested in tumor rejection in immunocompetent Balb/c mice, resistance to formation of spontaneous metastases and the development of immunological memory.

## Acknowledgements

This work was supported by the Ministry of Education and Science of the Russian Federation (grant # 14.W03.31.0005).

## References

1. G.J. Webb, G.M. Hirschfield, and P.J. Lane, *Clin. Rev. Allergy Immunol.*, 2016, **50**(3), 312–332.
2. G. Gri, E. Gallo, E. Di Carlo, P. Musiani, and M.P. Colombo, *J. Immunol.*, 2003, 17099–106.
3. E.O. Serebrovskaya, D.V. Yuzhakova, A.P.Ryumina, *et al.*, *Cytokine*, 2016, **84**, 10–16.

VI International Symposium

# TOPICAL PROBLEMS OF BIOPHOTONICS




## *Novel Laser Applications in Biomedicine*

# Chairs

**Alexander Sergeev**
Institute of Applied Physics RAS, Russia

**Alfred Vogel**
University of Luebeck, Germany

*Invited*

# NOVEL LASER AND FIBER OPTICS SOLUTIONS IN OPTICAL THERANOSTICS

**V. Artyushenko**

Art photonics GmbH, Rudower Chaussee 46, 12489 Berlin, Germany

Various biomedical applications of fiber optics in a broad spectral range 0.4–16 μm span more and more – from endoscopic imaging and Photo Dynamic Diagnostics (PDD) to laser power delivery for minimal invasive laser surgery, tissue coagulation and welding, Photo Dynamic Therapy (PDT), etc. Present review will highlight the latest results in advanced fiber solutions used for more precise diagnostics and intraoperative control of several therapy methods – for the so-called "theranostics". Spectral fiber sensing for label free analysis of tissue composition helps to differentiate malignant and normal tissue to secure minimal invasive, but complete tumor removal or treatment. All key methods of Raman, fluorescence, diffuse reflection & MIR-absorption spectroscopy will be compared when used for the same spot of tissue – to select the most specific, sensitive and accurate method or to combine them for the synergy enhanced effect. The most informative spectral features for distinct organs/ tumor can be used to design special fiber sensors to be developed for portable and low cost applications with modern IT-features (for software embedded in microprocessor, for data accumulation in clouds and treatment – to enable fast guidance for therapy *in-vivo*, etc.). Examples of multi-spectral tissue diagnostics will be presented toward the future clinical applications of tumor margin sensors. The promising trends of the synergy of Quantum Cascade Lasers coupled with IR-fiber optics or Hollow Waveguides will be also reviewed in areas of diagnostic screening of cancer and diabetes.

The 1st results on Mid IR-fiber endoscopy will be presented for thermography control of Radio Frequency Ablation (RFA) for pulmonary vein isolation (PVI) – for the common treatment used against a trial fibrillation (AF). Pilot study results obtained by Securus Medical will demonstrate how to prevent thermal injury in structures adjusting to the left atrium using PIR-fiber based thermography system for a fast non-contact thermal mapping over a 6cm length of esophagus.

A unique advantage of PIR-fiber transmission in Mid IR-range from 3 to 16μm enables to run non-contact temperature control for various laser-tissue operations: ablation, coagulation and welding of vessels, with precise control of tissue temperature at the spot of laser beam on tissue. This feature helps to design "smart" laser systems for minimal invasive operations – for external and endoscopic operations. Flexible delivery system for $CO_2$- and CO-lasers can be used for both directions in such systems as the temperature at laser spot on tissue can be measured between the laser pulses by its emission. This feed-back will provide the main advantage of "smart" laser systems – the automated support for a desired temperature of tissue treatment. The 1st trials prototypes of $CO_2$- & CO-laser systems with flexible cables will be presented for different operations.

Translation of described methods into clinical practice will be discussed in comparison with the other methods of optical diagnostics which should enhance modern medicine by less invasive, more precise and more effective methods of therapy to be fused with *in-vivo* diagnostics sensors & systems.

*Invited*

# THE SOUND OF PROTONS – IONOACOUSTIC RANGE MONITORING IN PROTON THERAPY

**W. Assmann**

Institute of Medical Physics, Faculty of Physics, LMU München
walter.assmann@lmu.de

**Abstract.** Range verification is the crucial issue in ion beam therapy to enable full clinical exploitation of its characteristic advantages over photon therapy. Detection of the ultrasound signal induced by the incident ions (ionoacoustics) promises a simple and direct possibility to measure the ion range. Here we demonstrate in experiments with proton beams of 20 MeV and 230 MeV the achievable accuracy and precision of this approach.

Ions offer a more advantageous dose distribution than photons for external beam radiotherapy, due to their inverse dose deposition and, in particular, a characteristic dose maximum at their end of range (Bragg peak). Therefore, a more conformal therapeutic dose can be applied to the tumor while sparing the surrounding healthy tissue, even if organs at risk are in striking distance. This makes, however, a precise positioning of the Bragg peak inside the tumor volume a challenging demand. Range verification in ion beam therapy relies to date on nuclear imaging techniques which require complex and costly detector systems, and none has still reached clinical maturity. In this project, we make use of the pressure pulse and related acoustic wave induced by ions stopping in tissue ("ionoacoustics") to measure the ion range with ultrasound methods. This technique could offer a simple and more direct possibility to correlate, in-vivo and in real-time, conventional ultrasound imaging of the tumor region with the position signal of the ion Bragg peak [1]. Despite several attempts in the past, the accuracy needed in radiation therapy could never been reached. However, to-day's more advanced irradiation schemes with active beam scanning and dose delivery with higher pulse intensities are in favor of a more accurate ionoacoustic approach.

This presentation will address our experimental and simulation work investigating the potential of the ionoacoustic method to enable sub-mm imaging of the Bragg peak, in proof-of-principle experiments with 20 MeV protons [2, 3] and in first test experiments at a clinical setup with up to 230 MeV protons.

### Acknowledgements

Parts of this work were performed in close collaboration with IBMI/MHZ and TUM (Germany), CAL (France) and IBA (Belgium). This work was funded by the DFG Cluster of Excellence Munich Centre for Advanced Photonics (MAP).

### References

1. K. Parodi and W. Assmann, *Mod. Phys. Lett.*, 2015, A **30**, 1540025.
2. W. Assmann, *et al.*, *Med. Phys,* 2015, **42**, 567–574.
3. S. Kellnberger, *et al.*, *Sci. Rep.*, 2016, **6**, 29305.

*Invited*

# SPATIO-TEMPORAL MODELING OF FEMTOSECOND LASER EFFECTS IN TRANSPARENT DIELECTRICS BASED ON SOLVING MAXWELL'S EQUATIONS

**N.M. Bulgakova**[1] and **V.P. Zhukov**[2,3]

[1] HiLASE Centre, Institute of Physics AS CR, Dolní Břežany, Czech Republic, bulgakova@fzu.cz
[2] Institute of Computational Technologies SB RAS, Novosibirsk, Russia
[3] Novosibirsk State Technical University, Novosibirsk, Russia

**Abstract.** This talk will overview the results of modeling of ultrashort laser pulse propagation in absorbing transparent media based on Maxwell's equations with demonstrating advantages of the approach compared to other models. The majority of simulations have been performed for fused silica irradiated by laser beams with linear and radial polarization. Effects of spatiotemporal coupling in ultrashort laser beams and pump-probe irradiation on laser energy absorption will be analyzed. Based on the absorbed laser energy balance, post-irradiation evolution of material will be discussed, including thermoelastic stresses and their consequences. First results of application of the model to water breakdown will be presented.

Processing of transparent materials with focused femtosecond laser beams is a fast-developing technique for applications in three-dimensional micro- and nanofabrication, surface nanopatterning, two-photon polymerization, etc. [1–3]. The technique enables highly localized laser energy deposition via non-linear photo-ionization of transparent media culminating in breakdown that makes it attractive for high precision surgery of cells and bio-tissues [4]. Swift formation of sub-micrometer-sized free electron plasma, which is strongly scattering laser light, makes the spatiotemporal dynamics of laser light propagation and absorption extremely complicated. There are no methods with enough resolution to directly follow the complexity of the processes at femtosecond temporal and nanometer spatial scales. Even small variation in laser irradiation parameters can cause heavy damage to processed matter, incompatible with the application goals. In such circumstances, theory and computer simulations are important means for understanding the processes and advancing the technique to real world applications.

In this talk an overview of the results of modeling of ultrashort laser pulse propagation in absorbing transparent media will be presented, obtained mainly for fused silica glass as an example [5, 6]. The model based on full Maxwell's equations accounts for the Kerr effect, photo-ionization, frequency dispersion of dielectric permittivity, and free electron plasma hydrodynamics with laser-induced electron acceleration and avalanche. It enables to study the effects of laser polarization, spatiotemporal coupling in the beam (such as lighthouse effect), defect accumulation in pump-probe and pulse shaping techniques, and can be extended to multi-pulse action. The dependences of laser light absorption efficiency and geometry of the light absorption zone will be analyzed as a function of pulse energy, numerical aperture, and beam polarization. For a number of irradiation regimes, the results will be compared with those obtained within the model based on the non-linear Schrödinger equation with demonstrating advantages of the full Maxwell's equations approach.

Based on the absorbed laser energy balance, post-irradiation evolution of material will be discussed, including thermoelastic stresses, generated shock waves, and their possible consequences. First results of application of the model to water breakdown will be presented.

**Acknowledgements.** N.M.B. acknowledges the support from the European Regional Development Fund and the state budget of the Czech Republic (project BIATRI: Grant No. CZ.02.1.01/0.0/0.0/15_003/0000445) and from the Ministry of Education, Youth and Sports of the Czech Republic (Programs NPU I Project No. LO1602, and Large Research Infrastructure Project No. LM2015086). The work of V.P.Z. was supported by the Russian Foundation for Basic Research (Project No. 15-01-02432).

## References

1. S.M. Yalisove, K. Sugioka, and C.P. Grigoropoulos, *MRS Bulletin*, 2016, **41**(12), 955–959.
2. M.V. Shugaev, Ch. Wu, O. Armbruster, A. Naghilou, N. Brouwer, D.S. Ivanov, T.J.-Y. Derrien, N.M. Bulgakova, W. Kautek, B. Rethfeld, and L.V. Zhigilei, *MRS Bulletin*, 2016, **41**(12), 960–968.
3. K. Sugioka, *Nanophotonics*, 2017, **6**(2), 393–413.
4. N. Linz, S. Freidank, X.-X. Liang, and A. Vogel, *Phys. Rev. B*, 2016, **94**, 024113.
5. N.M. Bulgakova, V.P. Zhukov, S.V. Sonina, and Y.P. Meshcheryakov, *J. Appl. Phys.*, 2015, **118**, 233108.
6. V.P. Zhukov, A.M. Rubenchik, M.P. Fedoruk, and N.M. Bulgakova, *J. Opt. Soc. Am. B*, 2017, **34**(2), 463–471.

*Invited*

# XUV COHERENCE TOMOGRAPHY WITH NANOSCALE RESOLUTION

**S. Fuchs**[1,2], **M. Wünsche**[1,2], **J. Nathanael**[2], **J.J. Abel**[2], **Ch. Rödel**[2], **J. Reinhard**[2], and **G.G. Paulus**[2]

[1] Institute of Optics and Quantum Electronics, Friedrich Schiller University Jena, Germany, silvio.fuchs@uni-jena.de
[2] Helmholtz Institute Jena, Jena, Germany

**Abstract.** We present a novel method for cross sectional imaging with nanometer resolution, which is referred to as XUV coherence tomography (XCT). XCT uses extreme ultraviolet light (XUV), e.g., from laser-driven high harmonic generation (HHG). In XCT, the coherence length of a few nanometers of broadband XUV sources is exploited. Thus, XCT extends optical coherence tomography (OCT) by improving the axial resolution from micrometers to nanometers. Axial resolutions down to 3 nm have been demonstrated in the water transmission window (wavelength range 2–4 nm) and 12 nm in the silicon transmission window (20–40 nm) highlighting possible applications in life sciences and semiconductor industry.

Optical coherence tomography (OCT) is a well-established method to retrieve three-dimensional, cross-sectional images of biological samples in a non-invasive way using near-infrared radiation. The axial resolution of OCT is in the order of the coherence length $l_c \propto \lambda_0^2/\Delta\lambda_{FWHM}$, which depends on the central wavelength $\lambda_0$ and the spectral width (FWHM) $\Delta\lambda_{FWHM}$ of a light source. OCT with broadband visible and near-infrared sources typically reaches axial (depth) resolutions in the order of a few micrometers [1]. XCT [2, 3] presented here takes advantage of the fact that the coherence length and therefore the axial resolution of OCT is significantly reduced when broadband XUV and SXR radiation is used. The broadness of the usable XUV spectrum is limited by absorption edges of the sample. For instance, the silicon transmission window (30–99 eV) corresponds to a coherence length and therefore a possible axial resolution of about 12 nm, thus suggesting applications for semiconductor inspection. In the water window at 280–530 eV a coherence length as short as 3 nm can be achieved and highlights possible applications of XCT for life sciences.

The usage of laser-based XUV sources like high-harmonic generation enables a laboratory-based experimental setup. Therefore, XCT becomes independent of large-scale x-ray sources like synchrotrons, which are usually used for EUV imaging. Fig. 1 shows a measured XCT volume with an axial resolution of approx. 20 nm. All structures could be resolved.

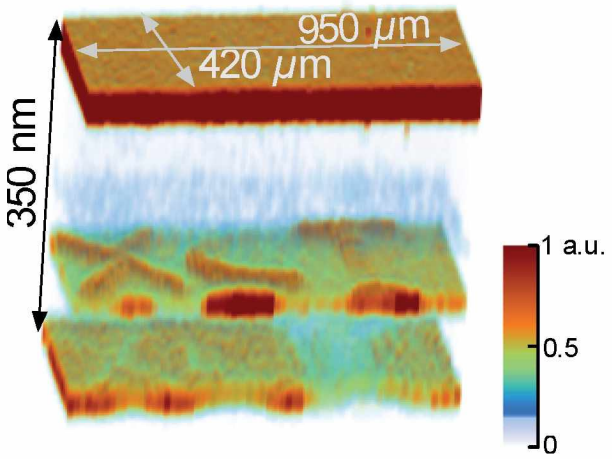



**Fig. 1.** *Tomogram of a silicon based sample with buried gold structures:* All buried structures are resolved. The axial resolution is approx. 20 nm and is independent of the focal spot size, which supports a lateral resolution of 23µm. The measurement was non-destructive

## References

1. D. Huang, *et al.*, *Science*, 1991, **254**(3), 1178–1181.
2. S. Fuchs, *et al.*, *Appl. Phys. B*, 2012, **106**, 789–795.
3. S. Fuchs, *et al.*, *Sci. Rep.*, 2016, **6**, 20658.

*Invited*

# NOVEL CLASSES OF EUBACTERIAL LIGHT-DRIVEN ION PUMPING PROTEINS FOR OPTICAL CONTROL TOOLS OF CELLS

**K. Inoue**[1,2]

[1] Nagoya Institute of Technology, Nagoya, Japan, inoue.keiichi@nitech.ac.jp
[2] PRESTO, JST, Saitama, Japan

**Abstract.** Microbial rhodopsins are the photoreceptive membrane proteins of various types of bacteria. The ion-transporting rhodopsins are used as molecular tools to control neuronal activity. This technique is called "optogenetics". Recently, we have discovered new classes of microbial rhodopsins, light-driven outward sodium pump and inward proton pump. The specific ion transports by these rhodopsins are expected to enable more efficient or low toxic optogenetic approach, and their molecular mechanism was studied to obtain basic insight to develop new optogenetic tools.

Microbial rhodopsins are the photo-receptive membrane proteins which are diversely found in mainly unicellular microorganisms such as eubacteria, archaea, algae and fungi. They share common structure composed of seven-transmembrane α-helices and chromophore all-*trans* retinal. Upon light-illumination, the retinal isomerizes to 13-*cis* form and then various types of biological functions are evoked by light. The most ubiquitous microbial rhodopsin is outward $H^+$ pump which can generate proton motive force for ATP-synthesis and so on. Recently, we identified a new types of rhodopsin, outward $Na^+$ pump (KR2) in the genome of marine bacterium [1]. Interestingly, it transports $H^+$ outward in the presence of only larger cation in the solution. We studied the $Na^+$-transport mechanism by spectroscopy and X-ray crystallographic analysis. They revealed that an aspartate near retinal transiently sequesters $H^+$ of retinal Schiff-base from $Na^+$ transport pathway [1, 2]. Furthermore, we found a cytoplasmic space with a bottle neck structure. This bottle neck structure works as a selective filter and artificial $K^+$ and $Cs^+$ pumps were developed by mutating the residues forming the gate [2, 3].

In 2016, we further reported inward $H^+$ pump (*Po*XeR) from deep-sea bacterium and spectroscopic study revealed the characteristic mechanism to transport $H^+$ inward [4]. We expect these new types of rhodopsin will be applied for optogenetics.

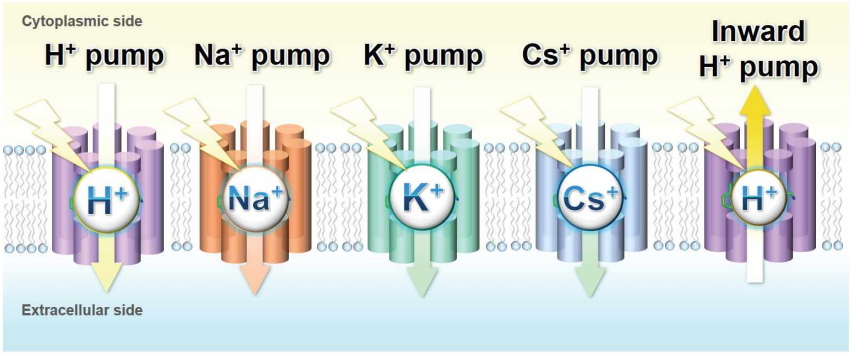



**Fig. 1.** The natural and artificial rhodopsins

## Acknowledgements

This work was supported by a Grant-in-Aid for Scientific Research from the Ministry of Culture, Sports, Science and Technology of Japan (JSPS KAKENHI) (15H04336, 16H00828 and 26104513) and PRESTO from Japan Science and Technology Agency (JST).

## References

1. K. Inoue, H. Ono, R. Abe-Yoshizumi, S. Yoshizawa, H. Ito, K. Kogure, H. Kandori, *Nature Commun.*, 2013, **4**, Article number:1678.
2. H.E. Kato, K. Inoue, R. Abe-Yoshizumi, Y. Kato, H. Ono, M. Konno, T. Ishizuka, M.R. Hoque, S. Hososhima, H. Kunitomo, J. Ito, S. Yoshizawa, K. Yamashita, M. Takemoto, T. Nishizawa, R. Taniguchi, K. Kogure, A.D. Maturana, Y. Iino, H. Yawo, R. Ishitani, H. Kandori, O. Nureki, *Nature*, 2015, **521**(7550), 48–53.
3. M. Konno, Y. Kato, H. Kato, K. Inoue, O. Nureki, H. Kandori, *J. Phys. Chem. Lett.*, 2016, **7**(1), 51–55.
4. K. Inoue, S. Ito, Y. Kato, Y. Nomura, M. Shibata, T. Uchihashi, S.P. Tsunoda, H. Kandori, *Nature Commun.*, 2016, **7**, Article number:13415.

# NEGATIVE IMPACT OF SELF-GENERATED MAGNETIC FIELDS ON ENERGIES OF IONS ACCELERATED BY ULTRA-HIGH INTENSITY LASER PULSES

**A.V. Korzhimanov**[1], **M. Nakatsutsumi**[2,3], **L. Grimellet**[4], and **J. Fuchs**[1,2]

[1] Institute of Applied Physics of the Russian Academy of Sciences, Nizhny Novgorod, Russia, kav@ufp.appl.sci-nnov.ru
[2] LULI — CNRS, École Polytechnique, CEA: Université Paris–Saclay; UPMC Univ Paris 06: Sorbonne Universités, Palaiseuax, France
[3] European XFEL, Schenefeld, Germany
[4] CEA, DAM, DIF, Arpajon, France

**Abstract.** Ion beams accelerated by hot electrons produced in solid targets irradiated by high-intensity laser pulses are widely believed to become a valuable tool for hadron cancer therapy. The current challenge is to reach therapeutic energies, *i.e.* above 200 MeV, which is commonly thought to be possible by increasing the laser intensity. Here, we present numerical results demonstrating that at intensities exceeding $10^{21}$ W/cm$^2$ magnetostatic fields self-generated in the sheath may have a detrimental effect on the ion energies and may pose a fundamental limit to target normal sheath ion acceleration for high enough laser intensities. We also discuss possible mechanisms of this effect.

The laser proton and light-ion acceleration is a perspective source for a hadron cancer therapy. Recent progress in developing laser sources producing pulses up to several petawatts make them widespread among laboratories across the world. A terawatt-level pulse focusing on a thin metal foil or plastic film is known to produce a bunch of ions with energies exceeding several MeVs. A regime of the acceleration for such pulses has been named Target Normal Sheath Acceleration (TNSA). It is based on laser heating of electrons to relativistic temperatures and subsequent expansion of a hot electron cloud beyond the target forming a sheath accelerating protons and light-ions from the rear target side by electrostatic forces. The known scalings show that to attain 200 MeV protons one needs to increase laser intensity level beyond $10^{21}$ W/cm$^2$. Now the pulses of this intensity are becoming available for routine experiments. Particularly, they were obtained by tightly focusing sub-ps laser pulses with elliptical plasma mirrors [1].

The experiments on proton acceleration utilizing these pulses have been conducted recently and show that the observed ion energies are well below predictions of simple models and popular scalings [2]. This observation has been attributed to the magnetic fields self-generated by hot electrons on the rear side of the target. These fields can be stronger than $10^9$ G at laser intensities above $10^{21}$ W/cm$^2$ efficiently magnetizing the sheath electrons and deflecting the protons off the accelerating region, hence degrading the energy transfer from the electrons to the protons.

Analysis shows that with increasing laser intensity the toroidal magnetic fields generated on the rear surface of the target by hot electron bunches ejected by the laser increase as well, but in a much faster manner. At the $10^{21}$ W/cm$^2$ intensity level they reach Gigagauss magnitudes and begin to significantly affect the electron trajectories. If the laser pulse is long enough, the Larmour radius of the electrons may become comparable to the size of the sheath, so that the electrons start to drift and their effective velocities decrease. When the drift velocity becomes less than the velocity of the accelerated ions the ejected electrons can't overcome the ion front and contribute to their acceleration. This is the main mechanism behind the detrimental effect the magnetic field has on ion energies.

Another mechanism is the deflection of protons away from the central axis where both the electron density and, consequently, accelerating fields are the highest.

In our talk we will discuss how the detrimental effect depends on the main parameters of the laser: intensity, duration and spot width. The results were obtained by means of 2D3V simulations performed with PICADOR code [3].

### Acknowledgements

The research was partially supported by the Ministry of Education and Science of the Russian Federation under Contract No.14.Z50.31.0007. The simulations were performed using the resources provided by the Joint Supercomputer Center of the Russian Academy of Sciences.

### References

1. M. Nakatsutsumi, *et al.*, *Opt. Lett.*, 2010, **35**, 2314.
2. M. Nakatsutsumi, *et al.*, *Nature Communications*, 2017, submitted.
3. I.A. Surmin, S.I. Bastrakov, E.S. Efimenko, A.A. Gonoskov, A.V. Korzhimanov, I.B. Meyerov, *Comput. Phys. Commun.*, 2016, **202**, 204–210.

*Invited*

# OPTICAL AND SENSORY CHARACTERISTICS OF OCEANIC BIOTA AND ORGANIC-INORGANIC NATURAL AND BIOMIMETIC MATERIALS

**Yu.N. Kulchin**[1,2] and **S.S. Voznesenskiy**[1,2]

[1] Institute of Automation and Control Processes, FEB RAS, Vladivostok, Russia, kulchin@iacp.dvo.ru
[2] Far Eastern Federal University, Vladivostok, Russia

This work is devoted to a review of marine biota research as the most promising sources of energy, mineral and biological resources that are produced in the Far Eastern Branch of the Russian Academy of Sciences, including in cooperation with the Far Eastern Federal University.

Monitoring of the state of aquatic environments requires obtaining information in real time, long before the appearance of visible signs of pollution, significantly exceeding the norms of maximum permissible concentrations. In recent years, living organisms that are highly sensitive to the effects of unfavorable factors are actively being studied as bio indicators for the ecological monitoring of the state of the water areas. The analysis of the publications and the results obtained in the Far East region demonstrate the sensitivity of the microalgae of phytoplankton to a fairly wide range of pollutants in aqueous media, including metal ions, herbicides, pesticides, cyanides, surface active agents, and others.

Investigation of the interaction of laser radiation with aquatic organisms has given rise to new methods of purification from the biofouling of the surface of underwater equipment and instruments.

Biomimetic and Bio-inspired Smart Nanotechnologies are actively developing on the basis of living organisms. Experts note that the development of biomimetic approaches in nanotechnology can have as revolutionary a role as genetic engineering in biotechnology.

The development of molecular and colloid chemistry and cell biology has determined the formation and intensive development of supramolecular chemistry, which serves as a kind of bridge between inanimate and living matter. The interaction of bio photonics with this direction gave an impetus to research in the areas of creating highly sensitive receptor centers for optical chemosensors based on spatially ordered natural and synthetic nanophase and supramolecular polymer complexes, technologies of creating optical chemosensory systems for detecting inorganic contaminants in aqueous media, and also for detecting metabolite gases in the environment and express analysis of the food freshness.

Much attention is devoted to the development of methods for the formation of submicron structures for obtaining multilayer spatially ordered optical elements and photonic crystals using natural biopolymers. We actively develop methods for the formation of nonlinear optical nanocomposite materials based on nanoparticles, which are synthesized using self-organization in biopolymer matrices as templates, as well as technologies for creating organo-inorganic nanophase materials for bioengineering of photonic biosensors based on molecular mechanisms of self-assembly on a protein matrix.

The development of this direction of biophotonics allows us to obtain a wide range of fundamentally new results with innovative potential.

**Acknowledgements**

This work was supported by a grant from the Russian Science Foundation (project No. 14-50-00034).

*Invited*

# FRONTIERS OF FEMTOSECOND LASER APPLICATIONS IN OPHTHALMOLOGY

**H. Lubatschowski**

ROWIAK GmbH, Hannover, Germany, h.lubatschowski@rowiak.de

**Abstract.** Ophthalmic femtosecond lasers promote safe surgery and fast healing times because they can process tissue and other materials within a 3-D volume without altering its surface. The success of this platform in refractive and, more recently, cataract surgery is based on two unique characteristics: the nonlinear absorption process and extremely high precision and low side effects, resulting from the low energy level needed for photodisruption. Consequently femtosecond lasers have potentially many more new ophthalmic applications, which are discussed in this presentation.

Since the launch of the first commercial femtosecond laser system for corneal surgery in 2001 by IntraLase, more than thousand systems have been sold and more than 20 million patients have been treated for refractive corneal surgery. Today fs lasers have developed from a pure flap-maker for LASIK surgery to a multiple tool for corneal surgery as well as for cataract surgery. In cataract surgery, the laser has extended its field of action from the cornea to the crystalline lens where it is used to open the capsular bag and performing lens fragmentation.

There is even more potential of "femto"-applications in ophthalmic surgery based on its unique features such as (a) simultaneous imaging of the target tissue while cutting or (b) processing even turbid tissue.

## Reversing presbyopia

In the near future presbyopia reversal might be possible by restoring the flexibility of the aged crystalline lens. Here, fs laser can be used to create micro-incisions inside the lens without surgically opening the eye. These micro-channels could reduce the inner friction of the lens tissue, acting as sliding planes. When delivered to rabbit eyes, these laser incisions did not cause cataract growth or wound-healing abnormalities. When applied to human autopsy eyes, an average increase of 100 μm in the anteroposterior lens thickness was seen, corresponding to a 2.00 to 3.00 D gain in accommodative amplitude.

## Treatment of tractional vitreous attachments

Another promising application of the femtosecond laser in the near future, ultrashort laser pulses may replace posterior vitrectomy for the treatment of tractional vitreous attachments. This noninvasive strategy requires the implementation of adaptive optics to compensate optical aberrations by the vitreous in order to achieve a well-focused, highly resolved laser spot near the retina.

## Refractive index shaping

If the intensity of the femtosecond laser remains just below the threshold of optical breakdown, it is possible to create low-density plasma, which will allow free electrons to interact with the surrounding tissue. These chemical reactions could result in slight changes in the refractive index of optical media, and this phenomenon could be used to program diffractive lenses into the cornea and crystalline lens. In animal studies, refractive index shaping has been shown to be stable for several weeks or months. This principle could also be used to adjust the power of an intra ocular lens in situ.

## Reversing cataract

Photo bleaching or using multiphoton absorption to photo-chemically destroy absorbing and scattering protein aggregates inside the nucleus can remove the yellowing of the crystalline lens. In one experiment, human donor lenses were treated with an 800-nm infrared femtosecond pulsed laser. After treatment, the investigators found that the age-related yellow discoloration of the lens was reduced and the transmission of light increased.

*Invited*

# ION BEAM THERAPY WITH LASER-ACCELERATED PROTON BEAMS – CHALLENGES AND SOLUTIONS

**U. Masood[1], T.E. Cowan[2], W. Enghardt[1,2], M. Gotz[1], T. Herrmannsdörfer[2], K.M. Hofmann[3], L. Karsch[1], F. Kroll[2], U. Schramm[2], M. Schürer[1,2], J.J. Wilkens[3], K. Zeil[2], and J. Pawelke[1,2]**

[1] OncoRay-National Center for Radiation Research in Oncology, Faculty of Medicine and University Hospital Carl Gustav Carus, Technische Universität Dresden, Germany
[2] Helmholtz-Zentrum Dresden-Rossendorf, Dresden, Germany
[3] Department of Radiation Oncology, Klinikum rechts der Isar, Technical University of Munich, Munich, Germany

**Abstract.** Proton acceleration on μm scale via high intensity laser has become a compelling alternative to conventional accelerators and gained interests for its potential to reduce size and costs for proton therapy (PT) facilities [1, 2]. Next generation petawatt lasers promise laser-driven protons (LDP) with therapeutic energies. But, in contrast to conventionally accelerated quasi-continuous mono-energetic pencil beams with about 30 Gy/sec dose rate, LDP beams have diverse properties, i.e. ultra-intense pico-sec bunches with up to $10^{10}$ Gy/sec dose rate, large energy spread and divergence, and with only up to 10 Hz repetition rate. These properties make it challenging to adapt LDP beams directly for medical applications. The presented work is an ongoing joint translational research project of several institutions aiming to establish laser-driven PT. We will present the recent progress in design concepts and the status of the development.

## Summary

The status of the development of laser-driven PT can be summarized in five main challenges:

I) Laser-based technology has been established, with protons (up to 20 MeV) via 150 TW laser system, for systematic radiobiological studies with human cell-lines and small animals with fixed beamline. In which, no overall difference in the radiobiological effectiveness between laser-driven and conventional beams was detected to date.

II) For translation towards patient irradiation, increase of proton energy from 20 to 230 MeV by increasing the laser power from 150 TW to ~1 PW is one of the fundamental requirements, and the development is in progress.

III) Furthermore, a compact gantry system is designed based on pulsed magnets (PM) which is ~2.5x smaller than conventional gantries. It is integrated with laser-particle acceleration chamber, novel beam capturing and energy selection system. A new pulsed scanning system for wide beams with broad energies is designed for irradiations with clinical accuracy. Also, a new 3D treatment planning software has been developed for new dose delivery and treatment planning strategies for laser-driven PT. The evaluation of treatment plans shows laser-driven broad energetic beams are feasible for clinical application [3, 4].

IV) The light-weight iron-less high-field PMs are being developed for gantry realization. These are non-trivial and challenging to design. A pulsed 40 T solenoid for particle capture and a novel 10 T compact iron-less 50° sector magnet has been successfully tested, furthermore, a pulsed 120 T/m gradient quadrupole is being developed.

V) Last, but not the least, dosimetric verification is a crucial part of radiotherapy. The pulse structure and high intensity of LDP require advanced theoretical understanding and experimental verification of the dosimetric equipment [5].

Laser-driven PT is a promising compact alternative and could change PT, yet requires substantial development towards clinical application.

## Acknowledgements

Supported by German BMBF, nos. 03Z1N511, 03Z1O511 & DFG cluster of excellence MAP.

## References

1. U. Masood, *et al.*, *Appl. Phys. B*, 2014, **117**, 41–52.
2. K.W.D. Ledingham and W. Galster, *New J. Phys.*, 2010, **12**, 045005.
3. K.M. Hofmann, *et al.*, *Med. Phys.*, 2014, **41**, 112.
4. S. Schell, *et al.*, *Med. Phys.*, 2010, **37**, 5330–5340.
5. L. Karsch and J. Pawelke, *Z. Med. Phys.*, 2014, **3**, 201–10.

*Invited*

# NANOPLASMONICS ENHANCED ULTRAFAST LASER NANOSURGERY: MODELING AND RATIONAL DESIGN

**M. Meunier**

Polytechnique Montreal, Montréal, Canada, michel.meunier@polymtl.ca

**Abstract.** Nanobubbles generated by ultrafast laser irradiation of plasmonic nanoparticles can induce highly localized damage to targeted cells, which makes them valuable for nanomedicine applications. In this presentation, we present a complete model that successfully describes all interactions occurring during the irradiation of plasmonics nanostructures by an ultrafast laser of various pulse widths and fluences. We have also developed a computational framework to screen for optimized nanostructures that are not damaged upon laser irradiation. Using this rational design approach, we demonstrate theoretically and experimentally that nanoshells can reduce significantly the cavitation threshold in the near-infrared.

## Introduction

Irradiating metallic nanostructures by a femtosecond laser beam produces highly localised processes on the nanoscale in the surrounding medium. This particular process is mainly attributed to the surface plasmon resonance of the nanostructures. When these nanomaterials are imbedded in a biological media, their irradiation by a femtosecond laser could results in a highly localized plasma, heat production and mechanical effects yielding to the nanosurgery of cells.

## Modeling plasmonics enhanced ultrafast laser nanocavitation

Vapor nanobubbles generated around plasmonic nanoparticles (NPs) by ultrafast laser irradiation are efficient for inducing localized damage to living cells. Killing targeted cancer cells or gene delivery can therefore be envisioned using this new technology [1, 2]. The extent of the damage and its non-lethal character are linked to the size of the nanobubble. Precise understanding of the mechanisms leading to bubble formation around plasmonic nanostructures is necessary to optimize the technique. Nanocavitation is caused by the interplay between heat conduction at the NP-medium interface and non-linear plasmon-enhanced photoionization of a nanoplasma in the near-field [3–5], the former being dominant for in-resonance and the latter for off-resonance irradiation. Modeling of the whole laser-nanoparticle interaction, together with the help of the shadowgraphic imaging and scattering techniques [3–6], give valuable insight on the mechanisms of cavitation at the nanoscale, leading to possible optimization of the nanostructure for bubble-based nanomedicine applications.

## Rational Design of Plasmonic Nanoparticles for Enhanced Cavitation and Cell Perforation

The highly non-linear interaction process is controlled by the NP material, shape and size. There is currently no systematic design approach that enables the engineering of optimized NPs that are not damaged upon laser irradiation. We thus developed a computational framework to efficiently screen a large library of spherical nanostructures [7]. Using this framework, we were able to define general principles for the design of robust nanoantennas. We also demonstrate that silica-metal nanoshells (NS) have the potential to reduce the bubble generation threshold in the NIR compared to homogeneous NPs, due to their extensive spectral tunability. AuNS optimized for NIR irradiation have been used to validate our design framework [8]. Using time-resolved bubble spectroscopy, shadowgraphy imaging and electron microscopy, we were able to confirm the particle structural integrity and a cavitation threshold reduction of 51% relative to optimal AuNP. AuNS have also been used to perforate cancer cells with an efficiency of 61%, using 33% less energy compared to AuNP, which demonstrate the transferability of our design method to biomedical applications.

## References

1. E. Boulais, R. Lachaine, A. Hatef and M. Meunier, *J. of Photochem and Photobio. C*, 2013, **17**, 26–49.
2. E. Bergeron, C. Boutopoulos, R. Martel, and M. Meunier, *Nanoscale,* 2015, **7**,17836–17847.
3. E. Boulais, R. Lachaine, and M. Meunier, *Nanoletters*, 2012, **12**, 4763–4769.
4. R. Lachaine, E. Boulais, and M. Meunier, *ACS Photonics*, 2014, **1**, 331–336.
5. C. Boutopoulos, A. Hatef, M. Fortin-Deschênes, and M. Meunier, *Nanoscale,* 2015, **7**,11758–11765.
6. A. Dagallier, E. Boulais, C. Boutopoulos, R. Lachaine, and M. Meunier, *Nanoscale*, 2017, **9**, 3023–3032.
7. R. Lachaine; E. Boulais; D. Rioux; C. Boutopoulos, and M. Meunier, *ACS Photonics*, 2016, **3**, 2158.
8. R. Lachaine; C. Boutopoulos, C.; P.-Y. Lajoie; E. Boulais, and M. Meunier, *Nano Lett.,* 2016, **16**, 3187–3194.

*Invited*

# THE POSSIBILITIES REALIZED IN SURGERY AND FORCED THERAPY BY MEANS OF DEVICES BASED ON THE FIBER AND DIODE LASERS

**V.P. Minaev**

NTO "IRE-Polus", Fryazino, Russia
e-mail: vMinaev@ntoire-polus.ru

**Abstract.** The characteristics and possible applications in surgery and forced therapy of devices developed with diode and fiber lasers emitting at wavelengths 0.97; 1.06; 1.55; 1.94 and 1.68 μmare are presented.

The appearance of fiber lasers allowed improving the operational parameters (reducing weight, dimensions and power consumption, increasing lifetime and effectiveness, resistance to environment and mechanical action) and creating medical devices with new characteristics due to:

– possibilities of support of the CW operation at the wavelengths formerly available only in a pulsed mode (1.55 and 1.94 μm);

– obtaining radiation at wavelengths unavailable before, for example, 1.68 μm by means of the fiber Raman converter;

– creation of devices in which two independent regulated radiations with different wavelengths are removed through one fiber.

These devices allowed, in turn, developing new effective techniques of treatment.

We present information on the implemented medical devices.

These devises were used for development of the effective treatment technologies in ENT, neurosurgery, cardio- and vascular surgery, urology and other areas of medicine.

The possibilities of use for medical purposes of the new fiber lasers developed at NTO "IRE-Polyus" and IPG corporation are considered.

The potential of the new fiber lasers developed at NTO "IRE-Polyus" and IPG photonics to be used for medical purposes is considered.

*Invited*

# RECENT DEVELOPMENTS IN JAI AND UK ON X-RAY BIO-IMAGING BASED ON LASER-PLASMA ACCELERATION

**A.A. Seryi**

John Adams Institute, University of Oxford, UK
andrei.seryi@adams-institute.ac.uk

The research directions of John Adams Institute for Accelerator Science range from gigantic future colliders to compact energy recovery linacs. Plasma acceleration is one of the central areas of JAI research. Our researchers have pioneered many breakthrough results such as higher than a GeV mono-energetic laser-plasma accelerated beam. Our present work on plasma acceleration is focused on creating higher brightness and higher efficiency compact light sources and using them for various applications. In this talk an overview will be given about the JAI and UK progress in the area of laser plasma acceleration in application to bio-imaging.

*Invited*

# BIO-PHOTONICS RESEARCH WORKS IN SAKIGAKE PROGRAM IN JAPAN

**K. Ueda**

Institute for Laser Science, University of Electro-Communications, Japan

**Abstract.** I introduce our SAKIGAKE program supported by JST. One of the major research targets is bio-medical and bio-photonics. We have many excellent young scientists challenging the critical scientific front using advanced photonics technology. Some of them will present their latest results in this conference. I introduce interesting research works of other members in my SAKIGAKE team.

*Invited*

# CAVITATION BUBBLE DYNAMICS IN PLASMA-MEDIATED NANOSURGERY OF CELLS AND TISSUES

**A. Vogel, X.-X. Liang, S. Freidank,** and **N. Linz**

Institute of Biomedical Optics, University of Lübeck, Germany

**Abstract.** The dynamics of cavitation bubbles in the µm and nm range such as occurring in plasma- and nanoparticle-mediated cell surgery is investigated experimentally and theoretically. Radius-times curves are recorded by interferometric single-shot measurements with nm accuracy and ps time resolution. Modeling provides information on the bubble size dependence of breakdown and collapse pressures and the partitioning of laser energy into vaporization, shock wave and bubble energy, and energy needed to overcome viscous damping.

Laser-induced plasma generation and plasmonics are used for intraocular, refractive and cataract surgery as well as for gene transfection into cells and targeted effects via antibody-conjugated nanoparticles. A profound understanding of the sequence of events from plasma formation through acoustic emission, bubble formation and subsequent bubble oscillations is essential for an optimization of these processes. In the past, the dynamics of bubbles with sizes from millimeters down to tens of micrometers has been extensively investigated, mostly by time-resolved photography in conjunction with modeling. In this parameter range, the bubble dynamics is "self-similar", i.e. the spatial extent of collapse region and shock wave width scale with the bubble size but collapse velocity and pressure remain constant. By contrast, for bubbles in the micrometer and nanometer range such as occurring in plasma- and nanoparticle-mediated cell surgery surface tension, liquid viscosity, and heat conduction play an important role and the bubble dynamics changes strongly for $R_{max} \rightarrow 0$. We established new experimental and theoretical tools enabling the investigation of this parameters range and applied them to explore the bubble dynamics in water and in transparent cells and tissues.

Interferometric measurements enabled us to record entire radius-times curves $R(t)$ of spherical bubble oscillations in single-shot measurements with nm accuracy and 160 ps time resolution (Fig. 1, a). For bubbles with maximum radius $R_{max} \leq 1.5$ µm, $R(t)$ can be recorded only for the first oscillation since the maximum radius of the rebound bubble becomes so small that it produces only Rayleigh scattering but no interference signal. Nevertheless, the oscillation time of the rebound bubble remains detectable and the durations $T_1$ and $T_2$ of first and second oscillation can serve as modeling input.

Modeling is based on the Gilmore model of bubble dynamics that considers surface tension and viscosity as well as the liquid compressibility. We achieve excellent agreement between measured and calculated $R(t)$ curves (Fig. 1, b). Based on experimental $T_1$, $T_2$ data for $R_{max} \rightarrow 0$ and assumptions on initial plasma energy density, we deduce a wealth of information on the bubble size dependence of breakdown and collapse pressures and the partitioning of absorbed laser energy into vaporization energy, shock wave energy, bubble energy, and energy needed to overcome viscous damping.

For bubbles of a few µm or larger, shock wave emission dominates damping and interactions. Viscous damping increases with decreasing bubble radius and dominates for $R_{max} < 1$ µm. However, since surface tension also increases with decreasing radius, a "hot" region with strongly elevated collapse pressures of ≈ 300 kbar is observed in the intermediate range 1 µm < $R_{max}$ < 3 µm. At large *NA* and close to threshold, femtosecond breakdown turned out to be more disruptive than ns breakdown, which is opposite to the pulse duration dependence at small and moderate *NA*s.

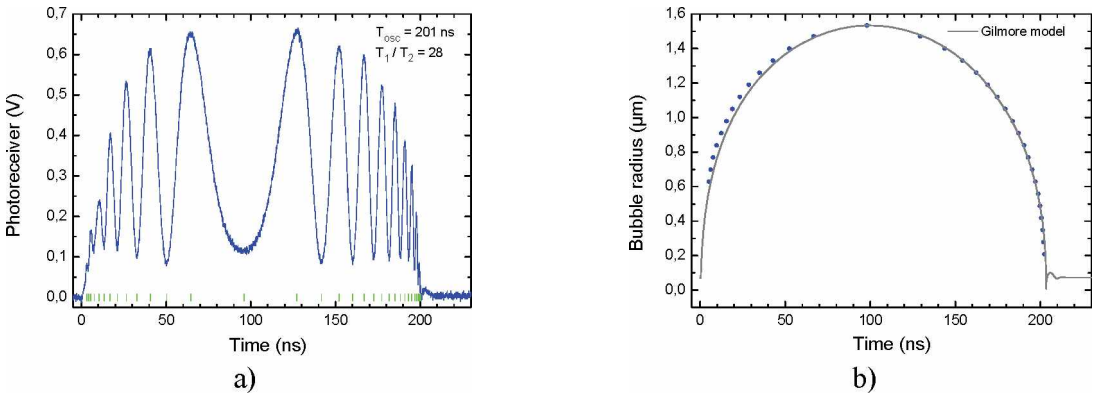



**Fig. 1.** Interference signal and $R(t)$ curve for a laser-induced bubble in water with $R_{max}$ = 1.52 µm

*Invited*

# DEVELOPMENT OF TUNABLE MID-IR LASERS FOR AGRICULTURE AND HEALTH SCIENCE APPLICATIONS

**S. Wada, T. Ogawa, M. Yumoto,** and **N. Saito**

RIKEN SPring-8 Center, Sayo, Hyogo, Japan
swada@riken.jp

Agriculture and health are of importance to keep human society and life of human. We develop optical systems using our original lasers, such as tunable MID-IR lasers and introduce them to plant factory and health checking systems with human breath.

*Invited*

# ANTIVASCULAR EFFECTS INDUCED BY PHOTO-MEDIATED ULTRASOUND

**X. Wang[1], H. Zhang[1], J. Li[1], Z. Hu[1], Y. Paulus[1], and X. Yang[2]**

[1] University of Michigan, Ann Arbor, MI, U.S.A. email: xdwang@umich.edu
[2] University of Kansas, Lawrence, KS, U.S.A. email: xmyang@ku.edu

**Abstract.** A novel antivascular technology, namely photo-mediated ultrasound therapy (PUT), was developed. By applying synchronized laser and ultrasound pulses simultaneously, PUT can treat microvessels in biological samples with excellent precision and controllability. Taking advantage of the high optical absorption of hemoglobin, PUT can selectively target microvessels without causing unwanted damages to surrounding tissue. PUT working at different optical wavelengths can selectively treat veins or arteries by utilizing the optical contrast between deoxy- and oxy-hemoglobin. Through the experiments on phantoms, chicken embryos, and rabbit eyes in vivo, the mechanism of PUT was studied, and its potential application in ophthalmology clinic was explored.

## Background and Motivation

Pathologic microvasculature plays a key role in the leading causes of blindness including diabetic retinopathy, retinal vein occlusions, and macular degeneration. Current treatments, including laser therapy, photodynamic therapy (PDT), and anti-vascular endothelial growth factor (VEGF) therapy, impose significant burdens on patients, their families, and our health system because of their invasive nature, frequent administration, and destructive nature. Using a combination of a low intensity laser concurrently with ultrasound, we developed a novel treatment technology, photo-mediated ultrasound therapy (PUT) [1], which can noninvasively remove microvessels without damaging surrounding biological tissues. Here, we present the first evaluation of PUT in treating microvessels in eye by working on rabbit choroidal vessel model.

## Methods

An integrated therapeutic ultrasound and laser treatment system was devised. Laser pulses, produced by a pulsed Nd:YAG laser at 532 nm with 3-ns pulse duration and 10-Hz repetition rate, synchronized with 10-ms ultrasound bursts. New Zealand white rabbits were used. For evaluating the treatment effects, Fundus photography and indocyanine green (ICG) angiography (ICGA) were acquired using the Topcon 50EX Fundus Camera. ICGA was performed before, immediately after, and weekly following PUT treatment for 1 month by injecting 0.2 mL/kg of ICG into the marginal ear vein.

## Results

Treatment with laser- or ultrasound-only resulted no changes on rabbit choroidal vessels. PUT treatment with concurrent laser and ultrasound was able to stop the blood flow in the choroidal vasculature with optimized parameters. Hemorrhage occurred with 2 MPa ultrasound + 150 mJ/cm$^2$ laser (estimated at the choroidal layer) whereas 2 MPa ultrasound + 30 mJ/cm$^2$ laser caused no effect. The optimal parameters were 2 MPa ultrasound + 75 mJ/cm$^2$ laser, which caused edema immediately after treatment. By 1 week, pallor occurred in the region of treatment with greatly diminished choroidal vessels which persisted to 4 weeks. ICGA demonstrated a decrease in number of choroidal vessels in the region by 1 week that persisted to 4 weeks after treatment. In conclusion, PUT holds significant promise as a novel non-invasive method to precisely remove microvessels in neurovascular eye diseases by more selectively treating vasculature with minimized side-effects and no systemic photosensitizing dye.

## References

1. Z. Hu, H. Zhang, A. Mordovanakis, Y. Paulus, Q. Liu, X. Wang, and X. Yang, "High-precision, non-invasive anti-microvascular approach via concurrent ultrasound and laser irradiation", *Scientific Reports*, 2017, 7, 40241.

*Invited*

# STATUS AND PERSPECTIVE OF AN X-RAY FREE ELECTRON LASER SACLA

**M. Yabashi**

RIKEN SPring-8 Center, Sayo, Hyogo, Japan, yabashi@spring8.or.jp

**Abstract.** After the inauguration in 2012, an X-ray free electron laser facility SACLA (SPring-8 Compact Angstrom free-electron LAser) in Harima, Japan has steadily provided hard X-ray FEL light for users. In this presentation, I will report the latest status of SACLA and their scientific achievements, which include investigation of structural change of photosystem II (PSII) in a water oxidation process, and observation of atomic motions in bacteriorhodopsin in a wide temporal range in nano- to milli-second after triggering of flash light.

Following five years construction, SPring-8 Angstrom Compact free-electron LAser (SACLA) in SPring-8, Harima, Japan [1] (Fig. 1) was inaugurated in March 2012, as the second X-ray free-electron laser (XFEL) facility after the Linac Coherent Light Source (LCLS) in the United States, and the first compact XFEL facility in the world. Since then, SACLA has steadily generated intense short-wavelength XFEL radiation around 1 Å for users .

Ultraintense femtosecond X-ray pulses have enabled single-shot detection of diffraction signals from complex molecules. One can thus elucidate static and dynamical molecular structures under chemical reactions without disturbing X-ray damages that cannot be avoided with conventional X-ray sources.




**Fig. 1.** SACLA and SPring-8

## Scientific achievements

Determination of structures and functions of photosystem II (PSII), a key catalytic protein complex for photosynthesis, is highly important for understanding the process and designing artificial photosynthesis. Shen and coworkers have determined a "radiation-damage-free" structure of PSII in the S1 state at a resolution of 1.95 A with SACLA, which shows differences in sub-angstrom levels compared to those obtained with a quasi-CW x-ray source of synchrotron radiation [2]. Furthermore, they determined a structure of an intermediate S3 state with two-flash illumination at room temperature at a resolution of 2.35 A with a time-resolved (TR) serial femtosecond crystallography (SFX) method, which suggests the insertion of a new oxygen atom close to another oxygen atom in the molecule [3]. These results have provided a critical basis for understanding mechanism of the oxygen evolution in photosynthesis.

The TR-SFX method also used for determining conformational changes in bacteriorhodopsin (bR), a light-driven proton pump and a model membrane transport protein, at 13 time points in a scale between nanoseconds to milliseconds following photo activation [4]. The molecular movie elucidated a fundamental mechanism of the directional proton transport in bR.

## Future perspective of SACLA

The limited availability of beamtime has been a common concern for world's XFEL activities. To address this issue, we have constructed the second XFEL beamline BL2 in 2013, and will start simultaneous operation of BL2 and BL3 for users in the autumn of 2017. We also started operation of a soft x-ray FEL beamline BL1. Furthermore, we have installed high-power laser systems including 500 TW lasers for investigating high-energy density science.

## References

1. T. Ishikawa, *et al.*, *Nature Photon.*, 2012, **6**, 540-544.; M. Yabashi et al., *J. Synchrotron Rad.,* 2015, **22**, 477-484.; http://xfel.riken.jp/research/indexnn.html.
2. M. Suga, *et al.*, *Nature*, 2014, **517**,99–103.
3. M. Suga, *et al.*, *Nature,* 2017, **543**, 131–135.
4. E. Nango, *et al.*, *Science,* 2016, **354**, 1552–1557.

*Invited*

# FIBER-OPTIC NEUROINTERFACES AND MULTIMODAL OPTICAL NEUROIMAGING IN OPTO- AND THERMOGENETIC STUDIES

**A.A. Lanin, M.S. Pochechuev, I.V. Fedotov, Y.G. Ermakova, A.B. Fedotov, D.A. Sidorov-Biryukov, O.I. Ivashkina, K.V. Anokhin, V.V. Belousov,** and **A.M. Zheltikov**

M.V. Lomonosov Moscow State University, Moscow, Russia
Texas A&M University, College Station TX, USA
Russian Quantum Center, Skolkovo, Moscow Region, Russia
Kurchatov Institute National Research Center, Moscow, Russia

We demonstrate multimodal optical imaging framework that combines single-neuron fluorescence microscopy with a variety of nonlinear-optical imaging techniques, including two-photon fluorescence, second- and third-harmonic generation, as well as coherent and stimulated Raman scattering. This provides a unique arsenal of tools for single-cell imaging of neurons expressing opto- and thermogenetic channels and/or fluorescent reporters in neuronal cultures, ex vivo brain slices, and precisely targeted regions inside the brain of awake transgenic mice and within the nervous system of zebrafish models.

VI International Symposium

# TOPICAL PROBLEMS OF BIOPHOTONICS




## *Clinical Biophotonics*

## Chairs

**Natalia Shakhova**
Institute of Applied Physics RAS,
Nizhny Novgorod State Medical Academy, Russia

**Herbert Stepp**
Laser Research laboratory, LIFE Center, University Clinic,
Munich, Germany

# CONTRIBUTION OF PHOTODIAGNOSIS AND PHOTODYNAMIC THERAPY TO THE TREATMENT OF LUNG CANCER: SAINT-PETERSBURG EXPERIENCE

**A. Akopov, G. Papayan**

Pavlov First State Medical University, Saint-Petersburg, Russia

Fluorescence diagnostics in combination with a variety of traditional and new methods of treatment has considerable potential to resolve of the complex medical issues. Its use in conjunction with photodynamic therapy is particularly effective, since it is easy to combine technically, allowing to perform the diagnosis and treatment of lung cancer as a single procedure. The possibility of photodynamic theranostics with various methodological improvements in experimental and clinical studies is shown as the use of tumour specific conjugates with biological nanocarriers; two-wavelength excitation; fluorescence image-guided surgery; stereotactic fluorescent biospectroscopy; using the near-infrared light to detect the tumour and sentinel lymph nodes; photodynamic irradiation in a pulsed radiation mode.

# BIOLUMINESCENCE-MEDIATED PHOTODYNAMIC THERAPY: A NOVEL TREATMENT FOR GRADE 4 ASTROCYTOMA

**J. Ng[1,2], N. Henriquez[1], N. Kitchen[1], and S. Bown[1]**

[1] Division of Surgery and Interventional Science, University College London UK. s.bown@ucl.ac.uk
[2] Providence Brain & Spine Institute, Portland, Oregon, USA

**Abstract.** Treatment for grade 4 astrocytoma is rarely curative due to infiltration of the tumour into adjacent normal brain. Photodynamic Therapy (PDT) can selectively destroy glioma cells, but is limited by light penetration through brain tissue. This new approach uses light generated chemically (bioluminescence). U87 glioma cells, transfected to express luciferase, could be killed *in vitro* with the photosensitiser mTHPC by adding luciferin for light generation on individual glioma cells. Transplanting these cells into mice, evidence of necrosis could be documented *in vivo* following administration of mTHPC and subsequent infusion of luciferin – the first evidence of bioluminescence activated PDT *in vivo*.

Despite advances in surgery, radiation and chemotherapy, grade 4 astrocytoma, the commonest primary brain tumour (glioblastoma multiforme), remains incurable with a dire prognosis related to its diffusely infiltrative nature. With photodynamic therapy, pre-treatment with a photosensitising drug and subsequent exposure to light of a specific wavelength can mediate selective tumour destruction. However, it is limited by light penetration. Bioluminescence results from conversion of chemical energy into light. Investigators have previously explored the potential for bioluminescence to activate a photodynamic effect [1–4]. This work builds upon these prior experiments, investigating whether bioluminescence generated inside astrocytoma cells *in vitro* and *in vivo* can mediate PDT: light generation by target cells requires no knowledge of the exact location of every cell, thereby potentially overcoming the unique diffusely infiltrative nature of astrocytomas.

*in vitro*: genetically modified U87 glioma cells expressing firefly luciferase (U87-*luc*) were generated, pre-treated with the photosensitisers hypericin or *m*THPC, then incubated with d-luciferin to induce bioluminescence. Cell viability was assessed by MTT assay, haemocytometry, and a growth assay. Inhibition by lycopene, an antioxidant that suppresses PDT, was assessed. Control studies used untransfected U87 cells. Bioluminescence-mediated PDT produced significant cell death with both photosensitisers in U87-*luc* cells, which was suppressed by lycopene. There was no effect in untransfected cells.

*in vivo*: U87-*luc* cells were xenografted subcutaneously and intracranially into CD1 nu/nu mice. Mice were pre-treated with intraperitoneal *m*THPC then given a 7 day infusion of d-luciferin (subcutaneously implanted pump). Tumour response was followed by bioluminescence imaging, volume measurements, and survival. Tumours were harvested for pathological examination and BrdU immunohistochemistry. In 3 out of 4 trials, including one in an intracranial model, a treatment effect was demonstrated by a significant reduction of proliferation, as assessed by the proportion of BrdU positive cells in the 'treatment' group compared with controls.

In conclusion, bioluminescence-mediated PDT kills tumour cells *in vitro*. Preliminary evidence of an effect *in vivo* supports the concept being explored further.

**Acknowledgements**

This work was generously supported by: The National Hospital Development Foundation Fellowship, The Royal College of Surgeons Rosetrees Fellowship and The B Braun Research Fellowship.

**References**

1. S. Carpenter, M.J. Fehr, G.A. Kraus, J.W. Petrich, *Proc Natl Acad Sci USA*, 1994, **91**, 12273–7.
2. J. Wen, P. Chowdhury, N.J. Wills, *et al.*, *Photochem Photobiol*, 2002, **76**, 153–7.
3. T. Theodossiou, J.S. Hothersall, E.A. Woods, K. Okkenhaug, J. Jacobson, A.J. MacRobert, *Cancer Res*, 2003, **63**, 1818–21.
4. M.L. Schipper, M.R. Patel, S.S.Gambhir, *Mol Imaging Biol*, 2006, **8**, 218–25.

# AUTOMATIC FEEDBACK GUIDED RETINAL LASER THERAPIES

**R. Brinkmann**[1,2]

[1] Institute of Biomedical Optics, University of Luebeck, Luebeck, Germany, brinkmann@bmo.uni-luebeck.de
[2] Medizinisches Laserzentrum Lübeck GmbH, Lübeck, Germany

**Abstract.** Laser photocoagulation of the retina is a very well establish standard of care for several retinal diseases over more than 40 years to date. However, with new methods and emerging precision of retinal diagnostics a demand for less invasive but as effective therapies arises. Therefore two minimal invasive retinal laser therapies with real-time feedback guidance in order to compensate for the inter and intra-individual variability in light scattering and absorption within the eye will be presented: Selective retina therapy (SRT) aiming to selectively damage the retinal pigment epithelium (RPE), and temperature controlled retinal stimulation and coagulation.

Laser grid photocoagulation according to the ETDRS study protocol was until recently the standard of care for the treatment of macular oedema, mainly associated with diabetic retinopathy [1]. However, retinal laser therapies for diabetic macular edema were recently challenged by anti-VEGF therapies. Prospective randomized and comparative multi center trials were conducted to investigate the efficacy for retaining vision by intravitreal drug administration. The RESTORE study for example using Ranibizumab showed a higher gain in visual acuity in the drug groups with and without laser, compared to the study arm treated by laser alone, after a periods of 12 months and 24 months, respectively [2].

However, when examining the study in more detail it shows that strong laser effects have been used, and the laser protocol was not defined in detail, in contrast to the drug administration. Interestingly, when using soft and well defined laser application after a first the drug loading phase of three administration, significantly lower numbers of injections over the following period of time were needed, while still no loss of vison was noticed [3].

Despite these results, nevertheless, the challenge to overcome the varying strengths of the laser effects owing to the eye's variability in absorption and light scattering remains. In order to overcome this drawback we realized two different new and innovative methods: Selective retina therapy (SRT) aiming to selectively address the retinal pigment epithelium (RPE) without any adverse effects to the adjacent neural retina and choroid [4]. In SRT a train of 1.7 µs laser pulses are applied with a repetition rate of 100 Hz which damages RPE-cells in a small therapeutic laser energy window. The therapeutic the aim is the rejuvenation of the RPE and Bruch's membrane in the healing phase. The second method involves an optoacoustic based real-time temperature measuring system with feedback control in order to generate uniform effects with a previously determined temperature increase, therapeutically aiming on temperature guided retinal stimulation and coagulation [5, 6]. Finally a completely sublethal temperature rise is under investigation in order to stimulate the retinal function to excite RPE cells to express cytokines and to trigger different intracellular reactions.

The talk will present both techniques in detail and will highlight preclinical and recent clinical results and future perspectives.

## References

1. Early Treatment Diabetic Retinopathy Study Reserach Group: Photocoagulation for Diabetic macular oedema: Early treatment diabetic retinopathy study report number 1, *Arch Ophth.,* 1985, **103**, 1796–806.
2. Diabetic Retinopathy Clinical Research Network. Randomized trial evaluating ranibizumab plus prompt or deferred laser or triamcinolone plus prompt laser for diabetic macular edema. *Ophthalmology.* 2010, **117**(6), 1064–77.
3. G. Barteselli, I. Kozak, S. El-Emam, J. Chhablani, M. Cortes, W. Freeman, *Br J. Ophthalmol.*, 2014, **98**(8), 1036–41.
4. R. Brinkmann, J. Roider, and R.. Birngruber, *Bull Soc Belge Ophtalmol.,* 2006, **302**, 51–69.
5. R. Brinkmann, S. Koinzer, K. Schlott, L. Ptaszynski, M, Bever, A, Baade, S. Luft, Y. Miura, J. Roider, and R. Birngruber, *J. Biomed. Opt.,* 2012, **17**(6), 061219.
6. K. Schlott, S. Koinzer, L. Ptaszynski, M. Bever, A. Baade, J. Roider, R. Birngruber, and R. Brinkmann, *J. Biomed. Optics.,* 2012, **17**(6), 061223.

# EFFECTS OF LOW-LEVEL LASER THERAPY (LLLT) IN THE PREVENTION AND TREATMENT OF RADIATION INDUCED MUCOSITIS ESTIMATED BY MULTIMODAL OPTICAL COHERENCE TOMOGRAPHY

**E.S. Finagina[1,2], E.B. Kiseleva[1], A.A. Moiseev[1,3], M.V. Sirotkina[1], A.V. Maslennikova[1], D.V. Shabanov[3], S. Ksenofontov[3], G. Gelikonov[1,3], L. Matveev[1,3], V. Zaitsev[1,3], E.V. Zagaynova[1], N.D. Gladkova[1], and A. Vitkin[1, 4]**

[1] Nizhny Novgorod State Medical Academy, Nizhny Novgorod, Russia
[2] Nizhny Novgorod Regional Oncology Hospital, Nizhny Novgorod, Russia
[3] Institute of Applied Physics, Russian Academy of Sciences, Nizhny Novgorod, Russia
[4] University of Toronto and University Health Network, Toronto, Canada

**Abstract.** Low-level laser therapy (LLLT) is a non-pharmacological method of treatment and prevention of mucositis induced by radio(chemo)therapy of oral and pharyngeal cancer. We monitored the effectiveness of LLLT using multimodal optical coherence tomography (OCT). A spectral domain OCT system with microvascular visualization was used. Twelve patients were included in the control group, and nine patients in the LLLT group. All patients in the LLLT group have shown less pain and duration of mucositis than in the control group. Structural OCT images for a longer time remain unchanged in comparison with the control ones. The density of the vasculature and the number of small vessels that increased as a result of the appearance of mucositis symptoms was much less in the LLLT group. Optical coherence tomography allows detecting early and "subtle" changes in living tissues and studying the "application points" and mechanisms of the action of therapy modalities.

Oral mucositis is the most important complication of radiation and chemoradiation treatment of oral and pharyngeal cancer [1]. Low-level laser radiation is used as a non-pharmacological method of treatment and prevention of mucositis [2]. Optical coherence tomography is a non-invasive method that allows evaluating the structural and functional changes in living tissues [3]. Our study objective was to evaluate the effectiveness of LLLT by multimodal optical coherence tomography.

Twenty-one patients with stage II-IV of oral and pharyngeal cancer were enrolled. Irradiation was performed by a linear accelerator or a $Co^{60}$ unit. Twelve patients received standard prevention and treatment of mucositis, nine patients were exposed to LLLT of oral cavity. LLLT was conducted by a "Matrix" unit (635 nm, power 5 mW for 3 min) before every radiotherapy session. A spectral domain OCT system (central wavelength = 1300 nm; speed = 20,000 spectral A-scans/sec; lateral resolution = = 15 μm) (Institute of Applied Physics RAS, Nizhny Novgorod, Russia) was used. Based on temporal speckle variations as the source of image contrast, 3D OCT angiography images were obtained. OCT imaging was carried out three times per week throughout the course of treatment on two symmetric sites on both cheeks. All patients were also evaluated by visual criteria and complaints.

OCT structural images of healthy buccal mucosa show three distinct layers corresponding to the epithelium, the lamina propria, and the submucosa. The main manifestation of mucosal reaction was a contrast reduction between the layers. Quantitative processing of the OCT microvascular images demonstrated an increase of the vascular density before visual signs of mucositis occur. Statistically significant changes of the vasculature compared to their initial levels were detected when grade two and three mucositis developed. Further, microvascular reaction is seen to be dose-level dependent. In the LLLT group, patients demonstrated a lower frequency and duration of severe mucositis (grade 0/1 – 52%, grade 2 – 29%, grade 3 – 19%) as compared to patients who received a standard treatment (grade 1 – 10%, grade 2 – 57%, grade 3 – 33%). OCT images remain unchanged for a longer time in comparison with the control group. The density of the vasculature and the number of small vessels increased slower compared to the initial level. Thus, multimodal OCT can be used when testing various agents for the prevention and treatment of mucositis and for studying their main "application points" (epithelium, connective tissue matrix or microcirculatory bed) and mechanisms of action.

## References

1. S.T. Sonis, *Nature Reviews Cancer*, 2004, **4**(4), 277–284.
2. R.J. Bensadoun, & R.G. Nair, *Current opinion in oncology*, 2012, **24**(4), 363–370.
3. N. Gladkova, *et al.*, *Medical Laser Application*, 2008, **23**(4), 186–195.

# INTRAVESICAL PDT FOR NON-MUSCLE-INVASIVE BLADDER CANCER

**S.V. Gamayunov**[1], **E.A. Tararova**[2], and **O.S. Streltsova**[3]

[1] Republican Clinical Oncologic Dispensary Health Ministry of Chuvashia, Cheboksary Russia
Gmajnovs@mail.ru
[2] Nihzny Novgorod Regional Oncologic Clinic, Nizhny Novgorod, Russia
[3] Nizhny Novgorod State Medical Academy, Nizhny Novgorod, Russia

**Abstract.** Non-muscle-invasive bladder cancer (NMIBC) can be effectively treated via transurethral resection and intravesical agents, although recurrence is common. Intravesical PDT has perspectives as one of new treatment approaches. This study aims at determining the optimal parameters of laser exposure for treatment of NMIBC with intravesical PDT. The following applied laser irradiation doses were tested: 10 J/cm$^2$ (group I, 5 cases); 20 J/cm$^2$ (group II, 10 cases); 40 J/cm$^2$ (group III, 5 cases). It is shown that the most safe and efficient regime is achieved with the dose of 20 J/cm$^2$.

Bladder cancer (BC) is the ninth-commonest malignancy worldwide [1]. Approximately 75–80% of urothelial carcinoma of the bladder (UCB) is manifested as non-muscle-invasive (NMI) disease [2]. Intravesical PDT appears to be a highly efficient, safe and well-tolerated technique for treatment of NMI (Ta, T1 and in situ) tumors [3–4]. The aim of this work is to determine safe and efficient light exposure regimes for intravesical PDT after transurethral resection (TUR) in patients with high risk of non-muscle-invasive bladder cancer (NMIBC).

Prospective multicenter stage I study was performed aiming at determining optimal PDT regimes and evaluation of achieved safety and efficiency intravesical PDT. A total of 20 patients with high risk of NMIBC were enrolled into the study. Intravesical PDT was performed in 24 hours after TUR. N-dimethyl-glucamine salt of chlorine e6 (Fotoditazin®; VETA-GRAND, Moscow, Russia) was used as photosensitizer for PDT (1.0 mg/kg, intravenous infusion 2.5–3.0 h before PDT). Radiation from a continuous wave (cw) laser diode operating at 662 nm (Lakhta-Milon; Milon Laser, Moscow, Russia) was delivered to mucosa with a cylindrical waveguide with 10-mm-long diffusor (QP UV 600; Polironik, Moscow, Russia) for bladder volume of 80 ml. The intensity of the laser lradiation on the tissue surface was 0.03 W/cm$^2$. The applied light doses were following: 10 J/cm$^2$ (group I, 5 cases); 20 J/cm$^2$ (group II, 10 cases); 40 J/cm$^2$ (group III, 5 cases). The study was approved by the Institutional Review Board of the Nizhny Novgorod Medical Academy (protocol 14, 03.12.2013) and the Nizhny Novgorod Oncology Clinic (protocol 1, 03.05.2015).

In group I (10 J/cm$^2$) minor pain syndrome in the suprapubic region was noted during 24 h after PDT procedure. A total of 3 recurrence cases (3 of 5) were detected in 5, 4.5 and 3 months after treatment. In group II (20 J/cm$^2$ ) minor pain syndrome in the suprapubic region was noted during 24–48 h after PDT procedure accompanied by short-term hematuria doped with intravesical gemostatics injection. In the follow-up varying in the range 4–17 month (median of 12 months) only 1 recurrence case was revealed (1 out of 10) in 13 months. In group III (40 J/cm$^2$ ) pronounced pain syndrome requiring anesthetics application in the suprapubic region was noted together with prolonged hematuria and formation of bladder fibrosis in 2 patients (2 out of 5). No recurrence cases were revealed in the follow-up varying in the range 4–17 months.

To conclude, PDT procedure after TUR is a perspective technique of organ-preserving treatment in patients with high risk of NMIBC. The PDT light dose was demonstrated to be most efficient due to low recurrence rate and absence of severe side effects. The stage II-III studies are appropriate for further investigation of the technique efficiency.

### Acknowledgements

The authors are grateful to the management and staff of Nizhny Novgorod Oncologic Clinic and Republican Clinical Oncologic Dispensary Health Ministry of Chuvashia for the possibility to conduct clinical studies.

### References

1. S. Antoni, J. Ferlay, I. Soerjomataram, *et al.*, *Eur Urol.*, 2017, **71**(1), 96–108.
2. A.M. Kamat, N.M. Hahn, J.A., *et al.*, *Lancet*, 2016, **388**(10061), 2796–2810.
3. M.J. Bader, H. Stepp, W. Beyer, *et al.*, *Urol Oncol.*, 2013, **31**(7), 1178–83.
4. J.Y. Lee, R.R. Diaz, K.S. Cho, *et al.*, *J Urol.*, 2013, **190**(4), 1192–9.

# MULTIMODAL OPTICAL COHERENCE TOMOGRAPHY MONITORING OF BASAL CELL CARCINOMA TREATMENT WITH PHOTODYNAMIC THERAPY

**E.V. Gubarkova[1], S.V. Gamayunov[2], E.V. Zagaynova[1], E.S. Finagina[1], M.A. Sirotkina[1], L.B. Timofeeva[1], A.A. Moiseev[1,3], S.Yu. Ksenofontov[1,3], A. Vitkin[1,4], and N.D. Gladkova[1]**

[1] Nizhny Novgorod State Medical Academy, Nizhny Novgorod, Russia, kgybarkova@mail.ru
[2] Republican Clinical Oncological Dispensary Health Ministry of Chuvashia
[3] Institute of Applied Physics Russian Academy of Science, Nizhny Novgorod, Russia
[4] University of Toronto, Toronto, Canada

**Abstract.** Nowadays, photodynamic therapy (PDT) is a common and efficacious method for basal cell carcinoma (BCC) treatment. In this study, a tissue monitoring method is introduced based on multimodal optical coherence tomography (MM OCT) as a combination of microangiographic and structural OCT modalities for tumor microvessel network and tissue structure visualization, respectively. It was demonstrated that MM OCT is a promising method of in vivo visualization of the different microvasculature in normal skin, BCC, in the scar formed after treatment, and assessment of the PDT tumor impact based on vascular changes.

**Introduction.** BCC is the most common cancer in fair skinned individuals and its incidence is still rising [1]. PDT treatment has been extensively developed as a new modality and an alternative to conventional therapies because of its high efficacy and good cosmetic outcome [2, 3]. OCT is fast emerging as an additional non-invasive modality for detection and visualization of the microvessel network skin tumor [4, 5].

The aim of this study was non-invasive monitoring of anticancer therapy used MM OCT based microangiography within human skin *in vivo*.

**Materials and Methods.** 30 patients with BCC who underwent PDT treatment and fluorescence imaging were imaged in this study. PDT was performed two hours after intravenous injection of Photoditazine (Chlorine E6, Veta Grant, Russia). The tumors were irradiated by a laser with a wavelength of 662 nm, energy density 150 J/cm$^2$, and power density 0.3 W/cm$^2$.

The vascular changes during and after PDT were evaluated *in vivo* by MM OCT. In this study we used a common path spectral domain MM OCT system with a central wavelength of 1310 nm, radiation power of 20 mW and spectral width of 100 nm, resulting in axial resolution of 15 μm, scanning depth of 1.7 mm, scanning speed of 20 000 A-scans per second. The system is capable of cross-polarization [6] and microangiography [7] OCT imaging.

The microcirculation and microstructure response was studied in an early period post PDT (within 24 hours) and in a late period when a scar is forming (in 3 months).

**Results.** MM OCT is capable of seeing *in vivo* the difference between microvasculature of normal skin, BCC, and a scar formed after treatment. It is also capable of assessing the PDT tumor impact based on visualized vascular changes. Microvasculature of BCC is characterized by abnormal shape and significant tortuosity. Immediately after PDT, the vessels disappear on the OCT images. It corresponds to a severe reduction of microcirculation on PDT treatment. 3 months after PDT a microcirculatory network of the formed scar becomes denser and has regular microvessels.

Thus, MM OCT based microangiography and cross-polarization is a promising non-invasive method for monitoring anticancer therapy in human skin *in vivo*.

### Acknowledgements

The study was supported by the grant no. 14.B25.31.0015 of the Ministry of Education and Science of the Russian Federation.

### References

1. S.V. Mohan *et al.*, *CurrDermatol Rep*, 2014, **3**(1), 40–45.
2. P. Agostinis *et al.*, *CA Cancer J Clin*, 2011, **61**(4), 250–81.
3. R.R. Allison and K. Moghissi, *Photodiagnosis Photodyn Ther.*, 2013, **10**(4), 331–41.
4. C. Blatter *et al.*, *Biomed. Opt. Express*, 2012, **3**(10), 2636–2646.
5. U. Baran *et al.*, *Skin. Res. Technol.*, 2016, **22**, 238–246.
6. E.V. Gubarkova *et al.*, *J. Biophotonics*, 2016, **9**(10), 1009–1020.
7. L.A. Matveev *et al.*, *Optics Letters*, 2015, **40**(7), 1472–1475.

*Invited*

# RETINAL AUTOFLUORESCENCE LIFETIME FOR OPHTHALMIC DIAGNOSTIC – WHAT CAN WE LEARN FROM IN-VIVO AND IN-VITRO FLIM?

**M. Hammer**[1], **L. Sauer**[1], **J. Schmidt**[1], **S. Peters**[1], **L. Kreilkamp**[1], and **M. Klemm**[2]

[1] University Hospital Jena, Jena, Germany
[2] Technical University Ilmenau, Ilmenau, Germany
Email: martin.hammer@med.uni-jena.de

**KEY WORDS**: Fluorescence lifetime ophthalmoscopy, retinal disease, animal models.

**Goal:** Fluorescence lifetime imaging ophthalmoscopy (FLIO) may provide a metabolic mapping of the retina. Full understanding of in vivo measured lifetimes, however, needs the *in vitro* investigation of pathologic processes, underlying fluorescence changes.

**Methods:** FLIO images were obtained from patients suffering from diabetic retinopathy, age-related macular degeneration, macular holes, and Alzheimer's disease. A 30° retinal field was investigated with a Heidelberg Engeneering Spectralis® fluorescence lifetime imaging ophthalmoscope (FLIO), detecting the temporal decay of the fluorescence in a short (498–560 nm; Ch1) and a long (560–720; Ch2) wavelength channel upon excitation with <100 ps (FWHM) laser pulses at 473 nm. The amplitude weighted mean fluorescence lifetime $\tau_m$ was calculated from a three-exponential approximation of the decay. For comparison, fluorescence lifetimes were recorded from porcine cadaver eyes, porcine ocular fundus organ cultures, and mice using the same FLIO technique as well as two-photon excited fluorescence lifetime imaging (FLIM).

**Results:** A general extension of lifetimes with age and disease was found. This correlated well with an increase of lifetimes in porcine organ culture as well as animal models due to oxidative stress, protein glycation, and sub-retinal deposition of metabolic byproducts. Melanin, lipofuscin, collagen, advanced glycation end products, macular pigment, and drusen material could be distinguished by fluorescence lifetime.

**Conclusions:** Various pathologic alterations of ocular fundus fluorophore composition, such as lipofuscin accumulation, modification, and clearing from retinal pigment epithelium cells, retinal atrophy, and protein glycation, may contribute to an extension of fluorescence lifetimes. The establishment of biological models of human disease and the investigation of their fluorescence characteristics is needed to understand *in vivo* FLIO data.

# MORPHOLOGY IN CONTROL OF PDT WITH CHLORINE PHOTOSENSITIZERS

**K.S. Korchagina[1], S.V. Gamayunov [1], S.S. Kuznetsov[2], V.V. Dudenkova[3], E.A. Sergeeva[4], and N.M. Shakhova[4]**

[1] Republican Clinical Oncological Dispensary Health Ministry of Chuvashia, Cheboksary, Russia, Ksenija-korchagina@rambler.ru
[2] State Medical Academy, Nizhny Novgorod, Russia
[3] Lobachevsky State University of Nizhni Novgorod, Nizhny Novgorod, Russia
[4] Institute of Applied Physics RAS, Nizhny Novgorod, Russia

**Abstract.** The results of studying tumor response to photodynamic therapy skin cancer with chlorine photosensitizers (PS) are presented. The study was performed using routine histological approaches. We demonstrate morphological changes in tumor typical for different time intervals after PDT. The obtained data allow dividing the morphological changes into two groups: early changes which occur within 24–48 hours, and late changes which develop in two days. For morphological verification of chlorine PS biodistribution in human tumors, a preliminary study of PS detection in biopsy samples of human skin carcinoma was carried out. Using laser scanning microscopy we show that PS is primarily distributed in the paratumoral zone.

Skin cancer is the most common type of oncological diseases in humans. Photodynamic therapy (PDT) can compete in efficiency with surgical and radiation methods of skin carcinoma treatment [1, 2]. However, there remain issues that need to be clarified. Among them are photosensitizer (PS) biodistribution in the tumor, photodynamic reactions which occur in human tumors, and morphological outcomes [2]. The purpose of the work is to study pathomorphism of human skin tumors after PDT and to show the possibility of laser scanning microscopy (LSM) to observe biodistribution of chlorine PS.

The protocol of the study was approved by the local Ethics Committee of the Nizhny Novgorod State Medical Academy. The study involved 32 patients. PDT was performed with morphologically verified basal cell carcinoma $T_{1\text{-}2}N_0M_0$ with the following parameters of laser radiation: wavelength, 662 nm, power density, 0.30 W/cm$^2$, dose density, 150–250 J/cm$^2$. As a photosensitizer, we employed Photoditazine in a dose of 1.0 mg / kg. To investigate developing morphological changes, biopsy was performed at definite time intervals: 2 hours after PS introduction, immediately after PDT, 2 hours after PDT, 1, 4, 6, 12 days after PDT. Study of PS distribution in *ex vivo* human skin carcinoma samples was conducted using LSM 510 META laser scanning microscope prior to laser exposure. Morphological changes in tumors after PDT were evaluated by two independent experts using routine histological staining study (H&E).

Immediately after PDT and after 2 hours no morphological features of pathomorphosis were detected while there was a slight swelling (edema) of tissues. In the early period after PDT (1 day) the main morphological changes were hemorrhages, plethora of blood vessels, thrombi formation, stasis and the sludge phenomenon. In the late period (4–6 days), necrotic changes of tumor prevailed, and by the 12th day reparation processes were observed. LSM imaging of samples prior to laser exposure showed that PS concentration in the tumor stroma (perivascular space and extracellular matrix) is higher than the concentration in the tumor cells.

It was demonstrated that the disorganization of tumor vascular bed is a key event in PDT with chlorine PS, which is probably due to the predominant accumulation of the drug in the tumor stroma.

**Acknowledgements**

The authors thank the Ministry of Education and Science of the Russian Federation (Project RFmEFI60414X0027, Contract No.14. B25.31.0015) and the Russian Foundation for Basic Research (grant 16-02-00974) for the financial support.

**References**

1. C. Matei, M. Tampa, T, Poteca *et al.*, *Journal of Medicine and Life*, 2013, **6**(1), 50–54A.
2. D.K. Cohen and P.K. Lee, *Cancers,* 2016, **8**(90), 2–9.

# OCT-BASED MICROANGIOGRAPHY FOR EVALUATION OF FUNCTIONAL VESSELS

**M.A. Lazareva**[1], **A. Moiseev**[2], and **N.M. Shakhova**[2]

[1] Nizhny Novgorod State Medical Academy, Nizhny Novgorod, Russia
gorozhanceva.m@gmail.com
[2] Institute of Applied Physics, Russian Academy of Sciences, Nizhny Novgorod, Russia

**Abstract.** Female breast reconstruction after surgical treatment of breast cancer is currently a standard. Combined treatment negatively affects the results of reconstruction inducing disorders in blood supply of the reconstructed tissues. For timely control of neovascularization process, effective and accessible monitoring techniques are required. The abilities of optical coherence tomography (OCT) in imaging of microcirculatory net vessels are demonstrated in this study. OCT-angiography of skin of different localizations is performed. In model studies the ability of monitoring vessel changes after functional tests is demonstrated. OCT-angiography technique is also demonstrated to be efficient for monitoring microcirculation in skin of reconstructed breast in the course of combined treatment.

Female breast reconstruction after surgical treatment of breast cancer is currently a standard. Radiation and chemotherapy negatively affect the results of reconstruction [1, 2]. One of the reasons for unsuccessful outcomes is the disorder in blood supply of the reconstructed tissues [3]. For timely control of neovascularization process effective and accessible monitoring techniques are required.

A spectral domain OCT (SD OCT) setup at 1.3 micrometer central wavelength with axial resolution equal to 10 micrometer and lateral resolution equal to 15 micrometers was used. Continuous 2D scanning was performed in the range of 3×3 mm, with 512 spectral measurements along the fast axis, from which 256 spectral A-scans were computed and 1024 B-scans along the slow axis formed the final 3D stack, thus it took about 26 seconds to scan the entire site. The study was performed on the volunteers of the research team. The skin areas located at breast (recipient zone) and in abdominal area (donor zone) were inspected. Functional tests were performed: for hot tests an applicator at 90 °C was applied resulting in the temperature of 42 °C on skin surface, while for cold tests an ice applicator at –20 °C was applied resulting in the temperature of 4 °C on skin surface.

In the study of various anatomical zones with OCT angiography, a different vascular pattern was observed indicating the possibility of visualizing the morphological features of the microcirculatory bed of superficial tissues. The results of the temperature tests clearly demonstrate the "depletion" of the vascular pattern in the cold test, followed by the restoration of functioning vessels and their obvious vasodilation. In the hot test after the applicator exposure, an increase in the number of functioning vessels and their vasodilation are detected with gradual relaxation after the normalization of skin surface temperature.

The obtained results show the ability of OCT-angiography to detect anatomical and functional features of the microcirculatory bed of superficial tissues. The proposed approach can be employed for in vivo monitoring of the condition of the microcirculatory bed of the skin of the reconstructed breast in the course of combined breast cancer treatment.

### Acknowledgements

The authors thank the Russian Foundation for Basic Research (grant 15-29-04884) for the financial support and the staff of the Nizhny Novgorod Oncology Center for making this study possible.

### References

1. E. Oh, H. Chim, H.T. Soltanian, *J. Plast Reconstr Aesthet Surg.*, 2012, **65**(10), 267–80.
2. M.B. Nava, A.E. Pennati, L. Lozza, *et al.*, *Plast Reconstr Surg.*, 2011, **128**(2), 353–9.
3. P. Andrades, R.J. Fix, S. Danilla, *et al.*, *Ann Plast Surg.*, 2008, **60**(5), 562–7.

# MULTIMODAL OPTICAL COHERENCE TOMOGRAPHY FOR EVALUATION OF THE NORMAL TISSUE STATE DURING ANTICANCER TREATMENT

**A. Maslennikova[1], E. Finagina[1,2], M. Sirotkina[1], M. Lazareva[1], A. Moiseev[1,3], S. Ksenofontov[3], G. Gelikonov[1,3], L. Matveev[1,3], E. Kiseleva[1], V. Zaitsev[1,3], N. Shakhova[3], E. Zagaynova[1], N. Gladkova[1],** and **A. Vitkin[1,4]**

[1] Nizhny Novgorod State Medical Academy, Nizhny Novgorod, Russia
[2] Nizhny Novgorod Regional Oncology Hospital, Nizhny Novgorod, Russia
[3] Institute of Applied Physics, Russian Academy of Sciences, Nizhny Novgorod, Russia
[4] University of Toronto and University Health Network, Toronto, Ontario, Canada

**Abstract.** The task of expedite *in vivo* evaluation of microvasculature state has many applications in oncology, in particular, for assessing the viability of tissues during surgery; in transplantology; in plastic surgery, for evaluating of wound healing and for monitoring the response of tissue to damage. A spectral domain OCT system with microvascular visualization, outfitted with an imaging probe, was used for in vivo monitoring of oral mucosa during the radiation therapy and for assessing the state of tissues in the area of plastic surgery after mastectomy. Fifteen patients were imaged longitudinally. Quantitative processing of OCT images demonstrated changes of vascular parameters before the appearance of clinical signs of mucositis. These were statistically significant compared to initial pre-treatment levels in patients that subsequently developed grade two or three mucositis.

The task of expedite *in vivo* evaluation of microvasculature state has many applications in oncology; in transplantology; in plastic surgery; for evaluating of wound healing and for monitoring the response of tissues to damage. Optical coherence tomography (OCT) is a noninvasive technique for microstructural in vivo bioimaging; OCT also allows sensitive microvascular visualization without any external contrast agents. Mucositis is the most common limiting toxicity of radio(chemo)therapy of head and neck cancer. Noninvasive quantifiable and robust methods for detecting subclinical changes of the irradiated mucosa that are impossible to register by subjective visual examination are highly desirable. Previous preclinical and clinical studies have suggested the feasibility and utility of using OCT for monitoring radiation mucositis [1].

Fifteen patients with stage II–IV of squamous cell carcinoma of the oral cavity and pharynx were enrolled. Irradiation was performed using a linear accelerator or $Co^{60}$ machine. Mucositis degree was scored by RTOG/EORTC scale. A spectral domain OCT system (central wavelength = 1 300 nm; speed = 20 000 spectral A-scans/sec; lateral resolution = 15 μm) was used. Based on temporal speckle variations as the source of image contrast, 3D OCT angiography imageswere obtained. The vessel thickness and volumetric vascular density metrics were then calculated; the 1-pixel-thick vessels (corresponding to diameters ≤ 25 μm) were used for the former calculation. OCT imaging was carried out three times per week throughout the course of treatment on two symmetric sites on both cheeks.

OCT images of the normal buccal mucosa show dense, uniform microvascular networks. Continued dose accumulation caused an increase in the clinical manifestations of reaction, as also seen by the OCT vascular density and the small vessel length. Statistically significant changes of vasculature parameters compared to their initial values were detected when grade two and grade three of mucositis developed. Microvascular reaction was dose-level dependent and was detected before clinical symptoms of mucositis were observed. In the cases of IMRT patients, similarity or dis-similarity of microvascular metrics in the different mucosal sites tracked with corresponding doses / DVHs. These findings may have relevance in the context of early intervention in patients who are likely to develop severe oral complications. The most important outcome of the work was the development of a clinical system for an in-vivo, well-tolerated, longitudinal, objective and quantifiable high resolution imaging of the microvasculature. Further work will explore correlation between the early OCT-detected microvascular changes in the oral mucosa in the course of RT, and the early and late RT oral complications.

**Acknowledgements** The study was supported by the Russian Federation Government contract No 14.B25.31.0015, RFBR project No16-02-00670 and No 15-29-04884.

## References

1. N. Gladkova *et al.*, *Medical Laser Application*, 2008, **23**(4), 186–195.

# DIFFERENTIAL DIAGNOSTICS OF VARIOUS FORMS OF CHRONIC RHINITIS WITH OPTICAL COHERENCE TOMOGRAPHY

**A. Meller[1,2], M. Shakhova[1,2], D. Sapunov[2], P. Agrba[1,3], A. Shakhov[2], and M. Kirillin[1]**

[1] Institute of Applied Physics RAS, Nizhny Novgorod, Russia
mellalina@mail.ru
[2] Nizhny Novgorod State Medical Academy, Nizhny Novgorod, Russia
[3] N.I. Lobachevsky State University of Nizhny Novgorod, Nizhny Novgorod, Russia

**Abstract**. Differential diagnostics of various forms of chronic rhinitis is necessary for elaboration of treatment tactics. OCT-rhinoscopy was performed for 85 patients with chronic rhinitis. OCT images of unaltered nasal mucosa (relative norm) were obtained from healthy volunteers. The features of OCT images of relative norm and two morphologically different chronic rhinitis forms were revealed. The potential of OCT in objectification of adrenalin test results is demonstrated. Numerical processing of OCT images allowed additional enhancement of diagnostic accuracy.

Chronic rhinitis is highly prevalent and affects the quality of life due to systemic symptoms [1]. Diagnosis of chronic rhinitis is often complicated due to the variety of morphological forms and clinical variants of the disease [2]. Recognition of morphological types of the disease determines the choice of treatment tactics [3]. OCT has high potential as a novel technique for differential diagnosis of chronic rhinitis forms.

The aim of this study is to demonstrate the cabilities of OCT in differential diagnosis of chronic rhinitis forms.

A total of 85 patients with chronic rhinitis were enrolled in the study; OCT inspection was performed in the course of standard rhinoscopy. We used the OCT-U1300 device operating at a central wavelength of 1280 nm, with spatial resolution of 15–30 μm and probing depth of up to 1.5 mm equipped with an endoscope probe of 2.4 mm in external diameter. Interpretation of OCT images of the nasal mucosa was performed on the basis of known morphological features and *post mortem* histology data from other patients. To enhance the diagnostic accuracy of OCT, numerical processing of OCT images, namely, histogram analysis, was employed.

In the frames of the study three morphologically different types were distinguished: relative norm, hypertrophic rhinitis and atrophic rhinitis. It is shown that OCT images of nasal mucosa in norm and with inflammatory process have specific features. In case of norm, two layers are visualized, the upper one, with moderate OCT signal corresponds to epithelium. It does not manifest a clearly distinguished boundary with lower layer corresponding to *lamina propria* with higher OCT signal that appears to be compact. The latter features small rounded zones of reduced signal corresponding morphologically to the blood vessels and glands. In the case of hypertrophic rhinitis, the upper layer in the OCT image is thickened, and the boundary between the epithelium and *lamina propria* is even more blurred. In the subepithelial layer, linear zones of the reduced signal typical for edema are observed. In case of atrophic rhinitis, it is impossible to distinguish epithelium as a separate layer in the OCT image, and the entire image represents a uniform layer. The reaction of tissue to the adrenalin test in case of neurovegetative rhinitis is much more evident in OCT images as compared to visual inspection in the course of rhinoscopy, while both norm and hyperthrophic rhinitis demonstrate a weak reaction to the test.

To conclude, the OCT images of nasal mucosa reflect morphologic and functional features of different form of chronic rhinitis which indicates high potential of the technique in differential diagnostics of different forms of this pathology.

**Acknowledgements**

The study is supported by the Russian Science Foundation (grant #17-15-01264).

**References**

1. E. Angier, J. Willington, G. Scadding, S. Holmes, and S. Walker, British Society for Allergy & Clinical Immunology (BSACI) Standards of Care Committee, *Prim Care Respir J,* 2010, **19**(3), 217–22.
2. E. Mølgaard, S.F. Thomsen, T. Lund, L. Pedersen, H. Nolte, and V. Backer, *Allergy*, 2007, **62**(9), 1033–7.
3. M. Quan, T.B. Casale, M.S. Blaiss, *Clin Cornerstone*, 2009, **9**(3), 54–60.

# MORPHO-VIDEO ENDOSCOPIC IMAGES IN DIAGNOSTICS OF AN EARLY CARCINOMA OF THE STOMACH

**N. Mitrakova[1], M. Gremyakina[2], V. Nefedov[1], A. Rozhentsov[2], and A. Mitrakov[3]**

[1] Republican Clinical Hospital, Yoshkar-Ola, Russia
endomitrakova@mail.ru
[2] Volga State University of Technology, Yoshkar-Ola, Russia
[3] Nizhny Novgorod Regional Clinical Oncological Center, Nizhny Novgorod, Russia

Oncologic diseases are among the main causes of high mortality rate all over the world. The identification of early forms of cancer of the upper parts of digestive tract, most accessible for visualization is very difficult for the majority of endoscopists. The standard research in white light is capable of diagnosing only mucosa pathology and early carcinoma of the stomach. Modern endoscopic devices with high resolution, possibility of magnification and spectral endoscopy allow to detect early forms of cancer of the upper parts of the gastrointestinal tract (GIT) with high precision. But differences in the level of resolving power of endoscopic equipment in medical institutions, and also differences in the level of training experts dictate the need for automation of processing video endoscopic images in white light.

The purpose of this work is creation of an automated system of digital processing of video endoscopic images in white light which would help the doctor to timely diagnose early forms of carcinoma of the stomach.

The main markers for detecting early carcinoma of the stomach, according to the references of the Japanese society of endoscopy, are changes of mucosa surface and its color, uneven edge and spontaneous bleeding, and also asymmetry of lesion contours. Digital processing of stomach mucosa lesion with early forms of cancer allows detecting asymmetry of lesion contours.

In the presented work performed in the period from 2011 for 2015 we analysed 6180 patients. First, every patient was subjected to standard video endoscopy in white light and then to narrow-band imaging (NBI). The pathological centers of mucous membrane were detected. For histologic verification target biopsy was performed.

The criteria of a neoplastic process in stomach mucosa, according to the Japanese society of endoscopy, are discolorations and existence of irregular vascular patterns, sharpness of lesion borders, asymmetry of the contour of lesion center (the so-called "Magic cross"). To avoid subjective diagnostics, we used the methods based on contour analysis of neoplasm images. There are two stages of quantitative assessment of signs:

1. Segmentation of the image for allocating areas corresponding to neoplasm, its localization and allocation of neoplasm contour.
2. Calculation of the characteristics of the contour related to diagnostic signs.

After allocation of the neoplasm contour we quantitatively assessed the diagnostic signs by the degree of symmetry of neoplasm shape, full information about which is contained within its contour. After geometrical transformations it becomes clear that the contours of malignant neoplasms have symmetry coefficient, and contours of benign neoplasms. This allows drawing a conclusion on a possibility of automated differentiation of neoplasms by analysing their shape.

Thus, our work has shown that precancerous changes of mucosa, serious dysplasia and early carcinoma of the stomach constitute a considerable part of the total number of detected pathology of the upper parts of GIT. Assessment of the endoscopic picture asymmetry of lesion contours of stomach mucosa will allow to unify digital processing of video endoscopic images and will enable the endoscopist to improve detectability of early forms of cancer of the upper parts of GIT, thereby prolonging the patients lifetime.

# THE PALLIATIVE ROLE OF ENDOSCOPIC PDT IN INOPERABLE CANCER

**A.A. Mitrakov[1], R.S. Alieva[1], V.A. Kryazhov[1], N.N. Mitrakova[2], and S.V. Gamayunov[3]**

[1] Regional Oncology Hospital, Nizhny Novgorod, Russia
alexandr_mit@mail.ru
[2] Republican Hospital, Yoshkar-Ola, Russia
[3] Republican Clinical Oncologic Dispensary of Chuvashia, Cheboksary Russia

**Abstract.** The cancer of lungs, stomach, esophagus and larynx takes a leading position among oncological diseases. Photodynamic therapy (PDT) is an alternative method in situations of contraindications to standard treatment. In our study we demonstrate the results of endoscopic PDT as a minimal invasive palliative procedure.

The cancer of lungs, stomach, esophagus and larynx takes a leading position among oncological diseases. Photodynamic therapy (PDT) is one of the methods that can be used for treatment of localized and advanced forms of cancer [1, 2]. In some cases standard treatment like surgery, radiotherapy or chemotherapy is impossible for many reasons: poor common condition, diseases, multiple centers of tumor. An alternative method in these situations is PDT [3].

PDT of lungs, esophageal, laryngeal and gastric cancer has been implemented in the Nizhny Novgorod Regional Oncological Hospital starting from October 2012. 36 patients have undergone PDT, PDT procedure was performed 64 times. The study involved 13 patients with gastric cancer (11 with local form, 2 with advanced form), 12 patients with esophageal cancer (5 with local form, 7 with advanced form), 11 patients with lung cancer (4 with local form, 7 with advanced form), and 2 patients with laryngeal cancer. Fotoditazin with absorption peak at 662 nm was used as a photosensitizer. Photoditazin was administered in a dose of 1 mg/kg of body weight followed in 1.5–2.0 hours by endoscopic illumination by laser light at 662 nm. Depending on the type and localization of tumor, cylindrical or front irradiation configuration was used with intensity of 300 mW/cm$^2$ resulting in a dose of 150–300 J/cm$^2$. The procedures were performed under local anesthesia. Optical fiber was delivered to the tumor through the instrumental channel of gastro- or bronchoscope. After the procedure, the patients followed less-light regimen during two days. The results were assessed on the basis of endoscopic image, mortality, morbidity, patient satisfaction with treatment, symptom relief and survival.

The observation period for gastric cancer patients ranged from 4 to 28 months, 10 of them are alive, 3 died. One patient with localized form died because of lung cancer, two patients with advanced form died in 13 and 21 months after PDT. The observation period for esophageal cancer patients ranged from 2 to 12 months, 4 patients are alive, 8 died. One patient with localized form died because of laryngeal cancer, 7 patients with advanced form died in 2, 3, 6, 5, 8, 11 and 12 months after PDT. The period of observation for lung cancer patients group ranged from 2 to 19 months, during which time six patients died in 4, 5, 6 and 8 months after PDT. The period of observation for laryngeal cancer patients ranged from 22 to 48 months. One of them died on the 22th month. We perform endoscopy examinations once in 2 months to control alive patients. There were no signs of stenosis and no complications caused by toxicity after PDT. In cases of tumor recanalization the quality of life became much better than before. Repeated procedures were done in cases of partial remission or stabilization of tumor.

Our results of endoscopic application of PDT showed good tolerance of this method, absence of allergic reactions and side effects. None of the patients with local form of cancer died because of primary tumor progression during the period of 28 months. In cases of advanced cancer the quality of life was improved and lifetime was increased after PDT compared to literature data [4]. There was a definite number of problems (the need of determining tumor thickness, more accurate light delivery, dosimetry and monitoring of the procedure) which we are working on.

## References

1. T. Yano, K. Hatogai, H. Morimoto, *et al.*, *Ann Transl Med*, 2014, **2**(3), 11.
2. C.B. Simone and K.A. Cengel, *Seminars in oncology*, 2014, **41**(6), 820–830.
3. Tetsuya, H. Fukui, M. Fujita, *et al.*, *Gastrointestinal Endoscopy*, 2000, **51**(4), AB258.
4. M.J. Aarts, B.E. van den Borne, B. Biesma, *et al.*, *Int J Cancer*, 2015, **136**(5), E387–95.

# NOVEL APPROACH TO ENDOMETRIUM EVALUATION IN PATIENTS WITH CHRONIC ENDOMETRITIS USING OPTICAL COHERENCE TOMOGRAPHY

**T.M. Motovilova[1], N.M. Shakhova[2], K.I. Chikalova[1], O.A. Kondratieva[3], S.S. Kuznetsov[1], O.V. Kachalina[1], P.A. Shilyagin[2], and M.Yu. Kirillin[2]**

[1] Nizhny Novgorod State Medical Academy, 603000, Minin Sq., 10/1, Nizhny Novgorod, Russia
tmshka@mail.ru
[2] Institute of Applied Physics RAS, Nizhny Novgorod, Russia
[3] N.I. Lobachevsky State University of Nizhny Novgorod, Nizhny Novgorod, Russia

**Abstract** Sclerosis in endometrium stroma and nearby vessels is a common indicator of chronic endometritis. However, hysteroscopy allows revealing chronic endometritis only in 35% of cases. The perspectives of optical coherence tomography (OCT) in diagnosing and grading endometritis in female patients with infertility have been studied. OCT is shown to increase the diagnostic accuracy of the endoscopic inspection and in particular cases to allow avoiding biopsy.

Disorders in female fertility are often caused by chronic inflammatory processes within uterus [1]. Hysteroscopy and morphological tissue examination are the gold standard in evaluation of endometrium. Sclerosis in endometrium stroma and nearby vessels is a common indicator of chronic endometritis. However, being based on macroscopic examination hysteroscopy allows revealing chronic endometritis in only 35% of cases while morphological examination is invasive and induces endometrium traumatism in the course of biopsy [2]. In this connection the potential of non-invasive diagnostic techniques as alternatives to standard approaches is of high importance to clinicians. In this study we investigate the perspectives of optical coherence tomography (OCT) in diagnosing and grading endometritis in female patients with infertility.

23 patients of reproductive age with fertility disorders were enrolled in the study, including 18 patients with confirmed chronic endometritis and 5 patients without confirmed pathology of endometrium. OCT inspection of endometrium was performed in the course of routine hysteroscopy procedure. The OCT-1300U device (IAP RAS, Biomedtech Ltd., Nizhny Novgorod, Russia) equipped with an endoscopic probe was employed. After the OCT hysteroscopy inspection an endometrium biopsy was performed followed by comparison of optical diagnostics and morphologic data. Sclerosis of endometrium was chosen as the most reliable imaging feature. A total of 48 OCT-images of the regions of interest were obtained.

An approach to numerical processing of the diagnostic OCT-images based on histogram analysis was developed allowing quantifying the grade of sclerosis in accordance with 5-level scale. Comparison of the OCT data and results of morphological analysis revealed that the presence of sclerosis significantly increases optical backscattering in the tissue resulting in a high level of the OCT-signal. A good agreement between sclerosis grade evaluation by independent specialists and the score obtained as a result of numerical processing is demonstrated. The diagnosis based on OCT data is confirmed by histology results. An advancement of OCT setup for optimal endometrium imaging is proposed.

To conclude, in this study the potential of OCT for evaluating endometrium condition in the course of OCT hysteroscopy is demonstrated. OCT is shown to increase the diagnostic accuracy of the endoscopic inspection and in particular cases to allow avoiding biopsy.

**Acknowledgements**

The study is supported by the RFBR (project #15-42-02572).

**References**

1. K. Kitaya, H. Matsubayashi, K. Yamaguchi, *et al.*, *Am J Reprod Immunol.*, 2016, **75**(1), 13–22.
2. H.J. Park, Y.S. Kim, T.K. Yoon, and W.S. Lee, *Clinical and Experimental Reproductive Medicine*, 2016, **43**(4), 185–192.

# TISSUE IMAGING WITH MUELLER POLARIMETRY FOR CANCER DETECTION

**T. Novikova[1], M. Kupinski[2], J. Rehbinder[1], S. Deby[1], A. Pierangelo[1], F. Moreau[1], B. Teig[3], and A. Nazac[4,5]**

[1] LPICM, CNRS, Ecole polytechnique, Palaiseau, France, tatiana.novikova@polytechnique.edu
[2] College of Optical Science, University of Arizona, Tucson, USA
[3] Department of anatomopathology, University Hospital of Bicêtre, Le Kremlin-Bicêtre, France
[4] Department of gynecology and obstetrics, University Hospital of Bicêtre, Le Kremlin-Bicêtre, France
[5] Brugmann University Hospital, Brussels, Belgium

**Abstract.** Due to the population growth and aging the cancer cases worldwide increased by 33% in the last decade (2005–2015). Cancer mortality is the second largest worldwide after cardiovascular diseases [1]. Early detection of cancer may significantly increase the survival rate and quality of patient life. We explore the potential of Mueller multi-wavelength wide-field imaging system to increase the contrast between imaged cancerous and non-cancerous zones and become a non-invasive technique for optical biopsy of tissue. The results of the studies of colon and cervical tissues will be presented, discussed and compared to the gold standard diagnosis of pathologist.

Current practice of cancer diagnosis implies an interaction of clinician (screening, biopsies if necessary) and pathologist (preparing and analyzing the histological cuts). This process may be quite long (up to several weeks) and strongly dependent on the expertise of both medical doctors because of a low contract between tumor and healthy tissue at the early stage of disease. Hence, there is an unmet need of the development of the fast, efficient and reliable methods of early cancer diagnosis.

It was demonstrated that precancerous modifications of epithelium, being invisible by naked eye, noticeably alter the optical properties of the tissue. The increase of light absorption is attributed to the increased vascularization and stromal angiogenesis, the decrease of light scattering is linked to the destruction of collagen matrix of underlying connective tissue [2]. Apart from scattering properties the presence of ordered stromal collagen in healthy connective tissue manifests itself via tissue optical anisotropy, which is broken even at early malignant transformations of epithelium.

We suggest that tissue birefringence may be measured with polarized light and exploited as an optical marker of cancer. For this purpose we use a wide-field Mueller imaging system [3] because Mueller polarimetry is the most complete optical technique for the measurements of both depolarizing and polarimetric properties of any sample. The multi-wavelength polarimetric measurements of cervical [4, 5] and colon [6] specimens and demonstrated the enhancement of contrast between cancerous and non-cancerous zones on Mueller matrix images. The Monte Carlo modeling [7] provides the insights on the origins of the observed polarimetric contrasts. The work on an efficient statistical algorithm for a binary segmentation of images [8] will help to choose the optimal combination of measurement wavelength and polarimetric parameters in order to increase the sensitivity and specificity of optical polarimetric Mueller imaging technique for cancer detection.

### Acknowledgements

This study was supported by funding from INCa (Institut National du Cancer) and Canceropole under Contract No. 2012-GYN-01-EP-1 and ANR project "TWIST4NET". One of the authors (M.K.) acknowledges the funding by "Jean d'Alembert" fellowship program Idex Paris-Saclay, France.

### References

1. C. Fitzmaurice *et al.*, *JAMA Oncol.*, December 2016, **3**,. doi:10.1001/jamaoncol.2016.5688.
2. I. Pavlova *et al.*, *Photochemistry and Photobiology*, 2003, **77**(5): 550–555.
3. T. Novikova *et al.*, *Biomedical Optics*, 2016, OSA Technical Digest, https://doi.org/10.1364/TRANSLATIONAL.2016.TTh3B.2.
4. A. Pierangelo *et al.*, *Opt. Express*, 2013, **21**(12), 14120–14130.
5. J. Rehbinder *et al.*, *J. Biomed. Opt.*, 2016, **21**(7), 071113(1–8).
6. T. Novikova *et al.*, *Optics and Photonics News OSA*, October 2012, 26–32.
7. T. Novikova *et al.*, *Appl. Phys. Lett.*, 2013, **102**, 241103–241107.
8. M.K. Kupinski and E. Clarkson, *J. Opt. Soc. Am. A*, 2015 **32**, 549–565.

# NONINVASIVE EVALUATION OF METABOLISM AND BLOOD SUPPLY IN BREAST CANCER POLYCHEMOTHERAPY

**M.V. Pavlov[1], P.V. Subochev[3], T.I. Kalganova[2], G.Yu. Golubyatnikov[3], V.I. Plekhanov[3], O.E. Ilyinskaya[1], A.G. Orlova[3], N.M. Shakhova[3], and A.V. Maslennikova[2,4]**

[1] Regional Oncological Hospital, Nizhny Novgorod, Russia
[2] State Medical Academy, Nizhny Novgorod, Russia
[3] Institute of Applied Physics RAS, Nizhny Novgorod, Russia
[4] Lobachevsky State University, Nizhny Novgorod, Russia

**Abstract.** Modern approaches to breast cancer treatment suggest assessment not only of structural but also metabolic changes of tumor tissue in the course of neoadjuvant chemotherapy. In our study, the dynamics of tumor oxygenation was determined by optical diffuse spectroscopy imaging (DOSI); ultrasound investigation (USI) in power Doppler mode was used to determine blood flow dynamics. Changes of these indicators were compared with pathologic tumor response. Dynamics of tumor oxygenation and changes in the number of vessels during chemotherapy demonstrated various changes depending on the tumor response to treatment.

Breast cancer is the most common form of malignant tumor in women and the morbidity continues to increase. Due to the extensive use of neoadjuvant chemotherapy (NACT), it is important to find criteria to predict the sensitivity of breast cancer to drug exposure. Important criteria which reflect changes in the neoplasms metabolism are oxygenation level and vasculature features [1, 2]. The goal of the study was complex evaluation of the dynamics of tumor oxygen state (by Diffuse Optical Spectroscopy, DOS) and tumor vasculature (by Ultrasound Investigation, USI) during NACT in patients with breast cancer.

Fifty-two patients with stage II-IV breast cancer were included in the study. The DOSI and USI changes and degree of tumor response were compared in 20 patients. Thirty-two patients continue chemotherapy now. DOSI and USI were performed before the start of treatment and before the second cycle of NACT. After completion of NACT the patients underwent surgery with the following pathological determination of the tumor response. Tumor oxygenation level was determined using the optical diffuse spectroscopy setup (IAP RAS, Nizhny Novgorod, Russia) [3]. Dynamics of tumor vasculature in the course of NACT was studied by the "Medison Accuvix-V20" setup using multifrequency linear sensor in power Doppler mode. The degree of tumor response was determined according to Miller and Payne.

Breast tumors demonstrated different changes of tumor oxygenation depending on the degree of tumor response. We observed the increase of tumor oxygenation in five of six patients with grade 4 and 5 of tumor response. Variable changes of the oxygenation level were mentioned in the patients with the third degree of tumor response. Tumor oxygenation decreased or was unchanged in case of one or two degrees of tumor response in seven out of eight patients. Dynamics of tumor vascularization did not demonstrate any correlation between this indicator and tumor response.

DOSI confirmed that tumor oxygenation after the first course of NACT was improved in the majority of patients responding to treatment. The results confirmed that the main source of tumor tissue reoxygenation under the influence of antitumor treatment is the decrease of the number of viable tumor cells and corresponding decrease of tumor oxygen demand. The reaction of tumor blood flow detected by USI in power Doppler mode seems to play a less significant role in the changes of oxygen state parameters in early time after beginning of chemotherapy.

### Acknowledgements

The authors thank the Russian Foundation for Basic Research (grants #15-42-02528 and #15-29-04884) for the financial support and the staff of the Nizhny Novgorod Oncology Center for making this study possible.

### References

1. A. Kumar, V. Srivastava, S. Singh, and R.C. Shukla, *Future Oncology,* 2010, **6**(8), 1265–78.
2. Q. Zhu, S.H. Kurtzman, P. Hegde, *Neoplasia,* 2005, **7**(3), 263–70.
3. A.G. Orlova, I.V. Turchin, V.I. Plehanov *et al.*, *Laser Physics Letters,* 2008, **5**(4), 321–27.

# THE FIRST CLINICAL EXPERIENCE OF PHOTODYNAMIC THERAPY OF PHARYNX INFLAMMATORY DISEASES

**D. Sapunov**[1], **A. Meller**[1,2], **M. Shakhova**[1,2], **A. Shakhov**[1], and **M. Kirillin**[2]

[1] Nizhniy Novgorod State Medical Academy, N. Novgorod, Russia
sapunow.nn@gmail.ru
[2] Institute of Applied Physics RAS, Nizhny Novgorod, Russia

**Abstract.** The first results of antimicrobial photodynamic therapy (PDT) of chronic pharynx inflammatory diseases (acute and chronic pharyngitis, chronic tonsillitis, 45 patients) are reported. At the diagnostic stage of the study, all patients underwent microbiological examination and PCR diagnostics of the mucosal detachable samples from posterior pharyngeal wall and palatine tonsils. PDT was performed with a local application of a photosensitizer of the chlorine series. The laser irradiation was performed at a wavelength of 405 nm. The efficacy of treatment was assessed based on patient complaints, pharyngoscopy data and control of microbiological examination.

Inflammatory diseases of the pharynx are highly prevalent and have a significant negative impact on the quality of human life [1]. Treatment that does not account for the etiologic factor or performed under microorganism resistance to a drug leads to the chronization of the process [2]. Microbiological examination is time-consuming leading to delayed treatment. Photodynamic therapy (PDT) has a nonspecific antimicrobial effect, including an impact on resistant microorganisms [3–5].

The aim of this study is to evaluate the efficacy of PDT in inflammatory pharynx diseases of different etiology.

The study involved 45 patients (25 females, 20 males) with chronic inflammatory diseases of pharynx. All patients underwent a microbiological study before the treatment to determine the etiology of the disease. The PDT procedure was performed in the course of standard pharyngoscopy using a local chlorine series photosensitizer (PS) Revixan (Russia). The laser action was performed at a wavelength of 405 nm with power of 0.5 W resulting in a dose of 50 J/cm$^2$. Each patient underwent 3 to 5 PDT procedures. The effectiveness of treatment was assessed by subjective (complaints) and objective (pharyngoscopy and microbiological examination) data.

Diverse bacteria were revealed in the group of examined patients: *St.haemolyticus*, *St.aureus*, *Str.pyogenes*, *Escherichia coli* and others less common. No correlation of etiological factors with severe clinical manifestations, frequent exacerbations and treatment efficacy was revealed so far. No complications or side effects were observed in the course of treatment. The PDT procedure was well tolerated by patients, pain relief was not required, however, complaints of discomfort when applying FS to the pharynx mucosa were registered. After the PDT course, all patients noted improvement in their well-being and pharyngoscopy revealed suppression of inflammatory phenomena. In some cases, hypervascularization of the mucosa was detected. According to the results of control microbiological studies after PDT, no pathogenic flora was detected, however, in several cases, activation of saprophytic flora was revealed.

Further studies are required for evaluation of treatment long-term effects. The study of morphofunctional reactions of pharynx mucosa to PDT will contribute to the development of optimal PDT protocols. Further optimization of FS application technique is also required.

### Acknowledgements

The study is supported by the Russian Science Foundation (grant #17-15-01264).

### References

1. T. Dai, Y.-Y. Huang, and M.R. Hamblin, *Photodiagnosis Photodyn Ther.*, 2009, **6**(3–4), 170–188.
2. M.R. Hamblin and T. Hasana, *Photochem Photobiol Sci.*, 2004, **3**(5), 436–450.
3. G.B. Kharkwal, S.K. Sharma, Y.-Y. Huang, T. Dai, and M.R. Hamblin. *Lasers Surg Med.*, 2011, **43**(7), 755–767.
4. T. Dai, G.P. Tegos, T. Zhiyentayev, E. Mylonakis, and M.R. Hamblin, *Lasers Surg Med.*, 2010, **42**(1), 38.
5. F. Cieplik, A. Pummer, J. Regensburger, K.-A. Hiller, A. Späth, L. Tabenski, W. Buchalla, and T. Maisch, *Front Microbiol.*, 2015, **6**, 706.

# OPTICAL MONITORING FOR PERSONALIZATION OF ENT DISEASES TREATMENT

**M. Shakhova[1,2], A. Meller[1,2], D. Sapunov[2], A. Novozhilov[2,3], A. Shakhov[2], and M. Kirillin[1]**

[1] Institute of Applied Physics RAS, Nizhny Novgorod, Russia, maha-shakh@yandex.ru
[2] Nizhny Novgorod State Medical Academy, Nizhny Novgorod, Russia,
[3] Volga District Medical Centre, Nizhny Novgorod, Russia

**Abstract.** To personalize management of patients with chronic ENT pathologies at diagnosis and treatment stages optical coherence tomography (OCT) was employed. OCT manifestations of different forms of chronic rhinitis, pharyngitis, and otitis were revealed. OCT is demonstrated to be an efficient tool for detecting alterations in nasal mucosa after drug treatment. When employing physical treatment techniques (cryotherapy and photodynamic therapy (PDT)) the OCT monitoring allowed correcting the treatment protocol in accordance with individual reaction to treatment. OCT diagnostics data was employed for individual planning of otitis treatment. For minimization of cosmetic complications of PDT of skin cancer localized at the most vulnerable areas of the ENT organs (nose wing and auricle) the OCT was used to study individual morphological features.

Treatment personalization is a modern trend in medicine. To implement personalized medicine (PM), bioimaging techniques are used to accurately diagnose, plan and monitor treatment, and to analyze each individual clinical case [1]. Optical coherence tomography (OCT) [2] is a modern imaging modality actively introduced in otorhinolaryngology in recent years [3, 4].

The aim of this work is to demonstrate the efficiency of OCT monitoring application for personalization of treatment of various ENT pathologies.

A total of 150 patients with chronic inflammatory diseases of ENT were enrolled in the study. The diagnostic stage of the study included OCT-rhinoscopy (85 cases), OCT-rhinoscopy combined with adrenalin test (local application of 0.1% adrenalin solution, 20 cases), OCT-pharyngoscopy (45 cases), OCT-otoscopy (20 cases). The treatment stage included OCT monitoring of photodynamic therapy (PDT) (photosensitizer "Revixan", 50 J/cm$^2$ at $\lambda$ = 405 nm, 17 cases) and cryotherapy (contact application of liquid nitrogen at –176 °C, 20 cases). The "OCT-1300U" device operating at central wavelength of 1280 nm with spatial resolution of 15–20 μm, image acquisition rate of 8 fps, probing depth of 1.4 mm, and the probe diameter of 2.4 mm was employed. The morphological features of skin of nasal wings and auricle were studied by OCT in 20 healthy volunteers.

OCT features of various morphological types of chronic rhinitis (hypertrophic and atrophic) as well as OCT features of chronic pharyngitis were revealed. Typical alterations of the tympanic membrane in OCT images were the basis for determining indications for surgical treatment. In the course of the OCT monitoring of different treatment procedures, the possibility of an objective real-time monitoring of changes was demonstrated. Analysis of the OCT images of the skin of the nasal wings and auricle from different patients demonstrated that individual characteristics are clearly traced, while common features are still preserved.

On the one hand, OCT manifestations of inflammatory diseases of different ENT organs are similar but, on the other hand, they are specific to morphologic types of inflammatory pathologies. OCT monitoring of treatment procedures allows real-time evaluation of treatment efficiency and timely treatment protocol correction. Application of OCT can contribute to the absolute personification of treatment tactics, however, further studies are required. The specificity and difficulty of OCT research in the ENT are related to unavailability of morphological verification for the interpretation of OCT images, since a biopsy is not indicated in case of benign ENT pathology.

### Acknowledgements

The study is supported by the Russian Science Foundation (grant #17-15-01264).

### References

1. European Society of Radiology (ESR), *Insights Imaging,* 2015, **6**(2), 141–55.
2. S. Andersson-Engels, P.E. Andersen, *J. Biomed. Opt.*, 2012, **17**(7), 071301.
3. Kibeom Park *et al.*, *Appl. Opt.*, 2017, **56**, D115–D119.
4. B.J.-F. Wong and J. Ligner, *Biomedical Optics in Otorhinolaryngology*, Springer, 2016, 529–623 (637 P).

# DEVELOPMENTS OF 2µM-LASER APPLICATIONS FOR CLINICAL USE

**R. Sroka**[1,2]

[1] Laser-Forschungslabor, LIFE-Center, Hospital of University, LMU-Munich, Germany
ronald.sroka@med.lmu.de
[2] Department of Urology, Hospital of University, LMU-Munich, Germany

**Abstract.** Based on lab-investigation and specified parameters, lasers emitting in the spectral range of 2 µm could be translated into different clinical applications for the envisioned clinical usage. Laser emitting at this wavelength range showed a lot of improvements and achievements in clinical routine of a variety of medical disciplines.

Pre-requisit for all clinical applications is the intense and careful investigation of the envisioned clinical application in laboratory environment. Based on that suitable laser parameter can be derived. Furthermore application devices can be developed and adopted for specific application purposes. Prior to clinical use the medical doctor in charge should be trained in the lab with regard to handling the laser system, to become aware of the in-situ laser-tissue interaction and finally in specific handling manoeuvres. In addition laser safety requirements should be trained with the personal in the laser OR. After approval of the local ethical committee first clinical application are allowed to perform under secured conditions.

With the aim of tissue reduction to achieve improvement in breathing, Ho:YAG as well as Tm-fiber laser assisted coagulation of hyperplastic nasal turbinates were performed [1]. In phlebology the Tm-fiber laser was used for endoluminal destruction of varicose veins [2]. In comparison to standard Nd:YAG laser therapy the advantages of using Tm-fiber laser assisted ablation for removal of endobronchial stents are shown [3]. In urology the 2µm-laser in pulsed manner were used for improvements in lithotripsy [4–6]. In addition to that benign prostate enucleation is in clinical routine using the Ho:YAG-laser and nowadays also using the Tm-laser emission [7]. Additionally laparoscopic laser assisted resection of kidney tumors could be performed.

In conclusion lasers emitting in the 2 µm wavelength range showed advantages of several other surgery treatments thus becoming more popular in clinical use.

## References

1. R. Sroka, P. Janda, T. Killian, F. Vaz, C.S. Betz, and A. Leunig, *Lasers Surg Med.*, 2007 Apr, **39**(4), 324–31.
2. R. Sroka, K. Weick, M. Sadeghi-Azandaryani, B. Steckmeier, and C.G. Schmedt, *J Biophotonics*, 2010 Jun, **3**(5–6), 269–76. doi: 10.1002/jbio.200900097.
3. W. Gesierich, F. Reichenberger, A. Fertl, K. Haeussinger, and R. Sroka, *J. Thorac Cardiovasc Surg.*, 2014 Jun, **147**(6), 1827–32. doi: 10.1016/j.jtcvs.2013.12.038. Epub 2014 Jan 15.
4. R. Sroka, T. Pongratz, G. Scheib, W. Khoder, C.G. Stief, T. Herrmann, U. Nagele, and M.J. Bader, *World J. Urol.*, 2015 Apr, **33**(4), 479–85.
5. M.J. Bader, T. Pongratz, W. Khoder, C.G. Stief, T. Herrmann, U. Nagele, and R. Sroka, *World J. Urol.*, 2015 Apr, **33**(4), 471–7.
6. B. Lange, D. Jocham, R. Brinkmann, and J. Cordes, *Lasers Surg Med.*, 2016 Nov, **12**, doi: 10.1002/lsm.22611.
7. C. Netsch, C. Magno, S. Butticè, L. Macchione, G. Mucciardi, T.R. Herrmann, and A.J. Gross, *Urol. Int.*, 2016, **96**(4), 421–6.
8. W.Y. Khoder, R. Sroka, S. Siegert, C.G. Stief, and A.J. Becker, *World J. Urol.*, 2012 Oct, **30**(5), 633–8.

# OPTICAL SPECTROSCOPY FOR THE DETECTION OF BRAIN TUMOR AND BLOOD VESSELS TO ENHANCE ACCURACY AND SAFETY OF STEREOTACTIC BRAIN TUMOR BIOPSY

**H. Stepp[1,2], N. Markwardt[1,2], A. Rühm[1,2], M. Goetz[3], P. Zelenkov[4], V. Loschenov[5], P. Grachev[5], and R. Sroka[1,2]**

[1] LIFE-Center, Klinikum der Universität München, Munich, Germany, herbert.stepp@med.lmu.de
[2] Dept. of Urology, Klinikum der Universität München, Munich, Germany
[3] MRC Systems GmbH, Heidelberg, Germany
[4] Burdenko Neurosurgical Institute, Moscow, Russia
[5] General Physics Institute, RAS, Moscow, Russia

**Abstract.** Objective: Increase accuracy and safety of brain tumor biopsy. Improved accuracy may be achieved by fiberoptic detection of protoporphyrin IX fluorescence. Fiberoptic recognition of blood vessels by remission spectroscopy promises to increase safety. To these ends, 3 or 4 optical fibers with outer diameters of 240 µm were integrated in a standard stereotactic biopsy needle. Fluorescence of protoporphyrin IX is preferentially excited with 635 nm. For detection of blood vessels, light transmitted between two fiber tips, separated by approx. 2 mm, was analyzed at two wavelengths with very different blood absorption, 578 nm and 650 nm, respectively.

## Introduction

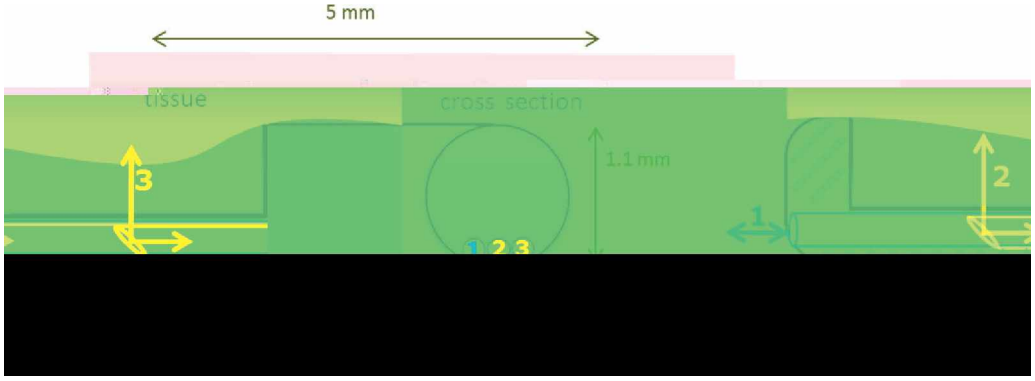
A fiber-based device for stereotactic brain tumor biopsies is developed. 5-ALA-induced protoporphyrin IX (PpIX) fluorescence is used to localize vital tumor tissue; the spectral analysis of polychromatic light diffusely transmitted through the investigated tissue between two fiber tips serves to detect blood vessels and thus helps minimize the risk of inducing cerebral hemorrhages.

## Methods

For both tasks, ray tracing simulations and experiments on phantoms mimicking the optical properties of brain tumor tissue were performed. The sensitivity of PpIX-based tumor detection was investigated for two different excitation wavelengths (405 nm, 633 nm). The effect of blood interference was studied by placing artificial blood layers of 10–400 µm thickness between fiber and phantom. Blood vessel detection with a two-fiber probe (inter-fiber distance: 2 mm) was experimentally tested by using a blood vessel dummy, which was submerged into the tumor-mimicking phantom. The remitted light was analyzed at two wavelengths with strongly differing hemoglobin absorption (578 nm, 650 nm).

## Results and Discussion

In general, 405-nm-excitation shows a 50-fold higher sensitivity, but physiological PpIX concentrations of a few µM should be well detectable with both wavelengths. In addition, 633-nm-excitation is considerably superior in case of blood-covered tumor tissue. For instance, a 50 µm blood layer blocks the 405-nm-excited fluorescence completely, but reduces the 633-nm-excited signal by less than 50%. Depending on their orientation, blood vessels are detectable up to 800–1200 µm ahead of the probe on the basis of a considerably reduced remission ratio $I_{578}$ / $I_{650}$ as compared to the background value. The implementation into a conventional biopsy needle is proposed.



# PREVENTION OF INFLAMMATORY COMPLICATIONS OF LASER LITHOTRIPSY

**O.S. Streltsova[1], D.P. Pochtin[2], I.D. Eranov[3], R.I. Kositsyin[3], V.I. Bredichin[3], O.L. Antipov[3], and V.A. Kamensky[3]**

[1] Nizhny Novgorod State Medical Academy, 10/1 Minin Square, Nizhny Novgorod, 603005, Russia, e-mail: strelzova_uro@ mail.ru
[2] Nizhny Novgorod Regional Hospital, Nizhny Novgorod, Russia
[3] Institute of Applied Physics RAS, Nizhny Novgorod, Russia

**Abstract.** Development of infectious and inflammatory processes in the kidney is one of common complications of lithotripsy. The study of different regimes of laser action on kidney stones is presented. It is demonstrated that laser exposure at a wavelength of 2000–2100 nm with a small pulse energy (from units to tens of mJ) and pulse duration of 20–50 ns at a high pulse repetition rate (tens of kHz) allows controlled destruction of concrements into large fragments without disseminating their content. The use of strongly absorbing coatings (SAC) of the laser fiber tip also provides controlled destruction and allows achieving an antimicrobial effect on the stone-associated biofilms. The presented approaches can ensure prevention of microbial dissemination in the course of contact lithotripsy.

**Introduction.** One of contact laser lithotripsy complications is the development of infectious inflammatory processes in the kidney due to bacteria dissemination from biofilm [1]. One of the options for dissemination prevention consists in the use of laser exposure regimes that provide controlled destruction of concrements without spreading microbial contents of stone-associated biofilms. The aim of this work is to demonstrate two options of laser action to provide controlled destruction.

**Materials and methods.** A total of 52 postoperative samples of renal concrements varying from 10 to 19 mm in size with different densities (127–1933 HU) were used as objects. Lithotripsy was performed with various types of lasers. Original laser systems (IAP RAS, Nizhny Novgorod) were used: a laser on an Ho: YAG crystal pumped by radiation from a thulium fiber laser [2] and a laser on Tm: Lu2O3 ceramics pumped by an erbium-fiber laser with a Raman wavelength shift (at 1670 nm) [3]. To implement the SAC technology, a 970 nm diode laser with tip initiation (with power of 10 W) was used [4].

**Results.** The fragmentation effect with a controlled fault was obtained in 9 cases out of 10 using a laser at a wavelength of 2097 nm at repetition rates of 10 and 30 kHz with pulse energy from 0.17 to 2.3 mJ. The concrement perforation time varied from 2 to 600 seconds, depending on the density and chemical composition of the stone. Exposure at the wavelength of 1967 nm at a repetition rate of 15 kHz with pulse energy of 0.4–0.6 mJ appeared to be ineffective in 7 cases out of 10. Employment of the SAC technology also proved to be effective for controlled fragmentation of concrements. The fragmentation time varied from 30 seconds to several minutes, depending on the density of the stone. The high temperature (2000 K) provided an antimicrobial effect on the stone-associated biofilms.

**Conclusion.** The reported regimes of kidney concrements fragmentation are perspective for prevention of infectious inflammatory complications of laser lithotripsy.

**Acknowledgements**

The work is supported by the RFBR (project No. 15-42-02654) and RSF (grant No.14-15-00840).

**References**

1. L. Didenko, E. Tolordava, T. Perpanova *et al.*, *Journal of Applied Medical Sciences,* 2014, **3**(4), 19–34.
2. O.L Antipov, I.D. Eranov, R.I. Kositsyin, *LaserPhys. Lett.,* 2017, **14**(1), 015002.
3. O. Antipov, A. Novikov, S. Larin, and I. Obronov, *Optics Letters*, 2016, **41**(10), 2298–2301.
4. N. Sapogova, V. Bredikhin, N. Bityurin *et al.*, *Biomedical Optics Express*, 2016, **8**(1), 104–111.

# LASER SCANNING MICROSCOPY STUDY OF THE BLADDER EXTRACELLULAR MATRIX AFTER RADIATION THERAPY

**O.S. Streltsova[1], V.V. Dudenkova[2], M.V. Kochueva[1], E.A. Tararova[3], D.K. Malikov[4], A.S. Vorobieva[4], E.B. Kiseleva[1], K.E. Yunusova[1], V.N. Krupin[1], and A.V. Maslennikova[1]**

[1] Nizhny Novgorod State Medical Academy, 10/1 Minin Square, Nizhny Novgorod, 603005, Russia
e-mail: strelzova_uro@ mail.ru
[2] Lobachevsky State University, Nizhny Novgorod, Russia
[3] Nizhny Novgorod Regional Oncologic Hospital, Nizhny Novgorod, Russia
[4] Nizhny Novgorod Regional Hospital, Nizhny Novgorod, Russia

**Abstract.** The results of inspection of the bladder extracellular matrix state in 75 patients with complications after radiotherapy are reported. Imaging of biopsy bladder samples is performed by laser scanning microscopy (LSM) in second harmonic generation (SHG) and two-photon autofluorescence excitation (TPEF) modes to study the state of collagen and elastin. Radiation damage is studied in comparison with bladder alterations in patients with chronic cystitis (80 patients). Verification of LSM data is performed by comparison with histology analysis. As a result, the difference in the state of collagen and elastin structures is demonstrated for different grades of bladder radiation damage. The obtained results can become a basis for the technique for diagnostics of bladder radiation damage.

Despite the development of techniques for conform irradiation, alterations in normal tissues induced by radiation therapy of malignant tumors is one of the actual problems of modern radiation oncology [1]. For understanding of the radiation damage of unaltered collateral tissues it is important to know the state of extracellular matrix of connective tissue [2]. In recent years the potential of nonlinear microscopy in second harmonic generation (SHG) and two-photon autofluorescence excitation (TPEF) modes to study the state of collagen and elastin was demonstrated [3].

The aim of this paper is to study the features of the state of extracellular matrix of the urinary bladder after radiotherapy by means of nonlinear microscopy.

Two groups of female patients were enrolled in the study: a group of patient with radiation cystitis with a period between 1 and 11 years after the exposure (75 patients); and a group of patients with chronic cystitis of bacterial etiology with a history of more than 3 years (80 patients). Cystoscopy and biopsy of bladder were performed in accordance with a standard protocol with standard equipment. Study of connective tissue state was conducted with an LSM 510 META laser scanning microscopy system in the modes of second harmonic generation (SHG) and two-photon excitation autofluorescence (TPEF) to examine the state of collagen and elastin, respectively. To verify the obtained images histological investigations with H&E, van Gieson, and picrosirius red staining were conducted.

It is demonstrated that collagen fibers in unaltered bladder are clearly visualized, have a crimp shape, are loosely located and accompanied by elastic fibers. In case of radiation cystitis the inflammatory reactions and tissue fibrosis are similar to those for chronic cystitis, however, are more pronounced. Moreover, nonlinear microscopy revealed a difference in the state of collagen and elastin structures at the bladder radiation damage of different grade.

The obtained results can become a basis for the technique for diagnostics of bladder radiation damage.

### Acknowledgements

The authors thank the Russian Foundation for Basic Research (RFBR grant # 16-07-00655) for the financial support.

### References

1. W. Dörr, *Nuklearmedizin,* 2010, **49**(1), 53–58.
2. J. Yarnold, M.C. Brotons, *Radiother Oncol.,* 2010, **97**(1), 149–161.
3. S.S. Kuznetsov, V.V. Dudenkova, M.V. Kochueva *et al.*, *Sovr. tehnologii v medicine*, 2016, **8**(2), 31–39.

# HYPERSPECTRAL NIRS: DEVELOPMENT AND APPLICATIONS

**V.Y. Toronov[1], S. Lin[2], R. Botero[3], H. Andrade-Caicedo[3], and T.N. Nguyen[1]**

[1] Ryerson University, Toronto, Canada, toronov@ryerson.ca
[2] Keenan Research Centre, Li Ka Shing Knowledge Institute, Toronto, Canada
[3] Centro de Bioingeniería, Universidad Pontificia Bolivariana, Medellín, Colombia

**Abstract.** We present a novel portable hyperspectral system for near-infrared spectroscopy of tissue and demonstrate its suitability in several clinical applications.

## Hyperspectral and Multispectral Near-Infrared Spectroscopy

Near infrared spectroscopy (NIRS) [1] is a non-invasive technique for in-vivo real-time brain and muscle imaging. It targets tissue chromophores having specific absorption spectra in the waveband 700–1100 nm. Most of commercially available NIRS systems are multispectral (i.e. they use light sources emitting at several isolated wavelengths). Measurements by multispectral NIRS qualitatively reflect trends in changes of blood oxygenation but suffer low quantitative accuracy. In order to improve quantitative accuracy and to extend the number of detectable chromophores we developed portable hyperspectral NIRS system. hNIRS hardware includes a tungsten lamp and portable fiber-optic spectrometers. In order to maximize the use of information contained in several hundreds of measurements corresponding to different wavelengths of light we developed special hyperspectral signal processing methods including noise filtering and spectral unmixing using blind signal separation and machine learning algorithms. Our technique allows for both relative and absolute measurements of chromophore concentrations including changes in the cytochrome C oxidase redox states, thus enabling the intracellular monitoring of oxygen metabolism [2]. In our presentation we will explain details of our hNIRS methods and demonstrate their suitability in several applications.

## Applications of hNIRS

### Assessment of septic patients

Sepsis is a major health problem associated with abnormalities of muscle tissue oxygenation and microvascular function. Early detection of sepsis is critical because delay in treatment may likely result in death of a patient. Our measurements using hNIRS show that the rates of changes of the chromophore concentrations in septic patients versus health subjects during the arterial and venous occlusion protocols are statistically significantly different.

### Measurements of functional brain activity

We extend the application of hNIRS to the measurement of event-related hemodynamic and metabolic functional cerebral responses during simulated driving. We used our portable hNIRS system and a driving simulator with a fully functional steering wheel and foot pedals. Each participant performed different driving tasks and participants were distracted during various driving conditions. We found that more complex driving tasks (non-distracted) deactivate prefrontal cortex while distractions during driving significantly activate it. Measured changes in the redox state of the cytochrome C oxidase were consistent with hemodynamic changes.

### Monitoring cerebral perfusion and metabolism during cardiac surgery

Measurements were done during Transcatheter Aortic Valve Implantation surgery simultaneously by our hNIRS and cerebral oxygen saturation monitor Nonin Equinox 7600. While cerebral oxygen saturations measured by both techniques were close, redox cytochrome C oxidase changes measured by hNIRS showed significant impact of short cardiac arrests on the cerebral metabolic rate of oxygen.

## Acknowledgements

This study was supported by the St. Michael's Foundation's Translational Innovation Fund, a ZOLL Foundation grant, and by Ruta N, Medellín, Colombia.

## References

1. F. Scholkmann, *et al.*, *Neuroimage*, 2014, **85**, 6–27.
2. O. Richter and B. Ludwig, *Rev. Physiol. Biochem. Pharmacol.*, 2003, **147**, 47–74.

# *IN VIVO* MEASUREMENT OF THE TISSUE OXYGENATION BY TIME-RESOLVED LUMINESCENCE SPECTROSCOPY: STRATEGIES TO MINIMIZE ARTEFACTS ASSOCIATED WITH THE PHOTOSENSITIZATION AND PHOTOPRODUCTS

**E. Gerelli[1], V. Huntosova[1,2], D. Horvath[2], and G. Wagnieres[1]**

[1] Swiss Federal Institute of Technology (EPFL), Lausanne, Switzerland
georges.wagnieres@epfl.ch
[2] Center for Interdisciplinary Biosciences, Faculty of Science, P. J. Safarik University, Kosice, Slovakia

**Abstract.** Protoporphyrin IX (PpIX) is an interesting probe to measure $pO_2$ in tissues by time-resolved luminescence spectroscopy. However, this probe is phototoxic and generates luminescent photoproducts. Consequently, we studied their influence on the PpIX lifetime *in vivo*. We established that this influence can be avoided if the PpIX emission is detected between 630±10 nm, or if the excitation dose at 405 nm is less than 1 J/cm$^2$. We also studied *in vivo* the oxygen sensitivity and phototoxicity of dichlorotris(1,10-phenantroline)-Ruthenium(II) Hydrate (Ru(phen)), a poorly (photo)toxic probe. We established that its phototoxic threshold is hundred times larger than the fluence necessary for $pO_2$ measurements.

## Introduction

The determination of the oxygen partial pressure ($pO_2$) in real time in living biological tissues is of high interest for numerous therapeutics, including photodynamic therapy (PDT) and radiotherapy. The real-time measurement of the $pO_2$ also enables to obtain interesting information regarding the metabolic activities. The development of time-resolved luminescence measurement methods combined with the availability of new oxygen-sensitive molecular probes is at the origin of the significant progress that have been achieved during these past decades to measure the $pO_2$ in living organisms. These probes include aminolevulinic acid-induced PpIX which is an approved photosensitizer (PS). Using this probe is of high interest in PDT since the $pO_2$ is measured at the precise location where the phototoxic mechanisms take place. Interestingly, PpIX is produced in the mitochondria, an important organelle for the cells respiration. Unfortunately, PpIX has drawbacks to measure the $pO_2$, including its significant phototoxicity and photobleaching. Therefore, we established radiometric conditions that minimize these artefacts. In addition, we studied the oxygen sensitivity and phototoxicity of an interesting alternative compound, Ru(Phen), a poorly (photo)toxic probe.

## Materials and methods

We studied the influence of the PpIX photoproducts luminescence on the PpIX lifetime in solution and *in vivo* on the Chick's Chorioallantoic Membrane (CAM) model, under various oxygen (between 0 and 155 mmHg) and light (405 nm emitted by a diode laser combined with a frontal light distributor; 0–15 J/cm$^2$ or 70–160 J/cm$^2$ for *in vivo* and solution experiments, respectively) conditions. The $pO_2$ was measured by time-resolved spectroscopy of the PpIX delayed fluorescence (DF), its phosphorescence being too weak to be detected *in vivo*. These measurements were performed with the spectrometer developed by our group and described in details by Piffaretti et al. [1]. The study of the Ru(Phen) phototoxicity and $pO_2$ sensitivity was performed in the CAM with the same setups adapted to the spectral properties of this promising $pO_2$ probe (PDT doses between 0 and 10 J/cm$^2$ at 470±20 nm; wavelength to measure the oxygen sensitivity between 0 and 155 mmHg: 470 nm).

## Results and discussion

Our results indicate that perturbations induced by the PpIX photoproducts can be avoided if its luminescence is detected between 620 and 640 nm, or if PpIX is excited at 405 nm with light doses < 1 J/cm$^2$. In addition, we established that the phototoxic threshold of Ru(Phen) is about two orders of magnitude higher than the fluence necessary for $pO_2$ measurements with this oxygen probe.

## Acknowledgements

This work was founded by SCIEX-NMSch project N° 10.142, by the Swiss National Science Foundation (projects N° CR32I3_159746), and the EU 7 FP grant CELIM (project N° 316310).

## References

1. F. Piffaretti, A.M. Novello, R. Senthil Kumar, E. Forte, C. Paulou, P. Nowak-Sliwinska, H. van den Bergh, and G. Wagnières, *Journal of Biomedical Optics*, 2012, **17**(11), 115007-1-9.

# PHOTODYNAMIC THERAPY OF MALIGNANT BRAIN TUMORS

**I.A. Medyanik, M.G. Volovik, A.V. Dydykin, K.S. Yashin, S.N. Bugrov,** and **N.N. Karyakin**

Privolgzhsky Federal Medical Research Center, Nizhny Novgorod, Russia

**Abstract.** Photodynamic therapy (PDT) is a promising method for local tumor control in surgery of malignant brain tumors. Nevertheless the thermal effect in PDT is known to have no damaging action and in general oncology this side effect can be paid no particular attention, in neurosurgery even relatively slight increase of brain tissue temperature, especially in eloquent brain areas, can lead to complications. In this study we present the role of the control of the temperature of tumor bed during PDTto prevent significant postoperative brain edema

Photodynamic therapy (PDT) is a promising method for local tumor control in surgery og malignant brain tumors [1, 2]. There are several parameters that should be calculated for the success of the procedure: a tumor size or the area exposed to radiation, laser radiation power, a photosensitizer type. If less estimated time is used, no desirable anti-tumor effect is reached. In neurooncology after removing large masses, the necessary estimation exposure time may reach up to 40 min. It can lead to one of the adverse effects- hyperthermia of surrounding tissues. Nevertheless the thermal effect in PDT is known to have no damaging action and in general oncology this side effect can be paid no particular attention, in neuro-surgery even relatively slight increase of brain tissue temperature, especially in eloquent brain areas, can lead to complications [3]. PDT contributes to the perifocal edema increase in a postoperative period, that can result in an increasing of neurological deficits [4]. But up to now the search for methods aimed at alleviating PDT-induced peritumoral edema is essential.

The aim of the investigation was to assess the role of infrared imaging for brain tissue heating when exposed to laser radiation in photodynamic therapy of bed of removed tumor, and its effect on postoperative brain edema.

**Materials and methods.** We studied the results of brain tumor surgeries with intraoperative PDT of 20 patients. The patients were divided into two groups: 1 – the study group (n = 12) had intraope-rative infrared imaging (IRI)-guided PDT, and 2 – the control group patients (n = 8) had no IRI control.

**Results.** Perifocal edema in the study group on the first postoperative day decreased, and was 50.4 [16.4; 79.3] and 88.5 [30.3; 110.6]% of preoperative values according to axial and coronary section study. In the control group postoperative edema increased and was 227.9 [92.4; 303.8] and 154.7 [84.5; 150.3]% of the initial.

**Conclusion.** PDT is accompanied by temperature rise of the exposed tissues, and increased perifocal edema in an early postoperative period. IRI control of exposed tissues heating in PDT of tumor bed enables to avoid edema augmentation of surrounding brain tissues.

**Acknowledgements**

The work was supported by the Federal Target Program "Research and development in priority areas of the development of the scientific and technological complex of Russia for 2014–2020" of the Ministry of Education and Science of Russia (Project ID RFMEFI57814X0074) and by grant No.16-15-10391 from the Russian Scientific Foundation.

**References**

1. H. Kostron, "Photodynamic Diagnosis and Therapy and the Brain", in *Photodynamic Therapy: Methods and Protocols*, C.J. Gomer, Editor. 2010, Humana Press: Totowa, NJ. P. 261–280.
2. D. Bechet, S.R. Mordon, F. Guillemin, and M.A. Barberi-Heyob, "Photodynamic therapy of malignant brain tumours: A complementary approach to conventional therapies". Cancer Treatment Reviews, 2012, **40**(2), 229–241. http://dx.doi.org/10.1016/j.ctrv.2012.07.004.
3. B. Karaszewski, J.M. Wardlaw, I. Marshall, V. Cvoro, K. Wartolowska, K. Haga, P.A. Armitage, M.E. Bastin, and M.S. Dennis, "Measurement of brain temperature with magnetic resonance spectroscopy in acute ischemic stroke", *Annals of Neurology*, 2006, **60**(4), 438–446; http://dx.doi.org/10.1002/ana.20957.
4. I.A. Medyanik, N.N. Karyakin, A.V. Dydykin, "A.P.F. The first experience of photodynamic application in the complex treatment of malignant brain neoplasms", *Lazernaya meditsina*, 2012, **16**(2), 49–52.

# *EX VIVO* STUDY OF HUMAN GLIOMAS WITH CROSS-POLARIZATION OPTICAL COHERENCE TOMOGRAPHY

**K.S. Yashin [1,2], E.B. Kiseleva [2], E.V. Gubarkova [2], A.A. Moiseev [2,3], S.S. Kuznetsov [2], M.M. Karabut [2], I.A. Medyanik [1], L.Ya. Kravets [1], and N.D. Gladkova [2]**

[1] Privolzhsky Federal Medical Research Center, Nizhny Novgorod, Russia, jashinmed@gmail.com
[2] Nizhny Novgorod State Medical Academy, Nizhny Novgorod, Russia
[3] Institute of Applied Physics, Russian Academy of Sciences, Nizhny Novgorod, Russia

**Abstract.** Optical coherence tomography (OCT) is a promising method of glial tumors borders diagnostics. This paper presents the results of cross-polarization OCT (CP OCT) usage for the glial tumors and their peritumoral area visualization. CP OCT detected the scattering and polarization properties of tissues and thereby it can be more informative method for tumor borders imaging than traditional OCT.

**The study was aimed** to evaluate the capabilities of CP OCT as an imaging tool for the glial tumors detection in peritumoral area.

**Materials and Methods.** The study was performed on 30patients with gliomas (intraoperative biopsies) of different malignancy degrees: Grade I-II (n = 8), Grade III (n = 7), Grade IV (n = 15). 176 *ex vivo* human gliomas samples of tumor and non-tumor tissue were studied by CP OCT and 865 images were acquired and analyzed. Spectral domain OCT setup at 1.3 μm central wavelength with axial resolution equals to 10 μm and lateral resolution equals to 15 μm was used (Institute of Applied Physics of the Russian Academy of Sciences, Russia) [1, 2]. To verify CP OCT images they were compared with histological data.

**Results.** The correspondence between the CP OCT images of human brain tissue and glial tumors and their morphological features was determined. The OCT signal of white matter in peritumoral area is characterized by high intensity and more homogeneity in comparison with the heterogeneity signal of the tumor. These differences are more clear in the CP OCT images than in traditional OCT images. Comparative evaluation of the glial tumors (Grade I–IV) and non-cancerous brain tissue CP OCT signalswas also carried out.

**Conclusion.** The white matter of peritumoral area and glial tumors can be differentiated based on the intensity, homogeneity and attenuation of the CP OCT signals. The CP OCT seems to have great potential in the surgery of infiltrative brain tumors.

**Acknowledgements.** The study was supported by the Russian Scientific Foundation grant No.16-15-10391 and RFBR project No. 16-32-60178 mol_a_dk. The CP OCT device development was funded by the Ministry of Education and Science of the Russian Federation, grant No. 14.B25.31.0015.

## References

1. V.M. Gelikonov and G.V. Gelikonov, *Laser Phys. Lett.* **3**, 445-451 (2006).
2. L. Matveev, V. Zaitsev, G. Gelikonov, *et al., Optics letters*, **40**(7), 1472–1475 (2015).

VI International Symposium

# TOPICAL PROBLEMS OF BIOPHOTONICS




## *Biophotonics in Stem Cell Research*

# Chairs

**Igor Adameyko**
Karolinska Institutet, Sweden; Medical University of Vienna, Austria

**Boris Chichkov**
Laser Zentrum Hannover e.V., Germany

*Invited*

# SINGLE CELL TRANSCRIPTOMICS REVEALS FATE SELECTION POINTS AND EARLY HETEROGENEITY OF THE NEURAL CREST

**M. Kaucka[1], R. Soldatov[2], T. Chontorotzea[3], J. Petersen[1], M.E. Kastriti[3], N. Akkuratova[3], V. Dyachuk[4], K. Fried[4], P. Kharchenko[2], and I. Adameyko[1,3]**

[1] Center for Brain Research, Medical University Vienna, 1090 Vienna, Austria
[2] Department of Biomedical Informatics, Harvard Medical School, MA 02115 Boston, USA
[3] Department of Physiology and Pharmacology, Karolinska Institutet, 17177 Stockholm, Sweden
[4] Department of Neuroscience, Karolinska Institutet, 17177 Stockholm, Sweden
e-mail: igor.adameyko@ki.se

**Abstract.** Lately, single cell transcriptomics methods bloomed and enabled a new approach to classify the cell types as well as to analyze developmental transitions. We took advantage of single cell transcriptomics to resolve neural crest heterogeneity and fate choice mechanisms. The results of our analysis showed that fate switches operate as sequential bifurcations of choices, and that prior to the fate selection, fate-specific gene clusters are heterogeneously activated in the early delaminating and migrating neural crest populations. Indeed, neural crest cells show the existence of active and passive differentiation-related biases operating at the gene expression level.

Neural crest cells are transient embryonic progenitors that are often called 4th germ layer since they give rise to a large number of differentiated cell types in the body. Thus, neural crest is a perfect model system to address the molecular mechanisms of a fate selection in case of several fate options. Cranial and trunk neural crest cells are different in terms of their competence: only cranial crest gives rise to ectomesenchymal fates that include cartilage and bone. We took advantage of a single cell transcriptomics (SCT) approach to address fate selection in the neural crest. For this we developed a new tool for multiple differentiation trajectory analysis to investigate the positons of fate splits and molecular mechanics behind fate choice. The results of our analysis showed that fate switches operate as sequential bifurcations of choices, and that prior to the fate selection, fate-specific gene clusters are heterogeneously activated in the early delaminating and migrating neural crest populations. These early fate-specific genes represent weak biases that still may assist eventual fate restrictions. Major biases differ between trunk and cranial crest: sensory neurogenesis bias dominates trunk crest while strong mesenchymal bias is present in the cranial crest. Finally, we provide a unique gene expression signatures and gene regulatory network transitions for every neural crest subpopulation along the developmental timeline and spatial distribution.

# LABEL FREE MICROSTRUCTURAL ANALYSIS OF THE HEALTHY AND DISEASED LIVER

**N. Bobrov[1], D. Kuznetsova[2], V. Dudenkova[2], F. Kulagin[2], N. Kiselev[1,2], M. Lukina[2], V. Zagaynov[1,2], and E. Zagaynova[2]**

[1] The Volga District Medical Centre of Federal Medical and Biological Agency, Nizhny Novgorod, Russia
[2] Nizhny Novgorod State Medical Academy, Nizhny Novgorod, Russia

Liver diseases are frequently encountered in clinical practice with high morbidity and mortality. A cholestatic liver disease is one of the most common liver diseases and can potentially progress to liver cirrhosis or even cholangiocarcinoma [1, 2]. Conventional techniques are insufficient to precisely describe the complex internal structure, het erogeneous cell populations and the dynamics of biological processes of the liver [3]. Currently, the methods of optical bioimaging and microstructural analysis are being actively introduced into biomedical research. These methods are extremely informative and non-destructive, which allows studying a large number of processes occurring inside cells and tissues, analyzing molecular cellular composition, as well as evaluating the state of connective tissue fibers due to their ability to generate a second optical harmonic. Of special interest for studying hepatic tissue in normal and pathological conditions are multiphoton lasers canning microscopy LSM, fluorescence-lifetime imaging microscopy FLIM, and second harmonic generation SHG. All these methods do not need additional staining of samples or incorporation of any markers to study certain parameters (metabolism, lipid composition, microstructure analysis, evaluation of fibrous structures, in particular, collagen and elastin) which have pronounced changes in hepatocytes and their microenvironment with common pathological diseases of the liver (cholestasis, steatosis, cirrhosis). Thereby in this study we investigated metabolic changes in the healthy and cholestatic liver based on the fluorescence of the metabolic co-factors NADH and FAD. Cellular metabolism was examined by monitoring the optical redox ratio (FAD/NADH), the fluorescence lifetime contributions of the free and bound forms of NADH and FAD. Two-photon fluorescence microscopy combined with FLIM and SHG was used to analyze this fluorescence in living hepatic cells of the healthy and cholestatic liver. The data can be used to develop new criteria for identification of hepatic pathology at the level of hepatocyte changes aimed at personalized medicine in the future.

**Acknowledgements**

This work has been financially supported by the Russian Science Foundation (No. 17-75-20185).

**References**

1. H. Wang, X. Liang, Y.H. Mohammed, *et al.*, "Real-time histology in liver disease using multiphoton microscopy with fluorescence lifetime imaging", *Biomed. Opt. Express*, 2015, **6**(3), 780–792.
2. R.G. Cameron, M.G. Neuman, N. Shear, L.M. Blendis, "Multivesicular stellate cells in primary biliary cirrhosis", *Hepatology*, 1997, **26**(4), 819–822.
3. H. Wang, X. Liang, G. Gravot, *et al.*, "Visualizing liver anatomy, physiology and pharmacology using multiphoton microscopy", *J. Biophotonics*, 2017, **10**(1), 46–60.

*Invited*

# 3D VISUALISATION OF SYNOVIAL JOINTS REVEALED NOVEL PROGENITOR CELLS WHICH FORM ENTIRE ADULT ARTICULAR CARTILAGE IN MICE

**A.S. Chagin**

KarolinskaInstitutet, Stockholm, Sweden
Sechenov Moscow State Medical University, Moscow, Russia
e-mail: andrei.chagin@ki.se

**Abstract.** Articular cartilage has limited regenerative capacity. Here, we describe novel chondrocyte progenitors responsible for formation of articular cartilage. 3D visualization with micro-CT revealed quantitative dynamics of cartilage growth and reshaping. Clonal genetic tracing revealed that chondro-progenitors generate chondrocytes and facilitate cartilage reshaping. Furthermore, chondro-progenitors renew their number by symmetric division, express mesenchymal stem cell marker CD73, and generate chondrocytes via both asymmetric division and symmetric differentiation. Finally, we found that adult articular cartilage is entirely formed by the progeny of chondro-progenitors. We conclude that chondro-progenitors are postnatal stem cells capable of maintaining their own population and form adult articular cartilage.

Articular cartilage has extremely little regenerative capacity. However, genetic tracing has recently revealed chondrocyte progenitors at the articular surface. Here, we characterized these progenitors utilizing in vivo genetic approaches. 3D visualization of articular cartilage growth with PTA-enhanced micro-CT revealed quantitative dynamic of tissue growth and reshaping. This approach, combined with clonal genetic tracing showed that superficial cells generate chondrocytes that contribute to the growth of the underlying epiphyseal bone and facilitate cartilage reshaping. Furthermore, superficial cells renew their number by symmetric division, express the mesenchymal stem cell marker CD73, and generate chondrocytes via both asymmetric division and symmetric differentiation, the classical behavior of adult stem cells referred to as population asymmetry. Finally, combined genetic tracing of superficial cells and neonatal chondrocytes revealed that adult articular cartilage is entirely formed by the progeny of the superficial cells.We conclude that superficial cells are postnatal stem cells capable of maintaining their own population. These cells are the source of adult articular cartilage.

*Poster*

# OBTAINMENT OF CAPILLARY-LIKE NETWORK FROM MSC SPHEROIDS FROM UMBILICAL CORD MMSC IN FIBRIN GEL

**A.A. Gorkun[1], I.M. Zurina[1], A.I. Shpichka[2], A.V. Koroleva[2], N.V. Kosheleva[1,4], D.V. Butnaru[2], P.S. Timashev[2], I.N. Saburina[1,5], and V.S. Repin[1,5]**

[1] FSBSI Institute of general pathology and pathophysiology, Moscow, Russia
[2] Sechenov First Moscow State Medical University, Institute for Regenerative Medicine, Moscow, Russia
[3] Laser Zentrum Hannover e.V., Hannover, Germany
[4] Lomosov Moscow State University, Faculty of Biology, Moscow, Russia
[5] FSBEI FPE "Russian Medical Academy of Continuous Professional Education" of the Ministry of Healthcare of Russia, Moscow, Russia

**Abstract.** In the current research, spheroids containing population of CD31+ cells were obtained from multipotent mesenchymal stromal cells from umbilical cord (MMSC UC) using induction with VEGF. After placing spheroids in the gel composed on the basis of fibrin, these cells activated the process of angiogenesis, which resulted in an active growth of tubules from MSC spheroids into the gel. In 7 days a primitive branched tubular network formed. The obtained results can become the basis for the development of the technology of 3D bio-printing of micro-vascularized tissues.

## Introduction

Formation of a capillary bed for the effective blood supply in de novo constructed tissues and organs is one of the most basic aims of modern tissue engineering. Combination of 3D bio-printing technology and cell technologies can become one of the most promising direction in this area. The use of 3D culture from multipotent mesenchymal stromal cells from umbilical cord (MMSC UC), which is induced towards endothelial differentiation and contains subpopulation of early endothelial progenitors, can allow obtainment of capillary network, formed by both endothelial and mesenchymal components.

## Materials and methods

MSC spheroids were obtained from human MMSC UC in 7 days in 3D culture under standard conditions (37°C; 5%$CO_2$) on agarose plates made with the use of 3D Petri Dishes (Microtissue, USA). Endothelial cell differentiation in spheroids was induced by adding vascular endothelial growth factor (VEGF) in growth medium. In 7 days some spheroids were fixed in 4% paraformaldehyde for immunocytochemical study of CD-31, Flk-1 and vimentin expression. The remaining spheroids were placed in non-modified andPEGylated fibrin to evaluate their capacity to form capillary-like network. To obtain stabilized hydrogel thrombin was added at the fibrinogen to thrombin ratio of 1mg to 02U. Gel based on modified fibrin was obtained by adding O,O'-bis[2-(N-succinimidyl-succinylamino)ethyl]poly(ethylene glycol) to fibrinogen at the molar ratio of 5 to 1. Reaction was carried for 2 hours at 37°. The control after the process of spheroid formation and tubule growth was performed using live time-lapse microscopy in Cell-IQ device (ChipMan Technologies, Finland).

## Results

Spheroids obtained from MMSC US after induction contained the population of CD31+ cells. After placing spheroids in both types of gel in 8 hours cells started to migrate from induced MSC spheroids and formed tubules. These cells expressed CD31, Flk-1 (endothelial cell markers) and some cells expressed vimentin (mesenchymal cell marker). In 7 days, we observed formation of a branched capillary-like network, where tubules connected with each other and with the tubules formed by the cells from neighboring spheroids.

## Conclusion

3D culture of MMSC UC in induction medium containing VEGF promotes the growth of number of endothelial cells, which are able of vasculo- and angiogenesis. The obtained results can become the basis for the development of the technology of 3D bio-printing of micro-vascularized tissues.

# A NEW APPROACH FOR SINGLE CELL IMAGING: MAMMALIAN OOCYTE CASE

**A.A. Gulin[1,2], A.V. Aybush[2], A.A. Astafiev[2], A.E. Solodina[2], A.G. Pogorelov[3], V.N. Pogorelova[3], A.I. Panait[3], and V.A. Nadtochenko[1,2]**

[1] Faculty of Chemistry, Moscow State University, Moscow, Russia
[2] N.N. Semenov Institute of Chemical Physics, Russian Academy of Sciences, Moscow, Russia
[3] Institute of Theoretical and Experimental Biophysics RAS, Pushchino, Moscow, Russia

**Abstract.** Combining imaging mass spectrometry with different microscopy techniques for the same sample on the same holder enables complex analysis of the sample morphology and chemical composition. A new sample preparation protocol was developed allowing complex analysis of germinal vesicles mice oocytes minimizing cellular chemistry redistribution and cell structure distortion. Mammalian oocytes can contain nucleolus-like body (NLB) units which were investigated. A domain structure of densely packed granules inside NLBs was revealed. Mass spectrometry shows increased amino acids and phosphate ions signal from the granules compared to cytoplasm area.

A combination of time-of-flight secondary ion mass spectrometry with a diversity of microscopy techniques, including coherent anti-Stokes Raman scattering microspectroscopy, atomic-force microscopy and scanning electron microscopy for the same sample allows characterizing both morphology and chemical composition of the examined sample. This type of analysis was successfully applied to the non-biological samples [1] and tissue sections [2], whereas a single cell study is a serious challenge.

A new sample preparation protocol based on preparation method used for electron microscopy and laser scanning microscopy [3] was developed for single isolated cells analysis. The protocol allowed us to analyze pre-selected GV-oocyte sections containing nucleolus-like bodies minimizing cellular chemistry redistribution and cell structure distortion. It would be important to mention briefly some crucial steps of the preparation technique. The obtained mice GV-oocytes were plunge-freezed followed by freeze-drying and immersed in Epon embedded media used for electron microscopy. On penetration into the embedding media, the samples were polymerized and cut by a microtome. Regions of interest were selected by sections examination using conventional light microscopy.

Nucleolus-like body composition and structure were investigated. Biological material in NLBs was found to be organized as a domain structure of densely packed granules with sizes from tenths of micron to a micron. Increased signal of amino acids and phosphate ions was observed in the NLB area compared to cytoplasm area. Epon was noted to poorly infiltrate inside NLBs. The work was supported by the Russian Foundation for Basic Research grant 16-53-52046.

## References

1. A. Diwan, B. Singh, C.J. Hurley, and M.R. Linford, "Layer-by-Layer Deposition of Nitrilotris (Methylene)Triphosphonic Acid and Zr(Iv): An Xps, Tof-Sims, Ellipsometry, and Afm Study", *Surf Interface Anal*, 2016, **48**, 105–10.
2. F. Le Naour, M.-P.Bralet, D. Debois, *et al.*, "Chemical Imaging on Liver Steatosis Using Synchrotron Infrared and Tof-Sims Microspectroscopies, *Plos One*, 2009, **4**, e7408.
3. A.G. Pogorelov and V.N. Pogorelova, "Quantitative Tomography of Early Mouse Embryos: Laser Scanning Microscopy and 3d Reconstruction", *J. Microsc*, 2008, **232**, 36–43.

# ELECTRON TRANSFER BETWEEN $Cd_{1-x}SeMn_x$ QUANTUM DOTS AND $MV^{2+}$: COHERENT EFFECTS REVEALED BY FEMTOSECOND LASER SPECTROSCOPY

**A.A. Gulin[1,2], I.V. Shelaev[1], F.E. Gostev[1], N.N. Denisov[3], A.V. Aybush[1], and V.A. Nadtochenko[1,2]**

[1] N.N. Semenov Institute of Chemical Physics RAS,Moscow, Russia
[2] Moscow State University, Chemical Department, Moscow, Russia
[3] Institute of Problems of Chemical Physics RAS,Chernogolovka, Moscow, Russia

**Abstract.** The exciton and charge carrier dynamics in CdSe, $Cd_{1-x}Mn_xSe$, and $Cd_{1-x}Mn_xSe$ / $MV^{2+}$ systems was studied by the fs pump-probe laser spectroscopy technique. The excitation was carried out to the low-lying exciton transition 1S (e) – 1S (h) 3/2 band (red edge of the CdSe absorption). The coherent wave packet oscillations were revealed in transient kinetics of CdSe, $Cd_{1-x}Mn_xSe$, and $Cd_{1-x}Mn_xSe$ / $MV^{2+}$. The oscillations correspond to the optical phonon of 206 $cm^{-1}$. The interfacial electron transfer from $Cd_{1-x}Mn_xSe$ to acceptor $MV^{2+}$ occurs with time constant close to 100 fs.

The excitons and charge carrier dynamics in CdSe, $Cd_{1-x}Mn_xSe$, and $Cd_{1-x}Mn_xSe$ /$MV^{2+}$ quantum dots were studied by the fs pump-probe spectroscopy technique with time resolution of 20 fs. The excitation was conducted to the band of the low-lying exciton transition 1S (e) – 1S (h) 3/2 (red edge of the absorption band). The excitation energy was varied from 20 nJ to 1300 nJ. The average number of excitons <N> per one quantum dot (QD) after the excitation was estimated taking into account the QD absorption cross section and the photon density in the pump pulse. The absorption cross section was determined according to W. William Yu *et al.* [1]. Transient absorption spectra were interpreted as the manifestation of different effects: 1) filling of electron and hole states due to excitation, which leads to a decrease in absorption after excitation (delta A < 0); 2) exciton stimulated emission (delta A < 0); 3) new optical transitions to higher excited states, for example, into biexciton states (delta A > 0); 4) the Stark shift of the QD absorption bands (delta A has S-shaped form with absorption and bleaching components). At low values of <N> delta A has a form closer to the first derivative of the linear absorption spectrum, at high values of <N>, delta A approaches the shape that is close to the shape of the second derivative of the QD linear absorption spectrum. Figure 1 shows transient kinetics at the wavelength of 567 nm. Fourier transform reveals the coherent wave packet corresponding to the optical phonon of 206 $cm^{-1}$. At high pump energy, Figure 1(B) demonstrates coherent wave packets related to the solvent toluene. Figure 2 shows that addition of MV2+ leads to the quenching of exciton. The time constant is close to 100 fs.

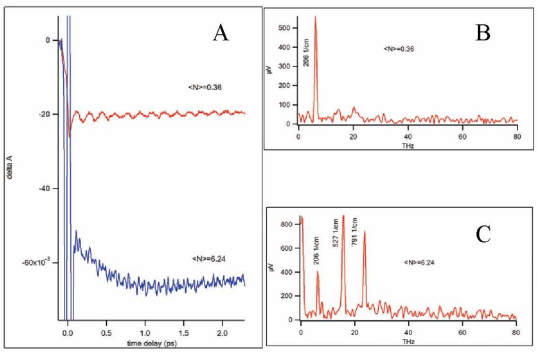



**Fig. 1.** A) transient kinetics at the wavelength of 567 nm. Two levels of excitation <N> = 0.36 and <N> = 6.24. B) Fourier transform of transient curves FFT under excitation of <N> = 0.36. C) FFT under excitation of <N> = 6.24

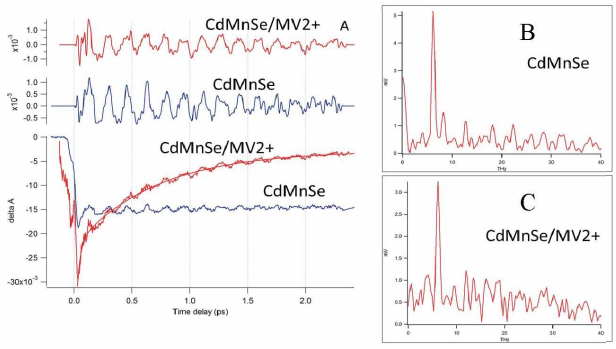



**Fig. 2.** A) transient curves of bleaching at 567 nm, <N> = = 0.14 with and without $MV^{2+}$. B) FFT,without$MV^{2+}$. C) FFT, with $MV^{2+}$

## Acknowledgements

The work was supported by RSF 17-13-01506.

## References

1. W.W. Yu, L. Qu, W. Guo, & X. Peng, *Chemistry of Materials*, 2003, **15**(14), 2854–2860.

# THE ROLE OF IMMUNOPROTEASOMES IN MAMMAL CELL DIFFERENTIATION

**E.Y. Ivanova[1,2], A.V. Selenina[2], S.A. Sinenko[2], E.I. Bakhmet[2], A.N. Tomilin[2], and A.S. Tsimokha[2]**

[1] Saint Petersburg University, Saint Petersburg, Russia, ivanoval.027@gmail.com
[2] Institute of Cytology, Russian Academy of Sciences, Saint Petersburg, Russia

The proteasome is a multisubunit protein complex responsible for selective protein degradation in the cell, playing important functions in various biological processes such as transcription, progression through the cell cycle, signal transduction, cell death, immune responses, metabolism, protein quality control and development. The proteasome is composed of a 20S core particle possessing proteolytic activity and one or two 19S regulatory complexes. In mammals, there also exists an immunoproteasome in which constitutive catalytic subunits β1, β2 and β5 are to be replaced with alternate β1i, β2i and β5i subunits, respectively. The immunoproteasome is believed to generate peptides specifically cleaved for antigen presentation. Recent data showed an increased gene expression of immunoproteasome subunit β5i in mouse embrionic stem (ES) cells during cell differentiation. The purpose of our study was to determine whether immunoproteasomes participate in cell differentiation. The experiments were carried out on the murine ES cell line E14 and cell differentiation was induced by removal of leukemia inhibitory factor (LIF) and by adding retinoic acid to growth medium. The expression of pluripotent markers such as Oct4 and Nanog was analyzed by quantitative PCR and immunocytochemistry. We confirmed that ES cells started to lose these markers 48 hours after the induction of differentiation. The expression of proteasomal subunit β5 and immunoproteasome subunits β1i, β2i and β5i was also analyzed by quantitative PCR. We found that the level of proteasome subunit β5 was similar in undifferentiated and differentiated cells. However, the level of β2i slightly increased in differentiated cells while stem cells did not express immunoproteasome genes at all. Additional tests such as Western-blotting, immunoproteasome activity inhibition assay, and immunosubunits knock-down are necessary to determine the extent of the influence of immunoproteasomes on the cell differentiation process.

**Acknowledgements**

This work was supported by the RSF 14-50-00068.

*Invited*

# EARLY MONOAMINES: DISCOVERING A NEW ANCIENT PATHWAYS IN DEVELOPMENT

**E. Ivashkin[1,2], M. Khabarova[2], A. Obukhova[2], M. Nikitin[3], I. Adameyko[1], and E. Voronezhskaya[2]**

[1] Karolinska Institutet, Sweden, evgeny.ivashkin@ki.se
[2] Institute of Developmental Biology RAS, Russia
[3] Lomonosov Moscow State University, Russia

**Abstract.** Already at the stage of very early embryo Metazoans show adaptations to the future challenges we will be facing in adult life. Mechanisms of such information transfer from mother to the developing embryo still remain largely unknown. We are trying to answer the question how the enigmatic world of ancient small molecules drives fate of progeny in animals and human. We discovered direct transmission of signal about the physiological condition of the mother's body to a progeny through the serotonergic system in female's reproductive organs. Our recent experimental and bioinformatical investigations brought us to understanding of exact targets and mechanisms.

External environmental factors significantly influence organisms at non-genetic level and, through this, impact the progeny that is generated at much later times. A number of important characteristics vary under the influence of parental effects and include the dynamics of development and growth, body size, metabolic levels as well as behavioral plasticity. The progenies may retain the non-genetic memory up to three generations after parents were exposed to abnormal temperature, nutrition level, dietary composition, hypoxia, photoperiod, social environment or activity of predators. Among behavioral programs that are sensitive to parental effects and are exceptionally important for survival we may list feeding behavior, escape from predators, learning capacity and dispersion of the offspring. Generally, non-genetic transfer of information to the progeny is widely spread in nature and varies in terms of molecular mechanisms. Despite recent success in studies of DNA modifications and the discovery of a histone code. It is worth mentioning that early developmental stages are especially crucial and are the key for implementation of parental effects. Many embryonic features that will influence the resulting fitness, behavioral modality and future reproductive success of the progeny are initiated during early development.

Monoamines and especially serotonin and dopamine are widely known as neurotransmitters and local humoral regulators of many processes in developing embryo and adult body. These substances and proteins related to them play many key roles in our motivation, memory, feeling of satisfaction. Their levels in our brain determine character, our decisions and after this drive our fate, fitness and life success. At the same time, it's much less known, that more than these substances seem to appear as a signaling molecules several billion years ago, at the very early steps of evolution. Serotonin may be found in prokaryotes, plants, protists and exists at least in some stages of life cycle in any of ever investigated animals including those ones who has no neurons at all such as an ancient and enigmatic placozoan trichoplax. In all vertebrates including human monoamines are expressed on all stages of life including male and female gametes, zygote and very early embryos. Their role in early pre-neuronal development is merely known, while about the functions we have only few hypotheses.

Recently we discovered an entirely new phenomenon in developmental biology and physiology – direct transmission of signal about the physiological condition of the mother's body to a progeny through the local serotonergic system in female's reproductive organs, level of serotonin in early embryo, the serotonin receptors, transporter, expressed in cells and the process of monoaminylation – covalent binding of serotonin to glutamines residues in proteins mediated by transglutaminase. We continued our study in this field and our recent experimental and bioinformatical investigations performed on the sea urchin, zebrafish shown us exact protein targets of monoaminylation. We could find differences in the roles of early dopamine and serotonin. Work in this direction revealed that both discovered molecular mechanism and principle itself is conservative and widespread in the animals' phyla. And brought us as close as possible to the most difficult question in our investigation: how does this ancient system works in viviparous animals such as most of mammals and human? Question about ourselves.

*Invited*

# NONINVASIVE MONITORING OF LIVING EARLY MAMMALIAN EMBRYO DEVELOPMENT

**A.V. Karmenyan[1], A.S. Krivokharchenko[2], E.V. Perevedentseva[1], H.-H. Chang[3], Ashek-i-Ahmed[1], L.-C. Liu[1], and C.-L. Cheng[1]**

[1] National Dong Hwa University, Hualien, Taiwan, artashes@gms.ndhu.edu.tw
[2] N. N. Semenov Institute of the Chemical Physics, Russian Academy of Sciences, Moscow, Russia
[3] Tzu Chi University, Hualien, Taiwan

**Abstract.** Optical methods are developed for applications in embryologic studies and practical use in artificial reproductive technologies (ART). These methods are nondestructive, low-invasive and informative and allow studying various structural and molecular biochemical processes inside living cells, without interfering in the living processes. Thus, new effective ways can be suggested for monitoring the status of ova with the aim to estimate developmental ability without losing quality for ART and investigation of fundamental mechanisms of early mammalian development. In presented work these methods were used to analyze impact of nanoparticles on ova. The main limiting factors for the laser-based analytical methods are discussed.

During last decades ART was wide used in scientific, medical, and biotechnological fields. One of ways to increase rate of the successful embryo implantation after *in vitro* manipulation is developing more effective methods for recognition qualitative ova for exploitation. To understand fundamental mechanisms underlying the early mammalian embryo (EME) development and to obtain information for EME evaluation and selection for ART new optical-spectroscopic methods on the base of advanced laser techniques are perfect candidates. These methods allow monitoring the status of mammalian gametes and embryos during preimplantation development without losing quality. However, limiting factor is the adverse effect of laser beam on the investigated biological sample depending on laser wavelength and dose of laser radiation.

In the present work, different optical-spectral methods, as Raman spectroscopy, 2-photon fluorescence spectroscopy, and fluorescence lifetime imaging microscopy (FLIM) are used and their applicability is discussed for diagnostics and control of EME conditions.

Raman spectra from different areas of mouse oocytes and 2-cells embryos have been measured and analyzed. The laser power and exposure were varied and further *in vitro* ova development was observed to select optimal conditions of the measurements. Safe parameters of the measurements were selected, which don't affect the embryo development up to morphologically normal blastocyst.

FLIM with 2-photon excitation was used to observe and analyze autofluorescence from metabolic cofactors reduced nicotinamide adenine dinucleotide (NADH) and flavin adenine dinucleotide (FAD). The distribution of lifetimes and intensity of autofluorescence in different areas of EME were analyzed to understand a relation between metabolic processes, their dynamics in various stages of development of gametes and embryos.

These methods' potential for estimation of an embryo state has been demonstrated via analysis and comparison of the spectra of fertilized and non-fertilized oocytes, EME subjected strong UV-irradiation and co-incubated with different nanoparticles (NP).

The development of nanotechnologies' bio-applications on one hand, and ART on the other hand increases probability of EME to be subjected to NP treatment. However, only a few previous studies consider the impact of NP on oocytes and EME. Physicochemical and biological mechanisms of NP toxicity for EME still unclear. In our work, the optical-spectroscopic methods have been applied to study effects of NP (nanodiamonds of different sizes and surface properties, $TiO_2$, etc.) on the development of mammalian ova *in vitro*.

High potential of the used methods in the embryology is demonstrated.

**Acknowledgements**

The authors appreciate the financial support of this research by the Ministry of Science and Technology of Taiwan, Grant numbers 104-2811-M-259-012, 104-2811-M-259-013, 105-2811-M-009, 105-2811-M-013 and 105-2923-B-320-001-MY3. ASK was supported in Russian Foundation for Basic Researches grant 16-53-52046.

*Invited*

# TWO-PHOTON POLYMERIZATION FOR FABRICATION OF TISSUE ENGINEERING SCAFFOLDS

**A. Koroleva[1], A. Deiwick[1], P. Timashev[2,3], D. Kuznetsova[4], and B. Chichkov[1]**

[1] Laser Zentrum Hannover e.V., Hannover, Germany, a.koroleva@lzh.de
[2] Institute of Photonic Technologies, Research Center of Crystallography and Photonics RAS, 108840, Troitsk, Moscow, Russia
[3] Sechenov First Moscow State Medical University, Institute for Regenerative Medicine, Moscow, 119991, Russia
[4] Institute of Biomedical Technologies, Nizhny Novgorod State Medical Academy, Nizhny Novgorod, 603005, Russia

**Abstract.** Two-photon polymerization (2PP) with femtosecond lasers provides many advantages for the fabrication of high quality 3-D microstructures with complex geometries [1]. 2PP technique uses non-linear absorption of femtosecond laser pulses to selectively polymerize photosensitive materials. Three-dimensional microstructuring by the 2PP technique provides many interesting possibilities for biomedical applications. This microstructuring technique is suitable for many biocompatible polymeric materials, such as polyethylene glycol, polylactic acid, polycaprolactone, gelatin, zirconium-based hybrids, and others [2, 3]. The flexibility in controlling geometries and feature sizes and the possibility to fabricate structures without the addition of new material layers makes this technique particularly appealing for fabrication of 3-D scaffolds for tissue engineering. Our recent progress in application of 2PP scaffolds for tissue engineering will be reported.

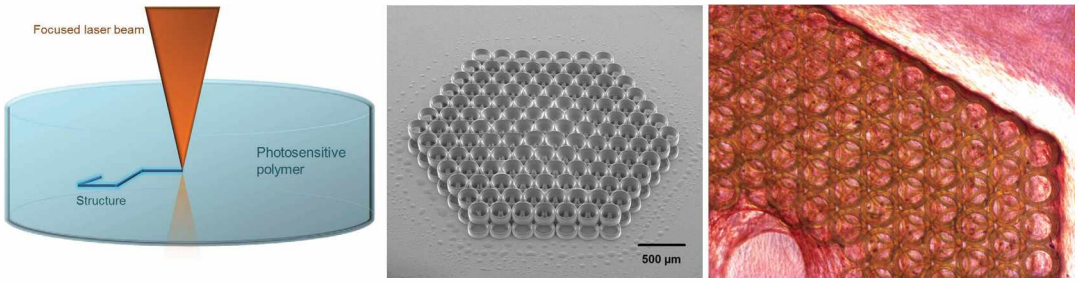



**Fig. 1.** Principle of 2PP process (*left*); 2PP fabricated scaffold from zirconium-based organic inorganic composite (*middle*); human mesenchymal stem cells (hMSCs) differentiated on 2PP scaffold towards osteogenic lineage (*right*)

## Acknowledgements

The work is supported by Excellence Cluster REBIRTH (Hannover, Germany) and Low Saxony project Biofabrication for NIFE.Institute for Regenerative Medicine of Sechenov First Moscow State Medical University is acknoweledged.

## References

1. J. Serbin, *et al.*, *Opt. Lett.,* 2003, **28**.
2. A. Koroleva, *et al.*, *Plosone,* 2015, **10** (2), e0118164.
3. P. Timashev, *et al.*, *Biomed. Phys&Eng Express,* 2016, **2**, 035001.

*Poster*

# DEVELOPMENT OF BIOENGINEERED CONSTRUCTION BASED ON OSTEOPLASTIC MATERIAL AND VEGF-INDUCED 3D CULTURE OF MESENCHYMAL STROMAL CELLS (MSC SPHEROIDS)

**I.M. Zurina[1], A.A. Gorkun[1], A.F. Fidarov[2], N.V. Kosheleva[1,3], and I.N. Saburina[1,2]**

[1] FSBSI "Institute of General Pathology and Pathophysiology", Moscow, Russia, e-mail: n_kosheleva@mail.ru
[2] FSBEI FPE "Russian Medical Academy of Continuous Professional Education" of the Ministry of Healthcare of Russia, Moscow, Russia
[3] Lomosov Moscow State University, Faculty of Biology, Moscow, Russia

**Abstract.** In the current research rat adipose-derived stromal cells in the presence of vascular endothelial growth factor (VEGF) were placed in non-adhesive conditions to form spheroids. 7-day VEGF-induced MSC spheroids were then placed on osteoplastic apatite-silicate composition material BAC-1000. 7 days later cells formed a dense layer as well as tubule-like structures both on the surface and in the pores of matrix. The current research describes a promising technology for obtainment of bioequivalents of vascularized bone tissue for fast and effective restoration of vast bone injuries.

**Introduction.** Nowadays creating tissue-engineered constructions is one of the most promising technology for repair of bone tissue defects. Traditionally a combination of osteoconductive carrier, osteoinducing growth factors and osteogenic progenitor cells is used in bone tissue engineering. However, for reparation of vast bone tissue injuries it is important to create vascularized constructions, where functionality and structure, regulation of osteogenesis and vasculogenesis would be well-balanced. The use of single-cell suspension for plating on osteoconductive micro-molds turned out to be not enough effective, in particular, because single cells rapidly lose their osteogenic potential in the absence of inductive culture media and special microenvironment. Cells in 3D culture – spheroids – survive better, have an elevated pro-angiogenic and anti-inflammatory potential, whilst their osteogenic potential does not reduce. In this aspect, adipose-derived stromal cells (ADSC) have more advantages for creating bio-engineered constructions. This cell population can be obtained in a large amount using not a very invasive procedure. Moreover, they contain not only multipotent mesenchymal stromal cell population, but also a vascular fraction. The aim of the current study was to develop a bio-engineered construction based on osteoplastic non-resorbable bioactive material – apatite-silicate composition material BAC-1000 and MSC spheroids from ADSC induced in angiogenic direction.

**Materials and methods.** Rat ADSC were obtained according to a standard protocol, cultured in standard conditions (37°C, 5%$CO_2$) up to the third passage, and characterized by flow cytometry analysis using standard MSC surface antigen panel. MSC spheroids were obtained from the suspension of the characterized ADSC in non-adhesive agarose plates made with the use of 3D Petri Dish (Microtissues, USA). To induce angiogenic differentiation in spheroids, vascular endothelial growth factor (VEGF) was added to culture medium. 7-day VEGF-induced spheroids were then put on the piece of BAC-1000 in a small volume of medium for two hours to initiate the adhesion of spheroids to the surface of material and afterwards the growth medium supplemented with VEGF was added to a necessary volume to fully cover the material. 7 days later the obtained constructions were fixed in 3% glutaraldehyde for the further analysis on the scanning electron microscope.

**Results.** Scanning electron microscopy 7 days after plating VEGF-induced MSC spheroids on BAC-1000 showed a great number of cells as well as tubule-like structures both on the surface and in the pores of matrix. This type of material in combination with cell material in the form of VEGF-induced MSC spheroids was shown to be the most optimal because it combines osteoprotection, osteoinduction, osteoconduction and biocompatibility. All these properties allowed us to develop a bio-engineered construction, where combine both support (osteoconductive) function and bio-integration (outgrowth of cells as well as newly developed vessels). The obtained results of the current research will help to develop new innovative methods and technologies for creating *in vitro* bioequivalents of vascularized bone tissue for fast and effective restoration of vast bone injuries.

*Invited*

# UNDERSTANDING OF DEVELOPMENTAL AND REGENERATION PATHWAYS OF TOOTH USING SINGLE CELL TRANSCRIPTOMICS

**J. Krivanek[1], T. Chontorotzea[2], K. Fried[2], and I. Adameyko[2]**

[1] Center for Brain Research, Medical University of Vienna, Vienna, Austria
jan.krivanek@meduniwien.ac.at
[2] Karolinska Institutet, Stockholm, Sweden

**Abstract.** Mouse incisor as a continuously growing tooth serves as an excellent model system to study stem cell niche, developmental differentiation pathways and importantly to study mutually interdependent epithelial to mesenchymal interactions. In our study we used single cell transcriptomics method by which we can elucidate levels of gene expression of all genes in each single selected cell. We analyzed obtained data by advanced algorithms which enabled us to distinguish different cell types, estimate their proportion and cluster them into different families. We characterized new cell subtypes and suggested cell differentiation pathways influenced by specific key factors.

## Introduction

Mouse is currently being probably most studied species in developmental biology field. Widespread use of mouse is caused by fast breeding capacity, extensive similarity to human body and importantly because of huge pool of available genetically modified strains which can be used for all various approaches. In past half century many studies had been published focused on tooth development. Nowadays we can say, that tooth development pathway serves as a well-described model system to explain mechanisms of epithelial-mesenchymal interactions and differentiation resulting from that. Mouse, instead of human evolution, developed mechanism how regenerate continuously their incisors. In these teeth we can find stem cell niche even in fully adult animals, keeping tooth growing. Understanding of stem cell renewal, interactions and differentiation is some kind of Holy Grail to decipher mechanisms we need to know for applicable and safe use in regeneration medicine.

## Methods

Our study is based on single cell transcriptomics approach, but combines also various methods as genetic tracing and immunohistochemistry combined to most advanced confocal microscopy and also *in situ* hybridization experiments designed to prove the transcriptomics data.

## Results

Our results shows expression of various important genes in different cell types which can be find in tooth. Among others, database contains also genes coding transcription factors, ligands or receptors. Based on these findings we can help to elucidate complicated interactome pathways between distinct cell types, understand some pathologic mechanisms and importantly follow developmental pathways responsible for differentiation of stem cells through transit-amplifying cells into pulp cells, odontoblasts or ameloblasts and moreover to follow their aging from maturation stage until apoptosis. Our findings provides deeper understanding of heterogeneity and homeostasis of pulp and give a clue how to decipher real physiology of maintaining of dental pulp.

## Acknowledgements

The research was supported by ERC-2014-CoG: FA629A0301.

# THE INVOLVEMENT OF ALLOGENEIC MESENCHYMAL STEM CELLS IN BONE FORMATION

**D.S. Kuznetsova[1], N.N. Prodanets[1], P.S. Timashev[2,3], V.N. Bagratashvili[3], and E.V. Zagaynova[1]**

[1] Nizhny Novgorod State Medical Academy,Nizhny Novgorod, Russia, dskuz@nizhgma.ru
[2] I. M. Sechenov First Moscow State Medical University, Moscow, Russia
[3] Institute of Photonic Technologies, Research center "Crystallography and Photonics", Troitsk, Moscow, Russia

**Abstract.** Currently there are three key elements in tissue engineering to treat bone defects: cells, scaffolds and growth factors. The cell approach consists of the preliminary seeding of cells onto scaffolds. Mesenchymal stem cells (MSCs) are thought to be the most attractive for making bone repair. However, much is unknown about MSCs which needs to be elucidated before this treatment can be widely applied in clinical situations. The goal of the present work was to study the involvement of seeded allogeneic MSCs in bone formation using the model of transgenic mice and genetically labeled cells.

Currently there are three key elements in tissue engineering to treat bone defects: cells, scaffolds and growth factors [1]. The cell approach consists of the preliminary seeding of cells onto scaffolds before these matrices are implanted. Several cell types can potentially be used as cellular material, but mesenchymal stem cells (MSCs) are thought to be the most attractive for making bone repair [2, 3]. However, much is unknown about MSCs which needs to be established before this treatment can be widely applied in clinical situations. The purpose of the present work was to study the involvement of seeded allogeneic MSCs in bone formation in vivo using the model of transgenic mice and genetically labeled cells.

The scaffolds were sterilized, individually seeded with MSCs from the bone marrow of male 5-week-old GFP(+) transgenic C57/Bl6 or GFP(–) male C57/Bl6 mice. Critical-sized defects were created on the calvarial bone of each animal. Scaffolds with or without seeded cells were implanted into the injury sites. The cranial bones were harvested either 6 or 12 weeks after implantation. All samples were stained with Hoechst and observed using fluorescence microscopes. GFP(+) transgenic mice having scaffolds with non-labeled MSCs were used for the observation of host cell migration into the scaffold. GFP(–) mice having scaffolds with GFP(+)MSCs were used to assess the functioning of the seeded MSCs. The control group comprised GFP(+) transgenic mice having scaffolds without any cells.

The data demonstrated that allogeneic MSCs were found on the scaffolds 6 and 12 weeks later. Moreover, by week 12 there was a newly formed bone tissue from the seeded cells without requiring osteogenic pre-differentiation. What is more important, host cells did not appear, and the control scaffolds without seeded cells remained empty. Also, the possibility was shown for vessel formation from seeded MSCs without preliminary cell cultivation under controlled conditions. Although the exact mechanisms of the involvement of the seeded allogeneic MSCs in bone formation need further investigation, our data contributes to the understanding of the positive results of MSC transplantation.

## Acknowledgements

This work has been financially supported by the Russian Science Foundation (grants No.17-74-20077).

## References

1. B. Chan and K. Leong," Scaffolding in tissue engineering: general approaches and tissue-specific considerations", *Eur Spine J.*, 2008, **17**, 467–479.
2. A. Undale, J. Westendorf, M. Yaszemski, *et al.*, "Mesenchymal stem cells for bone repair and metabolic bone diseases", Mayo ClinProc., 2009, **84**, 893–902.
3. Y. Qin, J. Guan, and C. Zhang, "Mesenchymal stem cells: mechanisms and role in bone regeneration", *Postgrad Med J*, 2014, **90**, 643–647.

*Invited*

# REPRODUCTION AND DEVELOPMENT *IN VIVO* WITH OCT

**I.V. Larina**

Department of Molecular Physiology and Biophysics, Baylor college of Medicine,
One Baylor Plaza, Houston, Texas 77030, USA
e-mail: larina@bcm.edu

**Abstract.** Understanding the dynamic process of reproduction is essential to advance the understanding and improve the management of reproductive disorders. However, the majority of what we know about the dynamics of these events is assumed based on histological analysis of extracted organs and studies in invertebrate animal models. To address this lack of knowledge, we developed a set of OCT-based imaging methods for *in vivo* structural, dynamic and functional visualization of the mouse reproductive tract, cilia function and sperm activity, which previously have not been accessible. These approaches reveal puzzling observations, which might contribute to uncovering the mechanisms of mammalian reproduction.

Understanding the dynamic process of reproduction is essential to advance the understanding and improve the management of reproductive disorders, such as infertility and ectopic pregnancy. However, the majority of what we know about the dynamics of these events is assumed based on histological analysis of extracted organs, low-resolution visualizations, and extrapolation of studies in invertebrate animal models. To address this lack of knowledge, we developed a set of OCT-based imaging methods for *in vivo* structural, dynamic and functional visualization of features of the mouse reproductive tract, cilia function and sperm activity, which previously have not been accessible. The micro-scale spatial resolution, millimeter-level imaging depth, large transverse field of view, high temporal resolving ability, functional capacity and compatibility with live imaging make this approach applicable for variety of reproductive and developmental studies. These approaches reveal puzzling observations, which might contribute to uncovering the mechanisms of mammalian reproduction.

# METABOLIC PLASTICITY OF MESENCHYMAL STEM CELLS DURING DIFFERENTIATIONS BY TWO-PHOTON FLIM

**A.V. Meleshina**[1,2], **V.V. Dudenkova**[1,2], **A.S. Bystrova**[1,2], **M.V. Shirmanova**[1], and **E.V. Zagaynova**[1]

[1] Nizhny Novgorod State Medical Academy, Nizhny Novgorod, Russia, almele@ya.ru
[2] Nizhny Novgorod State University, Nizhny Novgorod, Russia

**Abstract.** Metabolic plasticity and the versatility of different lineages of stem cells as they satisfy their energy demands are not completely understood. In this study we investigated the metabolic changes in mesenchymal stem cells undergoing differentiation in three directions, adipogenic, osteogenic and chondrogenic, using the two-photon fluorescence microscopy combined with FLIM. Based on the data for the FAD/NAD(P)H redox ratio and on the fluorescence lifetimes of protein-bound NAD(P)H we registered a metabolic switch from glycolysis to OxPhos in adipocytes, consistent switch from glycolysis to OxPhos to glycolysis in osteoblasts and switch to more glycolytic status in chondrocytes.

The role of cellular metabolism and macromolecular synthesis during differentiation has not been fully studied in stem cell biology. In this study we investigated metabolic changes in mesenchymal stem cells (MSCs) undergoing differentiation in three directions (adipogenic, chondrogenic, osteogenic) based on the fluorescence of the metabolic co-factors NAD(P)H and FAD. Cellular metabolism was examined by monitoring the optical redox ratio (FAD/NAD(P)H), the fluorescence lifetime contributions of the free and bound forms of NAD(P)H and FAD. Two-photon fluorescence microscopy combined with FLIM was used to analyze this fluorescence in living cells.

Undifferentiated MSCs and MSCs on 7, 14, 21 days of three differentiations were imaged with a Zeiss 710 microscope coupled to a FLIM system. The intrinsic fluorescence of NAD(P)H and FAD was excited at 750 nm and 900 nm respectively by a femtosecond Ti:sapphire laser. The data were analyzed with the commercially available SPCImage software. The fluorescence lifetimes and their contributions (free and protein-bound forms of NAD(P)H and FAD: $a_{free}$ NADH, $a_{free}$ FAD, $a_{bound}$ NAD(P)H, $a_{bound}$ FAD) for the areas of interest were calculated by finding the global minimum of the $\chi 2$ value for three-exponential fittings.

To estimate the general level of metabolic activity of the cells during differentiations, the fluorescence intensities of NAD(P)H and FAD were measured and represented as their redox ratio (FAD/NAD(P)H). The optical redox ratio FAD/NAD(P)H decreased during all differentiations. This was likely to be explained by the intensive biosynthesis of lipids (adipogenic differentiation) and collagen (chondrogenic, osteogenic differentiation). To study cellular energy metabolism during adipogenic, chondrogenic, osteogenic differentiation, we analyzed the fluorescence lifetime contributions of the free and protein-bound forms of NAD(P)H. A statistically significant increase in the contribution of bound NADH was shown during adipogenic differentiation, pointing to a shift toward oxidative phosphorylation (OxPhos). The contribution of protein-bound NAD(P)H in osteogenically and chondrogenicallydifferentiated MSCs gradually decreased, probably due to a bias toward more glycolytic metabolism.The fluorescence lifetime contribution of bound FAD was lower at all time points compared with the undifferentiated cells during osteogenic and adipogenic differentiation. A statistically significant increase in the protein-bound FAD contribution (in comparison with the undifferentiated MSCs) was revealed during chondrogenic differentiation.

So, we have elucidated the metabolic changes in MSCs during adipogenic, chondrogenic, osteogenic differentiation based on the fluorescence of the metabolic co-factors NAD(P)H and FAD using the methods of two-photon fluorescence microscopy combined with FLIM. Based on the data on the fluorescence lifetime contribution of protein-bound NAD(P)H, we registered a metabolic switch from glycolysis to OxPhos in adipocytes, consistent switch from glycolysis to OxPhos to glycolysis in osteoblasts and switch to more glycolytic status in chondrocytes. The fluorescence lifetime characteristics of FAD indicated the stimulation of an unknown metabolic pathway, where protein-bound FAD participates.

**Acknowledgements**

This work has been financially supported by the Russian Science Foundation (grants No. 14-15-00536).

*Invited*

# PRECISE CONTROL OF PROTEIN EXPRESSION BY LIGHT

**S. Ogasawara**

PRESTO, Japan Science and Technology Agency,
4-1-8 Honcho, Kawaguchi-, Saitama 332-0012, Japan
shinzi@cris.hokudai.ac.jp

**Abstract.** A photoresponsive cap that can be reversibly *cis-trans* isomerized by light irradiation was developed for the reversible photoregulation of translation. The photoresponsive mMe-2PA-cap in the *trans* form silences translation in zebrafish embryo, whereas treatment with the *cis* form provided a 7.1 times larger amount of translated protein compared to the *trans* form. An application of this approach in developmental biology was demonstrated by photo-inducing the development of double-headed zebrafish by controlling the expression period of squint protein.

## Introduction

Living processes are managed through the precise control of "when, where, and how long" proteins are expressed. The photo-control of protein expression enables the spatiotemporal induction of biological events in living cells or organisms. In transcriptional control, several hours elapse between light illumination and the beginning of protein expression, and protein continues to be synthesized for more than 10 hours after the light is turned off due to residual mRNA [1]. Therefore, direct regulation of mRNA translation is more suitable for controlling cellular functions occurring within a short time period, such as the determination of cell fate at the early development stage.

## Result and discussion

We synthesized three photoresponsive caps, 2-phenylazo cap (2PA-cap), 2-*para*-methyl-phenylazo cap (pMe-2PA-cap), and 2-*meta*-dimethyl-phenylazo cap (mMe-2PA-cap), such that the affinity for eIF4E could be modulated by steric hindrance. Differences in the translation of mRNA containing either the *trans* or *cis* forms of 2PA-cap, pMe-2PA-cap, or mMe-2PA-cap were investigated in zebrafish embryos. Yellow fluorescent protein (Venus) was used to estimate the amount of translated protein. Translation of mRNA was more efficient with photoresponsive caps in the *cis*-form than in the *trans*-form. mMe-2PA-cap exhibited the highest photomodulation efficiency. The fluorescence intensity of Venus protein in embryos injected with mMe-2PA-capped mRNA and illuminated with 370 nm light was 7.1 times higher than that of non-illuminated embryos. Next, we photo-controlled the duration of squint protein expression in early zebrafish embryos. squint is normally expressed on the dorsal side only during the period between the 8-cell stage and the shield stage. We thus examined the influence of the expression period of squint protein on the formation of head structure using our method. The results suggest that squint protein leads axis development in the earlier developmental stage and inhibits the formation of head structures when expressed at a later developmental stage.

## Summary

We succeeded in developing photoresponsive cap that can be reversibly *cis-trans* photoisomerized by alternate illumination with monochromic 370 nm and 430 nm light [2]. To demonstrate a potential application of our method in developmental biology, we showed photo-induction of the complete secondary axis of zebrafish embryo by regulating the duration of squint protein expression. Moreover, we found that the formation of head structures was inhibited by prolonged expression of squint. Our method will reveal the importance of when, where and how long protein expression occurs during specific biological events by spatiotemporally controlling translation in a reversible manner in living cells and organisms

## Acknowledgements

This work was supported by PRESTO, JST, and JSPS KAKENHI (Grant Number 16K14733). We are grateful to Prof. Karuna Sampath (University of Warwick) for providing the pCS2 squint plasmid.

## References

1. X. Wang, X. Chen, and Y. Yang, *Nat. Methods,* 2012, **9**, 266–269.
2. S. Ogasawara, *ASC Chem. Bio.,* 2017, **12**, 351–356.

*Invited*

# TEMPERATURE-RESPONSIVE BIOMATERIALS DESIGN FOR TISSUE ENGINEERING AND DRUG DELIVERY

**Yu. Rochev**[1,2]

[1] National University of Ireland Galway, Ireland
[2] Sechenov First Moscow State Medical University,
Institute for Regenerative Medicine, Moscow, Russia, yury.rochev@nuigalway.ie

**Abstract.** The regeneration of cells and cell sheets mediated by thermoresponsive substrates represents an important and ever growing area in tissue engineering. This presentation seeks to track the development of this field from inception to the present day by highlighting the most significant breakthroughs as well as focusing on important physical and chemical characterization of substrates produced for this specific purpose. Furthermore, a critical evaluation encompassing the advantages and disadvantages of different techniques used for producing such surfaces will be included as well as suggestions for possible future directions.

**Introduction.** Thermoresponsive polymers have numerous potential applications in areas such as drug delivery and tissue engineering. Over the last couple of decades a number of innovative conceptions to using thermoresponsive coating for tissue engineering and drug delivery have been developed and refined. In order to better understand the characteristics which influence the interfacial relationships between thermoresponsive coatings, biomolecules and drugs a summary of the most important physical and chemical characterization data related to poly(N-isopropylacrylamide) (pNIPAm) coatings prepared by different methods will be reported and the subsequent affect of these characteristics on cell compatibility and drug delivery assessed.

**Materials and Methods.** Copolymers of NIPAM/ N-tert-butyl-acrylamide (NtBAm) and ethylpyrrolidone methacrylate (EPM)/ NIPAM with varying ratios were synthesized. Also a photocrosslinkable NIPAm/ acrylamidobenzophenone (AcBzPh) copolymer was synthesised [1]. The solvent casting, spin coating and physically adsorption techniques has been used for the thermoresponsive film preparation. Surface analysis was facilitated through UV spectrophotometry, X-ray photoelectron spectroscopy (XPS), Fourier transform infrared spectroscopy (FTIR), atomic force microscopy (AFM), nanoindentation, white light interferometry and advancing contact angle measurements. A variety of primary cells including mesenchymal stem cells and cell lines has been used in cell culture experiments. A controlled drug delivery system fabricated from a NIPAm-AcBzPh copolymer was designed to obtain a pulsatile release profile which was triggered by altering the temperature of the dissolution medium [2].

**Results.** Based on contact angle results we found that NIPAM films above LCST are unstable, because the films can uptake significant amount of water even in hydrophobic state. The cell adhesion and proliferation depends on the film stability. The drug elution profile is also depends of the water content. The introduction more hydrophobic monomers NtBAm increase the film stability. Also, the method of the film preparation is important for the thermoresponsive coating design.

**Discussion and Conclusion.** The coatings based on PNIPAM homopolymer are generally poorly cell compatible and a number of techniques have been developed in order to overcome this issue. Our results demonstrate that NIPAM copolymer composition, water up-take level, coating thickness and method of preparation of the deposited films seems to have a considerable influence on cell compatibility and drug elution profile.

**Acknowledgments**

The authors would like to thank the Russian Science Foundation (Grant no. 15-15-00132) for providing financial support to this project.

**References**

1. Nash, *et al.*, *Soft Matter.*, 2012, **8**, 3889–3899.
2. R. Yang, *et al.*, *Int J Pharm.* 10, 2012, **427**(2), 320–7.

# THE STUDY OF THE DERMAL CELLS CULTURED IN COLLAGEN GEL BY OPTICAL AND MULTIPHOTON TOMOGRAPHY

**O.S. Rogovaya[1,2], V.V. Dudenkova[3,4], A.S. Bystrova[3,4], M.M. Lukina[3,4], E.A. Vorotelyak[1,4], E.V. Zagaynova[3], and A.V. Meleshina[3]**

[1] Koltzov Institute of Developmental Biology of Russian Academy of Sciences, Moscow, Russia
[2] Pirogov Russian National Research Medical University Moscow, Russia
[3] Nizhny Novgorod State Medical Academy, Nizhny Novgorod, Russia
[4] Nizhny Novgorod State University, Nizhny Novgorod, Russia

There are common mechanisms of connective tissue development in the course of various pathological processes. These processes are better studied in skin wounds and all types of regeneration and growth of connecting tissue. The contraction is one of the processes providing wound healing. We utilized the model of dermal equivalent (DE) manufactured from collagen gel containing stromal cells which contracted the gel within two weeks of cultivation in vitro. Murine dermal fibroblasts (DFB) and cells from the dermal papilla (DP) were used. In this system, collagen gel acted as an analog of a stroma which should be strengthened and contracted by cells to form collagen fibrils. The contraction of collagen gel and its structure were studied by standard laboratory and modern hardware methods with the use of optical coherence tomography (OCT) and a multiphoton tomography (MPT). The quality of cell component (according to the cells autofluorescence and a lifetime of NADH intracellular fluorophor) as part of DE was estimated by means of the multiphoton tomography equipped with FLIM system. The expression of specific proteins (vimentin (Vim), smooth muscleα-actin (α-sma), versican (Ver) and proliferation marker Ki67) by DFB and DP cells in collagen gel was determined with the use of an immunofluorescent method. Additionally, cells were stained for an activity of alkaline phosphatase as a stem cell marker. It was shown that throughout the cultivation period cells expressed Vim, α-sma, and Ki67. During the first 7 days Ver –DP specific marker –was found at the reliable level only in DP cells. But after 2 weeks of cultivation, it was also weekly expressed in DFB. The alkaline phosphatase was detected in DP cells at all terms of observations and, surprisingly, in some cells in DFB cultures after 14 days of cultivation in the gel. All types of DE showed similar patterns of formation of the ordered fibrils by the day 3 of cultivation that was shown by the OCT method. The formation of collagen fibers was visualized by means of the second harmonic generation (SHG) using the multiphotonMPTflex tomography. During the cultivation, we observed SHG signal enhancement that demonstrated emergence of an ordered structure of collagen fibers. On the basis of the lifetimes of an intracellular NADH metabolite and their contribution corresponding to the changes of the free and bound NADH forms in cell components by the day 14, the shift of the metabolic status towards oxidative phosphorylation was shown.

**Acknowledgments**

This work has been financially supported by the Russian Foundation for Basic Research (grant No.15-29-04851).

# HORMONAL REGULATION OF FUNCTIONAL HETEROGENEITY OF MESENCHYMAL STEM CELLS

**V.Yu. Sysoeva, N.I. Kalinina, P.A. Tyurin-Kuzmin, L.V. Ageeva,** and **V.A. Tkachuk**

Department of Biochemistry and Molecular Medicine, Faculty of Basic Medicine,
Lomonosov Moscow State University, Moscow, Russia
veroniks@mail.ru

Mesenchymal stem cells (MSCs) are necessary for renewal and regeneration of the most if not all tissues in human body. They closely interact with tissue-specific stem cells and control their functioning as well as differentiate into different cell lineages. These cells represent a functionally heterogeneous population; however, molecular mechanisms involved in the establishment and maintenance of MSCs heterogeneity remain poorly understood. Using MSCs isolated from human adipose tissue we have analyzed if hormones and their receptors could be involved in functional heterogeneity of these cells.

Using the genome-wide screening method and RT-PCR we identified the expression of a number of hormone receptors, including adrenergic receptors as well as receptors to angiotensin II. Adrenergic receptors mediate the interaction of MSCs with sympathetic neurons, which are important components of mesenchymal stem cells (MSCs) niche. We examined the mechanisms of regulation of MSCs responsiveness to noradrenaline. Using flow cytometry, we demonstrated that α1A adrenergic receptors isoform was the most abundant in adipose tissue-derived MSCs. Using calcium imaging in single cells, we demonstrated that only 6.9±0.8 % of MSCs responded to noradrenaline by intracellular calcium release. Noradrenaline increases MSCs sensitivity to catecholamines in a transitory mode. Within 6 hrs after incubation with noradrenaline the proportion of cells responding by Ca2+ release to the fresh noradrenaline addition doubled but declined to the baseline after 24 hrs. Increased sensitivity was due to the elevated quantities of α1A-adrenergic receptors on MSCs. Such elevation depended on the stimulation of β-adrenergic receptors and adenylate cyclase activation. Furthermore, other hormones, activating adenylate cyclase, such as serotonin and dopamine also up-regulated MSCs sensitivity to noradrenaline. Taken together, our data indicate that MSCs preserve embryonic adrenergic signaling regulation. Considering that noradrenaline exerts evident effects on MSCs secretory activity, these data are important for understanding their physiology and regulation of functional activity.

MSCs are often located within vascular wall and we suggested that angiotensin II could regulate their functional activity. We determined that adipose derived MSCs express mRNAs of main components of renin-angiotensin system (RAS): angiotensinogen, renin, angiotensin converting enzyme and angiotensin II receptors AT1 and AT2. Using flow cytometry analysis we demonstrated that almost all the MSCs express AT1 receptor and 5.7±1.7 % of MSCs express AT2 receptor. Using Ca2+-imaging with Fluo8 we examined activation of Ca2+-signaling pathway in response to angiotensin II treatment and determined that AT1 receptors on MSCs are functionally active. We analyzed angiotensin II effects on MSCs differentiation and secretion. Angiotensin II inhibited adipose differentiation of MSCs, which was registered by the reduction of mRNA expression of CEBPB, PPARG, ADIPOQ (adipose-differentiation master-genes). On the contrary, angiotensin II upregulated expression of neurotrophic factors on MSC and stimulated their neurogenic potential. Our data indicate that adipose derived MSCs produce functionally active local RAS, which regulates their differentiation and paracrine activity.

**Acknowledgments**

This study was supported by the Russian Science Foundation (RSF) grant 14-15-00439.

*Invited*

# COLLAGEN MORPHOLOGY IN THE EXTRACELLULAR MATRIX AS A MARKER OF TISSUE DAMAGE

**P.S. Timashev**[1,2], **S.L. Kotova**[2,3], **T.M. Zharikova**[2], **D.V. Butnaru**[2], and **A.B. Solovieva**[3]

[1] Institute of Photonic Technologies, Research center "Crystallography and Photonics", Troitsk, Moscow, Russia, e-mail: timashev.peter@gmail.com
[2] I.M. Sechenov First Moscow State Medical University, Institute for Regenerative Medicine, Moscow 119991, Russia
[3] N.N. Semenov Institute of Chemical Physics, Moscow, Russia

**Abstract.** We have applied atomic force microscopy (AFM) to diagnose morphological changes in the extracellular matrix of connective tissue caused by different pathological processes. AFM has been shown to reveal visible deviations from the normal morphology of the extracellular matrix in diseased tissues. The AFM data were found in a good agreement with the data of conventional histological studies. Thus, AFM may serve as either an independent, or a complementary diagnostic tool for tracking pathological changes in the connective tissue.

Atomic force microscopy (AFM) has been widely used in the life science and biomedical studies in the last decade (see, e.g., [1]). In particular, AFM studies of collagen-built structures, primarily, in the extracellular matrix (ECM) of connective tissue have attracted a significant attention [2]. Here we have applied AFM imaging to monitor alterations in the ECM of connective tissue from different pathological causes, including 1) abnormalities of connective tissue leading to development of pelvic organ prolapse (POP), 2) malignancy of connective tissue (chondrosarcoma), 3) radiation damage of the pelvic organs (bladder and rectum) resulting from radiation therapy.

Our AFM studies showed marked deviations from the normal ECM morphology of human skin and pelvic ligament for patients with POP. The deviations were observed at all the levels of the ECM texture, including microtexture (packing of collagen fibers), nanotexture (arrangement of collagen fibrils) and structure of individual collagen fibrils. The nanoindentation study revealed significant deterioration of the mechanical properties of the collagen fibrils bundles in the skin of POP patients, as compared to the skin of healthy subjects.

In the AFM study of bone tumor tissue, we compared the morphology of chondrosarcoma of histologically malignant grade I, II and III. A benign chondroma tumor was used as a control. The AFM imaging showed a clear correlation between the content of the fibrous collagenous elements in the ECM of a bone tumor and the degree of its malignancy.

The AFM study of the ECM of internal pelvic organs damaged by radiation therapy have shown the first ECM changes occur 1 week post-irradiation in the dose of 2 Gy. AFM studies have detected low-dose (2 Gy) effects on the extracellular matrix 1 week to 1 month post-irradiation and higher-dose (8–22 Gy) effects as early as 1 day post-irradiation.

The obtained AFM data demonstrated a good agreement with the conventional histological study data for the POP study and chondrosarcoma study. In the study of radiation therapy negative effects, the AFM capabilities in detecting early signs of radiation damage in the ECM appeared superior to the conventional optical microscopy-based methods.

## Acknowledgements

This study was financially supported by the Russian Foundation for Basic Research (grant No. 15-02-04505) and the Russian Science Foundation (grant No. 16-13-10295). The samples of tissues were provided by Prof. A.B.Shekhter, I.M. Sechenov First Moscow Medical University, Research Institute of Molecular Medicine, Moscow, Russia (patients with POP and chondrosarcoma) and by Prof. A.V.Maslennikova, Nizhny Novgorod State Medical Academy of the Russian Ministry of Health, Nizhny Novgorod, Russia (murine pelvic organs).

## References

1. U. Maver, T. Velnar, M. Gaberscek, O. Planinsek, and M. Finsgar, *Trends Analyt. Chem.,* 2016, **80**, 96–111.
2. H.K. Graham, N.W. Hodson, J.A. Hoyland, S.J. Millward-Sadler, D. Garrod, A. Scothern, C.E.M. Griffiths, R.E.B. Watson, T.R. Cox, J.T. Erler, A.W. Trafford, and M.J. Sherratt, *Matrix Biol.,* 2010, **29**, 254–260.

# BASIC AND APPLIED SIDES OF PLURIPOTENT STEM CELLS

**A. Tomilin**[1,2]

[1] Institute of Cytology RAS, St-Petersburg
[2] St-Petersburg State University, Russia
e-mail: a.tomilin@incras.ru

Pluripotent stem cells have gained considerable interest during the past decades because they represent a formidable tool for human disease modeling, drug screening and testing, and notably, because they possess a tremendous potential in regenerative medicine. During the talk I will give an overview of the field of pluripotent stem cell research with an emphasis on embryonic stem (ES) and induced pluripotent stem (iPS) cells as the most prominent pluripotent stem cell types. I will highlight three major issues standing on the way of efficient introduction of these cells into practical medicine (safety, immunogenicity, and oncogenic transformation) and will address possible ways of solving these issues. Basic and applied iPS/ES cell-related projects that are currently under way in the lab will be also incorporated into the talk.

**Acknowledgements**

The projects presented in this talk have been supported by the Russian Science Foundation grants No.14-50-00068 and 17-14-01407.

# IMMUNOPROTEASOME INHIBITOR PREVENTS REPROGRAMMING OF MOUSE EMBRYONIC FIBROBLASTS INTO INDUCED PLURIPOTENT STEM CELLS

**A.S. Tsimokha, A.V. Selenina, S.A. Sinenko, A.A. Kuzmin,** and **A.N. Tomilin**

Institute of Cytology, Russian Academy of Sciences, Saint Petersburg, Russia
atsimokha@incras.ru

The ubiquitin-proteasomal system plays an important role in several processes including maintenance of cellular quality control, transcription, cell cycle progression, DNA repair, cell stress and immune responses, apoptosis and development. The proteasome is a multi-subunit protease complex consisting of 20S core and one or two 19S regulatory particles. Under certain conditions, the constitutive catalytic subunits of the 20S particle β1, β2 and β5 can be replaced by alternative subunits – β1i, β2i and β5i. In this case, the proteasome is called immunoproteasome and plays a role in antigen presentation. It is known that there is an increased gene expression of the immunoproteasome subunits in embryonic stem cells (ESCs), while the expression of these subunits discernibly decreases during differentiation of these cells. This implies that immunoproteasomes take an active part in the maintenance of pluripotency of ESCs. The role of the immunoproteasomes in the induction of pluripotent cell state is also an interesting issue. To address this issue, we induced reprogramming of mouse embryonic fibroblasts (MEF) into induced pluripotent stem cells (iPSCs) by activating the OSKM construct (polycistronic sequence of factors Oct4, Sox2, Klf4, and c-Myc) by doxycycline. The expression of immunoproteasome subunits β1i and β5i was analyzed by PCR and western blotting. We found that the levels of immunoproteasome subunits β1i and β5i increased after 6 day of the process of reprogramming while resulting iPSCs and MEF did not express detectable immunoproteasome subunits. Furthermore, we assessed if the reprogramming process is affected by the presence of a selective inhibitor of subunit β5i – PR-957, and the proteasome inhibitor MG-132. Alkaline phosphatase staining, a marker of pluripotent cells, showed a significant decrease in the formation of iPSC clones, which indicates important functions of both proteasomes and immunoproteasomes in the process of cellular reprogramming. Our study reveals a critical role of ubiquitin-proteasome system in pluripotent stem cells.

**Acknowledgements**

This work was supported by the RSF 16-04-10343.

# AUTHOR INDEX


**A**

Abel J.J. 113
Adameyko I. 158, 165, 169
Ageeva L.V. 176
Agrba P. 43, 50, 140
Ahnen L. 39
Akarçay H.G. 26, 39
Akkuratova N. 158
Akopov A. 130
Aksenova N.A. 72
Alam S.R. 97
Alekseeva A.I. 87
Alieva R.S. 142
Andersson-Engels S. 27
Andrade-Caicedo H. 152
Anna T. 28, 30
Anokhin K.V. 127
Antipov O.L. 150
Antonova N.O. 74
Arteaga C.L. 23
Artyushenko V. 29, 110
Ashek-I-Ahmed 96, 166
Assmann W. 111
Astafiev A.A. 162
Aybush A.V. 162, 163

**B**

Bagratashvili V.N. 170
Bakhmet E.I. 164
Baklaushev V.P. 77
Balalaeva I.V. 74, 88, 90, 102
Balalayeva I.V. 66
Barroso M. 73, 98
Barry K. 62
Baum O. 61, 68
Becker W. 15, 101, 106
Belikova V. 29
Belousov V.V. 127
Belova A.S. 74
Betz V. 91
Bibikova O. 29
Bisinger D. 99
Boas D. 16
Bobrov N. 159
Bogomolov A. 29
Borisov A.V. 45
Botero R. 152
Bouchard R. 105
Bown S. 131
Bratashov D.N. 84
Bredichin V.I. 150
Breymayer J. 99
Brinkmann R. 132
Bugrov S.N. 154
Bulgakova N.M. 112
Butnaru D.V. 161
Butnaru D.V. 177
Bykov A. 52
Bystrova A.S. 34, 172, 175

**C**

Campagnola P.J. 75
Cannon T.M. 23
Cassidy J. 91
Chagin A.S. 160
Chakraborty S. 28, 30
Chandra D. 76
Chang Chia-Yuan 31
Chang H.-H. 166
Chaudhary A. 76
Chekhonin V.P. 77
Chen K. 73
Chen S.J. 41
Chen Shean-Jen 31
Chen Zhongping 32
Cheng C.-L. 78, 96, 166
Chernigina I.A. 79
Chernov V.V. 79
Chichkov B.N. 17, 167
Chidangil S. 80
Chikalova K. 43, 143
Chiou A. 28, 30
Chizhik A. 36
Chizhik Al. 36
Chontorotzea T. 158, 169
Cook R.M. 23
Cowan T.E. 118

**D**

Danielyan G. 29
Day C.R. 81
Day R.N. 82
Deán-Ben X.L. 33
Deby S. 144
Deiwick A. 167
Demidov V. 83
Deming D. 23
Deniso N.N. 163
Doronin A. 52
Druzhkova I.N. 103, 107
Dudenkova V.V. 34, 37, 46, 66, 92, 103, 137, 151, 159, 172, 175
Dyachuk V. 158
Dydykin A.V. 154

**E**

Eibl M. 35
Eichler H.J. 29
Elagin V.V. 104
Emelianov S. 105
Enderlein J. 36
Enghardt W. 118
Eranov I.D. 150
Ermakova Y.G. 127

**F**

Favreau P. 23
Fedoseeva V.V. 87
Fedotov A.B. 127
Fedotov I.V. 127
Feldchtein F.I. 37, 44
Feofanov A.V. 66
Fidarov A.F. 168
Fiks I. 53
Fiks I.I. 51
Finagina E.S. 44, 133, 135, 139
Flueraru C. 83
Franceschini M.A. 38
Freidank S. 123
Frenz M. 26, *39*
Fried K. 158, 169
Fuchs J. 115
Fuchs S. 113

**G**

Galanzha E.I. 84
Gamajunov S.V. 134
Gamayunov S.V. 135, 137, 142
Gavrina A.I. 103
Gelikonov G.V. 37, 40, 59, 68, 69, 104, 133, 139
Gelikonov V.M. 40, 59, 87
Gerelli E. 153
German S.V. 84
Gillette A. 23
Gladkova N.D. 37, 44, 60, 69, 87, 104, 133, 135, 139, 155
Glagolev N.N. 72
Goetz M. 149
Golovan L.A. 50
Golubiatnikov G.Yu. 95
Golubyatnikov G.Yu. 145
Gongalsky M.B. 50, 85
Gorin D.A. 84
Gorkun A.A. 161, 168
Gorokhova A.A. 102
Gostev F.E. 163
Gottschalk S. 33
Gotz M. 118
Grachev P. 149
Gremyakina M. 141
Grice J. 93
Grigoryev I.S. 88, 90
Grimellet L. 115
Gubarkova E.V. 34, 37, 60, 69, 135, 155
Gulin A.A. 162, 163
Gunther J. 27

**H**

Hakert H. 35
Hammer M. 136
Han S. 105
Haridass I. 93
Heaster T.M. 23
Heeger P. 18
Heinemann D. 18
Heisterkamp A. 18
Held K.G. 39
Henriquez N. 131
Herrmannsdörfer T. 118
Hoess P. 184
Hofmann K.M. 118
Holmes A. 93
Horvath D. 153
Hovhannisyan V.A. 41
Hu Z. 125
Huber R. 35
Huntosova V. 153

**I**

Ilyinskaya O.E. 145
Inoue K. 114
Intes X. 73, 98
Isomaki A. 85
Ivanova E.Y. 164
Ivashina T.V. 100
Ivashkin E. 165
Ivashkina O.I. 127
Iwata Y. 19

**J**

Jaeger M. 39, 53, 63
Johannsmeier S. 18

**K**

Kachalina O.V. 143
Kalganova T.I. 145
Kalinina N.I. 176
Kalinina S. 99
Kamensky V.A. 150
Kando M. 19
Karabut M.M. 155
Kardumjan V.V. 72

Karedla N. 36
Karmenyan A. 30, 96, 166
Karpf S. 35
Karsch L. 118
Kartha V.B. 80
Karyakin N.N. 154
Kasatkina I.V. 59
Kashaev F.V. 50
Kastriti M.E. 158
Kaucka M. 158
Khabarova M. 165
Kharchenko P. 158
Khilov A.V. 42
Khlebtsov B.N. 84
Khlebtsov N.G. 86
Kirillin M. 37, 42, 43, 50, 51, 56, 57, 63, 95, 140, 143, 146, 147
Kiriyama H. 19
Kiselev N. 159
Kiseleva E. 37, 43, 44, 87, 133, 139, 151, 155
Kistenev Yu.V. 45
Kitchen N. 131
Klapshina L.G. 88, 90, 102
Klementieva N.V. 89
Klemm M. 136
Kochueva M.V. 46, 151
Kondo K. 19
Kondratieva O. 43, 143
Korchagina K.S. 137
Koroleva A. 161, 167
Korzhimanov A.V. 115
Kosheleva N.V. 161, 168
Kositsyin R.I. 150
Kotova S.L. 177
Kravets L.Ya. 155
Kreilkamp L. 136
Krivanek J. 169
Krivokharchenko A.S. 166
Kroll F. 118
Krupin V.N. 151
Kryazhov V.A. 142
Ksenofontov S. 40, 59, 133, 135, 139,
Kuimova M.K. 88, 103
Kulagin F. 159
Kulchin Yu.N. 116
Kumar R. 76
Kumar S. 76
Kuo W.C. 28, 30
Kupinski M. 144
Kurochkina O.S. 45
Kuzmin A.A. 179
Kuznetsov S.S. 46, 60, 104, 137
Kuznetsov S.S. 143, 155
Kuznetsova D. 159, 167, 170

**L**

Lanin A.A. 127
Larin K.V. 47
Larina I.V. 171
Larson D.R. 81
Lazareva E.N. 48
Lazareva M. 138, 139
Lee K. 58
Leite-Silva V.R. 93
Lermontova S.A. 88, 90, 102
Leutenegger M. 49
Li J. 125
Liang X.-X. 123
Lilge L. 91
Lin S. 152
Lin Y.-C. 78, 96
Lin Z.-R. 78, 96
Linz N. 123
Liu D. 93
Liu L.-C. 96, 166
Loginova D.A. 42, 50, 51
Loschenov V. 149
Lubatschowski H. 117
Lugovtsov A.E. 58
Lukina M. 92, 101, 103, 159, 175
Lukyanov K.A. 89
Lukyanov S.A. 107

**M**

Madge V. 83
Maeda A. 83
Malik Z. 20
Malikov D.K. 151
Markwardt N. 149
Martin A. 81
Maslennikova A. 139
Maslennikova A.V. 44, 46, 66, 133 145, 151
Masood U. 118
Matkivskiy V.A. 59
Matveev L. 44, 60, 68, 69, 133, 139
Matveyev A.L. 60, 68, 69
Medyanik I.A. 154, 155
Meglinski I. 52
Melenteva A. 29
Meleshina A.V. 34, 172, 175
Meller A. 43, 140, 146, 147
Mel'nikov P.V. 77
Meunier M. 119
Mihailova I. 63
Mikhailova I. 53
Minaev V.P. 120
Minet O. 29
Mishin A.S. 89
Mitrakov A.A. 141, 142
Mitrakova N.N. 141, 142
Mizushima K. 19
Mohammed Y. 93
Moiseev A. 37, 44, 59, 60, 87, 104, 133, 135, 155, 138, 139
Moreau F. 144
Motovilova T. 43, 143
Muftieva D.A. 85
Muravyeva M.S. 88

**N**

Nadkarni S. 54
Nadtochenko V.A. 162, 163
Nakatsutsumi M. 115
Nathanael J. 113
Nazac A. 144
Nedivi E. 62
Nedosekin D.A. 84
Nefedov V. 141
Neubauer A. 101
Ng J. 131
Nguyen T.N. 152
Nikitin M. 165
Nikitin S.Yu. 58
Nikolaev V.V. 45
Nishiuchi M. 19
Noda E. 19
Novikova T. 52, 144
Novoselova M.V. 84
Novozhilov A. 147
Nuster R. 55

**O**

O'Donnell M. 21
Obukhova A. 165
Ogasawara S. 173
Ogawa T. 124
Ogawa M. 94
Omelchenko A.I. 68
Ongole R. 80
Orlova A. 56, 63, 74, 95, 101, 145
Osminkina L.A. 85

**P**

Pai K. 80
Pai K.M. 80
Paltauf G. 55
Panait A.I. 162
Papayan G. 130
Pasche C. 23
Pastore M. 106
Patil A. 80
Paulus G.G. 113
Paulus Y. 125
Pavlikov A. 101
Pavlov M.V. 145
Pavlova N.P. 92
Pavone F.S. 22
Pawelke J. 118
Peltonen L. 85
Perekatova V.V. 56, 57, 63
Perevedentseva E. 78, 96, 166
Periasamy A. 97
Peskova N.N. 90, 102
Peters S. 136
Petersen J. 158
Pierangelo A. 144
Plekhanov V.I. 145
Plekhanova E.S. 79
Pochechuev M.S. 127
Pochtin D.P. 150
Pogorelov A.G. 162
Pogorelova V.N. 162
Presnov D.E. 50
Priezzhev A.V. 58
Prodanets N.N. 170

**R**

Razansky D. 33
Rehbinder J. 144
Reinhard J. 113
Repin V.S. 161
Ricka J. 26
Ripken T. 18
Roberts M. 93, 106
Rochev Yu. 174
Rödel Ch. 113
Rodriguez J. 81
Rogovaya O.S. 34, 175
Romashov V.N. 40
Rowlands C.J. 62
Rozhentsov A. 141
Rück A. 99
Rudkouskaya A. 73, 98
Rühm A. 149
Ryan E. 93

**S**

Saarinen J. 85
Saburina I.N. 161, 168
Saito N. 124
Sakaki H. 19
Sakharova T. 29
Sanchez Majos S. 39
Sanchez W. 93
Santos H.A. 85

Sapunov D. 43, 140, 146, 147
Sarimollaoglu M. 84
Sauer L. 136
Savitsky A.P. 100
Schäfer P. 99
Schmidt J. 136
Schramm U. 118
Schürer M. 118
Selenina A.V. 164, 179
Semenov A.N. 58
Serebrovskaya E.O. 107
Sergeeva E.A. 43, 50, 51, 95, 137
Sergeeva T.F. 103
Seryi A.A. 121
Shabanov D.V. 40, 44, 59, 68, 133
Shah A.T. 23
Shakhov A. 140, 146, 147
Shakhova M. 43, 140, 146, 147
Shakhova N.M. 43, 137, 138, 139, 143, 145
Sharabrin E.G. 37
Sharick J.T. 23
Shcherbatyuk T.G. 79
Shcheslavskiy V. 101
Shcheslavskiy V.I. 103
Shchukina K.M. 74
Shelaev I.V. 163
Shilyagin P.A. 40, 59, 143
Shilyagina N.Y. 66, 88, 95, 102
Shimolina L.E. 103
Shirai T. 19
Shirmanova M.V. 88, 92, 101, 103, 104, 107, 172
Shirokov D. 101
Shirshin E.A. 58
Shoham S. 33
Shpichka A.I. 161
Sidorov-Biryukov D.A. 127
Sie Yong-Da 31
Sinenko S.A. 164, 179
Sinsuebphon N. 73, 98
Sirotkina M.A. 44, 60, 69, 87, 104, 135, 139
Sirotkina M.V. 133
Skala M.C. 23
Snopova L.B. 92, 103
So P.T.C. 62
Sobol E. 61, 68
Sokolov K. 105
Soldatov R. 158
Solodina A.E. 162
Solovieva A.B. 72, 177
Solviev I.D. 100
Song C.-Y. 96
Sovetsky A.A. 60, 68, 69
Spirina L.V. 45
Spokoynyy A.L. 72
Sroka R. 148, 149
Staforelli J.P. 52
Stähli P. 26
Stepp H. 149
Strachan C.J.85
Streltsova O.S. 134, 150, 151
Studier H. 93, 101, 106
Subochev P. V. 53, 56, 57, 63, 145
Sugita M. 83
Sukhov V.S. 66
Svindrych Z. 97
Sysoeva V.Yu. 176

## T

Takiguchi Y. 62
Tararova E.A. 134, 151
Teig B. 144
Terpelov D.A. 40
Timashev P.S. 72, 161, 167, 170, 177
Timofeeva L.B. 87, 135
Tkachuk V.A. 176
Tomilin A.N. 164, 178, 179
Torke P. 55
Toronov V.Y. 152
Torres L.M. 18
Tsimokha A.S. 164
Tsimokha A.S. 179
Tubbesing K. 73
Tuchin V.V. 48, 64
Turchin I.V. 42, 43, 53, 56, 57, 63, 95
Tyurin-Kuzmin P.A. 176

## U

Ueda K. 122
Ulrich L. 39
Unnikrishnan V.K. 80
Usenov I. 29
Utkina A.V. 102

## V

Varlamova A.V. 46
Vera Paz N.O. 52
Vinokurov L.M. 100
Vitkin A. 40, 44, 65, 68, 69, 104, 133, 135, 139
Vitkin I.A. 83
Vogel A. 123
Voloveckiy A.B. 66, 95
Volovik M.G. 154
Von Arnim C.A.F. 99
Von Einem B. 99
Vorobieva A.S. 151
Voronezhskaya E. 165
Vorontsov A.Yu. 60
Vorontsov D.A. 60
Vorotelyak E.A. 175
Voznesenskiy S.S. 116
Vrazhnov D.A. 45

## W

Wabnitz H. 67
Wachsmann-Hogiu S. 61
Wada S. 124
Wagner C. 58
Wagnieres G. 153
Wallrabe H. 97
Walsh A.J. 23
Wang X. 125
Weng D. 35
Wilkens J.J. 118
Wolf M. 39
Wu K.-T. 78
Wünsche M. 113

## X

Xue Y. 62

## Y

Yabashi M. 126
Yadav N. 76
Yakovlev V. 101
Yang X. 125
Yashin K.S. 87, 154, 155
Yaya F. 58
Yumoto M. 124
Yunusova K.E. 151
Yuzhakova D.V. 88, 107

## Z

Zabarylo U.J. 29
Zabotnov S.V. 50
Zagaynov V. 159
Zagaynova E. 101, 139, 159
Zagaynova E.V. 34, 44, 69, 74, 88, 89, 92, 103, 104, 107, 133, 135, 170, 172, 175
Zaitsev V.Y. 60, 68, 69, 104, 133, 139
Zeil K. 118
Zelenkov P. 149
Zhang H. 125
Zharikova T.M. 177
Zharov V.P. 70, 84
Zheltikov A.M. 127
Zhukov V.P. 112
Zurina I.M. 161, 168
Zurina I.M.

VI International Symposium

# TOPICAL PROBLEMS OF BIOPHOTONICS




## *Sponsors*

# EXTREME RANGE EXTENSION OF VISUAL SIGHT HAMPERED BY TURBID MEDIA

**P. Hoess**

Paul Hoess KG, Munich, Germany, phoess@stanfordcomputeroptics.com
Stanford Computer Optics, Inc., Berkely, CA-USA

**Abstract.** Range limitations in strongly scattering media are apparent. The visibility can be limited to even less than a few centimeters. Compact pulsed lasers open gated viewing to civil applications. These systems are able to take images with short (200 ps) gate times and delay steps down to 10 ps, highly reducing interference of scattered light and getting accuracy down to sub-mm-region. A visibility simulation is based on a 10 μJ laser for illumination and a 1.2 ns gated camera. The image was obtained through an opal glass diffuser causing scattering equivalent to over 2000 m thick sea water.

## Summary

Driving a car through dense fog, searching for victims in smoke filled rooms or scanning the ocean floor for sunken objects as RMS Titanic or the body of MH370 are all bound through well known limits of hampered visibility.

Since the invention of the laser there are proposals for gated (active) imaging, but mainly for military applications.

The primary purpose of our work was the proof that the otherwise invisible bottom of CO2 cooling tubes for spent nuclear fuel elements in a power plant, filled with a dusty atmosphere, will get visible and the exact depth of a potential dust layer can be determined.

We use a simulation setup as a replacement of real water or dusty air. It shall demonstrate the capabilities of gated imaging systems to get images through extremely high scattering media.

A milky ground glass plate is used as a diffuser. The laser beam is spread out to a spot of 1 m (FWHM) diameter in a distance of 11 m.The glass plate being in the optical path twice results in a reduction of the signal by a factor of around $5 \cdot 10^{6}$. The laser with a pulse length of 800 ps is set for a total illumination energy of 200 mJ for one recording.

The gate of the intensified CCD camera (4 Quik E) is triggered by the laser. From the time of receiving the trigger signal the camera needs around 70 ns before it turns the photocathode on. The first reflecting surface is 11 m from the laser, the roundtrip time to the camera right at the same place is roughly 73 ns. Minimum gate time is 1.2 ns, any multiple of 100 ps can be added. The delay can be programmed with a minimum of 100 ps steps.

The signal attenuation is linked to the distance in turbid media by the law of Lambert-Beer:

The extinction coefficient e in pure destilled water ranges from a minimum of 0.00442 $m^{-1}$ at 417.5 nm up to 1.678 $m^{-1}$ at 727.5 nm, being higher in muddy water. The water depths corresponding to our measured $5 \cdot 10^{-6}$ attenuation are 1750 m in the case of working with a fiber laser in the deep blue range. In the red regime this same intensity decrement would be reached at a water depth of only 4.5 m.

There is only a very weak wavelength dependency of scattering in air. Corresponding extinction coefficient numbers for smoke are 0.25 $m^{-1}$ in the case of light and up to 4 $m^{-1}$ in very dense smoke.

The range of values for e in air is much wider than what is observable in clear water. First noticable reductions of the visual range occur at a sighting distance of 10 km with an extinction coefficient of $4 \times 10^{-4}$, this being considered slightly hazy. It ranges up to a highest documented maximum of 13 $m^{-1}$, observed at the Great Smog in London in 1952. The resulting visibility was then only one foot.

Under such extreme foggy conditions a laser with a separated head at an optical fiber could still improve the sight range. With a detached output collimator that is connected through a few meters of fiber optic extension, the light source can be placed closer to the object.

Although the laser power used for the experiment presented in this paper was only 100 mW, a maximum visible range above 1000 m could be demonstrated. With multi-kW lasers and increased summation times a depth range of 5000 to 6000 m can be reached. An ocean floor telescope with an array of lasers in the high kW power range can be synchronized through individual lengths of the output fibers and therefore compensate for time of flight differences in between the center and the corners of the field of view.In such way the search for sunken objects from the ocean surface is in reach as a potential option.



**The organization of TPB-2017 was supported by the Government of the Russian Federation under the program designed to support research projects implemented under the supervision of the world's leading scientists at Russian institutions of higher learning**

**Grant No. 14.B25.31.0015**

"Development of new technologies of optical coherence tomography for problems of individual cancer therapy"

**Leading scientist – Alex Vitkin**

**by the Federal Agency of Scientific Organizations**

**agreement No. 007-02-1255/3**

**by the Russian Foundation for Basic Research**

**Grant No. 17-02-20342-г**
**Grant No. 17-02-20343-г**

**as well as by a number of Russian and foreign companies producing optical and medical equipment**

VI International Symposium

# TOPICAL PROBLEMS OF BIOPHOTONICS

TPB-2017

Proceedings